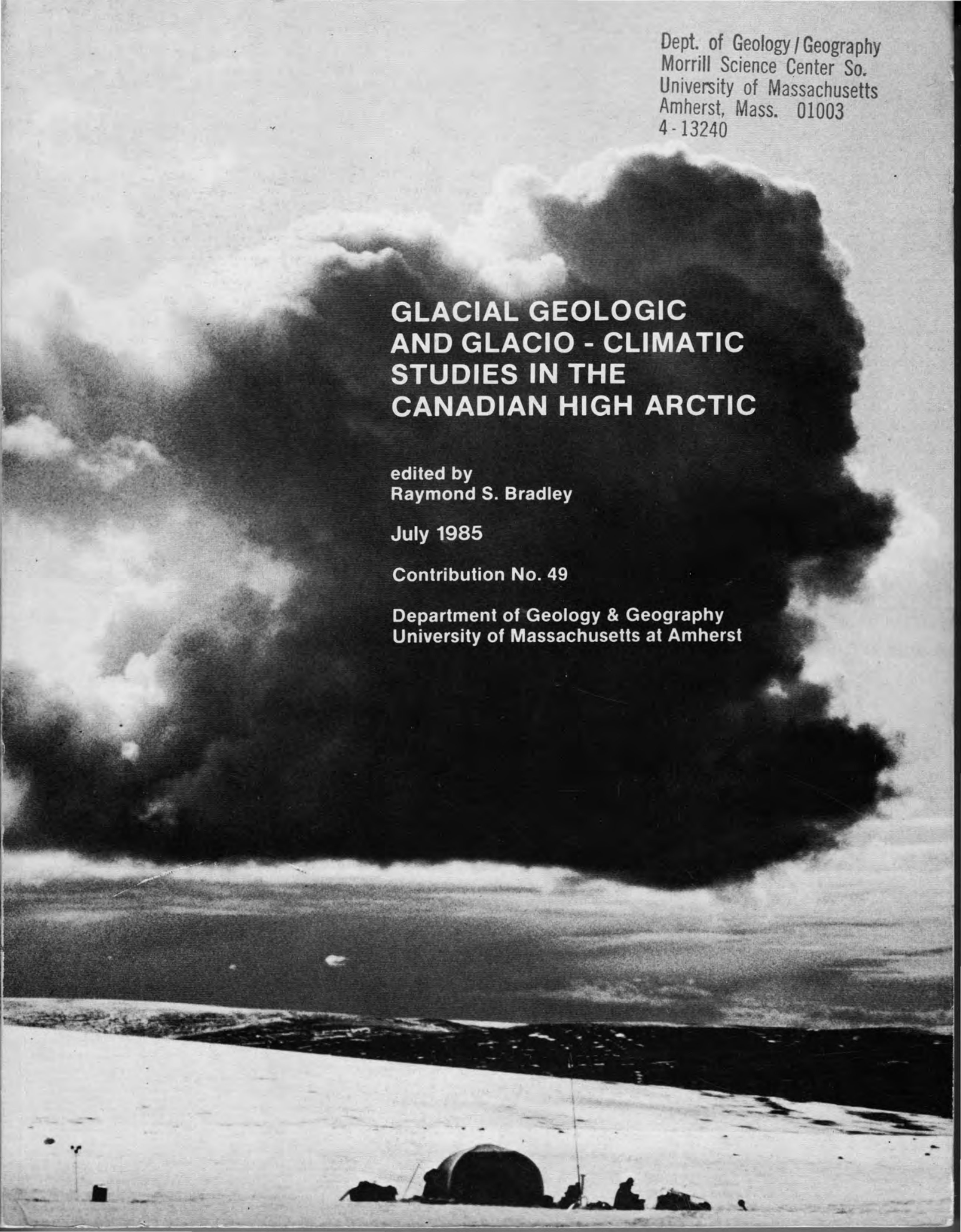

GLACIAL GEOLOGIC AND GLACIO - CLIMATIC STUDIES IN THE CANADIAN HIGH ARCTIC

edited by
Raymond S. Bradley

July 1985

Contribution No. 49

Department of Geology & Geography
University of Massachusetts at Amherst

GLACIAL GEOLOLGIC AND GLACIO-CLIMATIC STUDIES IN THE CANADIAN HIGH ARCTIC

Edited

by

Raymond S. Bradley

Final Report to the National Science Foundation

Grant ATM80-17745

Contribution No. 49

Department of Geology and Geography

University of Massachusetts

Amherst, MA 01003-0026

July

1985

TABLE OF CONTENTS

ACKNOWLEDGEMENTS

The authors gratefully acknowledge the financial support of the U.S. National Science Foundation, the Canadian Polar Continental Shelf Project (Department of Energy, Mines and Resources, Ottawa) and the University of Massachusetts Research Council. We also wish to thank: Dr. R. Stuckenrath, Smithsonian Institution for radiocarbon analyses; Dr. R. Feyling-Hanssen, University of Aarhus, Denmark; Dr. G. Vilks, Atlantic Geosciences Center, Halifax, Nova Scotia for faunal analysis of sediments; and Drs. J.T. Andrews, University of Colorado and Dr. J. Tull, University of Arizona for a C-14 accelerator date.

Many individuals provided assistance in the field, in the laboratory and in the office. We are particularly grateful to: John Fabel, Richard Friend, Christopher Allen, William McCoy, Jane Bradley, Dennis Anello Marie Litterer, Jimmie Terrell, Tony Kudrikow, Martha Terrell and Rita Montague.

PREFACE

This report comprises eight chapters arising from work accomplished as a result of NSF grant ATM80-17745 and logistical support from the Polar Contiental Shelf Project, Ottawa. Each chapter should be considered as a preliminary report and may be revised prior to publication in refereed journals.

Fieldwork on northeastern Ellesmere Island, N.W.T., Canada was carried out in the summers of 1981, 1982 and 1983.

The work had several objectives:

1. To provide further information on the timing and extent of glaciation on northeastern Ellesmere Island to help resolve differences between conflicting models of High Arctic glaciation (England 1976; England and Bradley, 1978; Denton and Hughes, 1980).
2. To study sediments from low elevation coastal lakes to provide information on the glacio-isostatic history of the area and on post-glacial environmental changes.
3. To monitor the mass balance of low elevation ice caps and to assess their ability to modify local climate, thereby enhancing prospects for survival.
4. To examine precipitation events in the Canadian High Arctic to understand contemporary climatic conditions favoring increased glacierization of the area, and to understand better the meaning of ice core isotopic records from the High Arctic.

The chapters presented herein represent the principal results of our work on these objectives. In addition, the following publications have also arisen from work accomplished on the project:

England, J., 1983: Isostatic adjustments in a full glacial sea. Canadian J. Earth Sciences, 20, 895-917.

Stewart, T.L. and England, J., 1983: Holocene sea-ice variations and paleoenvironmental change, northernmost Ellesmere Island, N.W.T., Canada. Arctic and Alpine Research, 11, 1-17.

Young, M. and Bradley, R.S., 1984: Insolation gradients and the paleoclimatic record, pp 707-713 in: Milankovitch and Climate, Vol. 2 (Berger, A.L., Imbrie, J., Hays, J., Kukla, G. and Saltzman, B. eds.) D. Reidel, Dordrecht.

Considerably more detail on topics discussed in this report may be found in the following theses:

Retelle, M.J., 1985: Glacial geology and Quaternary marine and lacustrine stratigraphy of the Robeson Channel area, northeastern Ellesmere Island, N.W.T., Canada. Ph.D. Geology, University of Masschusetts, Amherst, 229 pp.

Serreze, M.C., 1985: Topoclimatic studies of a small, sub-polar ice cap with implications for glacierization. M.S. Geography, University of Massachusetts, Amherst, 201 pp.

Palecki, M.A., 1984: Atmospheric boundary layer observations on a plateau in the Canadian High Arctic. B.S. Physics, Senior Honors Thesis, University of Massachusetts, Amherst, 125 pp.

REFERENCES

Denton, G.H., and Hughes, T., 1980. The Last Great Ice Sheets. John Wiley, New York. 484 pp.

England, J., 1976. Late Quaternary glaciation of the eastern Queen Elizabeth Islands, N.W.T., Canada: alternative models. Quaternary Research, 15, 603-617.

England, J. and Bradley, R.S., 1978: Past glacial activity in the Canadian High Arctic. Science, 200, 265-270.

GLACIAL GEOLOGY AND QUATERNARY MARINE STRATIGRAPHY OF THE ROBESON CHANNEL AREA, NORTHEASTERN ELLESMERE ISLAND, N.W.T., CANADA

Michael J. Retelle,

University of Massachusetts, Amherst.

Abstract

Glacial and marine deposits associated with two phases of glaciation are exposed along a 60 km corridor on Ellesmere Island that borders Robeson Channel. The oldest sediments, tentatively dated at $\geq$ 80,000 B.P. were deposited during a major advance of the northwest Greenland Ice Sheet across Robeson Channel. During subsequent retreat of this ice mass, glaciomarine sediments containing a high arctic macro- and microfauna, were deposited in the isostatic downwarp on Ellesmere Island. This marine unit was radiocarbon dated at 31,300 $\pm$ 900 and >32,000 B.P.; amino acid ratios (aIle/Ile) are 0.207 $\pm$ .02 and 0.062 for the free and total hydrolysate fractions.

The ice advance during the late Wisconsin to early Holocene did not extend into the field area from either interior Ellesmere Island or northwest Greenland. The ice marginal sea transgressed to the marine limit (ca. 116 m) and overlapped the deposits of the previous maximum Greenland advance. Local plateau ice caps did however, spill over into one major valley and delayed the establishment of the marine limit in this location. Radiocarbon dates on Holocene marine limit shorelines indicate initial emergence between 8000 and 8600 B.P. Amino acid ratios were not detectable in the free fraction and 0.037 $\pm$ .04 in the hydrolysate fraction.

Correlation of these units with other arctic sequences demonstrates similar early maximum ice extents and subsequently more restricted ice advances. The chronology for the Robeson Channel area supports a model for limited last ice extent that is non-synchronous with mid-latitude ice sheet expansion.

Introduction

During the field seasons of 1981 and 1982, a mapping program was conducted along a 60-km corridor bordering Robeson Channel, northeastern Ellesmere Island, N.W.T., Canada (Fig. 1). Because of

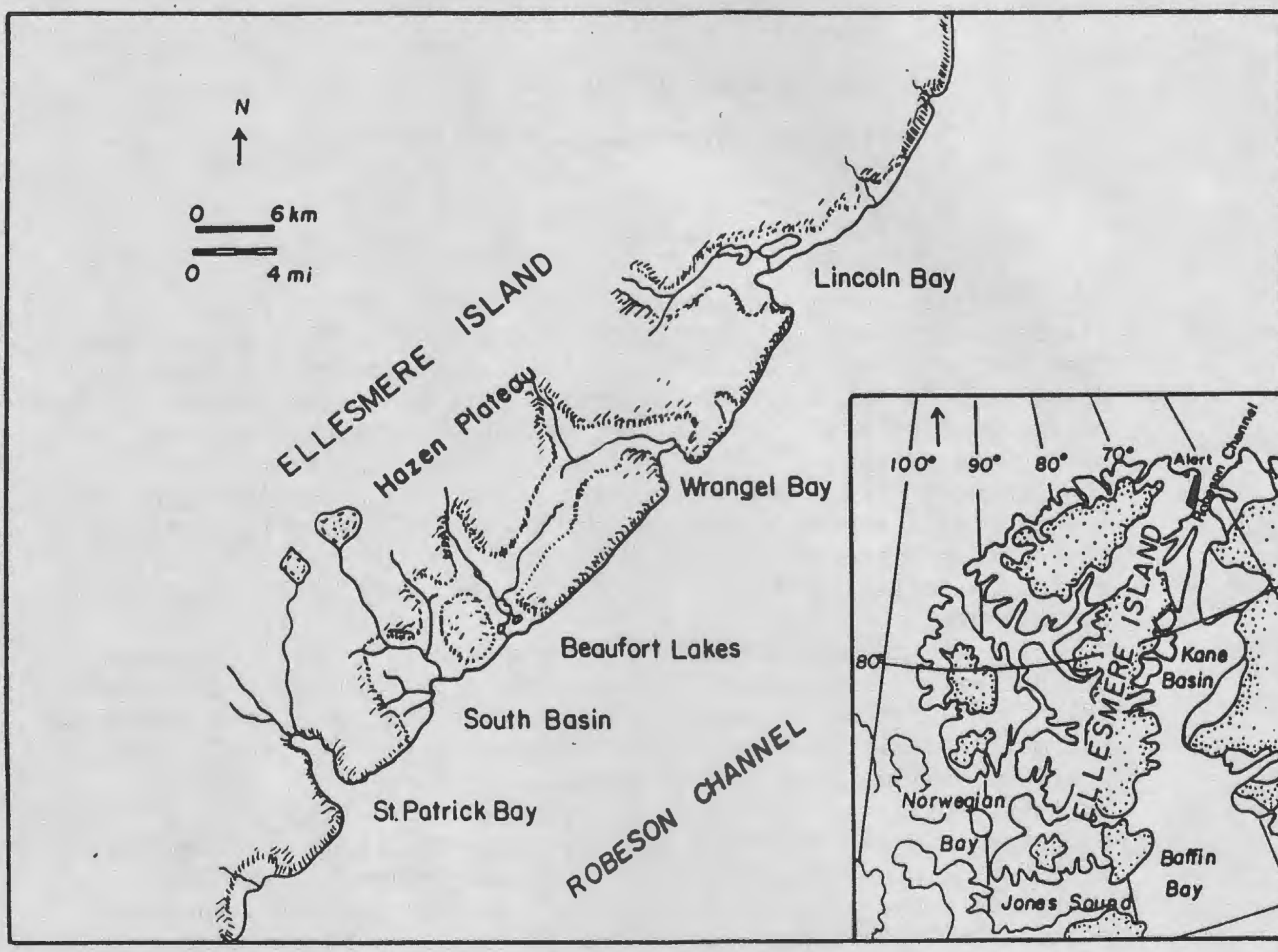

1. Location map of the field area on northeastern Ellesmere Island.

the proximity of this coastal zone to northwest Greenland, it is an ideal location for a study of the interaction between the northwest Greenland Ice Sheet and various ice masses originating on northeastern Ellesmere Island. In particular, the field site is in a critical location for evaluating proposed models of the timing and extent of glacial ice masses during the last glacial maximum. An extensive ice sheet covering the Arctic Ocean and the High Arctic islands has been proposed by Hughes, Denton, and Grossvald (1977). A dome of this ice sheet termed the Innuitian Ice Sheet (Blake, 1970) is thought to have covered the Queen Elizabeth Islands and merged with northwest Greenland ice over Nares Strait. In contrast, another model proposes far less extensive ice cover during the last glacial maximum. Over the Canadian High Arctic, this latter model proposes a non-contiguous ice cover termed the Franklin Ice Complex (England, 1976b) where ice cover is restricted to highland and plateau centers with extensive intervening ice-free areas. According to the "limited ice" model, Greenland and Ellesmere ice masses were approximately 100 km apart at the height of the last glacial. Previous glaciations were, however, more extensive. Northwest Greenland ice advanced across Robeson Channel onto the Hazen Plateau of northeastern Ellesmere Island sometime prior to 80,000 B.P.(England and Bradley, 1978). Ice from the interior ranges of northern Ellesmere Island advanced eastward to Robeson Channel and crosscut, at lower elevations, the deposits of the previous maximum Greenland advance. Glaciers terminated in fiords and formed ice-shelf moraines at 175 m asl (England et al.,1978). This advance has been radiocarbon dated at >28,000 to >30,000 B.P.; amino acid ratios suggest a $\geq$ 35,000 B.P. age for this advance (England et al., 1981). The last advance of Ellesmere Island ice was prior to 8000 B.P. and was more limited than the previous two periods of glaciation. Older deposits along the co astal zone were not overridden by this advance, as an ice-free corridor existed between the northwest Greenland Ice Sheet and interior Ellesmere Island ice. Holocene marine limit shorelines were cut into the till and bedrock at elevations of 90 to 120 m. Deepwater fossiliferous silts were deposited on the unglaciated forelands at the glacial maximum between ca. 12,000 and 8000 B.P.

Present Study

Field work was conducted along Robeson Channel in four major valleys and basins, from Lincoln Bay in the north to a large open basin, informally referred to as South Basin, located 5 km north of St. Patrick Bay, at the southern limit of the field area (Fig. 1). The four valleys, South Basin, Beaufort Lakes, Wrangel Bay, and Lincoln Bay, are incised into the eastern margin of the Hazen Plateau which is predominantly underlain by the lower Paleozoic brown to gray-brown-weathering sandstone and flysch sequence of the Imina Formation (Trettin, 1971). Locally, the Imina Formation is unconformably overlain by poorly consolidated Tertiary sandstones and siltstones correlative with the Eureka Sound Formation (Miall, 1982), which in several areas contains coal deposits. The Hazen Plateau is flat to gently rolling along its broad plateau summits; but structurally controlled northeast trending valleys and those perpendicular to this trend incised the eastern edge of the plateau to depths up to 600 m. The plateau presently supports several small ice caps, and in the past has supported more expanded plateau ice masses. Two relatively flat, thin ice caps northwest of St. Patrick Bay are found at elevations above 800 m. Morainic deposits and meltwater channels indicate previously greater extent for these ice masses. The Hazen Plateau terminates to the west against the Grant Land mountains, which exceed 2000 m in elevation and serve as a present-day accumulation area for coalescing mountain valley glaciers.

The plateau surface is mantled by rubbly tills (from various sources),landforms of ice-contact origin, and materials derived from permafrost action. In the valleys, waterlain deposits of glaciofluvial, glaciolacustrine, and glaciomarine origin are found.

In the following sections of this report, field evidence for several episodes of glaciation and related marine transgressions in the Robeson Channel area will be presented. The radiocarbon and amino acid chronology of these deposits supports correlations with similar glacial-marine sequences in the high latitude regions.

Glacial Geology And Quaternary Marine Stratigraphy

The chronology of glacial advances and related marine transgressions in the Robeson Channel area was determined as follows:

1) Maximum advance of the northwest Greenland Ice Sheet onto Ellesmere Island, covering the coastal plateau summits and extending inland at least 20 km. No evidence of any subsequent advance by Greenland ice was found in the area.

2) During retreat of this ice mass, ice-dammed proglacial lakes were formed on the upland plateau and also in the recently deglaciated valley between Wrangel Bay and Beaufort Lakes. In the Wrangel Bay area, the retreating valley ice lobe was in contact with the sea. Fossiliferous marine deposits extended from above the Holocene marine limit to a prominent shoreline at 286 m.

3) During the last glacial maximum, ice stood on the Hazen Plateau approximately 30 km to the northwest (England, 1983). A small plateau ice cap, however, expanded into Lincoln Bay approximately 7 km inland from the coast. At the glacial maximum, the sea

transgressed to an elevation of 116 m in South Basin, Beaufort Lakes and Wrangel Bay. In outer Lincoln Bay, sea level reached at least 100 m (minimum estimate); inner Lincoln Bay was occupied by ice during this transgression. When ice receded, marine waters extended into inner Lincoln Bay.

Evidence for each stage of this chronology is detailed in the ensuing sections.

Stage 1, Maximum Advance of Northwest Greenland Ice Sheet.

Distinctive red granite, red granite gneiss, and other crystalline erratics were mapped in the coastal zone and found to be widely distributed on coastal summits and in the interior plateau (Fig. 2). Christie (1967) mapped granite and gneiss erratics on Judge Daly Promontory and in several locations on the eastern Hazen Plateau. Christie points out that outcrops similar to these lithologies have been mapped in the Thule area and on Inglefiled Land further south in West Greenland, though for these areas to serve as a source for the erratics would imply that a trunk glacier flowed northward along Kennedy Channel at some time. As these erratics are also found in moraines bordering Polaris Promontory, it has been suggested that they may have been derived from beneath the present ice cover of the Greenland Ice Sheet (Davies, 1963). At the present time the exact source of these

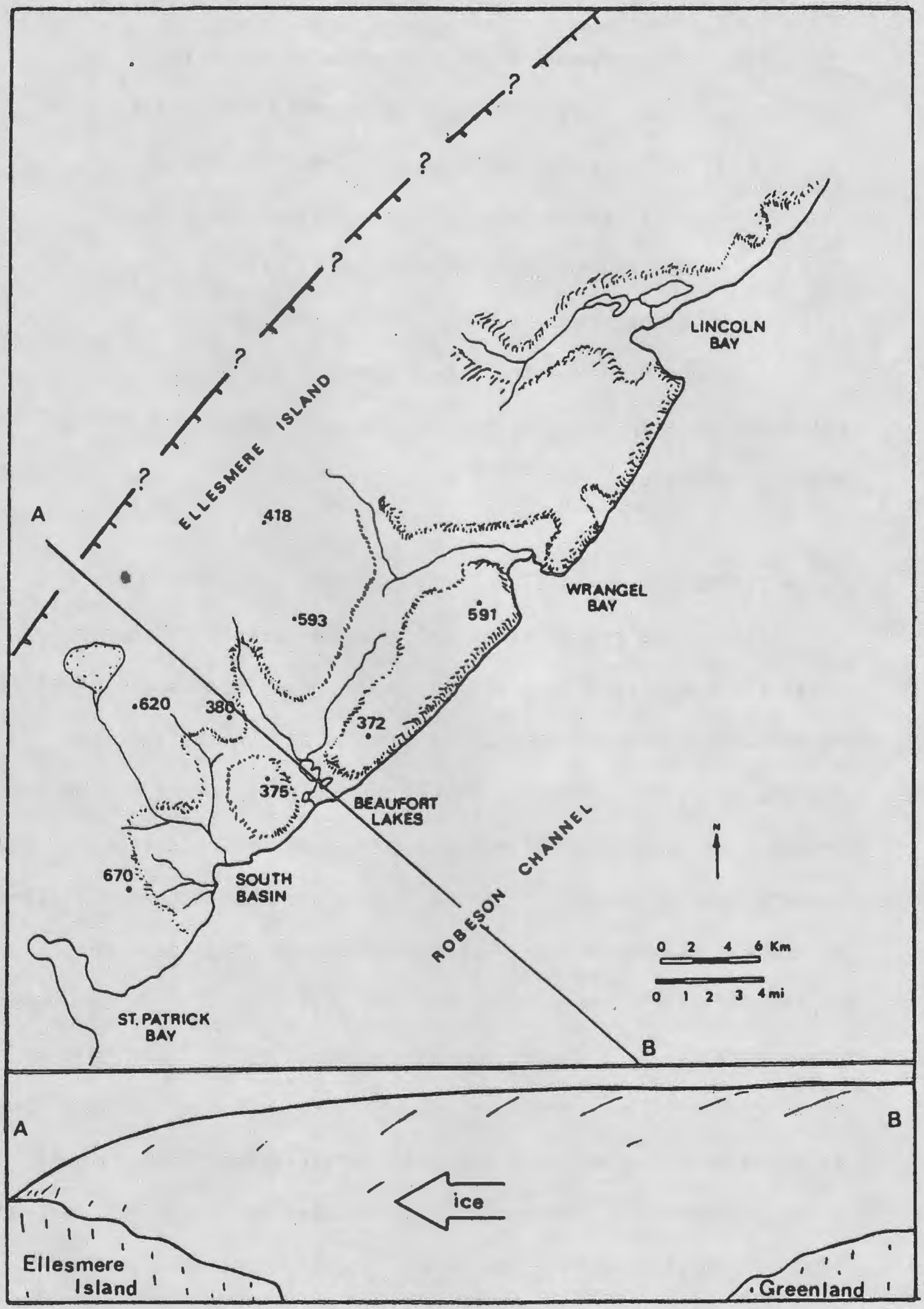

2. Distribution of crystalline erratics of Greenland provenance on northeastern Ellesmere Island. Elevations of erratics in meters asl.

erratics is not known; however, in this paper, the red granite and granite gneiss lithologies will be referred to as "Greenland erratics". Figure 2 shows the distribution of these distinctive erratics that overlie the Imina Formation. On a peak south of South Basin, erratics were found at elevations up to 670 m and up to almost 600 m at a location south of Wrangel Bay. Erratics were also found at locations up to 15 km inland from the coast. While traverses conducted during this study were not done beyond 10 to 15 km of the coast, Christie (1967) believes that the hypothesis of Taylor (1956), that Greenland ice advanced over the entire Hazen Plateau, is not justified. Rather, the advance of Greenland ice onto Ellesmere Island and possible confluence with interior and plateau ice, was probably limited to the eastern fringe of the plateau.

Stage 2: Recession of Greenland Ice.

The earliest recession of Greenland ice from Ellesmere Island is seen in high-level kames and meltwater channels located on the upland plateau surface. Both features contain abundant red crystalline erratics. The ice-contact features, kames and kame terraces, are found at elevations up to 415 m on the upland slopes to the west of South Basin. When Greenland ice retreated towards Robeson Channel, it was probably confluent with a plateau ice cap or ice from the interior mountains. As the two ice masses separated, an ice-dammed proglacial lake was formed between them.

A large delta (Figs. 3 and 4), consisting of several levels of delta plains, was fed by a meltwater stream issuing from an Ellesmere ice source. Lithologies of Hazen Plateau rock types were found in abundance on the topset plains of the deltas. The elevations of the frontal edge of these deltas ranged from 393 to 397 m. The delta was constructed into a small lake, held in by ice to the east. The ice frontal position to the east is shown by a kame-moraine topography that trends parallel to the delta front (m on Fig. 3). Fine laminated sands and silts at the toe of the delta lacked fossiliferous material.

As Greenland ice continued to downwaste, ice flow became confined to the major valleys. Lobate ice margins of this stage are defined by lateral and end moraines and kame terraces in the valley of Wrangel Bay and in the Beaufort Lakes basin (Fig. 5). All features contain abundant Greenland-type erratics.

When the terminus of this lobe was in upper Wrangel Bay valley, it was probably in contact with the sea. Segments of an end-moraine loop (m in Fig. 5) lie adjacent to a marginal meltwater channel that grades to the east. Adjacent to this terminal position is a broad shoreline at 286 m (Fig. 6) which extends along the south shore of Wrangel Bay for over a kilometer. This beach feature consists of cobble gravels, including many of Greenland provenance, and is over 100 m wide. Discontinuous outcrops of glaciomarine silts with dropstones are found from above the marine limit at 116 m almost up to the 286 m beach. These outcrops above

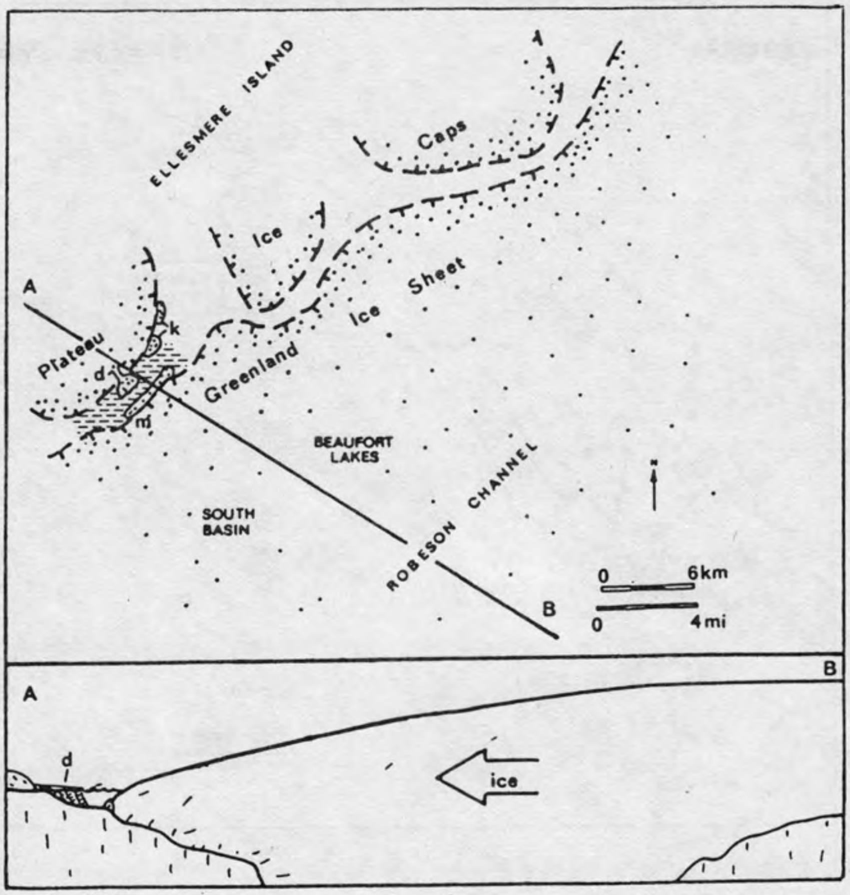

3. Initial recession of Greenland ice from Ellesmere Island.

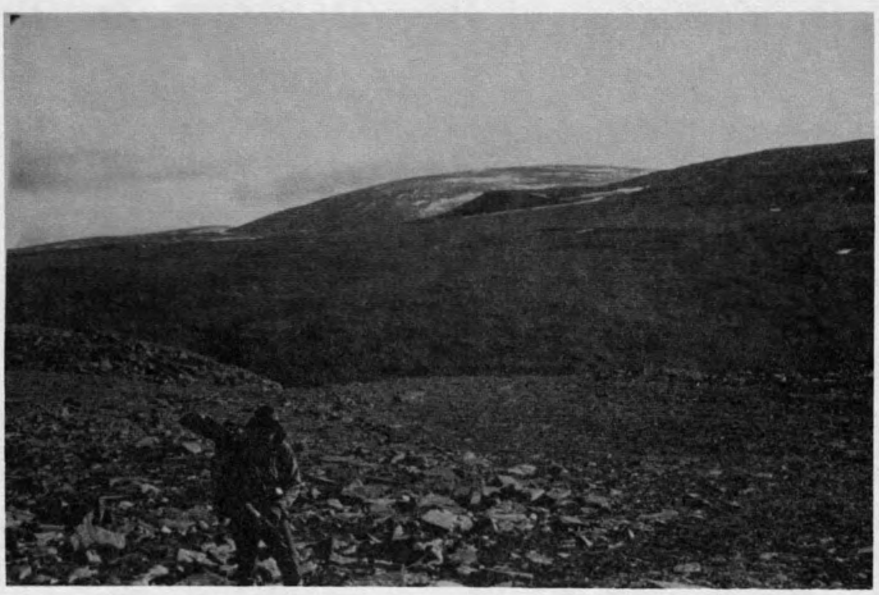

4. Photograph of ice-contact delta at 400 m asl on the Hazen Plateau. View is towards the south.

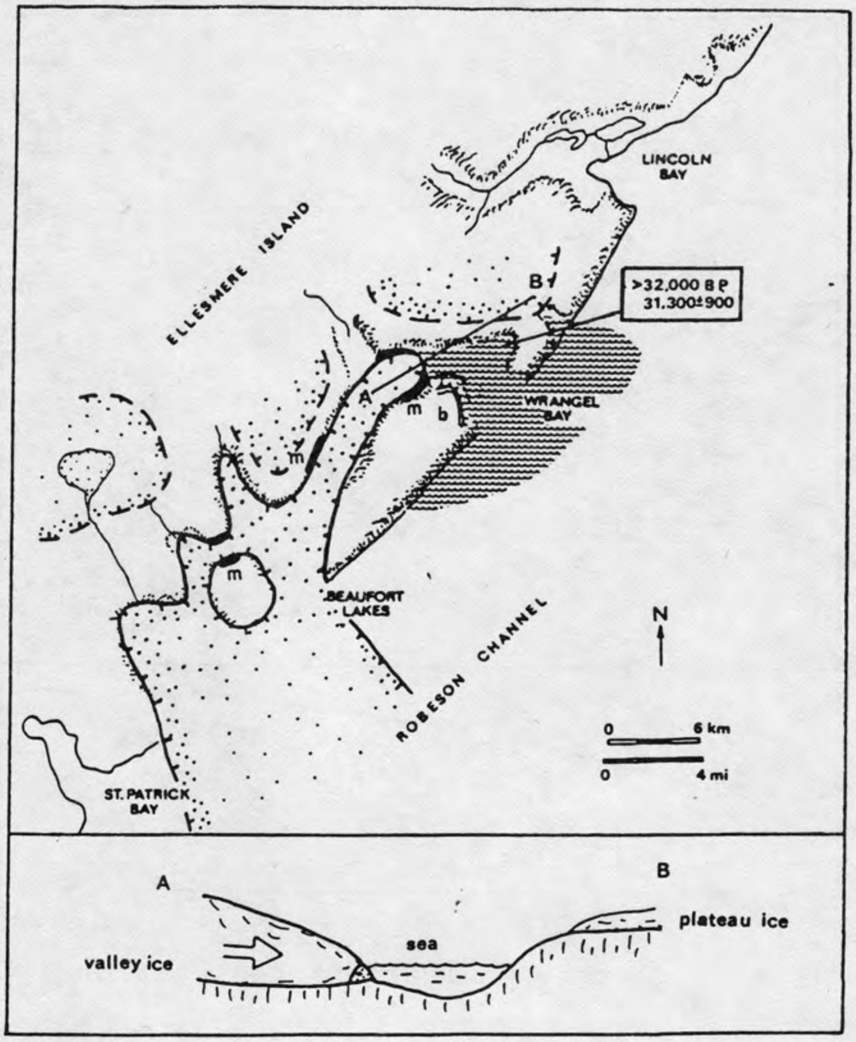

5. Lobate recession of Greenland ice from Ellesmere Island. b=beach at 286 m, m=moraine. Wavy pattern = marine incursion.

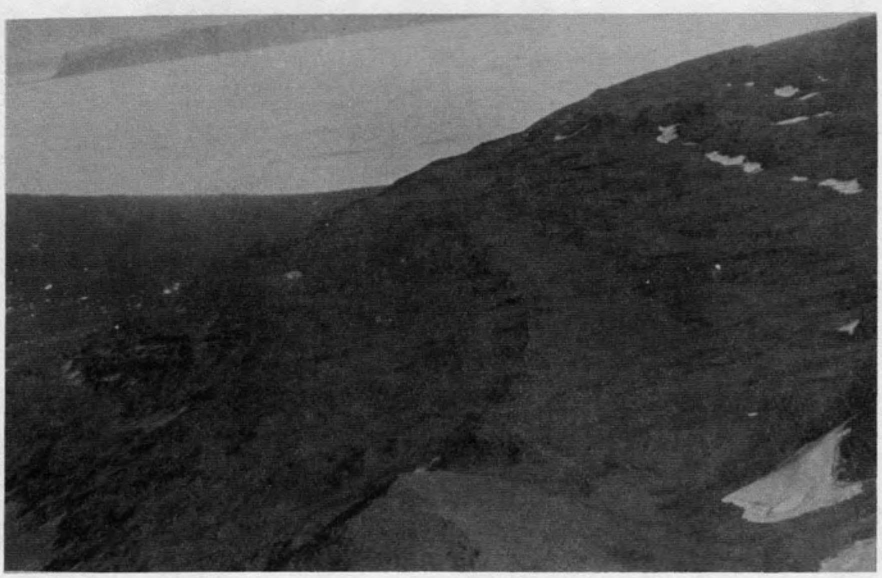

6. Photograph of beach at 286 m asl. View is towards the east with Robeson Channel and Greenland in the background.

the Holocene silts comprise discontinuous buttresses and patches of glaciomarine sediments associated with this older event. The outcrops have a reddish-orange to brownish-orange surficial weathering which differs from the gray to whitish-gray chalky surficial coloration typical of the Holocene silts that fill the valley floors and extend up to the Holocene marine limit. Two samples of mollusc shells were collected from these outcrops for radiocarbon dating; one sample, composed almost entirely of Portlandia arctica shell fragments, gave a date of 31,300 ± 900 (SI-5549). The other sample of Hiatella arctica fragments, from an adjacent outcrop at 125 to 140 m, was dated at >32,000 B.P. (SI-2112, England, pers. comm.,1984). Both of these dates are considered minimum estimates for the age of the deposit.

The microfaunal content of this unit included a well-preserved and unabraded assemblage dominated by the high arctic inner shelf foraminifera Islandiella helenae ,and is most likely of Quaternary, and possibly Wisconsinan in age (Rolf Feyling-Hansen, pers. comm., 1983).

Sequential retreat of lobate valley ice from the end moraine in upper Wrangel Bay valley is depicted in Figure 7. At the intersection of Wrangel Bay valley and the northeast-trending valley to Beaufort Lakes and behind several small moraines (m-1,m-2) a deltaic complex (d-1 on Fig. 7) at 250 m elevation, represents a stillstand of the Greenland lobe. The glaciomarine ice-contact delta was built into the regressing sea, which had

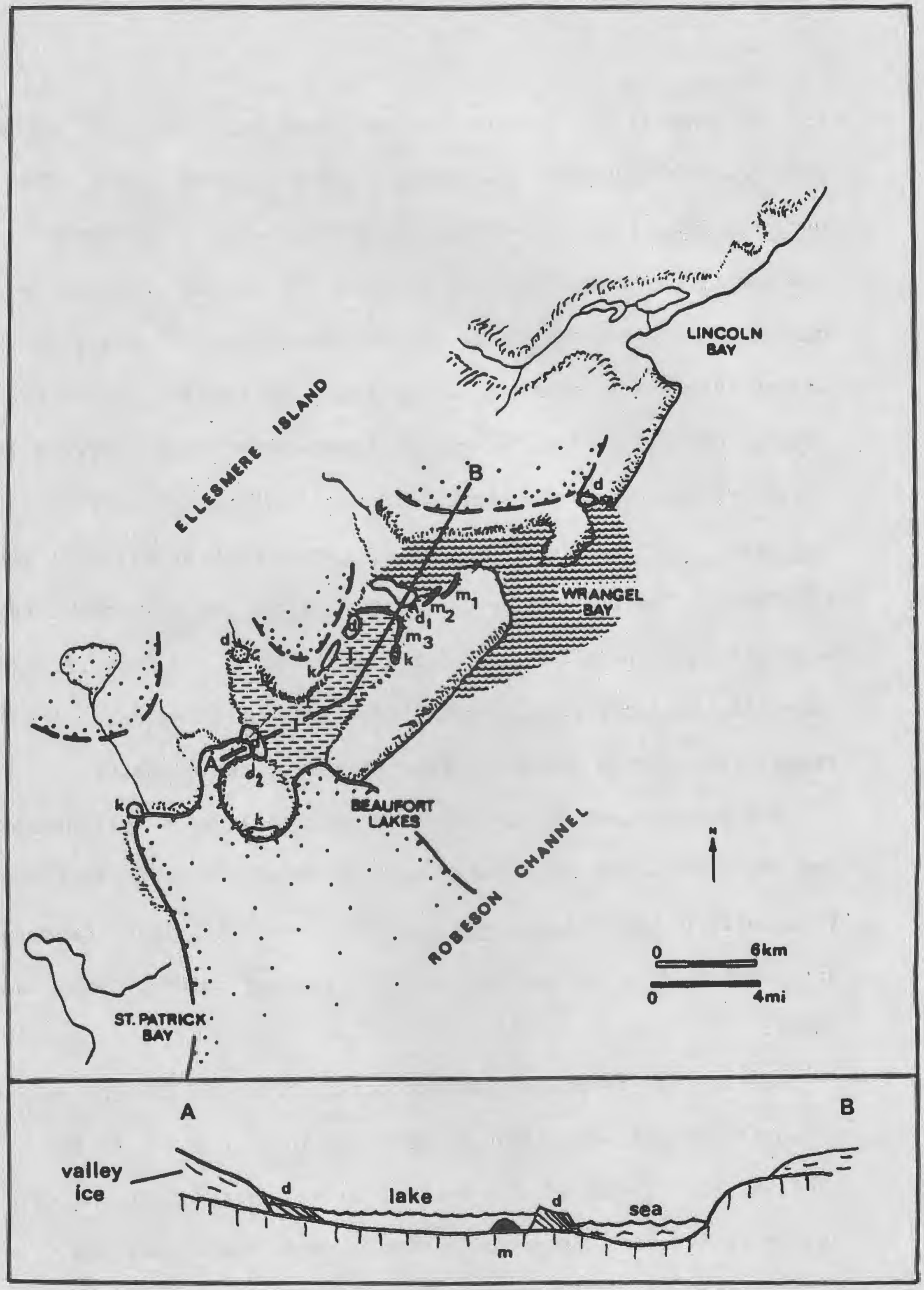

7. Continued recession of lobate Greenland ice and the formation of a proglacial lake in the Wrangel Bay-Beaufort Lakes basin. m-1 through m-3 are moraines formed during sequential retreat of the valley lobe toward Beaufort Lakes. d=delta, l=lake, k=kame.

dropped from the marine limit of 286 m. Another ice-contact delta north of Wrangel Bay was deposited into a coastal cirque basin facing Robeson Channel by meltwaters from a plateau ice cap to the northwest.

By the time that ice retreated from the delta at the head of Wrangel Bay valley (withdrawing towards Beaufort Lakes; Fig. 7) sea level had probably dropped below the level of the delta complex and retreating ice was no longer in contact with the sea. However, a glacial lake was formed in the valley on the proximal side of the delta, topographically ponded by the valley side to the north and to the south by rereating Greenland ice. An end moraine complex in the center of this valley (m-3, Fig. 7) consists of sheared and folded blocks of fine to medium-grained rhythmically bedded glaciolacustrine sands and silts, indicating a fluctuation of the Greenland ice lobe in the lake. This marginal position is also delineated by a prominent trimline on the east-southeast valley wall and a large kame-terrace deposit on the northwest wall (k on Fig. 7). The kame terrace was built by meltwater and sediment from both Greenland ice and plateau ice. A meltwater channel originating on the plateau to the west of the valley grades to the surface of the terrace. Hence, erratics of both Ellesmere provenance and Greenland provenance are found on the terrace surface. When the proglacial lake reached its maximum extent, it was 12 km in length, and extended 5 km inland towards the plateau (Fig. 8). Deltas were deposited into this water body at three

8. Glaciolacustrine delta complex in upper Beaufort Lakes basin. Upper levels are ice contact, lower level was fed by outwash flowing through the valley in background.

University of Massachusetts, Dept. of Geology & Geography, Contribution #49

ERRATA: Pages 25/26 and 27/28 have been transposed.

i.e. p. 27 should have been p. 25
p. 28 should have been p. 26
and *vice versa*.

Following this period of weathering, ice advanced to its maximum last-glacial position (Fig. 9). Greenland ice advanced from Petermann Fiord into Hall Basin and from Newman Bay into Robeson Channel (England, 1983). These lobes did not coalesce, nor overlap on Polaris Promontory (N.W. Greenland). This area remained unglaciated, and not until ice retreated from the Petermann Fiord moraine, did Holocene marine waters occupy the interior (England, 1983b). On the Ellesmere Island side of Robeson Channel, ice advanced from the interior ice caps, coalescing as piedmont glaciers on the plateau and flowing eastward toward Robeson Channel. Ice advanced to its maximum at the heads of Archer and Chandler Fiords, south of Lake Hazen (England, 1976, 1983a). Fifteen km northeast of Chandler Fiord, the ice probably stood at the Craig Lake Moraine, a prominent feature that loops around the south sides of Craig Lake and Kilbourne Lake (Fig. 9). It is not known exactly where the ice margin was on the plateau northeast of Craig Lake, however there is no evidence that ice from the interior of Ellesmere Island advanced within 10 km of the coastal zone between South Basin and Lincoln Bay. Small plateau ice caps (much like those located on the Hazen Plateau today near St. Patrick Bay and near the head of Archer Fiord) were present and probably in places were in contact with marine waters.

Thus, the margins of the Greenland and Ellesmere Island ice masses were separated by an ice-free zone during the last glacial maximum. Ice from Petermann Fiord in Hall Basin was separated from locations; the largest of these located at the junction of the upper Beaufort Lakes basin and the valley to the south (Fig. 13). Ice-channel fillings and kames behind the ice-proximal slope of the delta demonstrate the ice-contact nature of the deposit. The combinaton of ice thinning and retreat and isostatic rebound caused a lowering of the lake level. The largest delta plain, at 220 m, was deposited in the lower level . The ice margin during this stage was located at the topographic divide between Beaufort Lakes basin and South Basin, as this delta level was fed by a valley train deposit graded to this level.

The valley floor below the deltas and to the northeast is filled with laminated fine sand and silt. To determine if this basin was open to the sea, and hence was a marine equivalent to the Wrangel Bay marine sediments, samples of the silts were analyzed by Dr. Rolf Feyling-Hanssen of the University of Aarhus, Denmark, for the microfossil content. No foraminifera were found; plant debris and Cyclopyxis , a Thecamoebian genus characteristic of freshwaters, were present, indicating a lacustrine origin for the sediments. Although the uppermost level of this lake is lower than the marine limit associated with this advance in Wrangel Bay (286 m) it is evident that sea level had fallen below 250 m by the time ice retreated from upper Wrangel Bay valley. However, since the microfossil content was analyzed only from surface sediments, it is possible that older sediments at depth in the valley are of a marine origin and related to a sea level higher than the freshwater lake levels.

The silts at the toe of the delta and comprising the valley floor to the west of the delta contain abundant red granite, granite gneiss and other crystalline lithologies, presumably ice-rafted into place. Along the eastern margin of the lake, a cobble-gravel beach ridge at 213 m contained organic material interstratified with the coarse gravelly sand. Two black organic-rich horizons were excavated in a 1-m pit in the beach ridge. A sample of the organic material dated >33,000 B.P. (S-2182). Since this sample was dated, however, a sample of the organic material was analyzed for its pollen content and contained a temperate hardwood assemblage, including such taxa as *Juglans* and *Castanea* . This suggests that the organic material has most likely been redeposited from outcrops of Tertiary coal-bearing sediments located on the Hazen Plateau to the northwest. Hence, due to this contamination, the date from the beach sediments is considered unreliable.

As Greenland ice continued to retreat from northeastern Ellesmere Island toward Petermann Fiord on the Greenland coast, it melted down behind the topographic divide between Beaufort Lakes and South Basin and the lake no longer received its major sediment input. Several kames on the east slope of Mt. Beaufort and in the highlands above South Basin (191 m) document the retreat. With this withdrawal, the lake probably drained through the Beaufort Lakes basin.

Stage 3: Ice Extent During the Last Glacial Maximum

A substantial period of weathering, perhaps as long as 50,000 years, occurred between the retreat of Greenland ice from Ellesmere Island and the next major glacial advance (England and Bradley, 1978). The coastal highland areas were deglaciated first and projected above the valley ice lobes as nunataks, even before Greenland ice recession. These uplands (predominantly till-mantled bedrock) show signs of advanced weathering not encountered in recently deglaciated areas. Resistant tors, up to 3 m high, project above the topography. The tors are frost-riven and contribute debris to the surrounding felsenmeer surface. Tors on Mt. Beaufort, 2 km southwest of Beaufort Lakes, were found at elevations up to 260 m. Greenland erratics, exfoliated and reduced to gruss, were found among the felsenmeer at several localities. Clasts of the Imina Formation were also found to be comminuted to small tabular fragments and covered with a golden-brown desert vanish.

On surfaces of glaciofluvial landforms located above the Holocene marine limit (i.e., depositional features associated with the deglaciation of Greenland ice) advanced weathering is also apparent. Clasts of the Imina Formation were comminuted into small fragments (approximately 2 cm) and coated with desert varnish. Granitic clasts were spheroidally weathered, pitted, and etched, and in some cases reduced to gruss.

ice at the Craig Lake Moraine by almost 100 km. The isostatic loading of the two ice masses produced differential crustal warping, dominated by the larger Greenland ice load (England, 1976, 1983). Walcott (1970) has demonstrated that due to lithospheric rigidity, peripheral depression beyond an ice mass can extend up to 180 km from the ice margin. The "full glacial sea" (England, 1983) transgressed in this ice-marginal depression along the isostatically depressed coasts of Ellesmere Island and Greenland. Isostatic dominance of the Greenland ice is seen in Figure 9, which shows the elevations of marine limits in the Lady Franklin Bay-Robeson Channel area and along Polaris Promontory. These once-synchronous shorelines increase in elevation from 111 m at Discovery Harbour to 116 m along the outer coast from South Basin to Wrangel Bay, to 120 m on Cape Baird at the northern tip of Judge Daly Promontory. Marine limit elevations increase from 130 m on outer Polaris Promontory, to 140-150 m in the interior of Polaris Promontory (data from England, 1983a and this study).

Figure 10 depicts the maximum transgression of the sea along Robeson Channel during the last glacial maximum. Marine limit shorelines in the marginal depression were constructed and marine sediments deposited on the "old" till and bedrock topography except where the sea was in contact with local ice in Lincoln Bay. The "full glacial sea" (England, 1983) transgressed to 116 m in South Basin. No datable materials were recovered, however, from the highest shoreline feature, a raised marine delta.

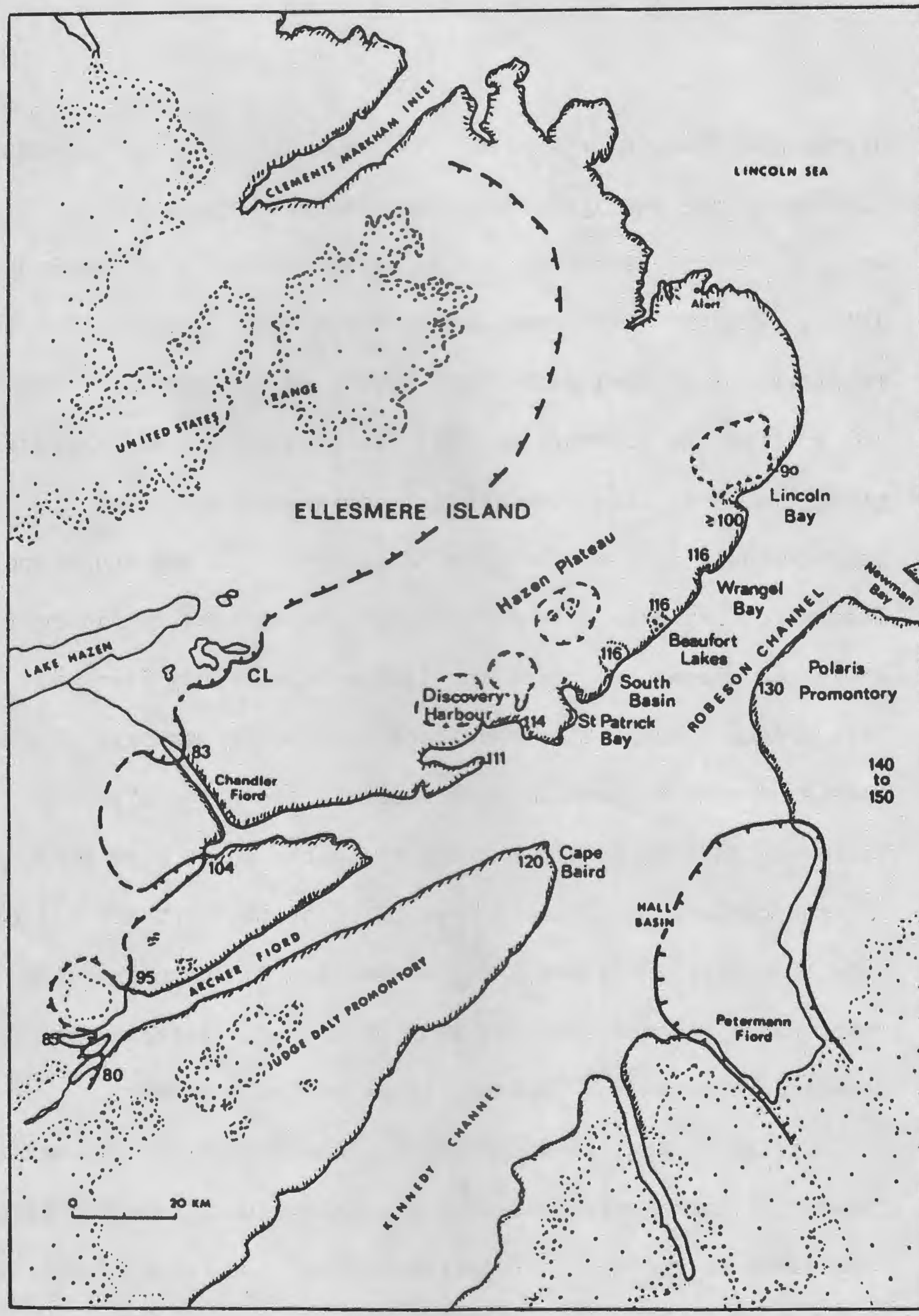

9. Ice extent and marine limit elevations during the last glacial maximum.

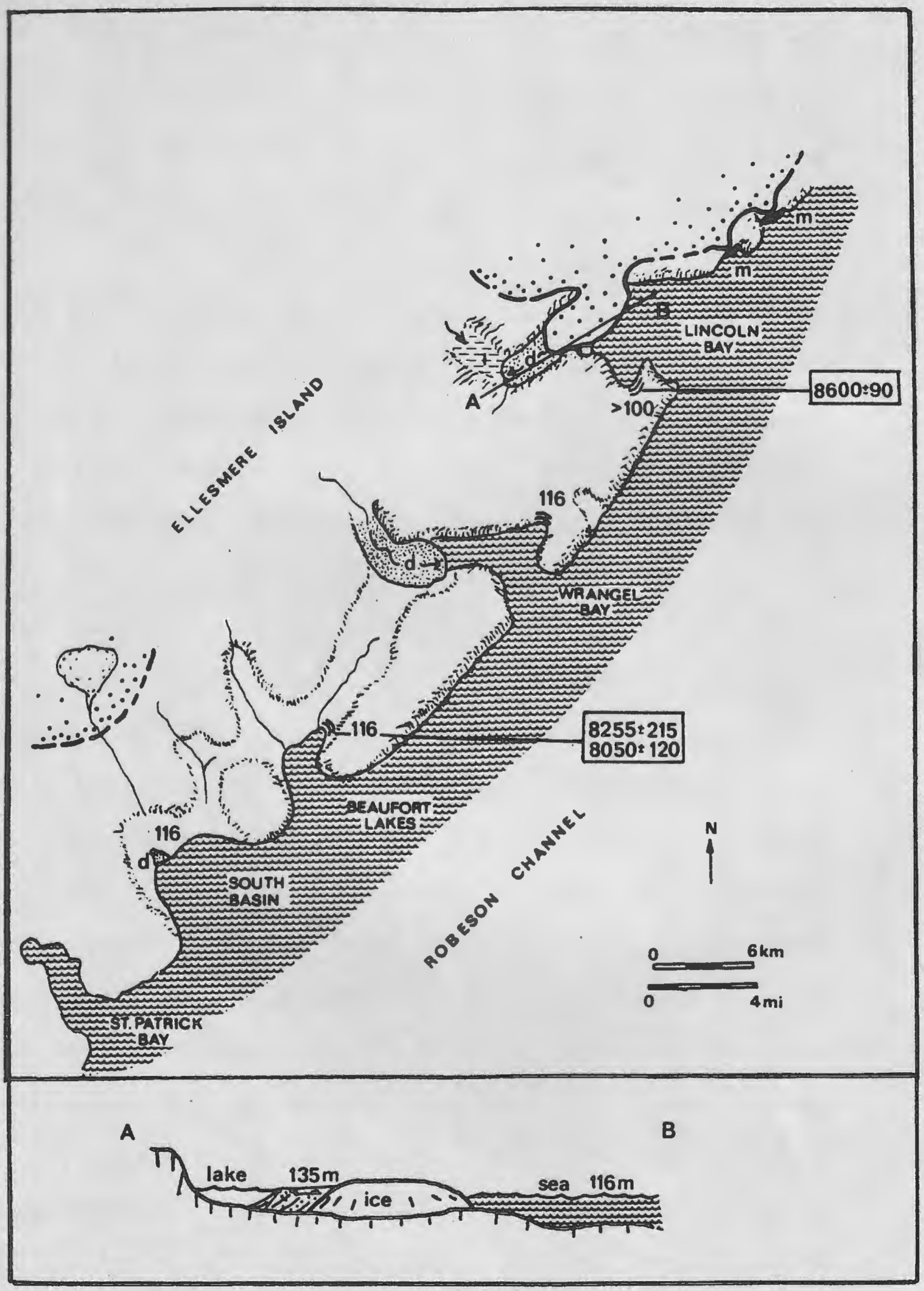

10. Marine limit elevations and plateau ice cap margins in the field area during the last glacial maimum.

Two samples of in situ shells from silts at 90 to 95 m grade upward to beach gravels at 116 m in the valley above Beaufort Lakes. Two similar collections dated 8050 ± 120 (SI-3041) and 8255 ± 215 (S-1990) (England, 1983).

No organic material or shell samples were found in stratigraphically equivalent deposits in Wrangel Bay. It is possible that landfast sea ice occupied this major fiord valley and prevented occupation by fauna until a later period. In Lincoln Bay, stratigraphic and morphologic evidence suggest that during the last glacial advance a plateau ice cap, such as previously described for Wrangel Bay, expanded and spilled over into inner Lincoln Bay and into coastal basins open to Robeson Channel. The latter locality has been described by Prest (1952) who described the moraines consructed in this basin. Distinct gravel terraces are incised into the moraines that are overlain by fossiliferous silts. The lobe of the plateau ice cap that spilled over into inner Lincoln Bay valley dammed drainage from the interior of the Hazen Plateau forming a proglacial lake (Fig.10). A complex of kame deltas which delineate he former ice front prograded inland to a lake surface of approximately 135 m elevation. Terraces also grade to this lake from the interior plateau to the northwest. The plateau ice did not extend to outer (southern) Lincoln Bay along Robeson Channel, and the sea transgressed to the marine limit as in the other basins to the south. Shells of *Bathyarca glacialis* and *Hiatella arctica* were collected in growth position in silts below a diffuse 100 m washing limit and dated 8600 $\pm$ 90 (SI-5551). This marine limit elevation is probably a minimum estimate as the topography at the marine limit is steep along the valley wall and there may be no evidence of the true marine limit.

Figure 11 illustrates the position of the sea subsequent to initial emergence from the marginal depression sea and the retreat of the Lincoln Bay ice cap. As the plateau ice lobe retreated from inner Lincoln Bay, the sea transgressed upon the deglaciated terrain and marine silts were deposited on the proximal, or ice-contact slopes of the deltas. The highest shoreline in this zone was at 90 m. A small collection of Portlandia arctica were collected in growth position in silts overlying the kame gravels and are dated at 7265 $\pm$ 215 B.P. (SI-5552). Upon deglaciation of the coastal basin to the north of Lincoln Bay, the sea overlapped the moraine at 84 m. A sample of Hiatella arctica found in situ in an erosional cut (78 m) below the moraine crest on the ice-proximal side of the moraine dated 7345 $\pm$ 75 B.P. (SI-5550).

In South Basin, shoreline features slightly below the marine limit record the initial emergence from the sea (Fig. 11). A gravel beach at 111 m contained abundant whole valves of Hiatella arctica that dated 7390 $\pm$ 90 B.P. (SI-5554). A collection of in situ Mya truncata and Hiatella arctica obtained from silts at 65 m that grade upward to a gravelly shoreline at 110 m and was dated at 7490 $\pm$ 70 B.P. (SI-5553).

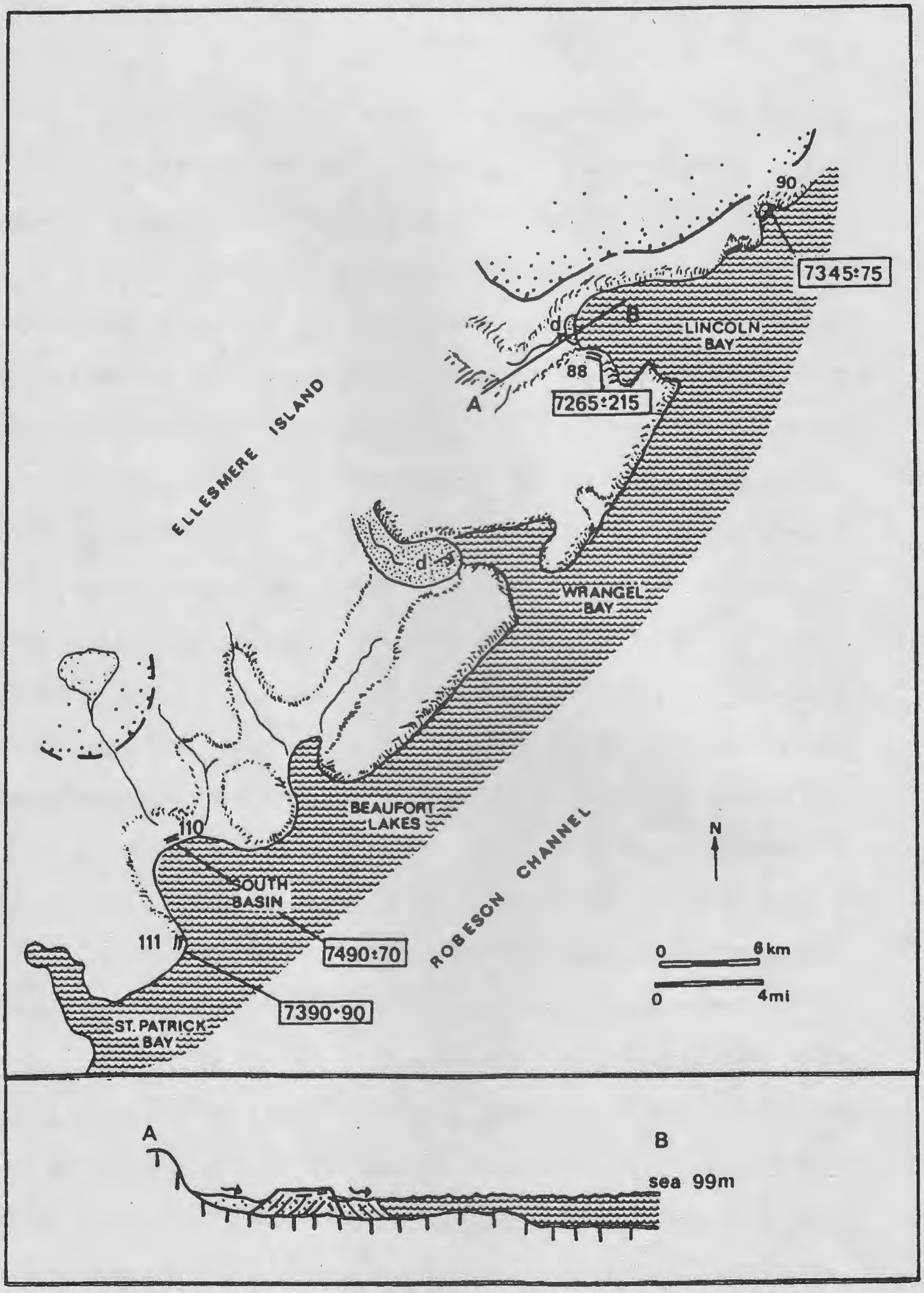

11. Initial recession of the ice marginal sea and retreat of plateau ice from inner Lincoln Bay.

Marine Chronology

Two glaciomarine units in the field area represent sedimentation associated with advances of Greenland and Ellesmere Island ice in the Robeson Channel area. Most of the area below below 110 m asl is mantled by Holocene marine silts deposited in a peripherally depressed sea between the Greenland and Ellesmere Island ice masses. In the Robeson Channel area on Ellesmere Island, the marine limit during this event was 116 m. Numerous radiocarbon dates, in the range of 7200 to 8200 B.P. have been obtained on shell collections from beaches and silts below the Holocene marine limit (Table 1). An older glaciomaine unit, at present mapped only in the Wrangel Bay area, is dated 31,000 ± 900 and >32,000 B.P. These sediments, exposed up to a maximum elevation of 286 m asl were deposited in an ice-marginal sea, isostatically depressed by a substantially larger ice load than during the last glacial advance. As the dates on the older marine unit should both be considered minimum age estimates, absolute age determinations and the correlation of this unit with other arctic glaciomarine units remains difficult. Correlations were attempted by aminostratigraphic techniques.

Comparsions of amino acid ratios from mollusc shells in sediments from a limited geographic area have proven to be effective for correlating fossiliferous sedimentary units, especially where radiometric control is lacking, or at the limits of the dating technique, or where stratigraphic units are not

1. Radiocarbon dates from raised marine deposits and proglacial lake sediments from the Robeson Channel area.

Site	Laboratory No.	Material	Age B.P.	Stratigraphy	Related Relative Sea Level
Wrangel Bay*		shells	>32,000	marine silts 140 m	116 to 286 m
Wrangel Bay	SI-5549	shells	31,300 ± 900	marine silts 90 m	116 to 286 m
Lincoln Bay	SI-5551	shells	8600 ± 90	marine silts 91 m	100 m
Lincoln Bay	SI-5552	shells	7265 ± 215	marine silts 82 m	88 m
Lincoln Bay	SI-5550	shells	7345 ± 75	marine silts 78 m	90 m
Beaufort Lakes++	S-1990	shells	8255 ± 215	marine silts 90 m	116 m
Beaufort Lakes++	GSC-3041	shells	8050 ± 120	marine silts 90 m	116 m
South Basin	SI-5553	shells	7390 ± 90	beach gravels 111 m	111 m
South Basin	SI-5554	shells	7490 ± 70	marine silts 65 m	110 m
Beaufort Lakes**	S-2182	organic material	>33,000	lacustrine beach gravel 213 m	-

* Unpublished date, J. England, pers. comm., 1982.

++ Previously reported in England, 1983.

** The validity of the date is questioned due to the presence of redeposited pollen in the sample, including arboreal species of temperate affinity.

Laboratory Identifications: SI- Smithsonian Institute, S- University of Saskatchewan, GSC- Geological Survey of Canada.

laterally contiguous (Andrews and Miller, 1976; Miller et al., 1977). Because the rate of racemization of amino acids in a shell is temperature dependent, it is very difficult to determine an absoulte age with this technique without having an independent temperature estimate of the deposit. It has been demonstrated however, that correlations of glaciogenic and marine units of similar relative age can be carried out for over a 1500 km distance (Miller et al., 1977).

Ratios of allo-isoleucine (aIle) to isoleucine (Ile) in mollusc shells collected during this study were determined at the University of Massachusetts Amino Acid Geochronology Lab. The method of sample preparation follows that described by Miller et al. (1982), so that fractionation effects in the total acid hydrolysate fraction are eliminated.

Results of the analyses from the northeastern Ellesmere Island samples are shown in Figures 12 and 13 and Table 2. Species analyzed from the collections include mostly Hiatella arctica ,although several samples of Astarte borealis were analyzed from core samples. No inter-species differences were detected in the Holocene age shells (Table 2). The mean aIle/Ile total hydrolysate ratio in Holocene shells from the field area is 0.037 $\pm$ .04. The free fraction in the Holocene unit shells was not detectable (N.D.). In contrast, the older unit has significantly higher ratios (0.207 $\pm$ .022 - 0.062 $\pm$ .012; free-total). These two groupings of ratios are termed aminozones (Nelson, 1981).

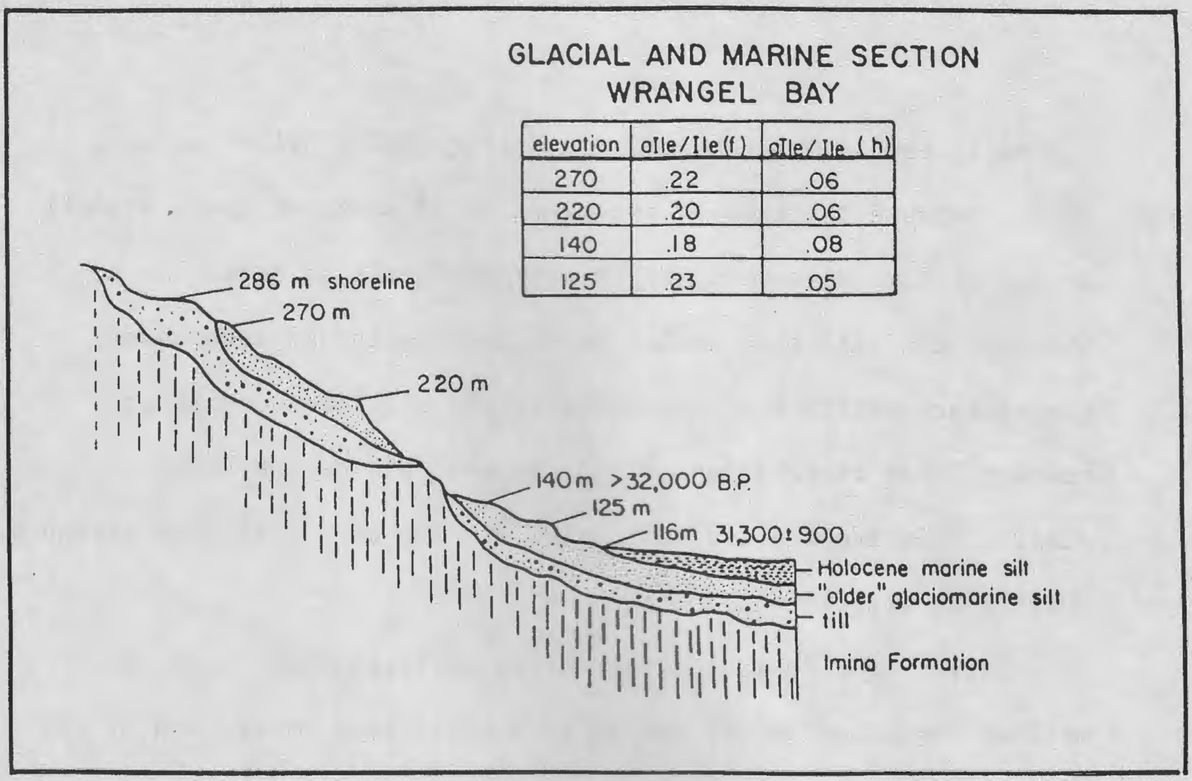

elevation	aIle/Ile (f)	aIle/Ile (h)
270	.22	.06
220	.20	.06
140	.18	.08
125	.23	.05

12. Glacial and marine stratigraphy at Wrangel Bay with amino acid ratios (aIle/Ile) for mollusc shells in glaciomarine sediments.

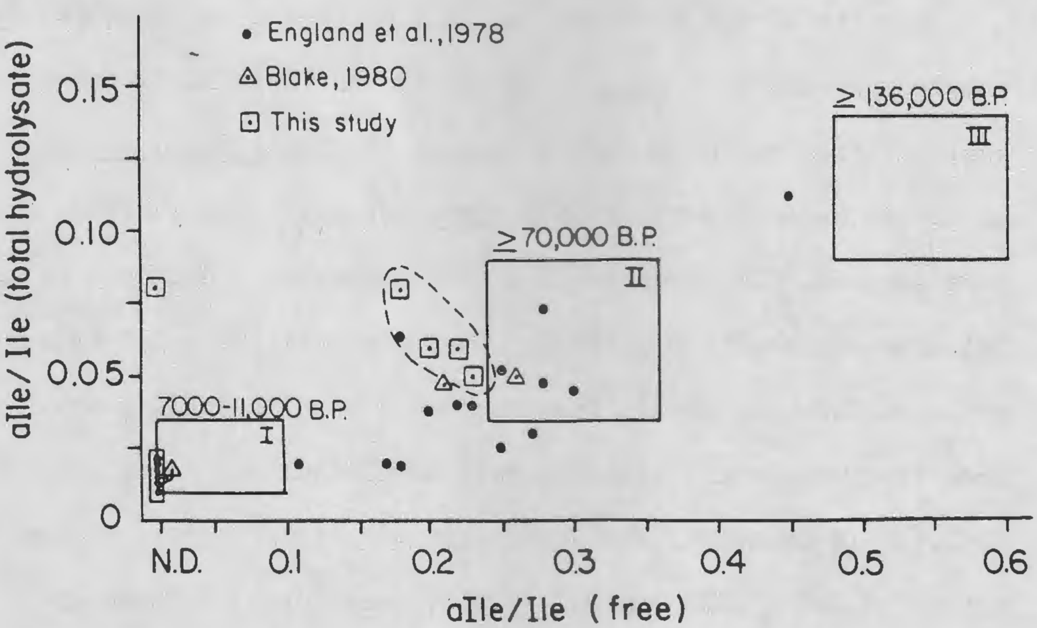

13. Comparison of aminostratigraphy of Robeson Channel area with other sites on Ellesmere Island and aminozones from eastern Baffin Island.

2. Amino acid ratios (allo-isoleucine/isoleucine) from marine mollusc shells in raised marine sediments and marine sediments from cores.

AGL NO.	SITE	DEPOSIT	SHELL TYPE	RADIOCARBON DATE B.P.	AMINO ACID AGE (B.P. est.)	aIle/Ile free	aIle/Ile total
077	Wrangel Bay	Glaciomarine silt 270 m	Hiatella arctica	-	≥ 35,000	0.22	0.06
079	Wrangel Bay	Glaciomarine silt 220 m	Hiatella arctica	-	≥ 35,000	0.20	0.06
031	Wrangel Bay	Glaciomarine silt 140 m	Hiatella arctica	>32,000	≥ 35,000	0.18	0.08
078	Wrangel Bay	Glaciomarine silt 125 m	Hiatella arctica	-	≥ 35,000	0.23	0.05
102	South Basin	Gravel Beach 111 m	Hiatella arctica	7390 ± 90	Holocene	N.D.	0.02
104	South Basin	Marine silt below 110 m beach	Hiatella arctica	7490 ± 70	Holocene	N.D.	0.01
105	Lincoln Bay	Marine silt below 100 m beach	Hiatella arctica	-	Holocene	N.D.	0.02
103	Lincoln Bay	Marine silt overlying moraine in coastal cirque	Hiatella arctica	7345 ± 75	Holocene	N.D.	0.02
106	Beaufort Lakes	marine sediment from piston core	Astarte borealis	-	Holocene	N.D.	0.02
107	Beaufort Lakes	marine sediment from piston core	Astarte borealis	-	Holocene	N.D.	0.014
108	Beaufort Lakes	marine sediment from piston core	Hiatella arctica	-	Holocene	N.D.	0.017
109	Beaufort Lakes	marine sediment from piston core	Astarte borealis	-	Holocene	N.D.	0.015
110	Beaufort Lakes	marine sediment from piston core	Hiatella arctica	-	Holocene	N.D.	0.019
008	Beaufort Lakes	gravel beach at 116 m marine limit	Hiatella arctica	8255 ± 215 8050 ± 120	Holocene	N.D.	0.080

N.D. denotes not detectable in the free aIle/Ile fraction.

Hereafter, the Holocene marine sediments will be referred to as the Beaufort aminozone , while the pre-Holocene marine unit is designated the Robeson aminozone . Aside from the clustering of amino acid ratios these units are lithologically, morphologically, and chronologically distinctive, and represent two unique intervals of glaciomarine sedimentation in the field area.

Regional Correlations

Although a local aminostratigraphy can be documented for the Robeson Channel area, an absolute age for the older Robeson aminozone has yet to be determined. Direct correlation of this marine unit is precluded by the lack of finite dates for the Robeson unit, and because of climatic variations between various sites, direct comparisons of amino acid ratios are difficult. Since the rate of amino acid racemization is temperature dependent (increased temperature yielding increased aIle/Ile ratios), it follows that temperature differences between northern Ellesmere Island and Baffin Island, for example, should account for lower aIle/Ile ratios at the more northerly site.

The data from this study is compared to eastern Baffin Island aminozones (Fig. 13) that have been assigned ages obtained from radiocarbon and uranium series dates on shell samples (Szabo et al., 1981). In addition to amino acid ratios from this study, data from southeastern Ellesmere Island (Blake, 1980 a,b) and from Judge Daly Promontory (England et al., 1978) are plotted in reference to aminozones I, II, and III from Baffin Island (Szabo et al., 1981). Group I comprises C-14 dated samples ranging in age from 7000 to 11,000 B.P. Group II has Th-230 ages between 21,000 and 68,000 B.P., and finite C-14 ages between 35,000 and 41,000 B.P., however the authors suggest that these samples are much older than 40,000 B.P. and assign a $\geq$ 70,000 B.P. age to the group. Group III shells gave Th-230 ages between 78,000 and 156,000 B.P. This grouping was assigned a $\geq$ 136,000 B.P. age, an average of these values. Both the Beaufort and Robeson aminozones plot to the left of Baffin Island groups I and II; thus they are less racemized than Baffin Island samples of the two different ages (Fig. 13). Correlation of the Holocene marine silts in both areas poses no problems, as many radiocarbon dates between 7000 and 11,000 B.P. have been reported for both sites. It is suggested however, that the pre-Holocene Robeson sediments are probably correlative to group II, which corresponds to the Kogalu aminozone of the Clyde Foreland (Miller et al., 1977). The difference in the cluster of the ratios between the Robeson and Kogalu aminozones is attributed to temperature differences between northeastern Ellesmere Island and Clyde Foreland, 1500 km to the south. Current mean annual temperature (CMAT) is approximately 6 C on northern Ellesmere Island (Table 3) although since amino acid racemizaton is more sensitive to warm temperatues, mean July temperature may be a better index of temperature dependence. The closest approximation to the intergrated thermal history that samples have experienced since burial is probably ground temperature, for which there is much less information. Ground temperature has been monitored on northern Ellesmere Iland at Alert and on Baffin Island at Mary River and Milne Inlet (Washburn, 1979) and measurements indicate concomitant decreases in mean annual temperature, mean July temperature, and ground temprature at depth (Table 3).

The timing and relative extents of ice masses in the two areas is also similar. The Ayr Lake Till, which underlies the Kogalu member of the Clyde Foreland Formation (Feyling-Hanssen, 1976), was presumably during the last glaciation to cover the foreland, as it in places extends out onto the continental shelf. Kogalu marine sediments were deposited in the isostatic downwarp in front of this ice mass (Miller et al., 1977). Similarly, the Robeson aminozone is associated with the maximum extension of Greenland ice onto Ellesmere Island, which created a major isostatic depression.

The amino acid ratios of the Robeson aminozone are also compared with those from other marine sediments on Ellesmere Island in Figure 13. Firstly, similar Free aIle/Ile ratios were measured on Hiatella arctica fragments in till in Makinson Inlet (Blake,1980b). Field evidence suggests that a substantial glacial advance filled Makinson Inlet (700 m thick) and entrained proglacial fossiliferous sediment and redeposited the shells at higher elevations (250 to 375 m). This event was tentatively correlated with the Kogalu aminozone by Blake (1980b). However, Miller (in press) has subsequently correlated the Makinson Inlet

3. Mean annual, mean July, and ground temperatures at several locations in the Canadian High Arctic.

Location	Latitude	Longitude	Mean Annual Temp.[1] °C	Mean July Temp.[1] °C	Ground Temp.[2] °C	Depth (m)
Alert N. Ellesmere	82°30' N	62° 20' W	-18	3.6	-16.1	15 - 18
Resolute Cornwallis Isl.	74° 43' N	94° 59' W	-16	4.1	-4.1	16
Milne Inlet[3]	73° 30' N	80° 00' W	-14.3	4.6	-12.2	15

[1] Canadian Climate Normals, 1951-1983

[2] Washburn, A.L.,(1979,

[3] Climate data from Pond Inlet, Baffin Island

deposits with the Loks Land aminozone, a younger event with less extensive ice extent. Secondly, the Robeson aminozone has ratios similar to Judge Daly Promontory pre-Holocene sediments, where shells were collected in silts beneath an ice-shelf moraine at relative sea level of 175 m. The ice-shelf moraine was deposited by floating Ellesmere Island ice that cross-cut deposits left by the maximum Greenland ice advance (England et al., 1978). Finite radiocarbon dates on the deposits range between 22,000 and 30,000 B.P., and are considered minimum estimates; amino acid ratios suggest a >35,000 B.P. age for this event (England et al., 1978). In contrast, shell fragments in a moraine deposited by Greenland ice on Judge Daly Promontory yielded free ratios of 0.45 $\pm$ .03 and 0.127 $\pm$ .002 (free and total fractions; Fig.13). These ratios do not necessarily conflict with the values for the Robeson aminozone, as the shells in the moraine probably pre-date the maximum Greenland advance, whereas the Robeson aminozone shells were taken from marine sediments deposited contemporaneously with recession of Greenland ice from Ellesmere Island. Thus, the Robeson aminozone shells and the oldest deposits from Judge Daly Promontory (England et al., 1978) most likely bracket the Greenland advance onto Ellesmere Island. The relation of the Robeson aminozone to the Makinson Inlet sediments is not clear, although if the shells are age-equivalent, a major glaciation would be necessary to deposit the shelly drift at high elevations in Makinson Inlet. Conversely, the Makinson Inlet samples may be older than the Robeson samples, with the equivalence in aIle/Ile ratios due to different effective diagenetic temperatures between northern and southern Ellesmere Island.

Figure 14 shows a compilation of some selected aminostratigraphic sequences in the High Arctic regions. Although several of the aminozones have not been named as such by the respective authors, local geographic (Melville) or stratigraphic (Hochstetter Foreland) terms are designated. Because of temperature variation and differences in radiometric age control at the sites, direct correlation by aIle/Ile ratios are difficult. However, visible correlations among aminozones in Baffin Island can be seen, as well as those from Spitsbergen. Boulton et al., (1982) have correlated the Spitsbergen glacial and marine chronology and aminostratigraphy with that on northeast Greenland (Hjort, 1981, 1982) demonstrating the similarity of Stadial 4 and Stadial 2 (Billefjord) with the Kap MacKenzie and Nanok Stadials of Greenland. The Kap Mackenzie Stadial in East Greenland was a major ice advance that reached the continental shelf. These deposits are dated by infinite C-14 dates and Th/U dates between 70,000 and 115,000 B.P. (Hjort, 1981). Ice advances subsequent to this (?) early Weichselian stadial were more restricted, as proglacial forelands and nunataks were exposed along the coast. This chronology is consistent with stratigraphy in northwest Greenland (Kelly, 1980), on Banks Island (Vincent, 1982), Baffin Island (Miller et al.,1977), and in this study, which demonstrates an

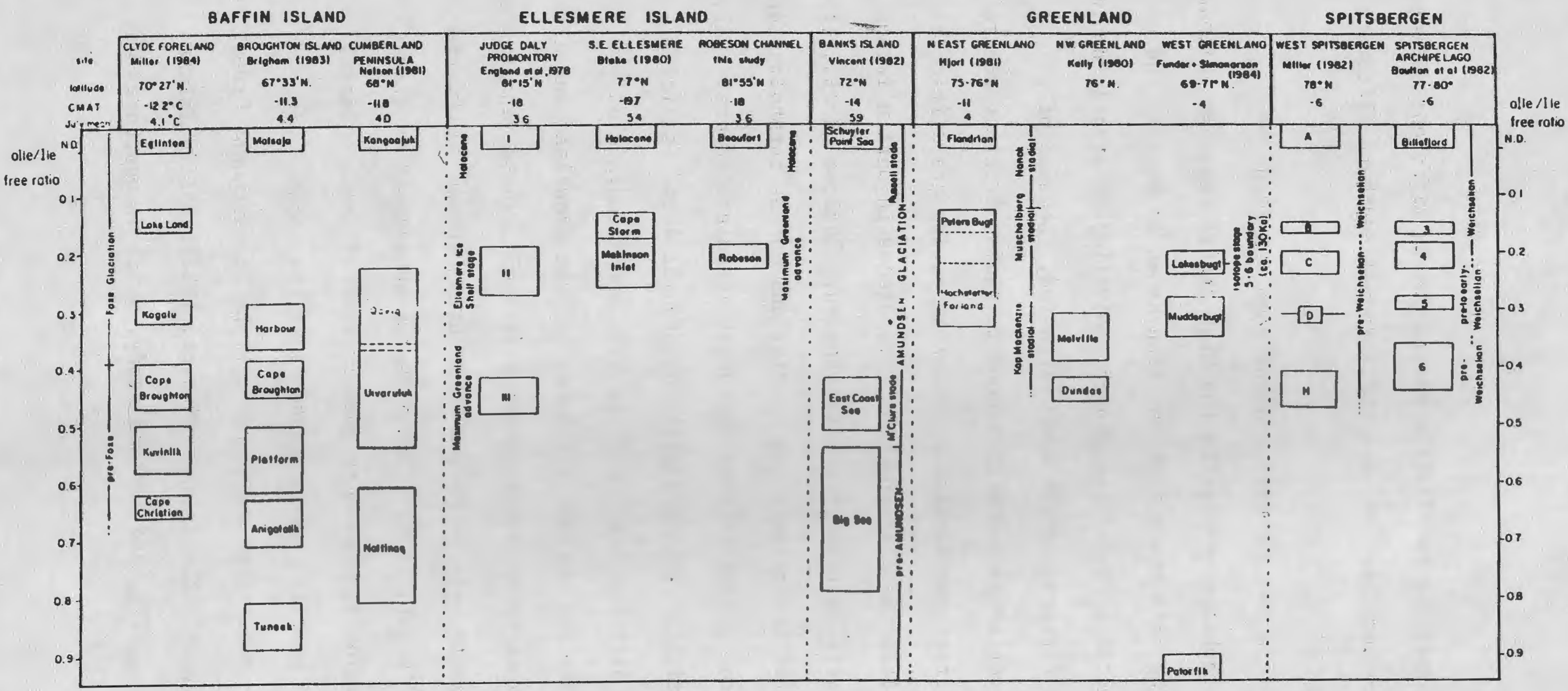

14. Compilation of amino acid ratios (free fraction) in stratigraphic sequences from various high arctic field sites.

early major glacial phase, followed by subsequently more restricted ice advances and associated marine events.

Discussion

In recent years, numerous studies have concluded that late Wisconsin ice cover at high latitudes was quite limited in extent (cf. Boulton, 1979). At that time, ice sheets to the south, in continental North America and Scandinavia, were extensive. Thus, it would appear that ice sheet margins at high and mid-latitudes have responded diachronously to climatic changes. Ice complexes in the High Arctic did not retreat and advance with their southerly counterparts. The dominant factor involved in the nonsynchroneity was the precipitation source for replenishing the ice sheets. While the southern margin of the Laurentide ice mass was nourished by the Atlantic Ocean to the south, the ice mass blocked precipitaton from moving into the High Arctic during the late Wisconsin glacial maximum at ca. 18,000 B.P. Therefore, High Arctic glacier expansion at this time was minimal. Although some authors (Ewing and Donn, 1956) have envisaged the Arctic Ocean as a moisture source for high latitude ice growth Koerner (1977) showed that Baffin Bay currently provides a greater moisture flux to High Arctic ice caps than does the Arctic Ocean. Moreover, Clark (1982) suggests that ice cover conditions in the Arctic Ocean have been constant for at least 700,000 years. If moisture flux from the Atlantic and Arctic Oceans was minimal, glacier expansion would likewise be limited during this time (Boulton, 1979). This seems likely, as expansion in high latitude areas occurred during disintegration of ice sheets and sea ice in the North Atlantic.

Geological evidence indicates that glaciers in high latitudes reached their last maximum between 11,000 and 8000 B.P., well behind the margins of previous Pleistocene advances. Morphostratigraphic evidence and isotope and amino acid chronologies from eastern Baffin Island, Spitsbergen, Greenland, Ellesmere Island and other locations suggest that glaciomarine sediments were deposited in isostatically-depressed forelands beyond their ice margins (Boulton et al., 1982). In these locations, marine silts with radiocarbon dates that range from 8000 to 11,000 B.P. overlie sediments of an older glaciomarine event that pre-dates the classical late Wisconsin/Weichselian glacial advance that occurred on the mid-latitude continents. No evidence of intervening glaciation is found between these deposits, hence, the timing and geographic placement of a major high latitude ice mass at 18,000 B.P. (Hughes et al., 1977) is questionable.

On the basis of field evidence on northern Ellesmere Island (summarized in Fig. 15), it is difficult to accomodate a model of expansive ice during the late Wisconsin maximum. According to this model, the Innuitian Ice Sheet (Blake, 1970) was confluent with the Laurentide and northwest Greenland Ice Sheets over Robeson Channel while centered over Norwegian Bay, southern Ellesmere Island. In subsequent papers, Blake (1975, 1977, 1978) presented evidence of fresh, large scale (but undated) glacial erosional and abrasional

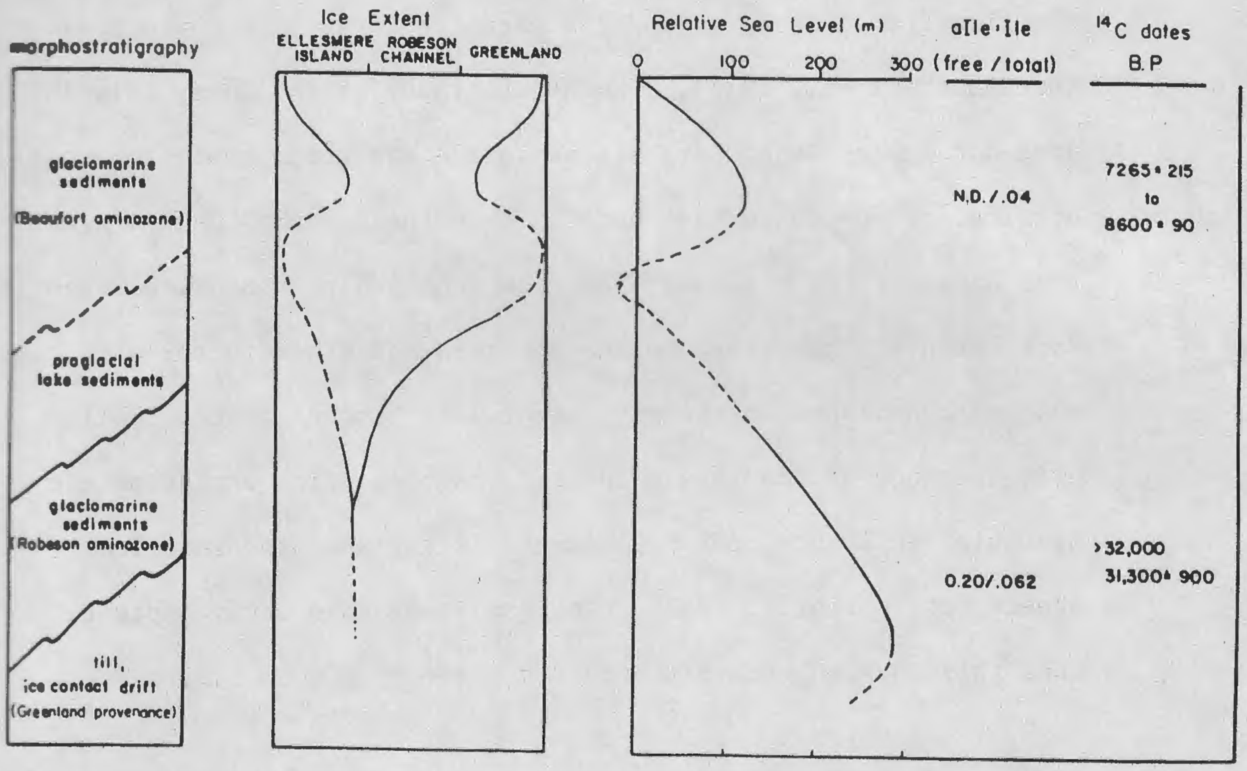

15. Summary of Quaternary glacial and marine stratigraphy in the study area.

features that indicate radial outflow from the Norwegian Bay area and erosional forms on the Carey Islands that indicate southerly ice flow from Kane Basin and the northern Nares Strait ice ridge (Dansgaard et al., 1970). The stratigraphy at the Carey Islands does not suggest that late Wisconsin ice was responsible for this erosion. No evidence has been found in the Robeson Channel area that demonstrates northerly ice flow from the proposed ice ridge in Kane Basin at this time, nor do moraines and other features in the coastal zone document the retreat of late Wisconsin ice. While evidence does demonstrate a one-time major glacial expansion and probable confluence of the Ellesmere Island and Greenland Ice Sheets (cf. Christie, 1983) the results of this study indicate that this advance probably occurred prior to 80,000 B.P.

Acknowledgements

The author sincerely thanks Drs. R.S. Bradley and J. England for introduction to the high arctic field study and for assistance through all phases of the research. R.S. Bradley and J.H. Hartshorn critically reviewed the manuscript. J. Fabel and R.L. Friend assisted in the field. Drs. R. Stuckenrath and J. Wittenberg provided radiocarbon dates. Dr. W. McCoy and M. Young are thanked for help with amino acid analyses. Dr. Rolf Feyling-Hanssen kindly provided several microfaunal analyses. The research was generously supported by the Polar Continental Shelf Project, Ottawa (G. Hobson, Director) and Division of Polar Programs, National Science Foundation Grant ATM80-17745 to the University of Massachusetts.

References Cited

Andrews, J.T. and Miller, G.H., 1976, Quaternary glacial chronology of the eastern Canadian Arctic: A review and a contribution on amino acid dating of Quaternary molluscs from the Clyde Cliffs: p. 1-32 in W.C. Mahaney (ed.) Quaternary Stratigraphy of North America, Dowden, Hutchinson, and Ross, Inc., Stroudsburg, Pa.

Bjorck, S. and Persson, T., 1981, Late Weichselian and Flandrian biostratigraphy and chronology from Hochstetter Forland, Northeast Greenland: Meddelelser on Gronland, Geoscience, volume 5, 18 p.

Blake, W., Jr., 1970, Studies of glacial history in Arctic Canada, I., Pumice, radiocarbon dates and differential postglacial uplift in the eastern Queen Elizabeth Islands: Canadian Journal of Earth Science, volume 7, p. 634-664.

__________, 1975, Radiocarbon age determinations and postglacial emergence at Cape Storm, southern Ellesmere Island, Arctic Canada: Geografiska Annaler, volume 57, Series A, p. 1-71.

__________, 1977a, Radiocarbon age determinations from the Carey Islands, northwest Greenland: Report of Activities, part A, Geological Survey of Canada, Paper 77-1A, p.445-454.

__________, 1977b, Glacial sculpture along the east-central coast of Ellesmere Island, Arctic Archipelago: Report of Activities, Part C, Geological Survey of Canada, Paper 77-1C, p. 107-115.

__________, 1978, Aspects of glacial history, southeastern Ellesmere Island, District of Franklin: Current Research, Part A, Geological Survey of Canada, 78-1A, p. 175-182.

__________, 1980a, Application of amino acid ratios to studies of Quaternary Geology in the High Arctic: in P.E. Hare et al. (eds.) Biogeochemistry of Amino Acids, Wiley and Sons, New York, 558 p.

__________, 1980b, Mid-Wisconsinan interstadial deposits beneath Holocene beaches, Cape Storm, Ellesmere Island, Arctic Canada: American Quaternary Association Sixth Biennial Meeting, Abstracts and Program, Orono, Maine, p.26-27.

Boulton, G., 1979, A model of Weichselian glacier variation in the North Atlantic region: Boreas, Volume 8, p. 373-395.

________, Baldwin, C.T., Peacock, J.T., McCabe, A.M., Miller, G., Jarvis, J., Horsefield, B., Worsley, P., Eyles, N., Chroston, P.N., Day, T.E., Gibbard, P., Hare, P.E., and von Brunn, V., 1982, A glacio-isostatic facies model and amino acid stratigraphy for late Quaternary events in Spitsbergen and the Arctic: Nature, volume 298, p. 437-441.

Brigham, J.K., 1983, Stratigraphy, amino acid geochronology, and correlation of Quaternary sea level and glacial events, Broughton Island, Arctic Canada: Canadian Journal of Earth Science, volume 20, p. 577-598.

Christie, R.L., 1964, Geological reconniassance of the north coast of Ellesmere Island, District of Franklin: Geological Survey of Canada, Memoir 331, 79 p.

________, 1967, Reconnaissance of the surficial geology of northeastern Ellesmere Island, Arctic Archipelago: Geological Survey of Canada, Bulletin number 138, 50 p.

________, 1976, Tertiary rocks at Lake Hazen, northern Ellesmere Island: Geological Survey of Canada, Paper 76-1B.

________, 1983, Lithological suites as glacial tracers, Eastern Ellesmere Island, Arctic Archipelago: in Current Research Part A, Geological Survey of Canada, Paper 83-1A, p. 399-402.

Clark, D.L., 1982, Origin, nature, and world climate effect of Arctic Ocean ice cover: Nature, volume 300, p. 321-325.

Dansgaard, W., Johnsen, S.J., Clausen, H.B., anf Langway, C.C. Jr., 1970, Ice cores and paleoclimatology: p. 337-348 in Olsson, I.U., (ed.) Radiocarbon Variations and Absolute Chronology, John Wiley and Sons, Inc., New York.

Dyke, A.S., 1979, Radiocarbon-dated Holocene emergence of Somerset Island, central Canadian Arctic: in Current Research Part 3, Geological Survey of Canada paper 79-1B, p.307-318.

__________ , 1976b, Late Quaternary glaciation of the eastern Queen Elizabeth Islands, N.W.T., Canada: alternative models: Quaternary Research, volume 6, p. 185-202.

__________ , 1978, The glacial geology of northeastern Ellesmere Island, N.W.T., Canada: Canadian Journal of Earth Science, volume 15, p. 603-617.

__________ , 1983, Isostatic adjustments in a full glacial sea: Canadian Journal of Earth Science, volume 20, p. 895-917.

__________ and Bradley, R.S., 1978, Past glacial activity in the Canadian High Arctic: Science, volume 200, p. 265-270.

__________ , Bradley, R.S., and Miller, G.H., 1978, Former ice shelves in the Canadian High Arctic: Journal of Glaciology, volume 20, p. 393-404.

__________ , Bradley, R.S., and Stuckenrath, R.S., 1981, Multiple glaciations and marine transgressions, western Kennedy Channel, Northwest Territories, Canada: Boreas, volume 10, p. 71-89.

Ewing, M., and Donn, L., 1956, A theory of ice ages: Science, volume 123, p. 1061-1066.

Feyling-Hansen, R.W., 1967, The Clyde Foreland> Field Report, North-Central Baffin Island, 1966, Edited by Loaf Loken,Dept. of Energey, Mines and Resources,Geographical Brance, Ottawa, Ontario, p. 35-55.

__________ ,1976, The stratigraphy of the Quaternary Clyde Foreland Formation, Baffin Island, illustrated by the distribution of benthic foraminifera: Boreas, volume 5, p. 57-94.

Funder, S., and Hjort, C., 1973,Aspects of the Weichselian chronology in central East Greenland: Boreas, volume 2, p. 69-84.

__________ , and Simonarson, L.A., 1984, Bio-and aminostratigraphy of some Quaternary marine deposits in West Greenland: Canadian Journal of Earth Science, volume 21, p. 843-852.

Hjort, C., 1981, A glacial chronology for northern East Greenland: Boreas, volume 10, p. 259-274.

__________ , 1982, Glacial and interglacial chronology in northeastern Greenland (abs.): Geological Society of America annual meeting, abstracts with program, p. 575.

__________ and Bjorck, S., 1983, A re-evaluated glacial chronology for northern East Greenland: Geologiska Foreningens i Stockholm Forhandlingar, volume 105, part 3, p. 235-243.

Hughes, T., Denton, G.H., and Grossvald, M.G., 1977, Was there a late Wurm Arctic Ice Sheet? : Nature, volume 266, p. 596-602.

Kelly, M., 1980, Preliminary investigations of the Quaternary of Melville Bugt and Dundas, northwest Greenland: Gronlands Geologisches Undersolgelses, Rapport no. 100, p. 33-38.

Koerner, R.M.,1977, Ice thickness measurements and their implications with respect to past and present ice volumes in the Canadian High Arctic ice caps: Canadian Journal of Earth Science, volume 14, p. 2697-2705.

Lehman, S., Forman, S., and Miller, G.H., 1983, Quaternary stratigraphy and ice limits;Forlandsun region, West Spitsbergen, Svalbard (abs.): Abstracts of the 12th Arctic Workshop, University of Massachusetts, Dept. of Geology and Geography, Contribution No. 44.

Miall, A.D., 1982, Tertiary sedimentation and tectonics in the Judge Daly Basin, Northeastern Ellesmere Island, Arctic Canada: Geological Survey of Canada, paper 80-30, 17 p.

Miller, G.H., 1982, Quaternary depositional episodes, western Spitsbergen, Norway: aminostratigraphy and glacial history: Arctic and Alpine Research, volume 14, number 4, p. 321-340.

__________ , in press, Amino acid geochronology of Baffin Island shell-bearing deposits : in J.T. Andrews and M. Andrews (eds.) Quaternary Environments, Eastern Canadian Arctic, Baffin Bay, and West Greenland, Pergamon Press, New York.

__________ , Andrews, J.T., and Short, S.K., 1977, The last interglacial/glacial cycle, Clyde Foreland, Baffin

Island, N.W.T.,stratigraphy, biostratigraphy and chronology: Canadian Journal of Earth Science, Volume 14, p. 2824-2857.

__________, Brigham, J.K., and Clark, P., 1982, Alternation of the total aIle/Ile ratio by different methods of sample preparation: Report of Current Activities, INSTAAR and Department of Geological Sciences, University of Colorado.

Nelson, A.R., 1978, Quaternary glacial and marine stratigraphy of the Qivitu Peninsula, northern Cumberland Peninsula, Baffin Island, Canada: unpublished Ph.D. dissertation, INSTAAR and Dept. of Geological Sciences, University of Colorado, Boulder.

__________, 1981, Quaternary glacial and marine stratigraphy of the Qivitu Peninsula, Baffin Island, Canada: Summary: Geological Society of America Bulletin, Part 1, volume 92, p. 512-518.

Prest, V.K., 1952, Notes on the geology of parts of Ellesmere and Devon Islands, Geological Survey of Canada, Paper 52-32.

Smith, D.I., 1961, The glaciation of northern Ellesmere Island: Folia Geographica Danica, Tom. 9, p. 224-234.

Szabo, B.J., Miller, G.H., Andrews, J.T., and Stuiver, M., 1981, Comparison of uranium series, radiocarbon, and amino acid data from marine molluscs, Eastern Baffin Island, Arctic Canada: Geology, volume 4, p. 451-457.

Taylor, A., 1956, Physical geography of the Queen Elizabeth Islands, Canada: American Geographical Society, New York, 12 volumes.

Trettin, H.P., 1971, Geology of the lower Paleozoic formations, Hazen Palteau and Southern Grant Land Mountains, Ellesmere Island, Arctic Archipelago: Geological Survey of Canada Bulletin 203.

Vincent, J.S., 1982, The Quaternary history of Banks Island, N.W.T.,Canada: Geographie Physique et Quaternaire, volume 36.

Walcott, R.I., 1970, Isostatic response to loading of the crust in Canada: Canada Journal of Earth Science, volume 7, p. 716-727.

Washburn, A.L., 1979, Geocryology, a survey of periglacial processes and environments: Edward Arnold Publishers, London.

Weidich, A., 1976, Glaciation of northern Greenland, new evidence: Polarforschung, volume 46, p. 26-33.

LATE QUATERNARY STRATIGRAPHY AND PALEOENVIRONMENTS OF THE BEAUFORT LAKES BASIN, NORTHEASTERN ELLESMERE ISLAND

M.J. Retelle

University of Massachusetts, Amherst

ABSTRACT

Late Quaternary environmental changes in a sedimentary basin on the coast of northeastern Ellesmere Island have been reconstructed using cores of sediment recovered from three contemporary lakes. The lake basins were isostatically depressed below sea-level in an ice-free corridor between ice sheets over northwest Greenland and Ellesmere Island during the last glaciation. They became isolated from the sea as the two ice sheets retreated and the coast isostatically readjusted to the reduced ice load. Each sediment core recovered comprised lacustrine sediments overlying glaciomarine sediments. Sedimentary properties such as grain size, loss-on-ignition, porewater geochemistry and faunal content were determined to characterize changes in the depositional environment from 'full glacial' to modern lacustrine conditions.

Present study

Three lakes (unofficially named the "Beaufort Lakes") are situated in a large south-facing cirque basin 2 km north of Mt. Beaufort and approximately 65 km south of Alert. The cirque, which opens towards Robeson Channel, was incised into the southeastern margin of the Hazen Plateau, which is made up of lower Paleozoic flysch sediments of the Imina Formation (a succession of interbedded sandstones, siltstones, and shales). The field site was situated beyond the limit of ice advance during the last glaciation in the ice-free corridor between interior Ellesmere Island ice and the northwest Greenland Ice Sheet. Ellesmere Island ice advanced out of the interior mountains and spread out as piedmont lobes on the Hazen Plateau, where it terminated at the Craig Lake Moraine.

Ellesmere ice also reached the heads of Archer Fiord and other major fiords to the south (England, 1978, 1983). Ice from northwest Greenland advanced out of Petermann Fiord and Newman Bay into Hall Basin and Robeson Channel across the channel from the field area and flanked, but did not cover, the Polaris Promontory foreland (Davies, 1963; England 1983). Thus, an unglaciated zone almost 100 km wide existed between Greenland and Ellesmere Island during the last glacial maximum. The crustal flexure produced by these ice loads extended well beyond the ice margins and produced a marginal depression in this ice-free corridor. Walcott (1970) has demonstrated that due to the rigidity of the lithosphere, the crust may be depressed for about 180 km beyond the ice margin. The depression produced by the ice loads caused marine submergence of the coastal zone in the Robeson Channel area up to a marine limit of 116 m. The sediments contained in isostatically depressed coastal lowland basins such as the Beaufort Lakes include: a) glaciomarine sediments that were deposited during a marine transgression as ice advanced to the last glacial limit. These sediments continued to accumulate until deglaciation of adjacent land areas led to isostatic emergence of the basins; b) lacustrine sediments deposited over the marine sediments subsequent to the isostatic emergence of the lakes from the sea.

Methods

Fieldwork was conducted at the Beaufort Lakes basin in 1981 and 1982 as part of a study of the Quaternary glacial and marine history and environments of the surrounding region. Piston cores of the lake-bottom sediments were recovered using a modified Livingstone corer with a stainless steel core tube 1.3m long and 4.5 cm in diameter. Magnesium-zirconium drive rods were used with the corer, which retrieved up to 4.8 m of sediment using repetitive drives down the same borehole. Core sections were extruded in the field, wrapped in plastic and heavy-duty aluminum foil, and stored in trays in insulated core boxes until returned to the lab. The cores were stored in a darkroom kept at +4°C. Segments of the cores were removed for radiocarbon dating at several intervals (Retelle, 1985a). Sub-sampling was then done on cores for paleomagnetics, bulk susceptibility, grain size, loss-on-ignition, microfauna, and geochemical analyses at various intervals. Grain size (% sand, silt, clay) was determined by centrifuge and wet sieve techniques on 2.5-cm sampling cubes that had been previously used for paleomagnetic studies. The sand, silt, and clay fractions were retained for further analysis.

The clay-size fraction (finer than 2 microns) was used for clay mineral analyses. Oriented smear mounts were prepared on glass slides. Air-dried, glycol-solvated and heat-treated samples (550°C) were run at 1 degree-2 theta/ minute on a Siemens diffractometer using Cu k-alpha radiation. A nickel filter with 1 and 0.4 degree slits was used at 35 kv and 20 ma.

Loss-on-ignition was measured after drying the sample overnight at 65°C, followed by combustion at 450°C for 2 hours.

The ionic concentrations of sediment porewaters were analyzed using a technique described by Patterson et al. (1978). Using a Delrin plastic press, interstitial waters were squeezed from the samples. Porewaters were diluted by a factor of 100 and ionic concentrations of Na, K, Ca, and Mg were measured on an Instrumentations Laboratories atomic absorption spectrophotometer. Lake-water samples, recovered from various depths in the lake by means of a Kemmerer sampler, were stored in opaque amber Nalgene plastic bottles for later laboratory analyses. Temperature, pH, and alkalinity analysis of the lake waters were carried out in the field. Chloride was measured with a specific ion electrode in the lab for lake and stream waters and sediment porewaters.

Present Environment of the Beaufort Lakes Basin

The three lakes at the field site are located at elevations of 12, 34, and 39 m a.s.l., below the Holocene marine limit of 116 m (Fig. 1). They are referred to as Lakes 1, 2, and 3, in order of increasing elevation. The lakes are held in by resistant northeast-trending bedrock ridges mantled by marine silts and beach gravels.

Lake 3 is the smallest of the lakes (0.6 km X 0.3 km) and is the shallowest, with ca. 12.4 m water depth. Inlet streams are few and small, with the largest originating from snow cornices on the northern headwall of the basin. The outlet of Lake 3 is very shallow (about 0.5 m) and flows into Lake 2.

Lake 2, the largest of the Beaufort Lakes, is the furthest inland from Robeson Channel. It is approximately 1.2 km long and nearly divided into two basins by a northeast/southwest-trending bedrock ridge. The northwestern half of the basin is about 30 m deep and shallows to the southeast. Most of the watershed is drained by two large streams which flow into the northwest end of the lake. Thus, Lake 2 has the greatest sedimentation rate, as the two inlet streams have built delta fans into the deep (northwestern) end of the lake. The combined outflow from Lakes 2 and 3 drains into Lake 1.

Lake 1, at 12 meters, has a maximum measured depth of 21.6 m.

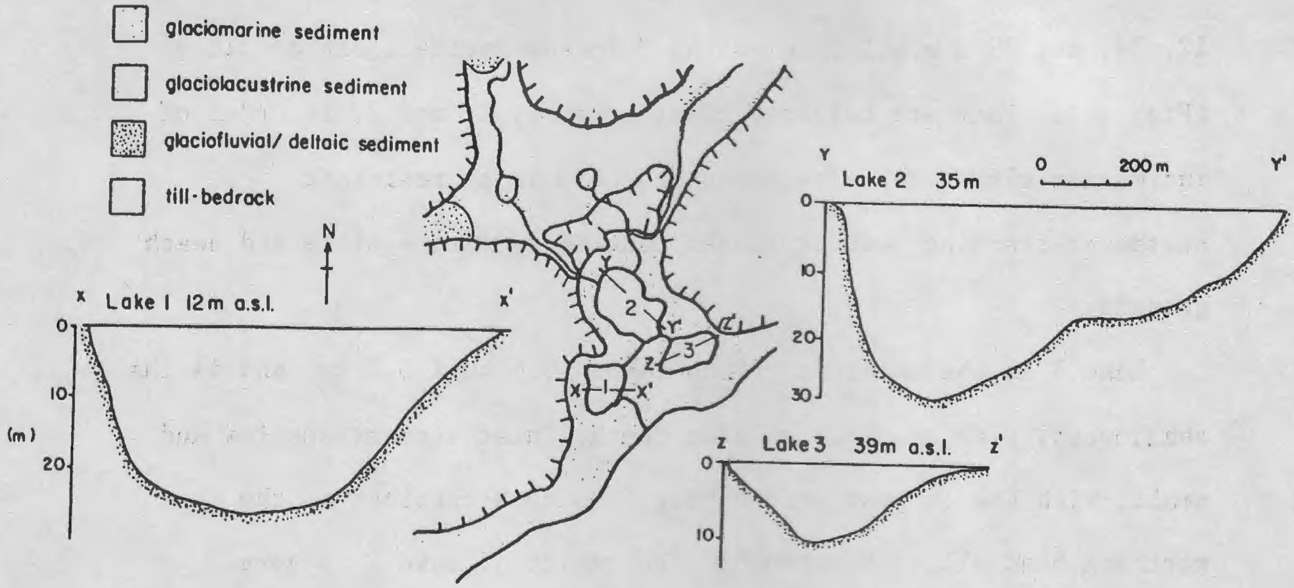

Figure 1. Bathymetry and surficial geology of the Beaufort Lakes basin.

Its outlet stream flows into Robeson Channel (Fig. 1). The immediate drainage basin of this lake is small, limited to the steep headwalls of the lower Beaufort Lakes basin which surround the lake.

To determine the present-day water chemistry in the lakes, limnological measurements were made in the three lakes in June 1981 (Fig. 2). Temperature profiles in all the lakes show isothermal conditions, with the exception of the water in contact with the drilled holes in the ice, in the top 2 to 2.5 m at each station. Lake 2 water registered the highest pH values (8.7), whereas in Lakes 1 and 3, the waters averaged 8.3. Mean values for temperature, alkalinity, and all the ionic concentrations, however, were greatest in Lake 3 (Fig. 2). Ionic concentrations averaged at least 4 times greater than those in Lakes 1 and 2. No evidence of chemical stratification was found in the lake waters.

Paleoenvironments of the Beaufort Lakes Basin

The Beaufort Lakes basin is floored by till, which is exposed at the surface above the marine limit. Abundant red granitic and gneissic erratics in this drift sheet (probably of Greenland provenance) stand out in contrast to the gray-brown Imina Formation. The till was probably deposited during the maximum advance of northwest Greenland ice onto northeastern Ellesmere Island, tentatively $\geq$ 80,000 years B.P. (England et al., 1981). Marine shorelines in the basin extend up to 116 m (the Holocene marine limit) and have been dated between 8200 and 8000 B.P. (England,

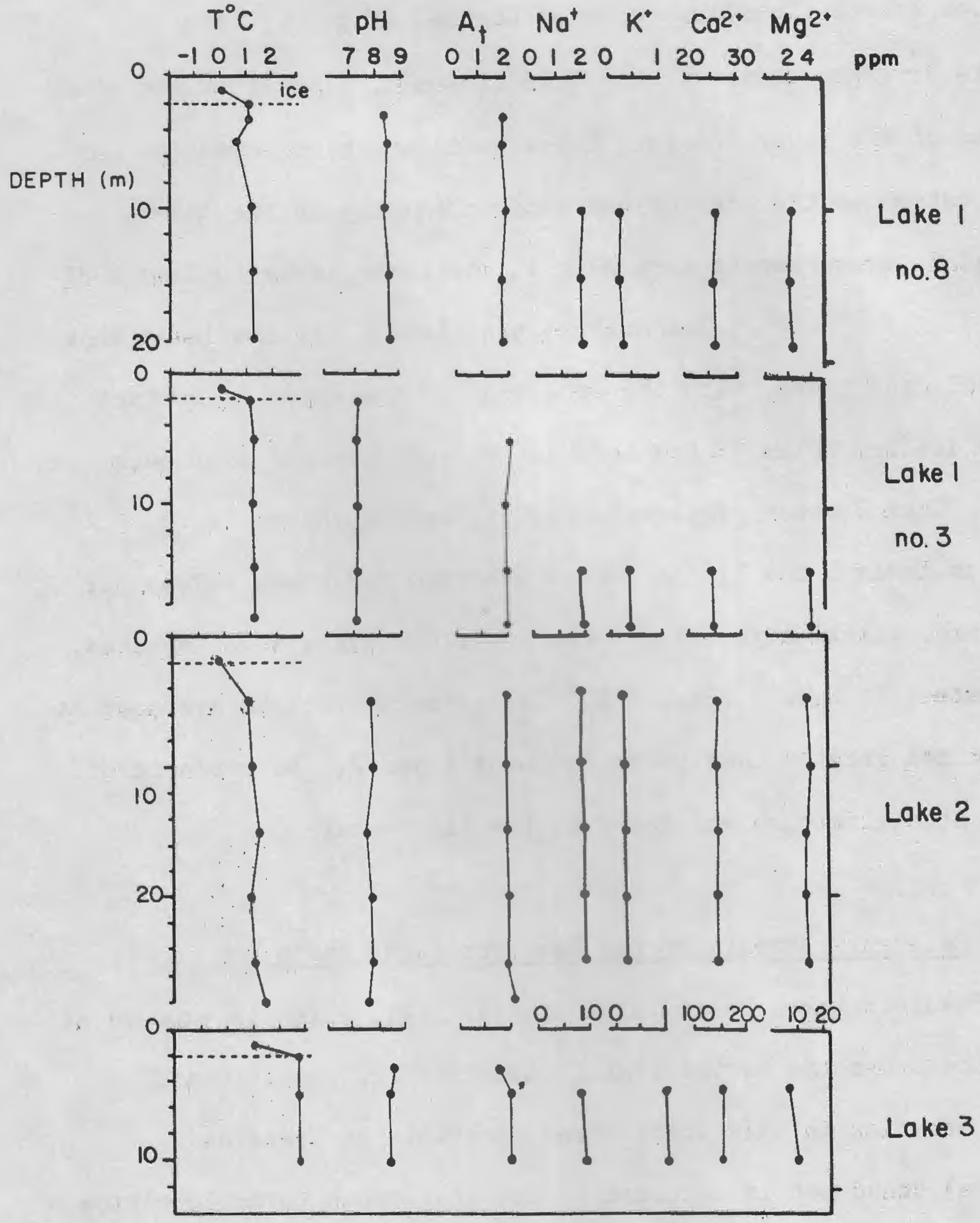

Joe's Hat Creek

T°C	pH	Na^+	K^+	Ca^{2+}	Mg^{2+}	Cl^-
1.5	8.5	1.76	0.95	19.4	2.70	22.0

Figure 2. Limnological measurements in the Beaufort Lakes, and inlet to Lake 2, June 1981.

1983).

Gravelly beach sediment and interfingering deeper-water glaciomarine silts overlie till below the marine limit. The glaciomarine silts have coarse sandy interlaminae and gravelly layers, presumably deposited by ice rafting or iceberg grounding. Abundant pelecypods found in the silt unit include Hiatella arctica, Portlandia arctica, Astarte borealis, and Mya truncata . Paired valves in growth position are often found in the silts, whereas on the gravel beaches, single unpaired and abraded shells are common. The duration of this marine event in the ice-marginal depression zone has not been determined; however dated shells from this area give minimum estimates from 8,000 to 11,000 years B.P. (England, 1983). The initial establishment of the marine limit, therefore, has not been documented. England (1983) points out that this event probably occurred as the "full glacial sea" transgressed in response to isostatic loading. Another possibility is that the marine limit, measured thus far, was established by sea level falling from higher levels associated with the crustal loading of an earlier glaciation. Radiocarbon dates on the total organic fraction from the base of the Beaufort Lakes cores indicate a duration greater than 40,000 years for this ice-marginal sea, however, it is very likely that these dates are overestimates, contaminated by dead carbon (Retelle, 1985a).

Sea level began to fall from the marine limit some time around 8000 B.P. in response to initial unloading of adjacent ice on the Hazen Plateau (England, 1983). The three Beaufort Lakes, responding to the changes in ice load, emerged progressively from the sea responding to the changes in ice load. In the sediment cores, this emergence is documented by a change from glaciomarine to lacustrine sediments. The change is very distinctive visually, texturally, and chemically, and is discussed in more detail below.

Lacustrine and Marine Sediment Cores

Stratigraphy

In total, thirty-three meters of cores of various lengths, ranging from 1 to 4.8 m, were recovered from the three lake basins. Lithostratigraphy from a representative core is shown in Figure 3 .

The lowermost sediment recovered in the cores is an olive-gray sandy and clayey marine silt that contains dropstones and marine invertebrate macro- and microfossils. Bedding is absent to faint due to bioturbation by the molluscs. Black sulfidic mottling and lamination are also present, mainly concentrated around the pelecypods.

Marine sediments were deposited in the basins by fluvial input from runoff, ice rafting by local landfast sea ice, pack ice or icebergs, mass flow deposits from the nearby shore, and eolian deposition.

The upper unit in the cores is a grayish-olive laminated lacustrine sediment with thickness averaging between 1 to 4.3 m in the cores. Primary sedimentary structures include thin horizontal

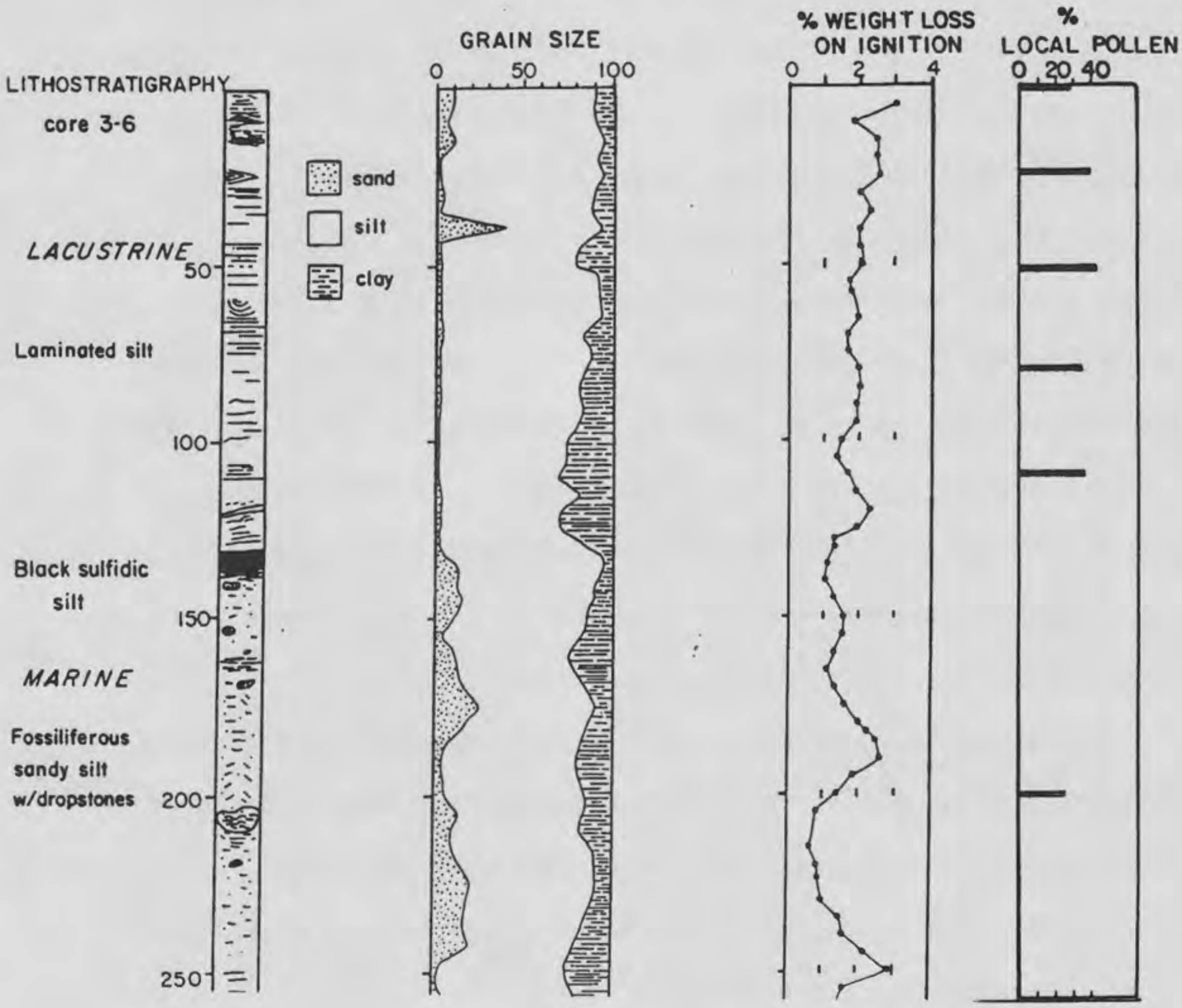

Figure 3. Stratigraphy of core 3-6 from Beaufort Lake 3.

laminae, massive beds, and graded beds which are irregularly spaced downcore. The graded beds are 0.2 to 0.5 cm thick and are separated by several centimeters of massive to faintly bedded clayey silt. The bulk of the lacustrine sediments in the basins was most likely deposited by fluvial input from spring and summer snowmelt runoff, although other prominent features in the lacustrine sediments include mudflow deposits and isoclinal folds formed by slumping of the lake bed or materials along the shore. Pebbly mudflow sediments found in the upper 20 cm of three cores spaced at ca. 50 m intervals on Lake 1 are probably redeposited glaciomarine sediments that slumped into the lake from the shore. Wind-transported sand and silt, as well as organic matter (Salix leaves and twigs) were found on the ice surface during coring operations .

The lacustrine and marine sediments are separated by a distinct transtion zone of massive to finely laminated black sulfidic clayey silt (Fig. 4) . Alternating black and light gray laminae, approximately 1 mm thick, grade upwards from the massive black silt to the laminated lacustrine sediments above.

Transition zones of this type have been described in similar sedimentary sequences in Sweden (Ericson, 1973) and Spitsbergen (Hyvarinen, 1970), where the marine to freshwater transition also results from deglaciation of a coastal site or subsequent isostatic rebound. Fine-grained black sulfidic clayey silt layers have also been documented in cores from fiords in Alaska (Hoskin and Burrell, 1972) and in cores from the Black Sea (Berner, 1970a), where the

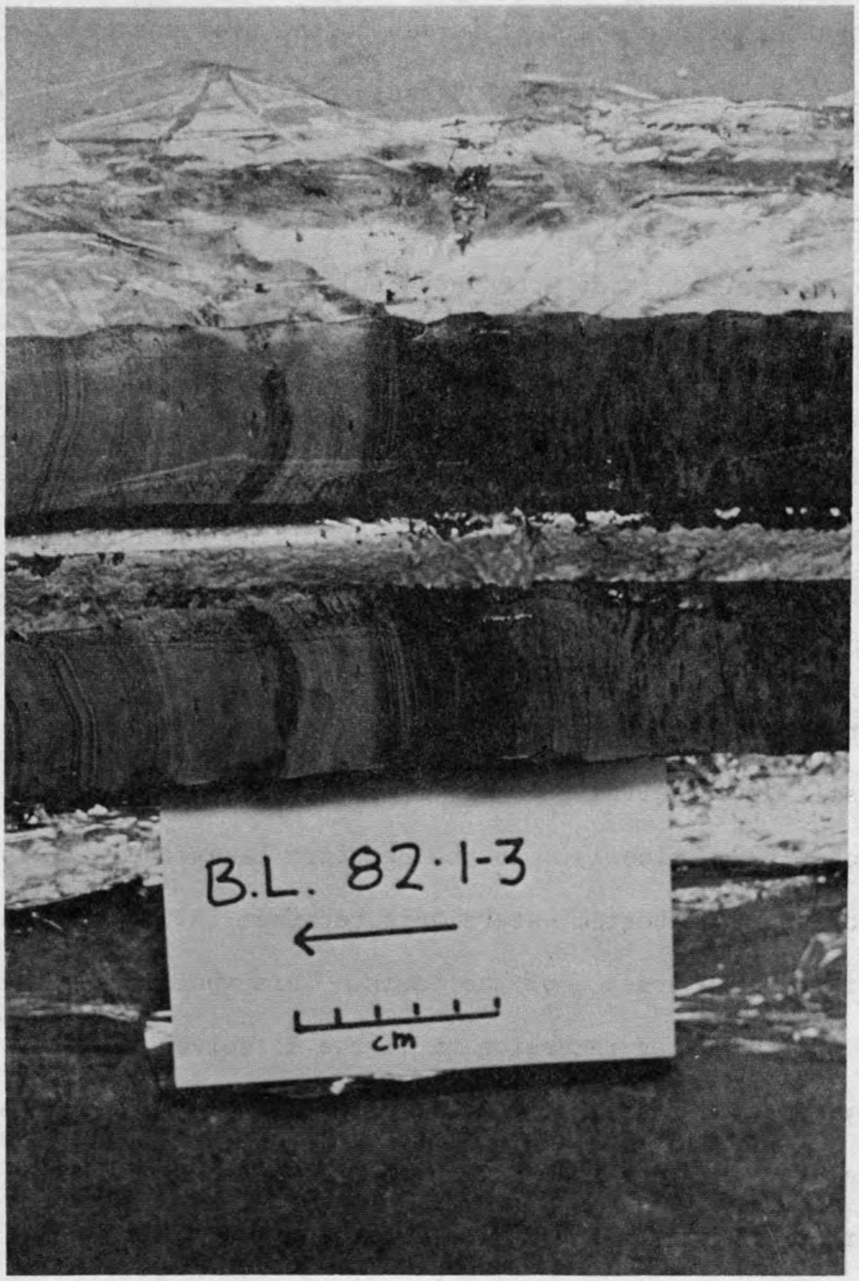

Figure 4: Photograph of the transition zone between marine and lacustrine sediments in core 1-2, Lake 2. Scale in cm.

black coloration of the sediment is due to the presence of iron monosulfides, mackinawite ($Fe_{1+x}S_x$) and greigite (Fe_3S_4). These unstable sulfide phases are precursors to pyrite ($Fe\ S_2$), which normally colors the sediment gray. The black precursor minerals usually form as a result of attenuated sulfate reduction and limited production of H_2S. Pyrite can form from monosulfides if there is organic material that can be metabolized and a sufficient sulfate supply for use by sulfate-reducing bacteria. Sulfate is usually supplied by downward diffusion from the overlying water column. Berner (1970a) cites evidence for black monosulfide occurrence in the Black Sea relating to periods of low sea level and increased freshwater influx. Fresh water entering the Black Sea contains only 0.35 umoles/l of dissolved sulfate, compared to sea water, which is more enriched (28 umoles/l). In the Beaufort Lakes area, it is possible that saline bottom waters were retained in the lake bottoms shortly after the emergence of the basin. This would delay the influence of freshwater incursion until the dissolved sulfate was removed by reducing bacteria. Black sediment would be deposited during emergence, as opposed to the gray pyrite-rich sediments typical of normal marine conditions. Although usually not the most limiting factor in the transformation of monosulfides to pyrite, the availability of elemental iron and elemental sulfur is also important (Berner, 1970b).

Loss-On-Ignition

An approximation of total organic material, although only a crude estimate, was made by studies of loss-on-ignition on two cores from Beaufort Lake 3. Percent weight loss in core 3-6 varied from a high of 3% in the upper lacustrine sediments to a low of 0.7% in the marine unit. Minima in percent weight loss appear to correlate with several black laminated zones at 120 cm (lacustrine), 165 cm (marine) and at the marine-lacustrine transition at 131 to 140 cm. Several low values are also observed in core 3-2 in the 115- to 120-cm zone and in the 135- to 140-cm zone. Weight loss in this core varied from 2.4% in the lacustrine sediments to 0.75% in the marine sediments. In both cases, the lowest average values are seen in the transitional units. These variations downcore may be the result of several processes operating simultaneously. Emergence of the basin from the sea exposes more wet lowlands in the basin for establishment of vegetation, increasing the available organic material. The establishment of vegetation would be delayed somewhat after emergence and a lag in organic input would be recorded in the sediments. Furthermore, the change from marine to freshwater decreases the sulfate flux to the bottom sediments and kills the marine biota, eliminating this source of organic matter.

Grain size variations

The variability of grain-size distribution (% sand, silt, clay) in the sediment cores was analyzed to detect changes in the depositional processes within the basin. While some of these processes are climate-dependent, and hence may record a climatic signal, others may result from physical processes that have little or no climatic significance. Sandy sediments (>62 um) can be introduced into deep water (both marine and lacustrine) by turbidity currents that flow into the basin from the prodelta slope. Stream water from snowmelt (which varied from 1.5 to 6°C) carries sediment into the lake, where present-day waters are less dense (ca. 1°C). As the stream water enters into the lake, it may flow beneath the less dense lake water as a turbidity current transporting sediment into the basin and producing graded beds (cf. Gustavson, 1975).

At Beaufort Lakes in 1981 and 1982, the two major streams flowing into Lake 2 started to flow in early to mid-June with discharge peaking in late June. Snowmelt decreased through early July and esentially terminated in August as snow rapidly melted from the basin. Although this annual pulse of discharge, with concomitant sediment influx, is clearly a response to seasonal warming, the amount of water discharged into the lake is limited by the volume of snow in the basin. Additional runoff is negligible because of the low precipitation and short melting season (Coakley and Rust, 1968). Since major precipitation events in the High Arctic areas depend upon open water for a source, such as an ice-free Baffin Bay during periods of climatic warming (Bradley, 1978; Bradley and England, 1979), both increases in warming and precipitation should correlate with periods of coarse fluvial input into the basins.
Alternatively, it should be stated that all graded beds are not

necessarily deposited as a response to seasonal warming. Graded beds in the glaciolacustrine environment may represent processes such as prodelta slope failure and turbidite deposition during the melt or frozen season (Shaw et al., 1978).

During marine submergence, sea ice (pack ice, icebergs and landfast ice) plays an important role in sediment transport. Coarse sediment may become entrained as sea ice becomes grounded onshore or compressed and buckled to the sea bed in up to 30 m of water (Reimnitz et al., 1978). Sediment incorporated into basal layers of ice by regelation may be rafted and released during transport. During cold periods, landfast ice and pack ice may have completely sealed off inlets to the extent of forming incipient ice shelves in coastal embayments and fiords (Crary, 1960; England, 1983). As s result, drifting ice may have been excluded from inlets resulting from minimal deposition due to ice rafting. In contrast, during warm periods sea ice may have penetrated fiords and inlets leading to more erosion, entrainment, and sediment deposition.

During emergence of the lake basin, as the threshold of the basin passes through wave base, coarse sediments may be winnowed from previously deposited glaciomarine sediments and transported into the basin by estuarine currents (Rust and Coakley, 1970) or by icebergs and sea ice grounding over the shoal. This latter process is also most effective during periods when the embayment is not locked in ice.

While the observed changes in grain size in the cores from the

Beaufort Lakes basin reflect environmental changes in the basin or changes in regional climate, it is difficult to reference these changes to a rigorous chronologic framework (Retelle,1985a)Estimates on some of the more obvious changes can be made using the revised relative sea level curve described in the previous chapter. Thus, the black sulfidic marine to lacustrine transition sediments in the cores represent time lines for each basin and can be used to predict the emergence of that lake basin. Sedimentologic changes downcore will be referenced to these horizons.

The longest marine record from core sediments is contained in core 3-8 (Lake 3), where approximately 2 meters of glaciomarine sediments underlie lacustrine sediments (Fig. 5). The marine to lacustrine transition contact at 200 cm is estimated at ca. 5600 B.P. (Retelle, 1985a). In addition, an accelerator radiocarbon date was obtained on <u>in situ</u> bivalves at 220 cm and was dated at 7060 ± 660 B.P. Several pronounced changes in sand percentage are visible in this core. Sand content decreases from 28% below the contact (210 cm) to only 1% at 95 cm. This decrease and the other abrupt decreases in the marine-lacustrine contact in other cores, most likely reflect shoaling of the basin and reworking of the threshold by waves, currents, and drifting ice. Other high percentages of sand, from a period of higher sea level than during emergence, most likely reflect increases in runoff and ice rafting when sea ice was mobile during climatically warmer periods. At 335 cm, the abundant sand content drops off abruptly to a mean of 4 % between 335 and 380

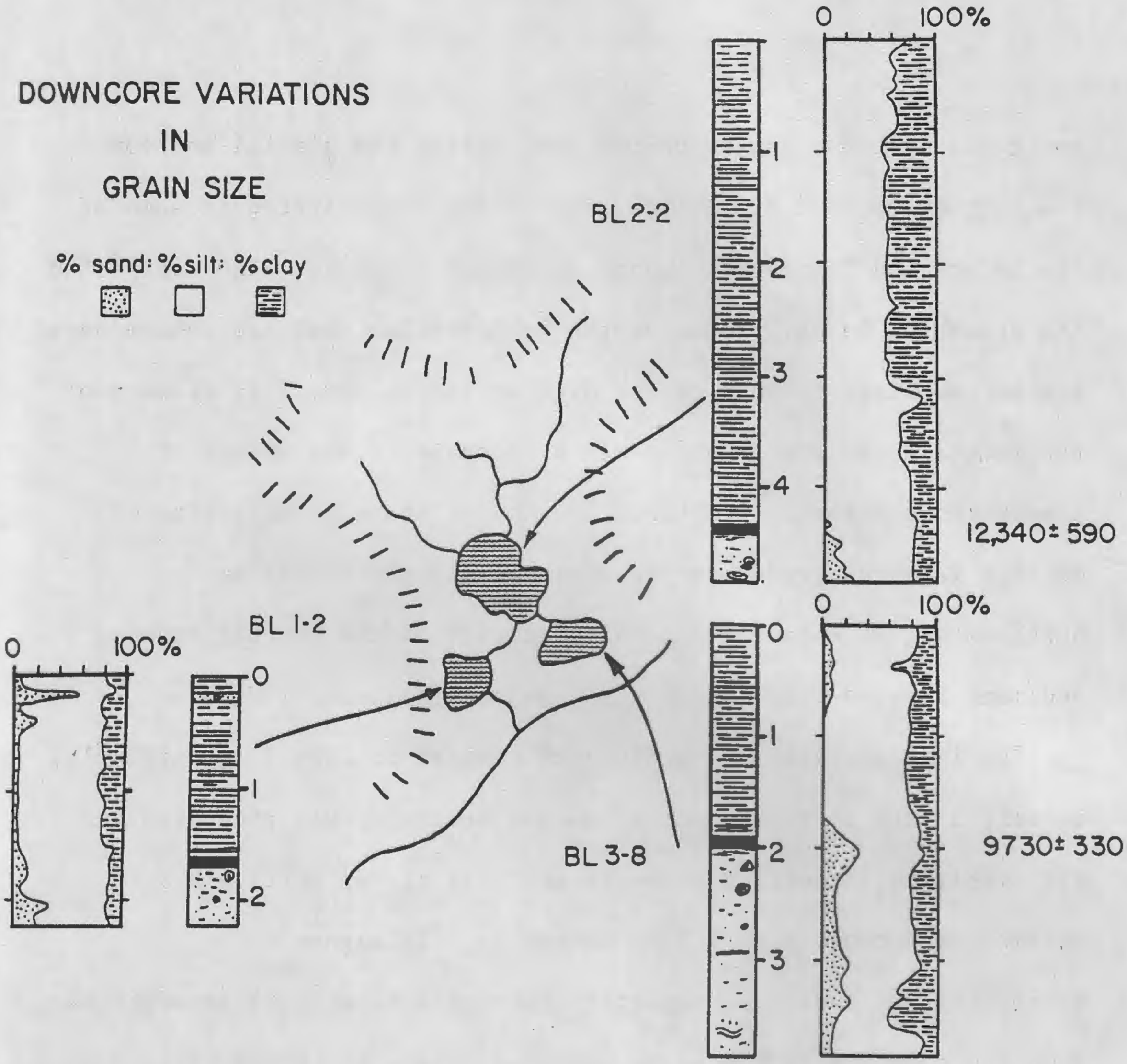

Figure 5. Downcore variations in grain size (% sand, silt,clay) in three cores from the Beaufort Lakes.

cm. England (1983) has suggested that during the glacial maximum (ca. 11,000 to 8000 B.P.), ice shelves may have existed in some of the inlets and fiords precluding driftwood entry and also restricted the growth of fauna, producing the barren silts that are common near the marine limit in some of the High Arctic inlets. This closure of the inlets would also resulted in a decrease in the amount of ice-rafted sediment. Additionally, the relatively small size of deltaic features graded to the marine limit shorelines on northeastern Ellesmere Island also attests to the limited fluvial sediment input during the glacial maximum (England, 1983).

The interpretation of grain size changes in Lake 2 is difficult, as only a very short segment of marine sediments was recovered and the overlying lacustrine sdiments are fine clayey silts wih a maximum sand content of 1 %. Changes in bulk magnetic susceptibility (which is magnetic grain size dependent) demonstrate some fluctuations in the basin hydrology since emergence (Fig. 6). A gradual upcore decrease in susceptibility, visible from 420 cm to the surface may reflect either overall decrease in availability of 62 um magnetite (Chernicoff, 1984) or a decrease in stream capacity since emergence (Bjorck et al., 1980; Thompson et al., 1980). Superimposed on this overall decreasing trend are minor susceptiblity inceases that may indicate periods of increased runoff due to warming and increased precipitation (260 cm, 230 cm, 100 cm), although it is difficult to estimate when these changes occurred.

In Lake 1, which emerged at approximately 2600 B.P., a gradual

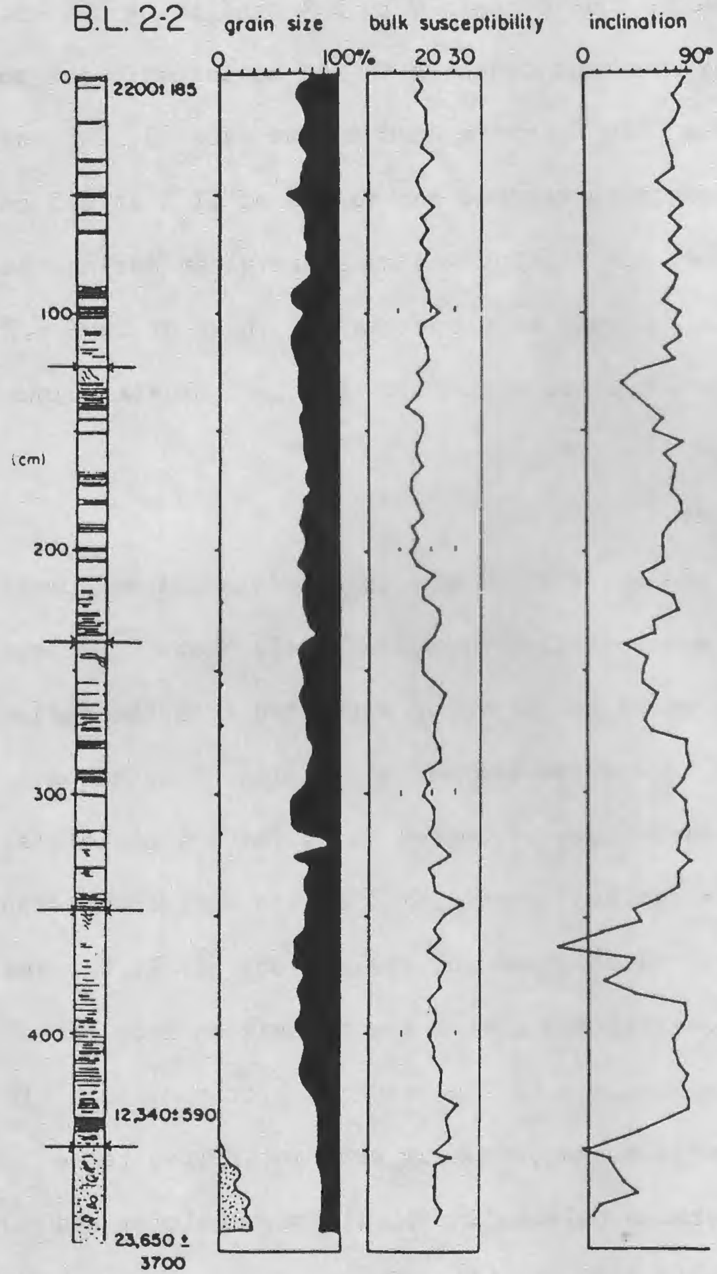

Figure 6. Paleomagnetic and lithostratigraphy of sediment core 2-2, Beaufort Lake 2.

transition from the marine sediments at 190 cm (14 % sand) occurs through the emergence contact (167 cm, 6 % sand) to the overlying lacustrine sediments that contain 0 to 3 % sand below 100 cm. Additionally, maximum sand contents in the marine unit are not as high as those from Lake 3 (where sand maxima are 23, 24, and 28 %). In Lake 1, sand contents reached one maxima of 21 % at 215 cm. This may illustrate that ice rafting was more prevalent during the emergence of Lake 3 (hence more open water) than at 2600 B.P., when Lake 1 emerged during a colder period with less fluvial input and extensive landfast sea ice.

Porewater chemistry

To estimate the water chemistry in the depositional environment during different sedimentation episodes in the basin, geochemical analyses were conducted on porewater extracted from the marine, transitional, and lacustrine sediments. Similar studies on depositional sequences have attempted to estimate depositional paleosalinities in various transitional environments. Ericsson (1972, 1973) extracted chloride and the cations Na, K, Ca, and Mg to estimate the paleosalinities during the transition from the freshwater Ancylus Ice Lake to the brackish Littorina Sea. In that study, chloride, sodium and potassium were determined to be inadequate to determine paleosalinity, although calcium and magnesium were considered valuable. The analyses were correlated to a diatom stratigraphy which paralleled changes in the geochemistry. Friedman and Gavish (1970) compared interstitial water with overlying waters in several transitional environments (shelf, lagoon, deltaic, estuarine, and salt marsh). Trends of various ions in their study show that, in several environments, porewaters had either higher or lower ionic concentrations than that of the overlying water column. Several factors that influence the ionic concentration present in the porewater including the composition of the inflowing water, geochemical conditions at the sediment/water interface, post-depositional exchange with clay minerals, dissolution and precipitation of minerals, and post-depositional diffusion of porewaters.

The analysis of porewaters from Lake 2 (Fig.7) shows very slight changes downcore; however, small increases in all the ions are seen at the 400-cm level in the lacustrine unit. The values for Na range from a low of 26 ppm at 145 cm to a high of 91 ppm at 425 cm. A single sample from the marine unit in this core was only 35 ppm. A similar parallel increase at 425 cm is also seen for potassium. Concentrations of calcium and magnesium in this lake are the lowest of the three lakes with ranges of 15 to 62 ppm and 5 to 17 ppm, respectively. Chloride concentrations vary in parallel with Na and K and are less than 200 ppm.

Porewater chemistry from Lake 1 (core 1-1, Fig. 8) shows the greatest variations through the sedimentary sequence. Average sodium values decrease from the marine (210 ppm) to transitional (188 ppm) to the lacustrine sediments (43 ppm). Parallel decreases are seen for K (74 to 71 to 10 ppm) and Mg (210 to 244 to 9 ppm). Calcium ion trends do not parallel the other three; a distinct decrease is seen in the black transition unit. A marked decrease of Ca from 1039 ppm in the marine facies to 9 ppm in the lacustrine sediments demonstrates a salinity decrease. Chloride shows similar

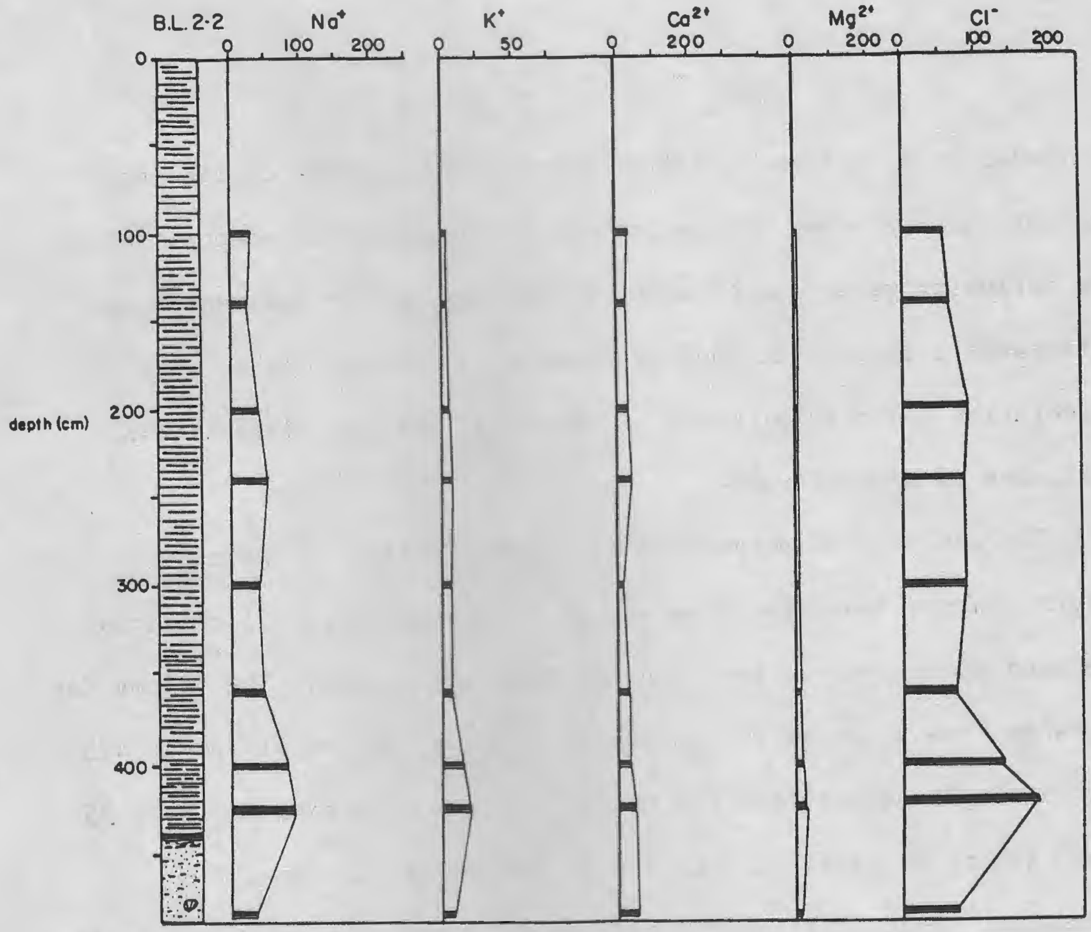

Figure 7. Porewater ionic concentration (in ppm) plotted versus depth downcore. Core 2-2, Lake 2.

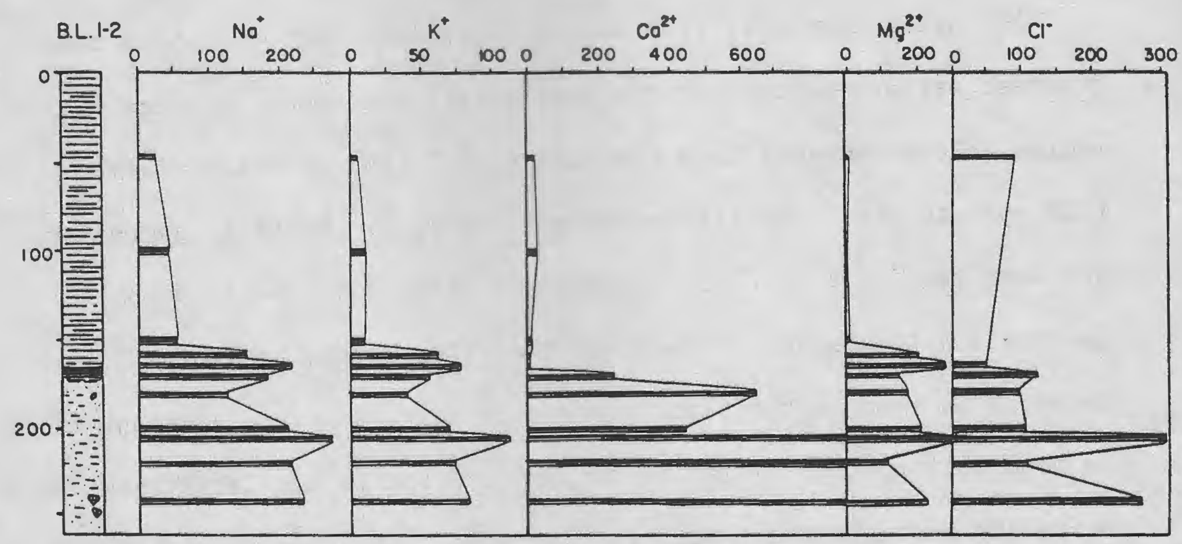

Figure 8: Porewater ionic concentration (in ppm) plotted versus depth downcore. Core 1-2, Lake 1.

fluctuations as the cation concentrations. The highest values for chloride in the three lakes are found in the glaciomarine unit in Lake 1 reaching approximately 300 ppm.

The present day waters of Lake 3 have the highest ionic concentration of the three lakes, however the porewater concentrations are neither the most concentrated nor do they show abrupt gradients at the lacustrine-marine transition. High Ca concentrations in both cores from this lake are found at or below the transition zones from the cores. Values exceed 1600 ppm, and Ca concentration is thus more concentrated than in sea water (1290 ppm). Slight decreases for Na, K, and Mg are found at the lacustrine-marine contact and above in cores 3-4 and 3-5 (Figs. 9 and 10). Mean values for the lacustrine, transition, and marine sediments all indicate slightly higher concentrations downcore in the marine unit.

In all these lakes, it is evident that ionic concentrations in the marine unit interstitial waters are lower than those of sea water, and that porewaters in the lacustrine sediments are more concentrated than the overlying lake waters. Thus, downcore profiles of ionic concentrations do not accurately represent paleosalinities of the depositional waters. Moreover, the actual concentrations and downcore profiles differ significantly among the three basins. To ascertain whether these changes represent a simple dilution of seawater during the evolution of the basin, or an interaction of the porewaters with the solid phase of

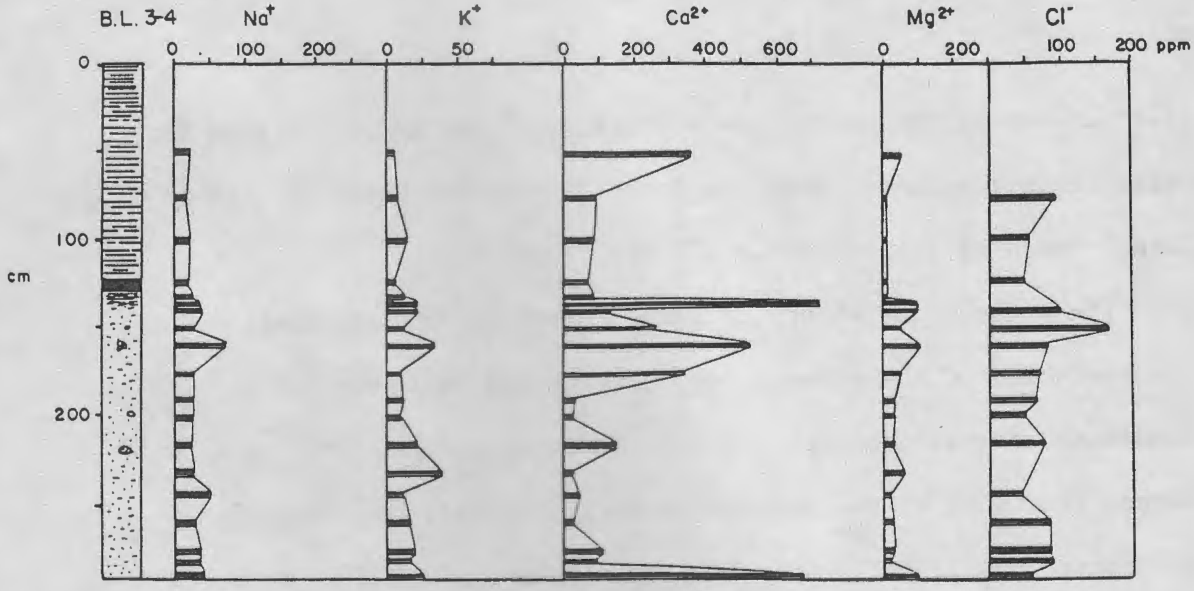

Figure 9 Porewater ionic concentration (in ppm) plotted versus depth downcore. Core 3-4. Lake 3.

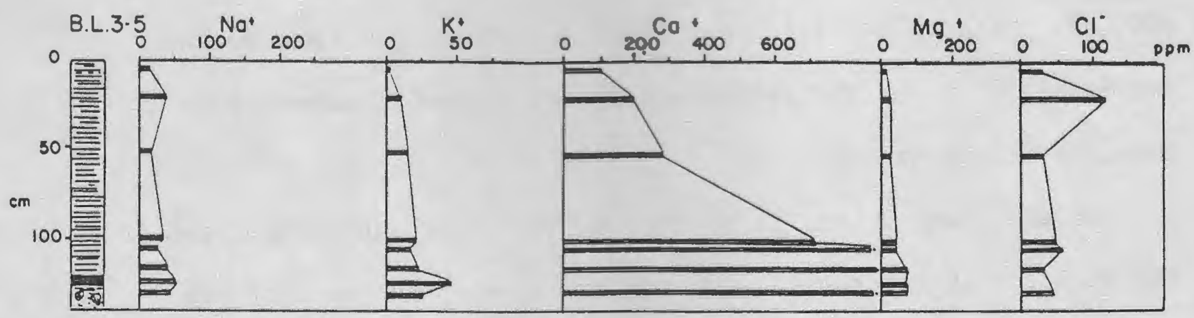

Figure 10 Porewater ionic concentration (in ppm) plotted versus depth downcore. Core 3-5, Lake 3.

the sediments, cation concentrations were normalized to chloride, a relatively conservative ion which does not enter into the same exchange reactions as the cations. If simple dilution of the seawater was the cause of the variation, as in fiord waters (Knight, 1971), cation/chloride ratios would essentially remain the same as in sea water (Tepper, 1980).

Figures 11 and 12 show downcore variations in the cation/chloride ratios relative to the ratios of mean ocean water, overlying lake water, and snowmelt runoff values from the inlet of Lake 2. The profiles of cores from lakes 2 and 3 indicate that the cations, except for Na, are enriched with respect to chloride in the marine sediment porewaters, as compared to the ocean cation to chloride ratios. Sodium varies closely around the mean for ocean waters in all three cores from lakes 2 and 3 (Figs. 11 and 12), and thus appears to be a simple dilution of sea water, unaffected by other post-depositional changes. Potassium/chloride ratios are variable within the three lakes. In Lake 2, the ratio is equal to or slightly greater than lake water, while in Lake 3 (core 3-4) the ratio is lower than the lacustrine waters. In Lake 1, the ratios are much greater than ocean water. Calcium in the marine sediments is enriched compared to ocean water; however, the ratio is much lower than that in present lake water and more closely approximates that of the inlet water. Magnesium/chloride ratios follow approximately the same trend as calcium/chloride, indicating enrichment relative to marine waters and depletion relative to

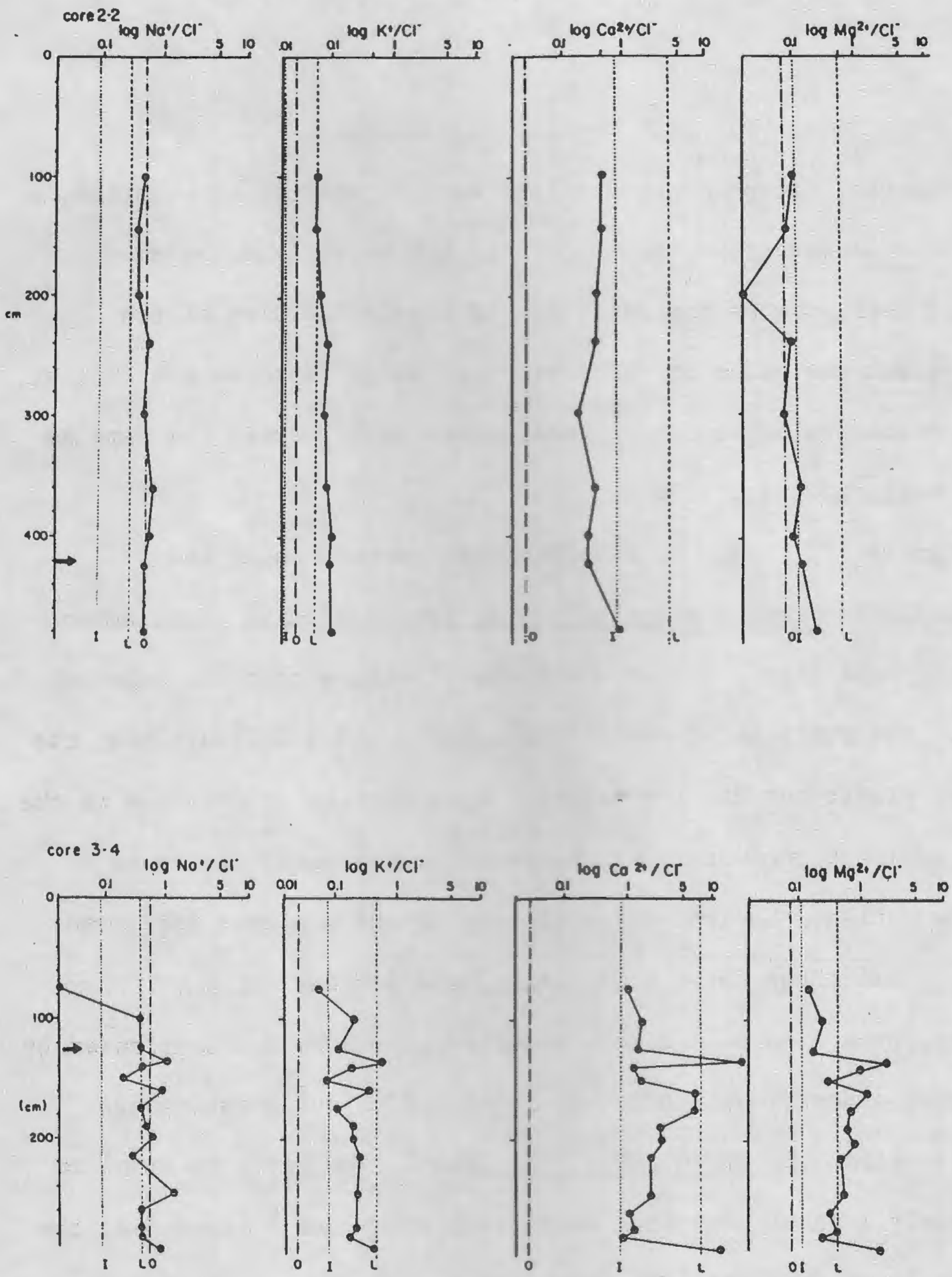

Figure 11 : Cation/chloride ratios of interstitial waters from cores2-2 & 3-4 plotted versus depth downcore. Arrow on left represents the location of lacustrine-marine transition in the core sediments. Line L = ratio of cation to chloride in present-day lake water. Line O = ratio of cation to chloride in ocean water. Line I = ratio of cation to chloride in inlet water from Lake 2.

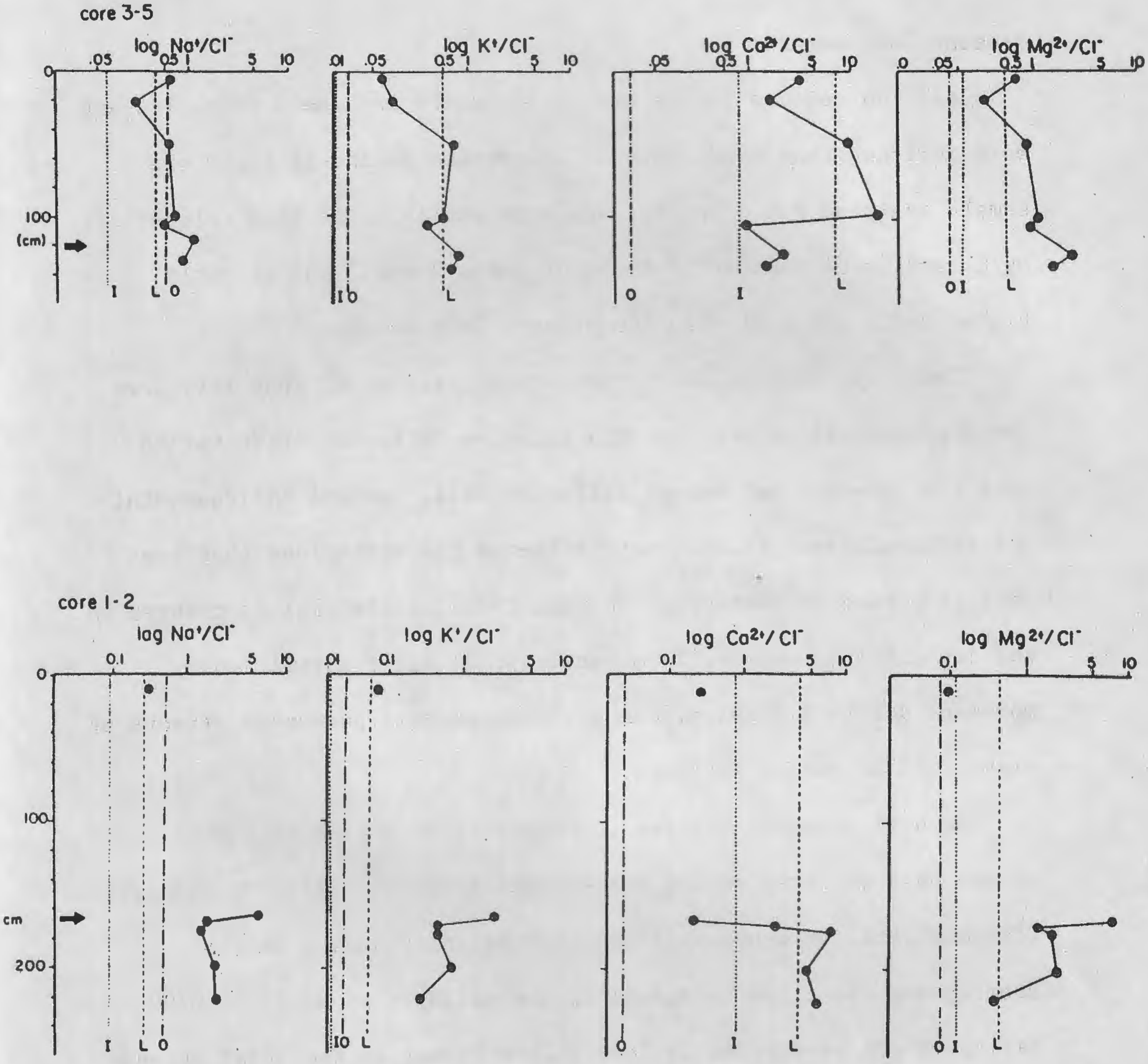

Figure 12 : Cation/chloride ratios of interstitial waters from cores 3-5 & 1-2 plotted versus depth downcore. Arrow on left represents the location of lacustrine-marine transition in the core sediments. Line L = cation/chloride ratio in present-day lake water. Line O = cation/chloride ratio in ocean water. Line I = cation/chloride ratio from inlet water of Lake 2.

present lake waters.

All the cations in the marine sediments in Lake 1 (Fig. 12) are more enriched than ocean water. Lacustrine sediments (only one sample analyzed for chloride) are more variable but show values for Mg/Cl and Ca/Cl similar to those of Lakes 2 and 3 and slightly higher Na/Cl and K/Cl than the present lake waters.

Thus, not only do the actual concentrations of ions vary from the depositional waters, but the relative cation:chloride ratios from the interstitial waters differ as well. Several environmental and sedimentologic factors may influence the variations that are seen in porewater chemistry (Sharma, 1970), including: 1) changes in the depositional waters, 2) mineralogy, 3) differential ionic movement due to diffusion, compaction, and semi-permeable effects of clays, and 4) cation exchange.

Several distinct changes in chemistry of the depositional waters have occurred during the evolution of the basin. Microfossil (foraminifera) evidence suggests that salinity during marine submergence was close to normal marine salinity of 33 to 34 0/00. Marine waters were probably less saline closer to the inlet streams near the margin of Lake 2, yet the cations were diluted in proportion to sea water, as in fiord water (Knight, 1971). As isostatic uplift progressed, estuarine conditions would have prevailed and chemical stratification would have developed (Rust and Coakley, 1970). At that time, exchange of sea water would have occurred until the basin thresholds emerged beyond the highest tidal range. Saline conditions probably existed at the sediment-water interface after the basin was isolated as a lake. Remnant sea water, trapped in lake bottoms since emergence, has been discovered in several high latitude lakes on northern Ellesmere Island (Hattersley-Smith et al., 1970; Jeffries et al., 1984) one of which had bottom water dated at 3000 years B.P. (Long, 1967). Other chemically stratified arctic lakes of this type have been reported in Norway (Strom, 1957, 1961). Saline conditions were probably prevalent long after emergence, but this changed as the chemocline dissipated due to diffusion (Jeffries et al., 1984).

Changes in the lake chemistry have occurred since emergence either by mixing of old sea water, once isolated at the base of the lake, with freshwater or by evaporative concentration. A combination of these factors possibly explains the differences in Lake 3 from the other lakes, as it has much less freshwater input and a very restricted, shallow outlet.

Many previous studies have also indicated that mineralogic composition dictates the interstitial water composition, either by dissolution of the solid phase contributing to the porewater, precipitation depleting the porewater, or by cation exchange (Siever et al., 1964; Friedman and Gavish, 1970; Sharma, 1970; Sayles, 1979). Friedman and Gavish (1970) report decreasing cation/chloride ratios for magnesium, potassium, and sodium, which all move into exchange positions in the surface sediments. It is suggested that Na ions undergo rapid exchange with Ca at the sediment/water interface as fluvially entrained sediments enter the sea (Sharma, 1970). Other studies have provided conflicting evidence, citing dissolution of K from potassium feldspar, which increases the concentration in the pore fluids (Siever et al., 1964; Friedman and Gavish, 1970) Increases in calcium may be attributed to dissolution of sand- and silt-size hornblende and biotite (Sharma, 1970).

In the Beaufort Lakes porewater studies, all the ions in the marine sediments appear to have been enriched compared to the cation/chloride ratios in sea water, with the exclusion of sodium in Lakes 2 and 3, which appears to be rather conservative. As mentioned above, the clay mineralogy is a chlorite-illite detrital assemblage, which would probably deplete Mg and K by adsorption. However, there are no correlations between the clay mineral assemblages and the porewater cation concentrations in the sediments, with the possible exception of the cores from Lake 3. These cores demonstrate that there is twice as much illite as chlorite than in the other two lakes. The water chemistry in this lake is several times more concentrated than the other lakes, possibly indicating a longer residence time of old sea water and a prolonged interaction of the sediments with more saline solutions. Cation exchange studies may prove some of this variance.

A likely contributor to high concentrations of calcium and magnesium in the sediments and waters of the lake is dissolved carbonate from the underlying calcium carbonate and dolomite-cemented Imina Formation. In some instances, especially below the lacustrine-marine contact in cores from Lakes 1 and 3, calcium concentrations exceed that of sea water. Magnesium concentrations are below those of sea water; however, the magnesium/chloride ratios exceed marine values.

A very important factor in the variation in porewater chemistry is the post-depositional diffusion and migration of the porewaters, influenced by sediment compaction and flow of groundwater through the sediment column. This factor may explain major changes in both the original concentrations below the sediment/water interface and later alteration by dilution after the basin has been isolated from the sea. During sediment compaction, cation concentrations may be increased by clay minerals and other fine particles acting as semi-permeable membranes, allowing passage of water and retaining ions (DeSitter, 1947; Siever et al., 1964;. Sharma, 1970). The results of this process are difficult to quantify, however, due to variations in mineralogy, grain size, and overburden pressure.

Post-depositional diffusion due to the flow of groundwater, however, is probably a more influential and obvious factor in this study. Downcore chemical profiles (Figs. 7 to 10) illustrate that the diffusion effect has progressively altered the porewater composition since the emergence of the basins from the sea. Profiles from Lakes 2 and 3 (Figs. 7 , 9 and 10) are essentially isochemical downcore, the marine units having no greater concentration than the lacustrine sediments. Lake 1, however, shows abrupt concentration changes at the lacustrine-marine transition

(Fig. 7). This illustrates that Lake 1, which probably emerged from the sea over 2000 years after the other lakes (Retelle, 1985a) has been less affected by post-depositional fluid migration through the sediment column. Porewaters driven out of the marine sediments would migrate upwards through the lacustrine sediment and enrich these sediments relative to the overlying lacustrine waters (Fig. 13). This type of migration has been documented in a temperate lake in southern Canada (Frape and Patterson, 1981), where a tritium-contaminated groundwater plume has migrated down the hydrologic gradient from a waste site into sediments underlying a lake. Interstitial waters from deep in the sediment column migrated vertically through the sediments in the middle of the lake and at more of a shallow trajectory near the shore. Vertical migration such as this could indeed have had an effect on the porewater assemblage of the Beaufort Lakes cores, as most of the cores were recovered in the centers of the lake basins.

Paleontology

Evidence from micro- and macrofossil assemblages from the core sediments further demonstrate that the porewater ionic concentrations do not reflect the original depositional salinities.

In Lake 3 (cores 3-4 and 3-5) the marine microfauna was sampled at about 10 cm below the lacustrine-marine contact. The assemblage was dominated by Islandiella helenae ,a species abundant in High Arctic water with salinities of 33 to 34 0/00. In contrast, an

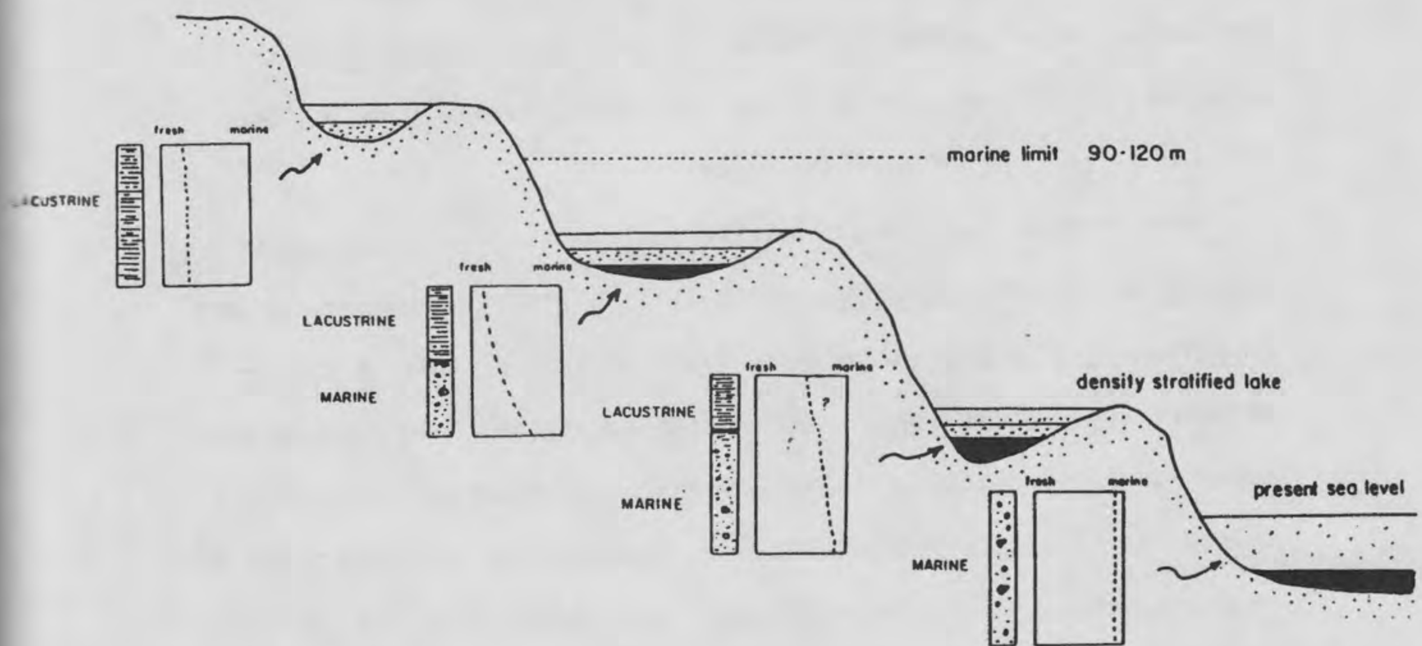

Figure 13. Hypothetical model for the post-depositional diffusion of porewaters in lakes that were formerly isostatically depressed below sea level.

analysis of sediments directly below the emergence contact in Lake 1 shows that estuarine conditions prevailed during the isolation of the basin (Vilks, pers. comm., 1983). It is highly possible that the normal marine assemblage below the emergence contact in Lake 3 is unconformably exposed, with the estuarine sediments having been removed by iceberg or fast ice scour.

Macrofossils found in the marine sediments include Portlandia arctica and Astarte borealis , both with paired valves and in growth position. Portlandia valves were found in growth position in the sediment cores among forams repesenting estuarine (Lake 1 core) and normal marine conditions (Lake 3 cores), demonstrating the variable conditions tolerated by this species. This bivalve was also found in growth position within the black sulfidic sediments of the emergence zone in the cores, further illustrating its tolerance for low salinity conditions. Portlandia have been recovered from fiords in eastern Baffin Island in water depths up to 230 m (approximately 0° C) with bottom water salinities of 30 to 32 0/00 (Gilbert, 1982). In contrast, Spjeldnaes (1978) describes that the Portlandia community lived in a layer of "fiord water" at 0°to 5°C and salinity $\leq$ 25 0/00 at depths up to 200 m in Oslo Fiord. As the Portlandia valves were found within approximately 20 cm of the marine-lacustrine emergence contact in the cores, the inferred water depths for these communities ranges from 10 to 30 m, which is at or slightly deeper than the present water depths of the lakes.

Summary

The sedimentary sequence in the Beaufort Lakes basin represents glaciomarine sedimentation followed by progressive uplift and isolation of the three lakes from the sea and subsequent lacustrine sedimentation. A transitional facies between the marine and lacustrine units in each basin represents a period during which denser saline bottom water lay beneath freshwater of the newly formed lake basin. Sedimentological and paleontological evidence from the sediment cores demonstrate periods when sea ice was mobile, fluvial input was increased, and the embayments were relatively open. These findings can be correlated with other evidence for Holocene climatic change in the arctic regions.

Pre-8000 B.P.

Prior to initial isostatic emergence in the Robeson Channel area, the sea stood at the marine limit in the Beaufort Lakes basin (116 m, Fig. 14). At this time, northwest Greenland ice and interior Ellesmere Island ice masses were at their last glacial limit, separated by a 100-km corridor. In the Beaufort Lakes embayment, the marine limit shoreline (dated at 8050 ± 120 and 8255 ± 215 B.P.) consists of a poorly defined gravelly washing limit overlying glaciomarine silts. The fossil assemblage that was dated includes a relatively sparse collection of *Hiatella arctica* and *Portlandia arctica* in growth position at 90 to 95 m. Beaches at the marine limit in other nearby embayments (Retelle,1985b) were also

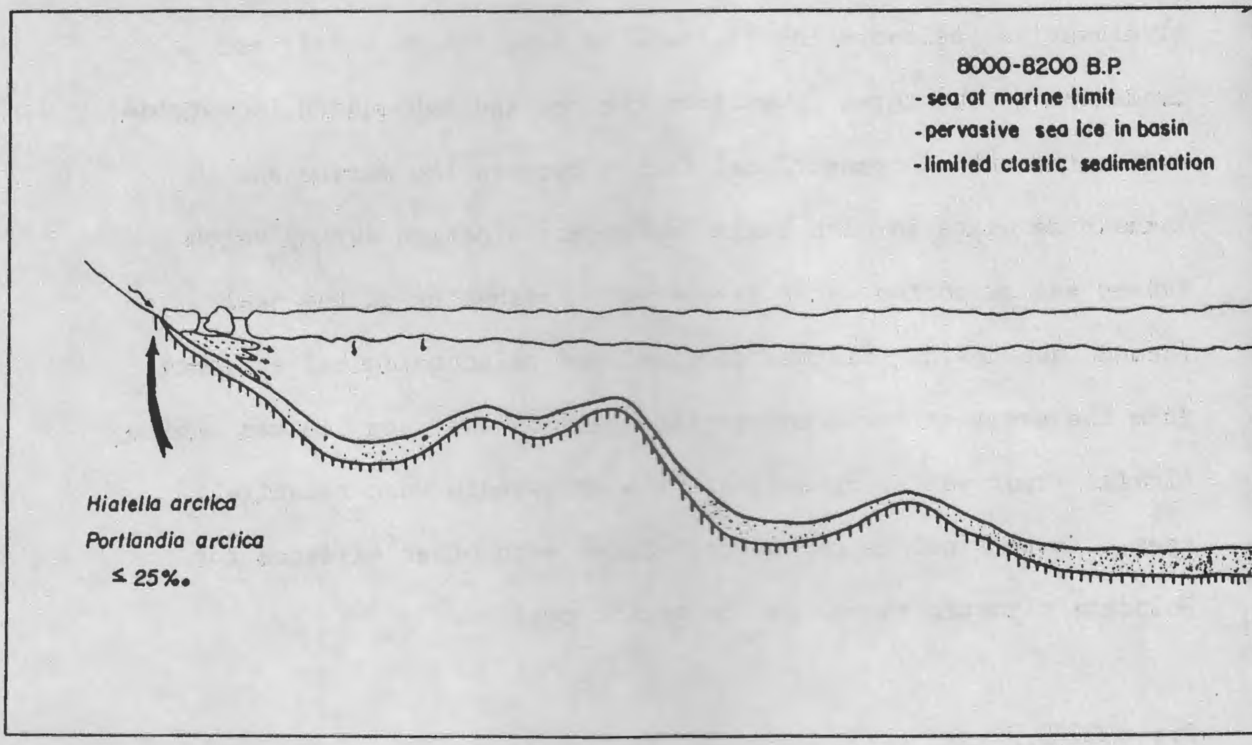

Figure 14: Environmental conditions in the Beaufort Lakes Basin during the last glacial maximum, ca. 8000 to 8200 B.P.

poorly develop ed and contained a sparser fauna in comparison to younger, lower elevation marine deposits. England (1983) interpreted the presence of "barren silts" prevalent in some of the inlets of northeastern Ellesmere Island as due to pervasive landfast sea ice or ice shelves that seal off the inlets and fiords and inhibit faunal occupation and driftwood penetration. Sediments from the base of core 3-8 (Lake 3) demonstrate a period when ice rafting and fluvial input decreased due to climatic deterioration during the glacial maximum. No macrofossils were found at lower depths (below 3 m) in this core, further suggesting that condiions were unfavorable for fauna in deeper portions of the embayment (ca. 100 m depth) although the presence of _Hiatella arctica_ and _Portlandia arctica_ near the shoreline of the embayment may indicate an open shallow lead where a marginal community could live.

6000 to 7000 B.P.

Initial isostatic uplift in the Robeson Channel area resulted from the retreat of Greenland and Ellesmere Island ice from their maximum last glacial stands at around 8000 B.P.(Retelle, 1985b). As climate ameliorated in the High Arctic and glacier retreat progressed more rapidly, uplift proceeded at a faster rate (Retelle, 1985a).

The basins of Lakes 2 and 3 emerged during this period of climatic warming (ca. 5600 B.P., Fig. 15). The warming of climate and subsequent breakup of sea ice in the inlets can be demonstrated by the increased sand contents in the Lake 3 cores. This is

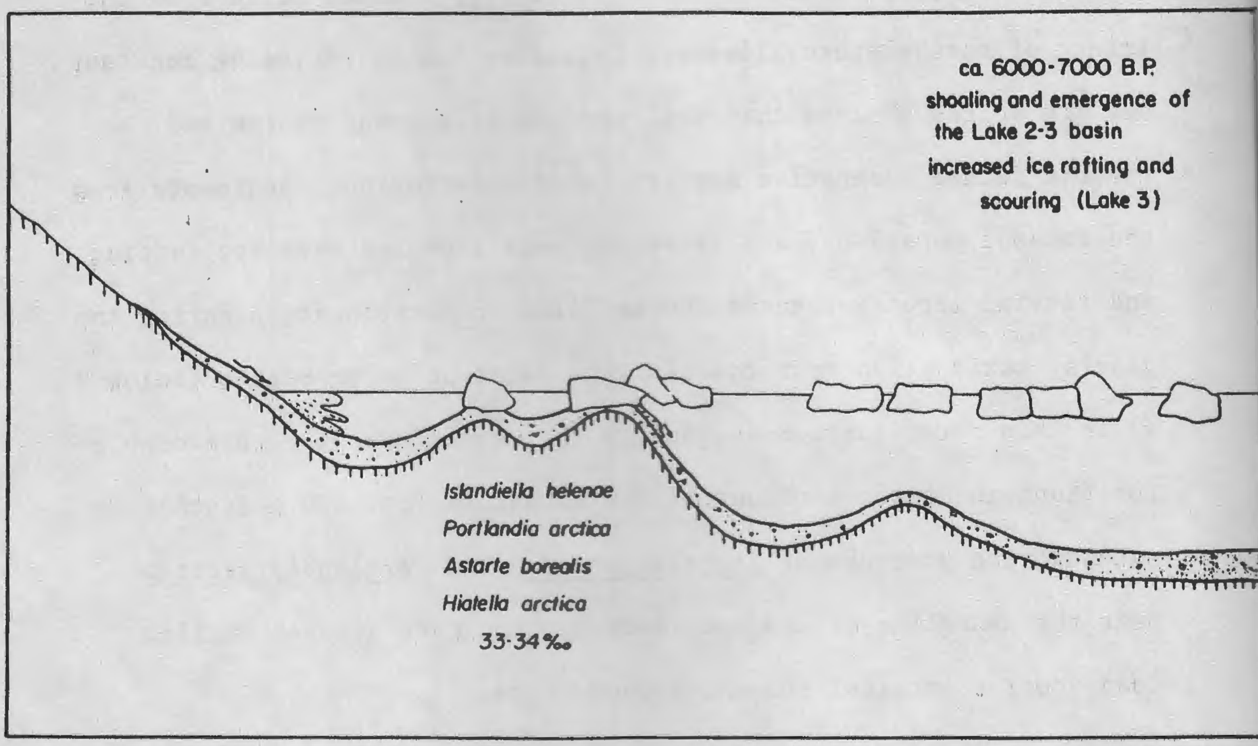

Figure 15: Environmental conditions in the Beaufort Lakes Basin during the shoaling and emergence of Lakes 2 and 3 (ca. 6000-7000 B.P.).

presumably due to increased runoff and ice rafting. In addition, macrofauna are relatively abundant in the cores, with the occurrence of Portlandia arctica, Astarte borealis and several gastropod species. Microfauna indicate normal marine salinities in the basin at this time.

Evidence from other areas in the arctic regions demonstrate climatic warming during this period. Because of the breakup of sea ice between 6000 and 4200 B.P., driftwood penetrated High Arctic fiords and inlet with greater ease (Stewart and England, 1983). Similarly, because of the generally more open circulation in the northern seas, drifted pumice accumulated on shorelines that dated ca. 5000 B.P. on southern Ellesmere Island and Devon Island and in Spitsbergen on shorelines that date between 4800 and 7000 B.P. (Blake, 1970).

Stewart and England (1983) also report that the marine bivalve Limatula subauriculata, a subarctic mollusc normally found below 72° N inhabited a north coast fiord on Ellesmere Island at ca 6400 B.P. Similar northerly range extensions of the species Mytilus edulis, Macoma balthica, and Chlamys islandicus have occurred in the north Atlantic and Arctic waters due to the northward encroachment of warmer Atlantic waters between 8200 and 2800 B.P. (Andrews, 1972).

The oxygen isotope record from ice cores from the Greenland Ice Sheet and various ice caps in the Canadian Arctic concur with evidence cited above that suggests an early to mid-Holocene warm period. The isotope record from the Camp Century ice core

(Dansgaard et al., 1970) shows $\delta^{18}O$ maxima (> -29 0/00) between 7000 and 4400 B.P. The Devon Island ice core record (Paterson et al., 1977; Fisher and Koerner, 1980) shows trends broadly similar to the Camp Century core, with the Climatic Optimum occurring at ca 5000 B.P. The isotope record from both cores indicates a deterioration or cooling trend from the mid-Holocene toward the present.

ca.3000 B.P. to present

The Lake 1 basin emerged from the sea during a period of climatic cooling that followed the mid-Holocene Climatic Optimum. In the High Arctic, this cooling is seen in the ice-core records, the relative scarcity of driftwood due to an increase in landfast sea ice (Stewart and England, 1983), and late Holocene glacier advances (Hattersley-Smith et al., 1955; Blake, 1975; Davis, 1980).

Sedimentologic evidence from the Lake 1 basin demonstrates a period of moderately coarse sediment influx prior to the lake emergence (Fig. 5) and a gradual transition from coarse to fine sedimentation through the emergence contact. The decrease in coarse material during emergence may indicate the formation of landfast sea ice, which sealed off the basin during this colder period (Fig.16). The stabilization of ice in the embayment would preclude the entry of icebergs carrying sediment, as well as decrease the coarse sediment input from erosion of the shorelines and basin thresholds by mobile sea ice. The microfaunal assemblage below the transition sediments reflects estuarine conditions during emergence of the

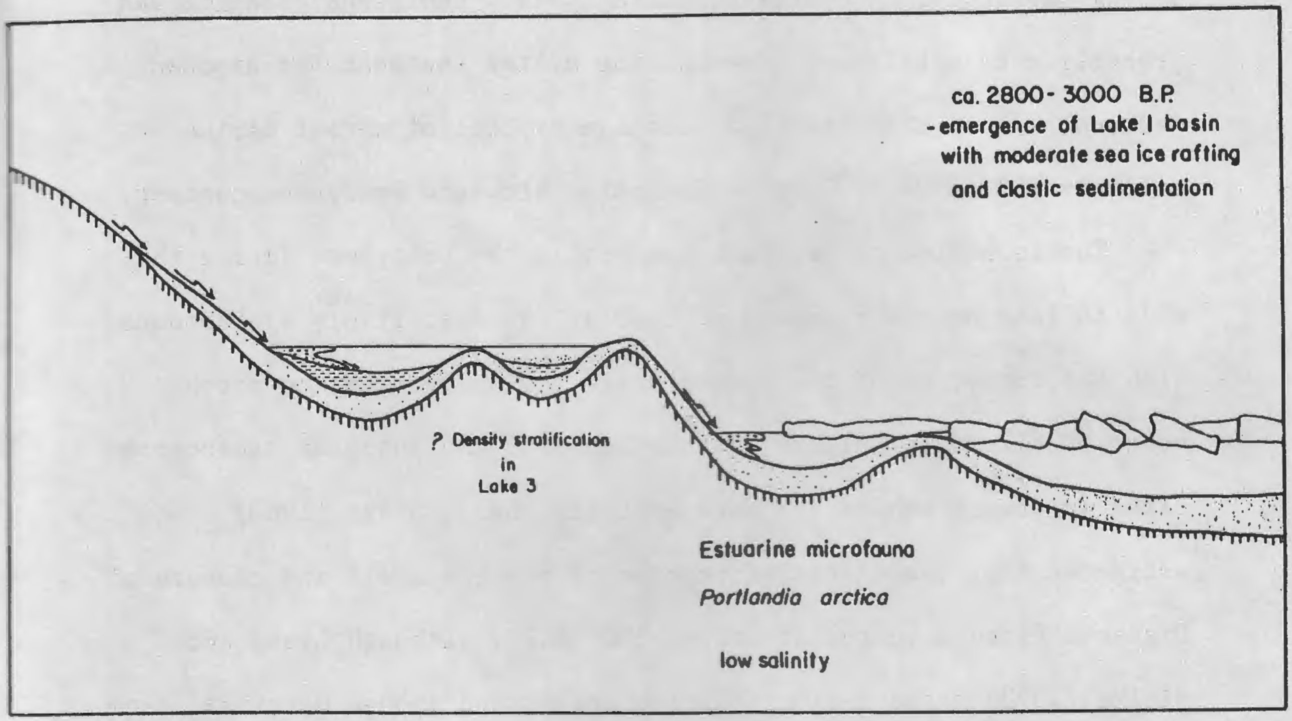

Figure 16: Environmental conditions in the Beaufort Lakes Basin during the emergence of Lake 1 (ca. 2800-3000 B.P.).

basin. The presence of this fauna immediately below the contact further illustrates that scouring did not occur on the sediment bed during emergence. In contrast, during Lake 3 emergence, sea ice was probably more mobile and ice-scouring of the sediment bed exposed sediment with a microfossil assemblage typical of normal marine salinity (33 to 34 0/00) unconformably below the emergence contact.

The formation of landfast sea ice in the embayment during the mid- to late Holocene period of cooling was most likely synchronous with the formation of the larger scale ice shelves on the north coast of Ellesmere Island. On the basis of the youngest radiocarbon dated driftwood behind the Ward Hunt Ice Shelf, Crary (1960) estimates that the initial formation of the ice shelf and closure of Disraeli Fiord occurred at around 3000 B.P., although Lyons and Mielke (1973) dated marine fossils (shells and sponge material) from basal layers of the ice shelf and indicate that initial formation was underway by at least 3700 B.P. Likewise, driftwood exclusion from Clements Markham Inlet, also on the north coast of Ellesmere Island, began at ca. 4200 B.P. Hence, the trends of decreasing coarse sediment input in the Lake 1 basin prior to emergence at around 2600 B.P. probably reflect the same cooling cooling trends seen in other climate proxy records for the period prior to 3000 B.P.

REFERENCES

Andrews, J.T., 1972. Recent and fossil growth rates of marine bivalves, Canadian Arctic, and Late Quaternary Arctic marine environments. Paleogeography, Paleoclimatology and Paleoecology, 11, 157-176.

Berner, R.A., 1970a. Pleistocene sea levels possibly indicated by buried black sediment in the Black Sea. Nature, 227, 700.

Berner, R.A., 1970b. Sedimentary pyrite formation. American J. Science, 268, 1-23.

Bjorck, S., Dearing, J.A. and Johsson, A., 1980. Magnetic susceptibility of Late Weichselian deposits in southeastern Sweden. Boreas, 11, 99-111.

Blake, W. Jr., 1970. Studies of glacial history in Arctic Canada, I. Pumice, radiocarbon dates and differential postglacial uplift in eastern Queen Elibaeth Islands. Canadian J. Earth Science, 7, 634-664.

Blake, W. Jr., 1975. Radiocarbon age determinations and postglacial emergence at Cape Storm, southern Ellesmere Island, Arctic Canada. Geografiska Annaler, 57A, 1-71.

Bradley, R.S., 1978. Recent climatic fluctuations of the Canadian High Arctic and their significance for glaciology. Arctic and Alpine Research, 10, 715-731.

Bradley, R.S. and England, J.H., 1979. Synoptic climatology of the

Canadian High Arctic. Geografiska Annaler, 61A (3-4), 187-201.

Chernicoff, S.E., 1984. Using isotropic magnetic susceptibility to delineate glacial tills. J. Geology, 92, 113-118.

Coakley, J.P. and Rust, B.R., 1968. Sedimentation in an arctic lake. J. Sedimentary Petrology, 38, 1290-1300.

Crary, A.P., 1960. Some remarks on glaciers and climate in northern Ellesmere Island. Geografiska Annaler, XLVII, 45-48.

Davies, W.E., 1963. Glacial geology of northern Greenland. Polarforschung, 5, 94-103.

Davis, P.T., 1980. Late glacial, vegetational, and climatic history of Pangnirtung and Kingnait Fiord area, Baffin Island, N.W.T., Canada. Unpublished Ph.D. dissertation, University of Colorado, Boulder.

DeSitter, L.U., 1947. Diagenesis of oil field brines. American Association of Petroleum Geologists Bulletin, 31, 2030-2040.

England, John, 1978. The glacial geology of northeastern Ellesmere Island, N.W.T., Canada. Canadian J. Earth Science, 15, 603-617.

England, John, 1983. Isostatic adjustments in a full glacial sea. Canadian J. Earth Science, 20, 895-917.

England, J., Bradley,R.S. and Stuckenrath, R.S., 1981. Multiple glaciations and marine transgressions, western Kennedy Channel, Northwest Territories, Canada. Boreas, 10, 71-89.

Ericsson, B., 1972. The chlorinity of clays as a criterion of paleosalinity. Geologisches Foreningens Stockholm Forhandlingar, 94, 5-21.

Ericsson, B., 1973. The cation content of Swedish post-glacial sediments as a criterion of paleosalinity. Geologisches Foreningens i Stockholm Forhandlingar, 95, 181-220.

Frape, S.K. and Patterson, R.J., 1981. Chemistry of interstitial water and bottom sediments as indicators of seepage patterns in Perch Lake, Chalk River, Ontario. Limnology and Oceanography, 26(3), 500-517.

Freidman, G.M. and Gavish, E., 1970. Chemical changes in interstitial waters from sediment of lagoonal, deltaic, river, estuarine and saltmarsh and cove environments. J. Sedimentary Petrology, 40, 930-953.

Gustavson, T.C., 1975. Sedimentation and physical limnology in proglacial Malaspina Lake, southeastern Alaska. pp. 249-263 in Jopling, AQ.V./ and McDonald, B.C. (eds.), Glaciofluvial and Glaciolacustrine Sedimentation. Society of Economic Paleontologists and Mineralogists, Special Publication Number 23.

Hattersley-Smith, G. and other members of the expedition, 1955. Northern Ellesmere Island, 1953 and 1954. Arctic, 8(1), 2-36.

Hattersley-Smith,G., Keys, J.E., Serson, H. and Mielke, J.E. 1970. Density-stratified lakes in northern Ellesmere Island. Nature, 225, 55-56.

Hoskin, C.M. and Burrell, D.C., 1972. Sediment transport and accumulatrion in a fiord basin, Glacier Bay, Alaska. J. Geology, 80, 539-551.

Hyvarinen, H., 1970. Flandrian pollen diagrams from Svalbard. Geografiska Annaler, 52A, 213-222.

Jeffries, M.O., Krause, H.R., Shakur, M.A. and Harris, S., 1984. Isotope geochemistry of stratified Lake A, Ellesmere Island, N.W.T., Canada. Canadian J. Earth Science, 21, 1008-1017.

Knight, R.J., 1971. Distributional trends in the recent marine sediments of Tasiujaq Cove of Ekalugad Fiord, Baffin Island, N.W.T. Maritime Sediments, 7, 1-18.

Long, A., 1967. Age of trapped water at bottom of Lake Tuborg, Ellesmere Island, N.W.T. (abs.). Transactions of the American Geophysical Union, 48, 136.

Lyons, J.T. and Mielke, 1973. Holocene history of a portion of northernmost Ellesmere Island. Arctic, 26, 314-323.

Patterson, R.J., Frape, S.K.,Dykes, L.S. and McLeod, R.A., 1978. A coring and squeezing technique for the detailed study of subsurface water chemistry. Canadian J. Earth Science, 15, 162-169.

Patterson, W.S.B., Koerner, R.M., Fisher, D., Johnsen, S.J., Clausen, H.B., Dansgaard, W., Bucher, P. and Oeschger, H., 1977. An oxygen isotope climatic record from the Devon Island Ice Cap, Arctic Canada. Nature, 266, 508-511.

Reimnitz, E., Toimil, L. and Barnes, P., 1978. Arctic continental shelf morphology related to sea-ice zonation, Beaufort Sea Alaska. Marine Geology, 28, 179-210.

Retelle, M.J., 1983. Glacial geology and Quaternary marine stratigraphy, northeastern Ellesmere Island, N.W.T., Canada. Abstracts, 12th Annual Arctic Workshop, University of Massachusetts, Department of Geology and Geography Contribution No. 44.

Retelle, M.J., 1985a. A comparison of emergence chronologies from raised marine sediments and sediments in isostatically adjusted coastal lake basins along Robeson Channel. Chapter 3 in Glacial Geology and Quaternary Marine and Lacustrine Stratigraphy of the Robeson Channel Area, northeastern Ellesmere Island, N.W.T., Canada. Unpublished Ph.D. thesis, Department of Geology and Geography, University of Massachusetts, Amherst.

Retelle, M.J., 1985b. Glácial geology and Quaternary marine stratigraphy: Robeson Channel area, northeastern Ellesmere Island, N.W.T., Canada. Chapter One in Glácial Geological and Glacio-Climatic Studies in the Canadian High Arctic, Department of Geology and Geography Contribution No. 49, University of Massachusetts, Amherst.

Rust, B.R., and Coakley, J.P., 1970. Physico-chemical characteristics and postglacial desalination of Stanwell-Fletcher Lake, Arctic Canada. Canadian J. EarthScience, 7, 900-911.

Sayles, F.L., 1979. The composition and diagenesis of interstitial solutions I. Fluxes across the seawater-sediment interface in the Atlantic Ocean. Geochimica et Cosmochimica Acta, 43, 527-545.

Sharma,G.D., 1970. Evolution of interstitial waters in recent Alaskan sediments. J. Sedimentary Petrology, 40(2), 722-733.

Shaw, J., Gilbert, R. and Archer, J.J., 1978. Proglacial lacustrine sedimentation during winter. Arctic and Alpine Research, 10(4), 689-699.

Siever, R., Beck, K.C. and Berner, R.A., 1964. Composition of interstitial waters of mode4rn sediments. J. Geology, 73, 39-73.

Spjeldnaes, N., 1978. Ecology of selected late- and post-glacial faunas in the Oslo Fiord area. Geologisches Foreningens i Stockholm Forhandlingar, 100, art. 2, 189-202.

Stewart, T.L. and England, J., 1983. Holocene sea-ice variations and paleoenvironmental change, northernmost Ellesmere Island, N.W.T., Canada. Arctic and Alpine Research, 1, 1-17.

Strom, R.M., 1957. A lake with trapped seawater. Nature, 180, 982.

Strom, R.M., 1961. A second lake with trapped seawater. Nature, 189, 913.

Tepper, D.H., 1980. Hydrogeologic setting and geochemistry of residual periglacial Pleistocene seawater in wells in Maine. Unpublished M.S. Thesis, Department of Geological Sciences, University of Maine, Orono.

Thompson, R., Bleomendal, J., Dearing, J.A., Oldfield, F., Rummery,T.A., Stober, J.C. and Turner, G.M., 1980. Environmental applications of magnetic measurements. Science, 207, 481-486.

Walcott, R.I., 1970. Isostatic response to loading of the crust in Canada. Canadian J. Earth Science, 7, 716-727.

GLACIO-CLIMATIC STUDIES OF A HIGH ARCTIC PLATEAU ICE CAP,

PART I: MASS BALANCE

Raymond S. Bradley and Mark C. Serreze

University of Massachusetts, Amherst.

ABSTRACT

Mass balance measurements have been renewed on two small ice caps on northeastern Ellesmere Island. Original stake networks were established in 1972 and 1976. Since then, both ice caps have experienced significant mass losses averaging -70 to -140 kg m ^{2}a . They have also decreased in area. The equilibrium line in this area has averaged around 1150 m for the last decade or so. The ice caps are remnants of former climatic conditions and are out of equilibrium with contemporary climate.

INTRODUCTION

The Hazen Plateau of northeastern Ellesmere Island is a broad upland area extending 70 km from the United States Range in the west to Robeson Channel in the east (Figure 1). The upland is dissected by deep glacial troughs, which formerly drained ice from the mountains in the northwest towards the southeast. Hill summits are extremely flat, generally exceeding 600 m in elevation and occasionally reaching >850 m above sea-level (Figure 2). Most of these upland surfaces are currently unglacierized, the local glaciation level ranging from 700 m to 1000 m (Miller, et al., 1975). A noteable exception to this is the region north of St. Patrick Bay (Figure 1) where two small ice caps occur; these are the northeasternmost ice bodies in the Queen Elizabeth Islands. They are referred to, unofficially, as the "St. Patrick Bay Ice Caps". The larger of the two ice caps is the primary focus of this report. Meteorological studies on and around the ice caps are discussed elsewhere

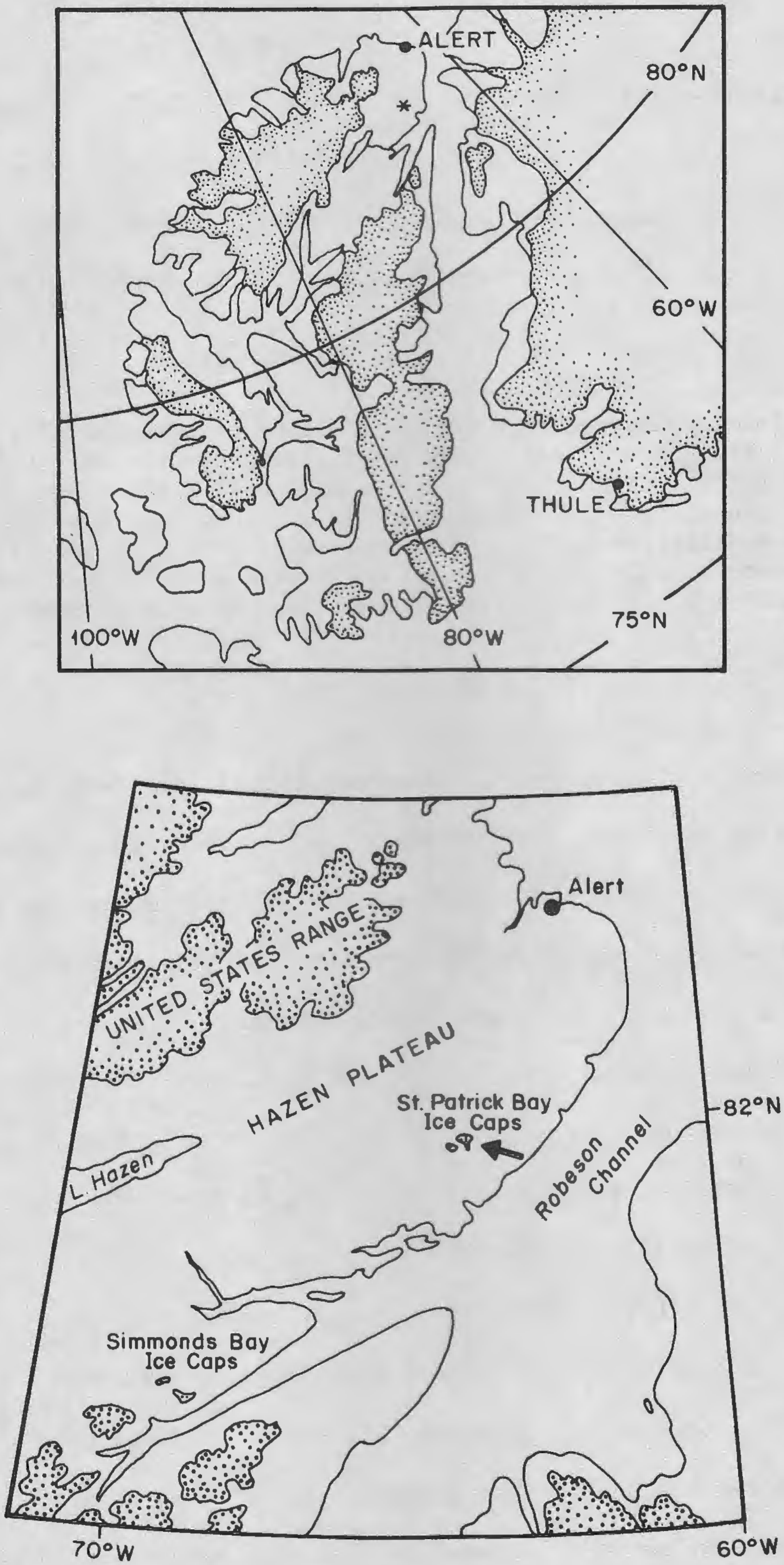

Figure 1 Location map: northeastern Ellesmere Island, N.W.T., Canada. Arrow refers to view shown in Figure 2.

(Bradley and Serreze, 1985, Serreze and Bradley, 1985).

PREVIOUS WORK

No reference to the ice caps has been located in any historical literature in spite of the fact that they are relatively close to where both the Greely and Nares expeditions spent considerable time (in 1875-76 and 1881-84 respectively). In particular, the Greely expedition explored much of the region around Fort Conger, but no notation of these features was made. Possibly extensive snow cover on the higher reaches of the plateau in the late 19th Century would have made Greely, et al. oblivious to their presence.

Photographic coverage of the ice caps is quite good beginning with the POLARIS trimetrogon survey in 1947 (Table 1). Although of poor quality these photographs show extremely snow-free conditions across the Hazen Plateau at the time of the survey (July 24)(Figure 2). Similar conditions prevailed in 1959; by July 6th, all winter accumulation had disappeared and the underlying dirt-laden ice was exposed (Figure 3). Recent low-level coverage in 1974 followed a period of snowfall so the ice caps appear snow-covered, even though the surrounding plateau was snow-free at that time (August 4th). Finally, low-level coverage was repeated in 1978, revealing a dirt-laden ice surface with meltwater channels clearly visible.

The ice caps were first visited in 1972 when conditions, late in the ablation season, were radically different from those shown on the 1959 aerial photographs. By August 20-21 there was "partial cover of winter snow all around the ice margin for at least a kilometer" (Hattersley-Smith

TABLE 1

Aerial Photographs of the St. Patrick Bay Ice Caps

Date	Survey	Scale	Type	Conditons
24 July 1947	Polaris Trimetrogon		Oblique only Black & white	Plateau completely snow-free
6 July 1959	Dept. Energy Mines & Resources	1:80,000	Vertical and oblique Black & white	Plateau and ice caps snow-free; ice cap surface is dirt-laden ice showing layering and surface drainage channels.
4 August 1974	Glaciology Division	1:20,000	Vertical Color	Plateau snow-free; ice caps with snow-cover possibly from just before the survey.
1 August 1978	Glaciology Division	1:23,000	Vertical Color	Plateau and ice caps snow-free, prominent ablation surface on ice caps, dirt-laden meltwater channels visible.

Figure 2 Oblique aerial photograph of Hazen Plateau looking towards United States Range and Lake Hazen (left, rear) from location of arrow in Figure 1. (Copyright: Canadian National Map Collection: NMC-7M154 186 RT, July 24, 1947).

Figure 3 Vertical aerial photograph of St. Patrick Bay Ice Caps (Copyright: Canadian Government; air photograph A-16608-15, July 6, 1959).

and Serson, 1973). A network of eight ablation stakes was installed at that time; one additional stake was added in 1975 (H. Serson, Pers. Comm.). The area was not re-visited again until the summers of 1982 and 1983 when a topoclimatic study of the ice caps was initiated by the University of Massachusetts. As part of this work, the original stake line was re-surveyed. A more extensive stake network was established (Figure 4a) and two extensive snow depth and density surveys were made. Five stakes were also installed on the smaller (southwestern) ice cap in 1983. In additiion, an ablation stake network established in June, 1976 on the "Simmonds Ice Cap", ~110 km to the southwest (Bradley and England, 1977) was re-surveyed in July 1983 (Figure 1). Results of these measurements are discussed in the next section. The radiation climate, energy balance and topoclimatic studies carried out on the main St. Patrick Bay Ice Cap in 1982 and 1983 are reported elsewhere (Serreze and Bradley, 1985, Bradley and Serreze, 1985).

ICE CAP ELEVATION AND MASS BALANCE

Elevations of stakes and other features are shown in Table 2. Repeated measurements with a precision surveying altimeter provided an internally consistent set of elevations relative to base camp (Station Yankee; Figure 3). Helicopter traverses to sea-level provided estimates of base camp elevation. We estimate the stake elevations shown in Table 2 are accurate to within ±1 m relative to one another and within 10 m of absolute elevations relative to sea-level. The important point is that the entire elevational range of the larger ice cap is only about 50 m, with a summit elevation of approximately 900 m. It is thus extremely

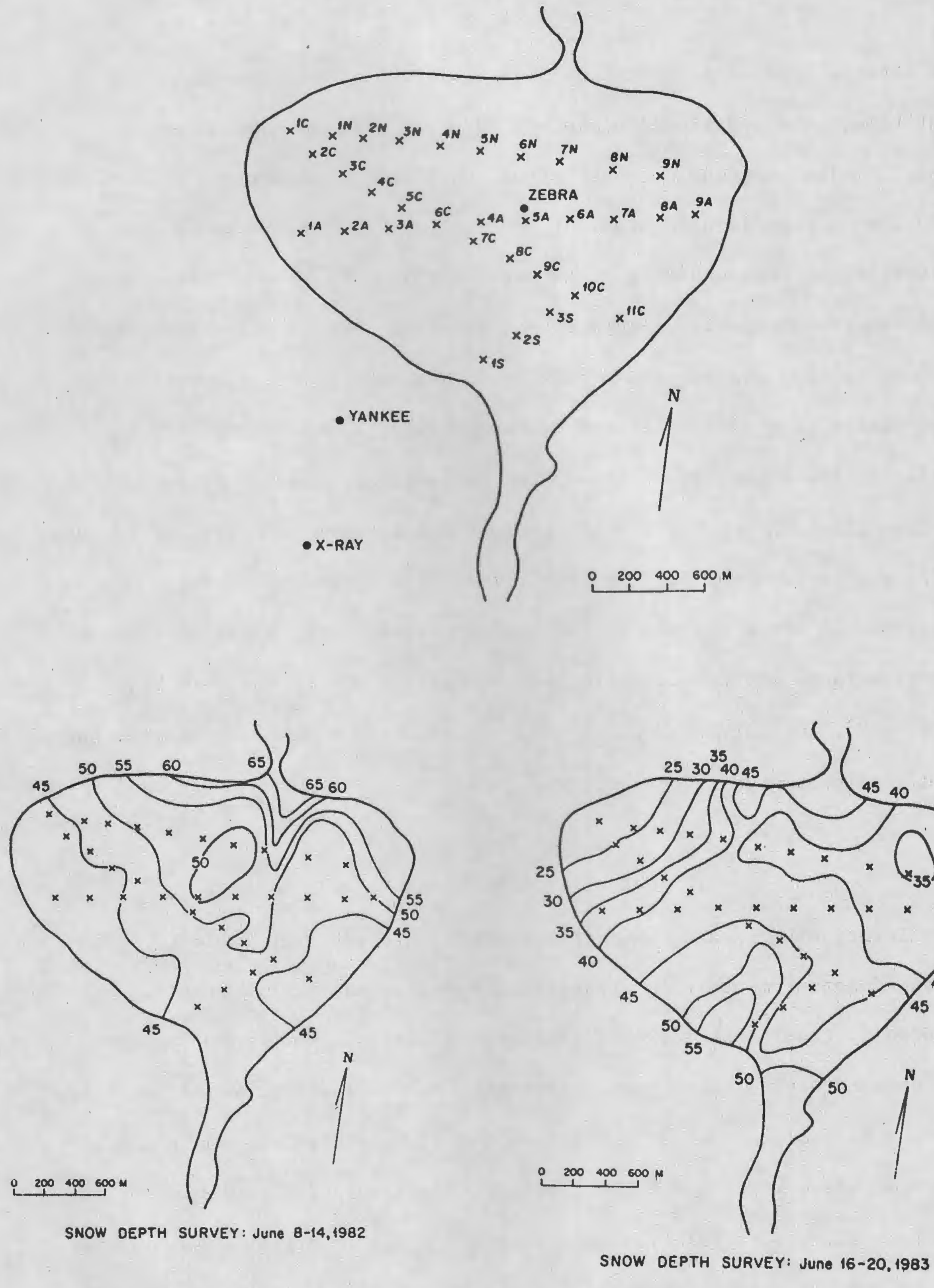

Figure 4 a) Ablation stake network established on main ice cap. Zebra, Yankee, and X-Ray refer to meteorological stations maintained in the summers of 1982 and 1983 (Bradley and Serreze, 1985). b) Snow depth survey (cm), June 8-14, 1982. c) Snow depth survey (cm), June 16-20, 1983.

TABLE 2

Elevation of Stakes and Meteorological Stations (m)

on and Around St. Patrick Bay Ice Caps

Meteorological Stations

X-Ray	828	Yankee	842	Zebra	860

Stakes on Large Ice Cap

1N	887	1C	882	1A	892
2N	887	2C	894	2A	893
3N	881	3C	898(summit)	3A	885
4N	867	4C	894	4A	862
5N	855	5C	883	5A	858
6N	847	6C	871	6A	862
7N	848	7C*	867	7A	867
8N	858	8C	863	8A	868
9N	865	9C	857	9A	854
		10C	854		
		11C	856		

Stakes on Small Ice Cap

1	810
2	790
3	773
4	759

*Stake Missing 1983

flat, and similar in elevation to the surrounding unglacierized hills. Considering its topographic setting, the ice cap is probably no more than 25 m thick at the summit. The smaller ice cap to the west does not cover a hill summit and is entirely lower than the larger ice cap. It is situated on a northeast-facing slope and ranges in elevation from ~740 to 820 m above sea level. It seems likely that this ice body formerly occupied the summit to the northwest (at ~865 m) and possibly the southwest, but continued ablation has resulted in ice only being able to survive in the most topographically-favored site.

Mass balance data are shown in Table 3. Although Hattersley-Smith and Serson (1973) were impressed by the extensive firn on the plateau in the summer of 1972, the climatic conditions which led to that situation have not prevailed. From 1972-1982, the net balance was quite negative (average net balance: -1300 kg m^{-2}, based on re-measurements of the 1972 stake line). This result is supported by changes in ice cap area which are apparent between the 1959 and 1978 photographic surveys. We estimate that the larger and smaller "St. Patrick Bay Ice Caps" have decreased in area by 7% and 11%, respectively, over this interval.

A network of 18 stakes was established on the "Simmonds Ice Cap" (Figure 1) June 7-10, 1976. This ice cap also occupies a small higher elevation summit of the Hazen Plateau, but is considerably higher in elevation than the St. Patrick Bay Ice Caps and has greater relief, ranging from <1050 m to >1150 m (Bradley and England, 1977). The stake network was re-surveyed on July 11, 1983. Twelve of the original 18 stakes could not be located and are assumed to have melted out. Mass balance for the interval 1976-1983 was estimated as follows. For the six

TABLE 3

Mass Balance Data for Northern Ellesmere Island Plateau Ice Caps*

A. St. Patrick Bay Ice Cap
($kg\ m^{-2}$)

	Average Balance**	Southwestern	Northeastern
1972-82			-1300
1981-82	Winter (6/12/82)		+159
	Summer (7/28/82)		-303
	Net		-144
1982-83	Winter (6/18/83)	+183	+118
	Summer (7/27/83)	-18	-19
	Net	+165	+137

B. "Simmonds Ice Cap"

1976-83	Net balance		-488 Minimum estimate

*Rates in parentheses are times of initial and final snow surveys at the start and end of the field seasons.

**Winter balance calculated from stake network and associated snow pit density measurements areally weighted by snow depth distribution; summer balance calculated from mean of measurements at stakes. Net balance 1972-82 and 1976-83 are averages of measurements at stake line.

remaining stakes, the difference from the top of the stake to ice surface measurements in 1976 and 1983 was calculated and multiplied by an assumed ice density of 0.9. To this value, the difference in water equivalent of the snow and firn above the ice surface for the two years was subtracted (using calculated water equivalents in 1976 and estimated values in 1983). For the missing stakes, the same procedure was followed except the ice lost was assumed to be only equivalent to the original depth of stake insertion into the ice. Weighting the resultant values at each stake to sub-areas of the ice cap (using Theissen polygons) gave a mean value of -488 kg m^{-2}. Clearly, this is a minimum estimate since the stakes which survived were all at higher elevations (>1090 m). It also appeared that marginal recession of the ice cap had occurred since the 1959 aerial photographic survey. Interestingly, stake 8, at the summit of the ice cap showed very little mass loss over the 1976-1983 interval (-10 kg m^{-2}) suggesting that the equilibrium line in the area has averaged around 1150 m during this period.

Detailed snow depth and density measurements on the larger St. Patrick Bay Ice Cap in early June, 19872 indicated a mean winter balance of ~159 kg m^{-2}. In 1983 the figure was 118 kg m^{-2} for 1971-72 (Hattersley-Smith and Serson, 1973) though no snow density measurements were made at that time and the survey was limited to the stake line. Ablation season conditions in 1982 and 1983 were markedly different resulting in quite different mass balance conditions for each year. In 1982, mass losses of the previous decade (or more) continued at the same rate, the net balance averaging -144 kg m^{-2}. However, the summer of 1983 was much colder and snow was common throughout the normal ablation season. As a result, when the field party left at the end of July, there had been a net gain in mass on the ice cap of 137 kg m^{-2} for the year. Similarly, the smaller, southwestern ice cap registered a net gain of 165 kg m^{-2}. It is unlikely that subsequent conditions in August changed the situation significantly.

DISCUSSION

Although no long-term climatic data are available for the ice caps themselves, meteorological observations have been made at Alert, ~ 70 km to the north, since 1950. These provide the best available index of long-term climatic variations in the region. Melting degree days (cumulative totals of daily above freezing mean temperatures) are a useful index of total ablation season warmth. Figure 5 shows annual and July totals of melting degree days (MDD) for the last 34 years. Three aspects of the record are worth noting; firstly, there is large inter-annual variability, particularly in the early part of the record. Secondly, there has been a statistically significant decline in MDD over the period of record, amounting to 22 MDD per decade, on average. Thirdly, it is clear that July MDD account for most of the summer "warmth", particularly in cold summers. The Alert record also enables the recent summers to be placed in a longer time perspective. 1983 ranked in the lowest quartile of annual MDD, and the lowest decile of July MDD. This was obviously reflected in the positive mass balance estimate for 1982-3. By contrast, 1982 had MDD totals closer to the average of the last 30 years. Judging by the MDD values for the period prior to the mid-1960s, and the fact that the ice caps have lost considerable mass during the 1970s, there seems little doubt that mass losses were considerably greater in the 1950s and

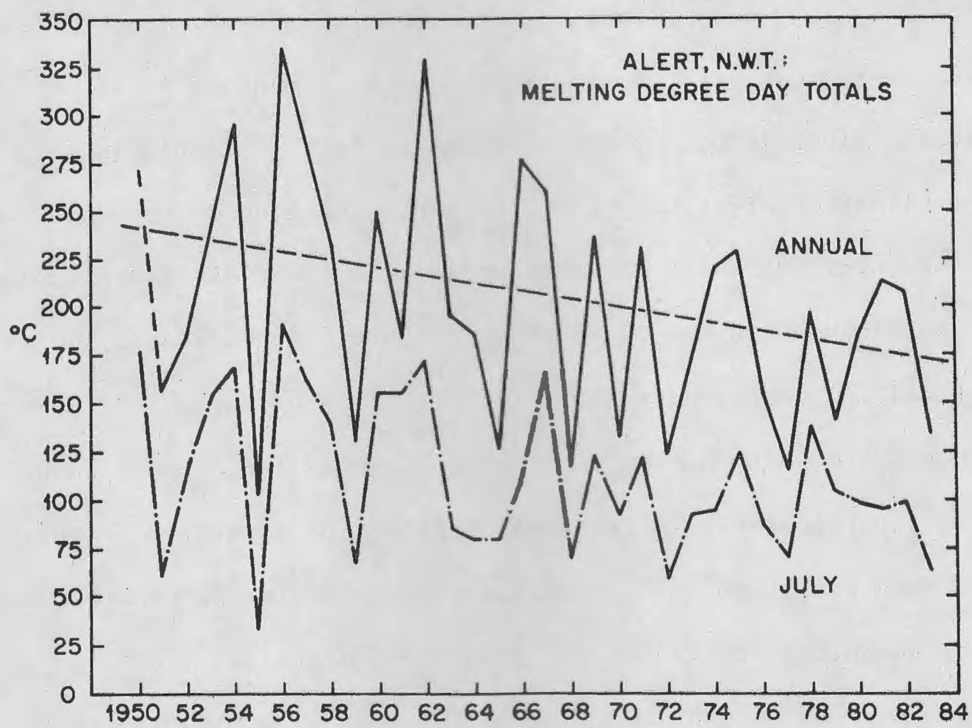

Figure 5 Melting degree day totals (°C) at Alert, annually (solid line) and for July (dashed line). Values derived from mean daily temperature. A linear regression on the annual data ($y = -2.16x + 4454$) is also shown. The correlation coefficient (r) is -0.34 ($p = 0.02$).

early 1960s.

To investigate whether scattered glaciological observations on northern Ellesmere Island and/or photographic evidence could be used in conjunction with Alert data to provide a general yearly index of ice cap mass balance, Alert winter precipitation totals were plotted against the subsequent summer MDD totals (Figure 6).

Two points on the diagram are well established; 1971-2 and 1982-3 were clearly very positive mass balance years. It is also very likely that 1964-5 was too; according to observations by Hattersley-Smith (1969) the snowline in mid-August 1964, near Tanquary Fiord (~200 km to the southwest) was ~850 m. Other observations (e.g.Hattersley-Smith and Serson, 1970, Hattersley-Smith, 1972) indicate that this was probably representative of a larger area of northern Ellesmere Island. Comparison with the Alert data suggests that positive balance years are associated with MDD totals of <140. It seems likely therefore that 1954-5, 1967-8, 1979-80 and 1976-7 were also positive balance years. It should be noted, however, that by this reasoning 1958-9 should also have been a very positive mass balance year, but aerial photographs taken on July 6 (Figure 3) clearly show the St. Patrick Bay Ice Caps devoid of snow with bare ice exposed. It is difficult to imagine how this situation arose since (at least at Alert) mean daily temperatures had only been above 0°C for two weeks prior to this photographic survey. Possibly the plateau had received very little snowfall during the winter and/or had been swept clear by strong winds. Alternatively, the Alert data may not have been representative of a wider area in 1959; indeed Hattersley-Smith and Serson (1970) in their study of mass balance on the Ward Hunt Ice Shelf,

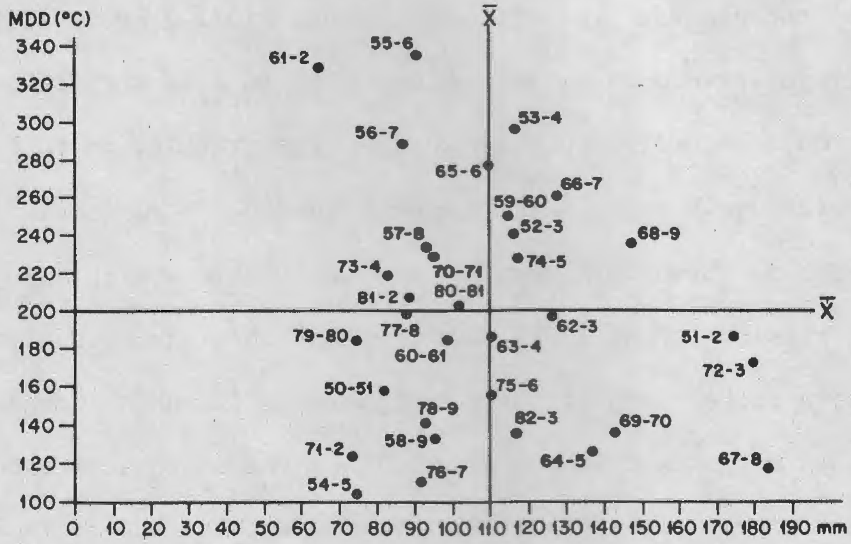

Figure 6 Snowfall (mm water equivalent) during winter months and melting degree days the following summer at Alert. Winter is defined as the time between the last period of mean daily temperatures continuously above 0°C for 5 days or more in the autumn and the first period of same in the spring (mean dates, 1951-83 were August 25 and June 18).

note that the ice shelf lost mass in 1959 and gained mass in 1964, when the Alert data suggest that the reverse would have been true. Clearly the Alert data can only be used as a general guide to regional climate as conditions along the northern coastal strip of Ellesmere Island may be quite different from the interior.

Observations of mass balance on the Gilman Glacier in the 1950s provide another assessment of ELAs in the region. In 1957 and 1958, ELAs in the area (100 km west-southwest of the St. Patrick Bay Ice Caps) were 1240m and 1200 m respectively; in 1959, the ELA was lower (Hattersley-Smith, et al. 1961). This is what would be expected from the Alert data (Figure 6). Aerial photographs of the St. Patrick Bay Ice Caps in August 1978 show a prominent ablation surface on the ice caps indicating a negative mass balance year. These observations, coupled with the 1981-2 observations of a negative mass balance on the St. Patrick Bay Ice Caps, suggest that summers with MDD at Alert exceeding 190m probably resulted in mass losses on the ice caps. Winter snowfall variations seem to be of little significance. It is worth noting that the 1982-3 winter balance on the St. Patrick Bay Ice Caps was only 75% of the 1981-2 winter balance (cf. Alert, Figure 6) yet the lower MDD of 1983 resulted in a positive mass balance*.

We estimate that the climatic threshold between net mass loss and net mass gain on the St. Patrick Bay Ice Caps corresponds to a summer with between 140 and 190 MDD at Alert. Since summers over the last 35 years

---

*With lower summer temperatures, precipitation is commonly in the form of snow rather than rain, which further retards the melt process.

have ranged from a minimum MDD total of ~105 to a maximum of ~330, it is clear that the dominant tendency has been towards mass losses, particularly during the 1950s. Interestingly, daily maximum temperatures at Alert during the 1950s commonly exceeded 15.5°C (with an absolute maximum of 20°C recorded in 1956). Since 1963, maxima have rarely even reached 15°C.

Are the St. Patrick Bay Ice Caps a "sensitive" indicator of climatic variation? They are certainly vulnerable to small shifts in mean summer conditions but, given the range of MDD at Alert experienced over the last three decades, the ice caps are by no means in equilibrium with contemporary climate. In spite of occasional small mass balance gains, larger mass losses in other years preclude any overall ice cap growth. They are remnants of a period when MDD totals exceeding 200 must have been quite rare and/or when snowfall was very much higher than in recent years. Overall, the ice caps today are wasting away and will eventually disappear if contemporary conditions are any guide to the climate of the next century or two. In the sense that they provide no long-term record of climate, they do not really provide any better indication of climatic variability than the Alert instrumental record. A more useful "sensitive" indicator of regional climate, in the sense of providing a yard-stick by which to assess contemporary climatic variations, would be provided by a long continuous record from higher elevations such as the ice core recently recovered from the Mer de Glace Agassiz 200 km to the southwest. Monitoring of annual accumulation and ablation season conditions can then be placed in a longer term perspective, beyond the limited 35 year instrumental record, available for the High Arctic.

CONCLUSIONS

Mass balance studies on small plateau ice caps of northern Ellesmere Island indicate significant wastage has occurred during the 1970s, in spite of occasional positive balance years. Mass balance on the St. Patrick Bay Ice Caps was -144 kg m^{-2} in 1981-2 and +137 kg m^{-2} in 1983. Analysis of these and other regional glaciological and photographic observations has been attempted, to place the observations in a longer term perspective. From this analysis it is clear that over the last 30 years the ice caps must have lost considerable mass and that they are not in equilibrium with the climate of recent decades. They are remnants of a period in the past when MDD totals at Alert were rarely >200 and/or when snowfall was heavier. If contemporary conditions persist, the ice caps will disappear within the next 100-200 years.

ACKNOWLEDGEMENTS

This work was supported by the U.S. National Science Foundation, Grant ATM80-17745 to the University of Massachusetts. Logistical support was provided by the Polar Continental Shelf Project, Department of Energy, Mines and Resources, Ottawa. We are grateful to M. Palecki, C. Allen, M. Retelle, J. Fabel and R. Friend for assistance in the field.

REFERENCES

Bradley, R.S. and England, J.H., 1977. The Simmonds Ice Cap, pp. 177-182 in Past Glacial Activity in the High Arctic. Bradley, R.S. and J.H. England (1977), Contribution No. 31, Dept. Geology and Geography, University of Massachusetts, Amherst.

Bradley, R.S. and M.C. Serreze, 1985. Glacio-climatic studies of a high arctic plateau ice cap, part II: topoclimate (submitted).

Hattersley-Smith, G. 1960, Operation Hazen. Glaciological studies: snow cover, accumulation and ablation. Report D. Physical Research (G) Hazen 10, Defense Research Board, Ottawa.

Hattersley-Smith, G. 1969. Glacial features of Tanquary Fiord and adjoining areas of northern Ellesmere Island, N.W.T. Journal of Glaciology, 8(52), pp. 23-50.

Hattersley-Smith, G. 1972. Climatic change and related problems in northern Ellesmere Island, N.W.T., Canada. Acta Univ. Oulouensis, Ser. A3, Geol. No. 1, pp. 137-148.

Hattersley-Smith, G. and Serson, H., 1970. Mass balance of the Ward Hunt Ice Rise and Ice Shelf: a 10 year record. Journal of Glaciology, 9(56), pp. 247-252.

Hattersley-Smith, G. and Serson, H., 1973. Reconnaissance of a small ice cap near St. Patrick Bay, Robeson Channel, northern Ellesmere Island, Canada. Journal of Glaciology, 12(66), pp. 417-421.

Hattersley-Smith, G. Lotz, J.R. and Sagar, R.B., 1961. The ablation season on Gilman Glacier, northern Ellesmere Island. Int. Assoc. Sci. Hydrol., Helsinki, 1960, Publication No. 54, pp. 152-168.

Miller, G.H., Bradley, R.S. and Andrews, J.T., 1975. The glaciation level and lowest equilibrium line altitude in the High Canadian Arctic: maps and climatic interpretation. Journal of Arctic and Alpine Research, 7, pp. 155-168.

Serreze, M.C. and Bradley, R.S., 1985. Glacio-climatic studies of a high arctic plateau ice cap, part III: radiation climate (submitted).

GLACIO-CLIMATIC STUDIES OF A HIGH ARCTIC PLATEAU ICE CAP, PART II: TOPOCLIMATE

By

Raymond S. Bradley and Mark C. Serreze

University of Massachusetts, Amherst.

ABSTRACT

Meteorological observations on and around a small, exposed plateau ice cap on northeastern Ellesmere Island, N.W.T., Canada were carried out in the summers of 1982 and 1983. The objective was to assess the effect of the ice cap on local climate as the melt season progressed. In 1982 seasonal net radiation totals were lowest on the ice cap and greatest at the site farthest from the ice cap. The ice cap site received only 35% of net radiation totals on the surrounding tundra. This reflects a gradient in albedo; albedo changed most markedly away from the ice cap as the summer progressed. A thermal gradient was observed along a transect perpendicular to the ice cap edge; this gradient was greatest at low levels (15cm) and was maximized under cloud-free conditions. The 'cooling effect' of the ice cap was less at the start of the ablation season than later. Low level inversions occurred more frequently over the ice cap than over the snow-free tundra. Overall, melting degree days on the ice cap were only 40-65% of those on the adjacent tundra. A model of interactions between the atmosphere and a snow and ice cover, or a snow-free tundra/felsenmeer surface is proposed. Observations indicate that the ice cap has a cooling effect on the lower atmosphere relative to the adjacent snow-free tundra; this effect is absent when snow cover is extensive (as in 1983). However, any cooling effect of the ice cap on adjacent areas involves heat flux to the ice which may eventually lead to enhanced ablation.

INTRODUCTION

It has often been noted that positive feedbacks between snow and ice-covered surfaces and the atmosphere must have played an important part in maintaining (and perhaps even enlarging) ice or snow-covered areas during the initial stages of glacierization (e.g. Bonacina, 1948; Kellogg, 1975). Indeed, this feedback process is an implicit part of the "theory of instantaneous glacierization" (Ives, et al., 1975). In spite of this, the actual effect of snow or ice-cover on local climate has not been adequately studied. *A priori*, it seems likely that an ice/snow cover will increase albedo, reduce net radiation and lower temperatures locally, but the magnitude of these effects and their spatial dimensions have rarely been quantified (cf. Muller and Roskin-Sharlin, 1967; Braithwaite, 1978).

To assess the magnitude of the "ice cap effect," a study was initiated on a small plateau ice cap on the northeastern edge of the Hazen Plateau of Ellesmere Island, N.W.T., Canada (Figure 1). The "St. Patrick Bay Ice Cap"* (81° 57'N, 64°10'W) is a thin, extremely flat ice mass with a total relief of less than 50 m. It is completely unshaded by adjacent terrain and surrounded by unglacierized plateau summits at similar elevations (Figure 2). It thus represents an ideal situation to study the effect of the ice cap itself on the local climate. To this end, a network of meteorological stations were established on and around the ice cap during the summers of 1982 and 1983 (Figure 3). The sites differed in elevation by less than 50m; the major difference between the sites was thus the underlying surface and proximity to the ice cap. We hypothesized that by initiating the study each year before any significant ablation had taken place, all observations would start with an essentially

---

*Unofficial name; the ice caps have previously been referred to as the "Hazen Ice Caps" (Bradley and Serreze, 1983); this study was conducted around the larger of the two small ice caps north of St. Patrick Bay

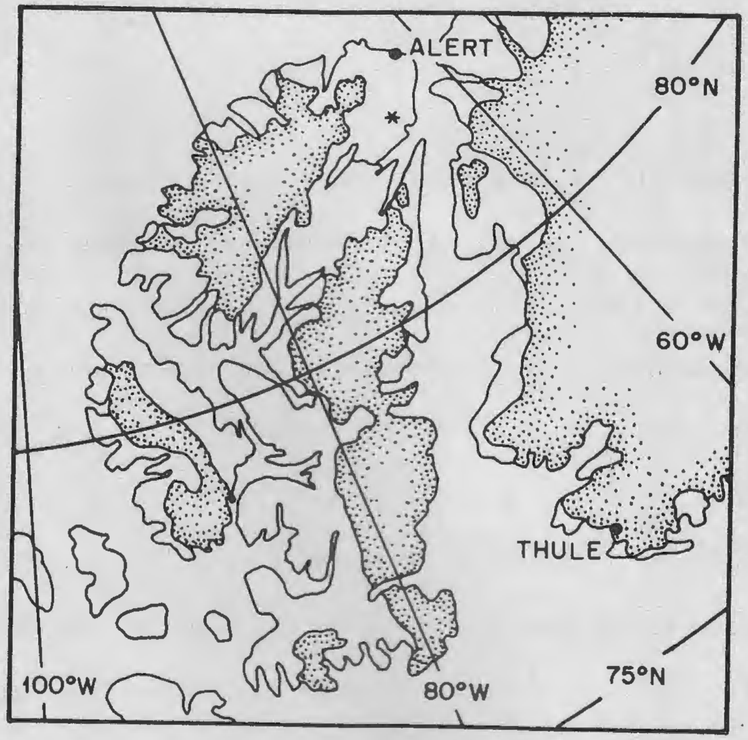

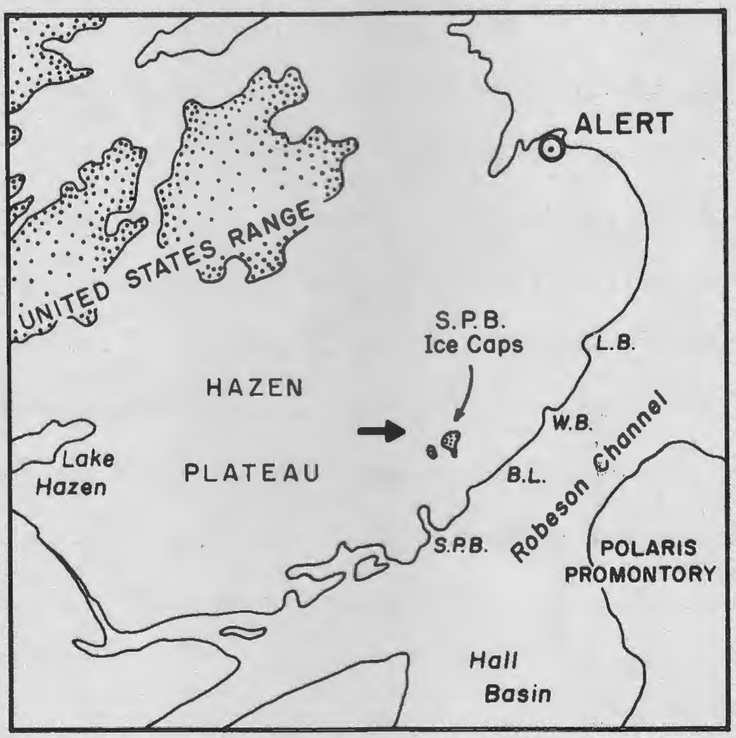

Figure 1 Regional location maps: S.P.B. = St. Patrick Bay, B.L. = "Beaufort Lakes;" W.B. = Wrangel Bay; L.B.= Lincoln Bay.

Figure 2 Oblique aerial photograph looking eastwards across St. Patrick Bay ice caps (delimited by dashed lines). Photograph is taken from the perspective of dark arrow in lower panel of Figure 1, looking across the outer Hazen Plateau. (Copyright Canadian Government aerial photograph T397R-189; June 24, 1950).

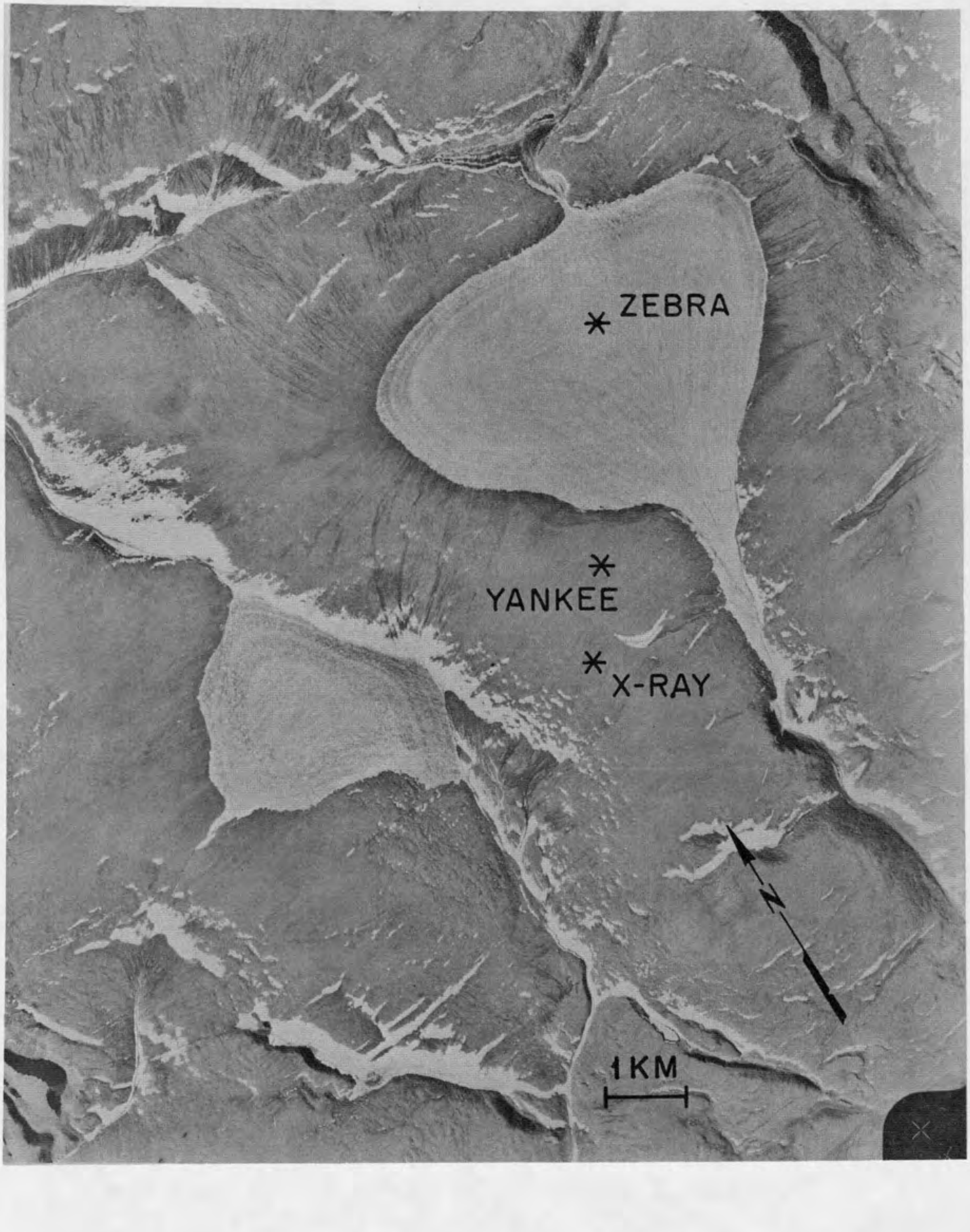

Figure 3 Vertical aerial photograph showing location of principal meteorological stations (Copyright Canadian Government aerial photograph A-16608-15; July 6, 1959).

uniform, snow-covered surface. As the season progressed and snow cover on the land melted off, the topoclimatic effect of the ice cap should become apparent. In fact, this was more or less what happened in 1982, but in 1983 summer conditions were quite different and the entire plateau remained snow-covered for much of the season. This prevented any further assessment of the "ice cap effect" but provided a valuable data set from both ends of the spectrum of summer ablation conditions. Mass balance of the ice cap has been discussed by Bradley and Serreze, 1985a. Here we discuss the observations made in 1982 and 1983 with particular emphasis on topoclimatic variations. Radiation balance measurements and the low level atmospheric structure over the ice cap are discussed elsewhere (Serreze and Bradley, 1985a and Palecki, _et al_., 1985 respectively).

MEASUREMENT PROGRAM

Table 1 summarizes the measurement program carried out at the stations shown in Figure 3. Table 2 documents the instruments used and sampling frequency. In both 1982 and 1983, incoming short and longwave radiation was measured only at station Yankee, near the edge of the ice cap (Figure 4). These measurements were assumed to be representative of the entire study area. It is possible that under certain cloud conditions, multiple reflection between clouds and snow and ice at the surface may have made this assumption invalid, but in the vast majority of cases the assumption of uniform radiation receipts is probably reasonable for this small (lessthan 10 km) area. This factor is discussed further in Serreze and Bradley, 1985a. Development of local clouds or fog (e.g. specifically over the tundra or over the ice cap) occurred only rarely.

TABLE 1

"St. Patrick Bay Ice Cap" Meteorological Measurement Program, 1982 and 1983: parameters recorded and height of instruments (cm)

1982

Station	Air Temp.	Relative Humidity	R	Q	Q	I	Ground Temp.*
X-Ray	15 150 300	15 150	150		150		
Yankee	15 150 300	15 150	150	150	150	150	-5 -15 -25cm
Zebra	15 150 300	15 150	150		150		

1983

Station	Air Temp.	Relative Humidity	R	Q	Q	I	Snow Temp.(cm)*	Wind Speed	Wind Direction
X-Ray	15 150		150		150				
Yankee	15 150 300	15 150	150	150	150	150	-2 -17 -37	15 150	300
Zebra	15 150	15 150	150		150			15 150	

In 1982, sub-surface temperatures were recorded within a frost hummock and in 1983 within the surface snow-cover. In addition ice temperatures at an adjacent site (on the smaller ice cap) were recorded at 100 cm below the snow-ice interface.

In addition, an hourly record of synoptic weather conditions was kept during waking hours; observations included: cloud type and amount, opacity, wind speed and direction (in 1982 wind speed from totalizing anemometer and wind direction estimated; both were recorded instrumentally in 1983). Barometric pressure (microbarograph) and precipitation (standard U.S. Weather Bureau gage) were also recorded. Albedo was calculated from incoming shortwave radiation (Q) at Yankee and Q at other stations. Temperature, humidity and wind profiles at Yankee and Zebra (1983) provided estimates of latent and sensible heat fluxes (Serreze and Bradley, 1985b). In 1983, an instrumented tethered balloon system was used to obtain low-level (<0.5 km) measurements of pressure, temperature, humidity, wind speed and direction on selected days (see Palecki, et al. 1985).

TABLE 2

Meteorological Instrumentation Used on St. Patrick Bay Ice Cap

Sensors:

Temperature: Campbell Scientific Inc. (CSI) model #101 thermistor probes, CSI model #201 temperature/relative humidity probes.
Relative Humidity: CSI model #201 temperature/relative humidity probes.
Radiation:
Net Radiation: Micromet Instruments net radiometers
Incoming Shortwave & Reflected Shortwave: Eppley Model#8-48 black and white pyranometers.
Incoming Longwave: Eppley modelPSP pyrgeometer
Windspeed: Weathertronics model #2031 DC generator and model #2032 contact closure Micro-Response anemometers (2 of each).
Wind Direction: CSI model #024A Met-One direction sensors.

Data Acquisition:

CSI model CR-21 microloggers (user programmable, battery operated microcomputer. Features a real-time clock, serial data interface and programmable analog-to-digital converter). Data recorded on cassette tapes.

Sensor Calibration:

All Eppley radiometers calibrated at Eppley Laboratories Spring 1982. Micro-response anemometers calibrated by Weathertronics, Inc. Spring 1983. Wind direction sensors, calibrated in field. CSI model #101 thermistor probes and model #201 temperature/relative humidity probes: fixed calibrations. Net radiometers checked against one another before and after field season. One net radiometer factory calibrated, 1983.

Sampling Frequency and Statistics Computed:

Hourly:	Temperature:	mean	Wind direction:	mean
	Relative humidity:	mean	Windspeed:	mean
	Radiation:	mean		

Daily:	Temperature:	max., min., standard deviation
	Relative humidity:	mean, standard deviation
	Windspeed:	max. gust
	Wind Direction:	mean
	Radiation:	total, max., min.

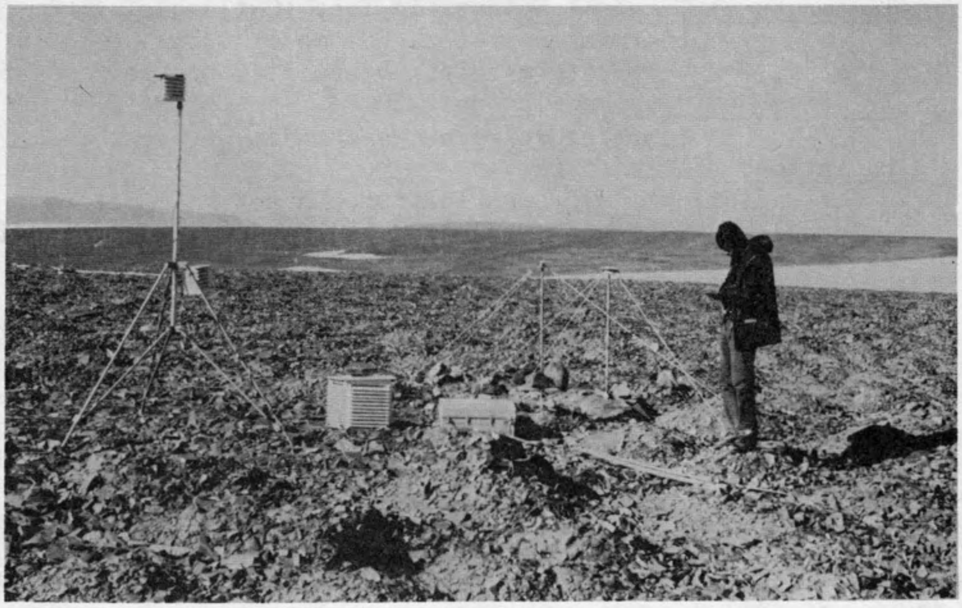

Figure 4 Instrument array at Station Yankee (July 9, 1982).

THE SUMMERS OF 1982 AND 1983

Summer conditions in 1982 and 1983 were significantly different, as reflected in the ice cap mass balance for the two years (-144 kg m^{-2} in 1981-2 and 137 kg m^{-2} in 1982-3; Bradley and Serreze, 1985a). In 1982, the snowpack became isothermal by Julian Day (JD) 177 (June 26) and runoff commenced soon thereafter. By JD 185 the snowpack over the surrounding tundra was completely melted. By the end of July bare ice exhibiting a cryoconite surface was exposed over much of the ice cap. By contrast, in 1983, short periods of melt were interrupted by episodes of snowfall and low temperatures (Figure 5). Riming was also common, occurring on 33% of all days in the summer of 1983. The snowpack only became isothermal on JD 193 (July 12) after 3 days of rain which warmed the snow by refreezing at depth. Snowfall continued intermittently during the rest of July and by the end of the month, an almost continuous snow cover existed around the perimeter of the ice cap for at least 2 km. This was similar to conditions in 1972 when the net balance (1971-72) was estimated at approximately +140 kg m^{-2} (Hattersley-Smith and Serson, 1973). Interestingly, climatic data from Alert,the only long-term weather station in the area, 70 km to the north, shows that 1972 and 1983 summer temperatures (June-August) were the lowest of at least the last 30 years. On the other hand, 1982 was well above the 30 year mean.

Table 3 summarizes the marked differences in principal climatic parameters at station Yankee for the period of overlapping records in both seasons (JD 270-207). In the radiation balance equation [$R = Q_i(1 - \alpha) + I_i + I_o$] all parameters were measured except outgoing infrared radiation

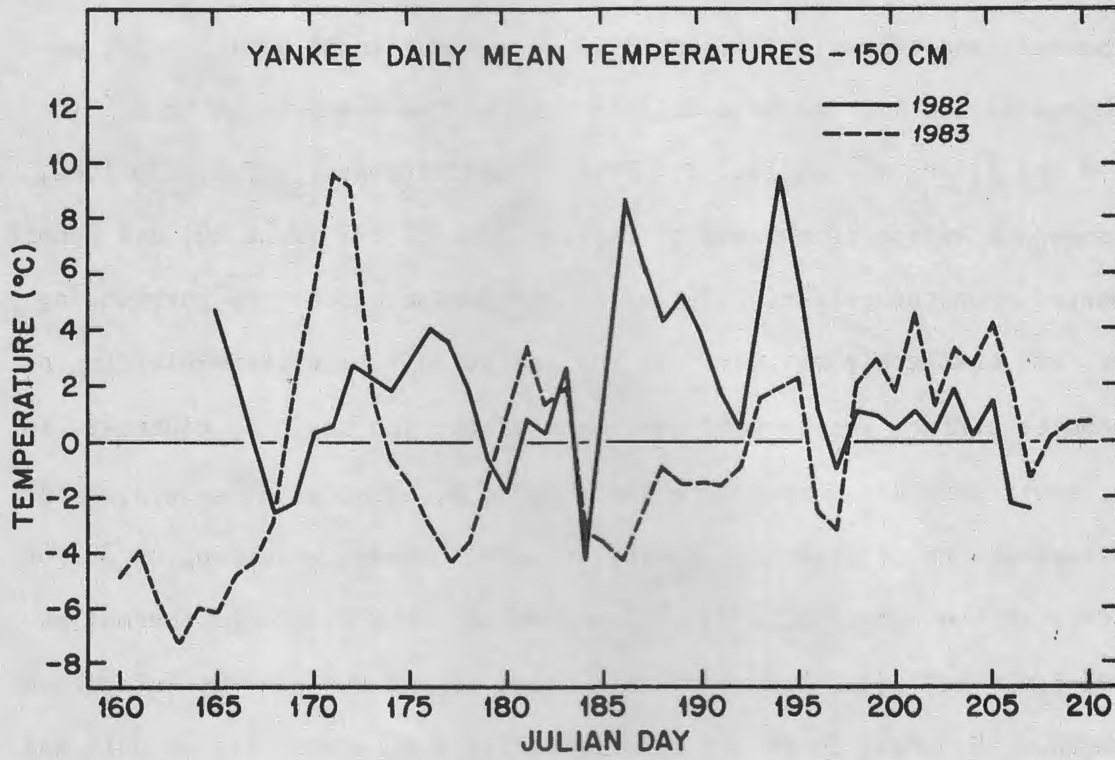

Figure 5 Mean daily air temperatures at 150 cm, Station Yankee 1982 and 1983. (Daily mean based on average of 24 hourly mean values).

TABLE 3

Average Values of Major Climatic Parameters at Station Yankee in 1982 and 1983 (JD 170-207)+

	1982	1983	units
Incoming shortwave radiation ($Q_{\downarrow}$)	0.946	0.924	MJ m^{-2} h^{-1}
Albedo (α)	0.280	0.770	
Reflected shortwave radiation ($Q_{\uparrow}$)	- 0.259	- 0.713	MJ m^{-2} h^{-1}
Incoming longwave radiation (I_{i})	0.949	0.888	MJ m^{-2} h^{-1}
Outgoing longwave radiation (I_{o})	-1.183	-1.020	MJ m^{-2} h^{-1}
Net longwave radiation (I_{i} - I_{o})	-0.233	-0.132	MJ m^{-2} h^{-1}
Net radiation (R)	0.453	0.079	MJ m^{-2} h^{-1}
Cloudiness	6	7	tenths
150 cm air temperature (hourly mean)	1.77	0.83	Centigrade
150 cm relative humidity (hourly mean)	81*	80*	%
Total precipitation	1.25	2.50	cm (water equivalent)

+Differences in seasonal means are statistically significant ($p = 0.01$) unless noted by an asterisk. All downward radiation fluxes are defined as positive.

which was solved as a residual*.

Seasonal averages of incoming shortwave radiation were slightly lower in 1983, probably as a result of the greater cloud amounts, but the differences are not statistically significant. Incoming longwave radiation was significantly lower in 1983, largely as a consequence of the lower temperatures. The lower surface temperatures and slightly higher cloud amounts in 1983 probably resulted in the less negative net longwave radiation balance in 1983. Many previous studies have noted the importance of counter-radiation from clouds in increasing the net infrared flux (e.g. Hoinkes, 1970; Holmgren, 1971; Ambach, 1974). The major contrast between the two seasons was in surface albedo, reflected short-wave radiation and net radiation. The overall lower temperatures and frequent snowfalls maintained an extremely high surface albedo for most of the summer (Figure 6). Albedo only dropped below 50% at station X-RAY, and not until after JD 201 (July 20). As a result, net radiation was markedly lower in 1983.

Although no detailed synoptic analysis of the two seasons has yet been undertaken, some insight into the contrasting conditions of the two seasons can be obtained by stratifying the data by wind direction. Figure 7 shows wind direction frequency and mean wind speed, mean

---

During periods of a melting snow surface in both summers, the radiation balance was checked by comparing I_o calculated as a residual and corresponding values calculated using the Stefan-Boltzmann equation ($I_o = \varepsilon\sigma T^4$) with an assumed surface temperature of 0 degrees C and an emmissivity (ε) of 0.95. In nearly all cases, values were in close agreement.

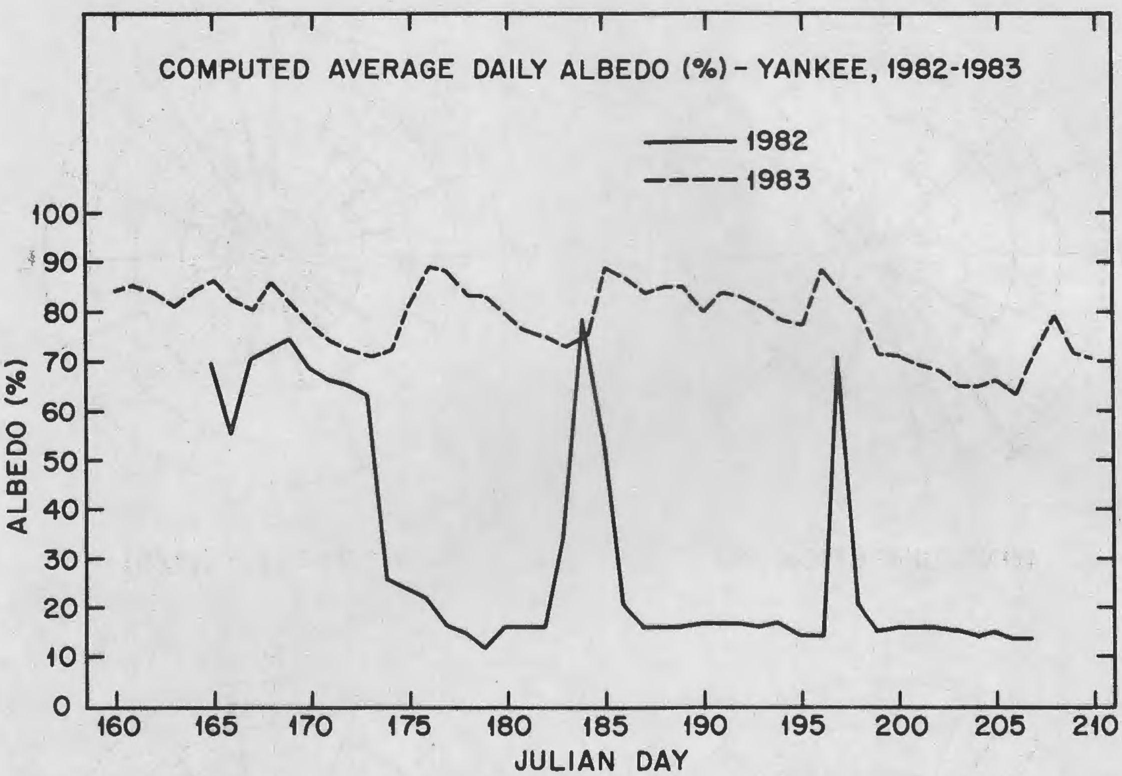

Figure 6 Mean daily albedo at Station Yankee, 1982 and 1983.

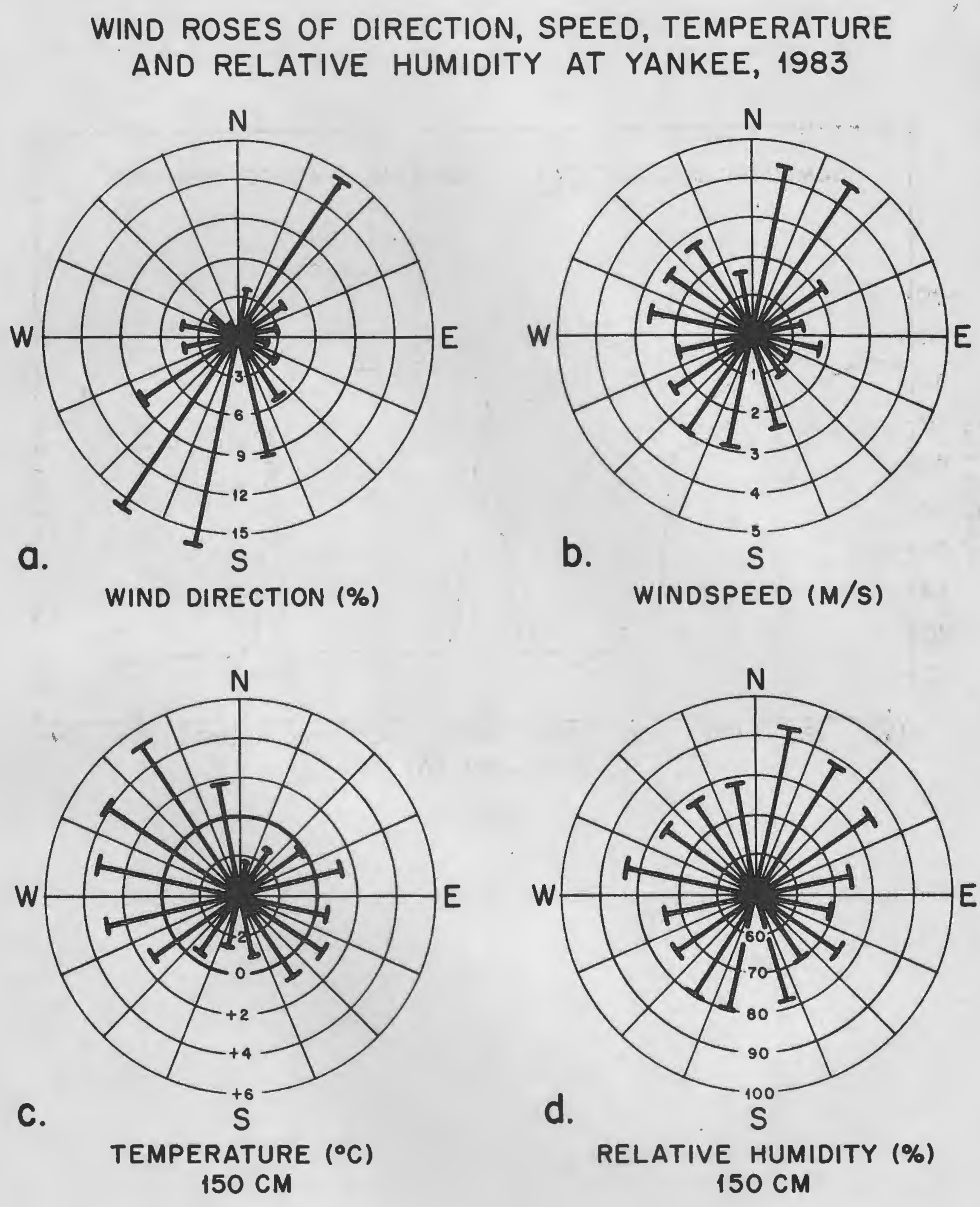

Figure 7 Wind roses of hourly wind direction frequency and mean wind speed, mean temperature and mean relative humidity stratified by wind direction.

temperature and mean relative humidity for periods with winds from different directions (data from 1983). Winds were most frequently from either the NE or SW which corresponded to the lowest temperatures, highest wind speeds and generally high relative humidity, particularly from the northeast. By contrast, wind from the relatively infrequent NW and SE quadrants was generally much warmer, less strong and of lower relative humidity. Wind data were not logged automatically in 1982 so data cannot be so precisely stratified for comparison. South/southwesterly and northeasterly airflow were also the principal wind directions in 1982, though northeasterly flow was less common. It appears that air temperatures associated with SW and SSW airflow were higher, probably as a result of the early removal of snow cover on the plateau in that direction in 1982.

TOPOCLIMATIC VARIATIONS: 1982

a) Radiation Balance

Mean hourly totals of the radiation balance components at the three principal stations (X-RAY, YANKEE and ZEBRA; Figure 3) are shown in Table 4. We assume Q_s and I_i were the same at all three sites. Strong gradients in Q_0 (reflected short-wave radiation) and R were observed from ice station ZEBRA through the marginal site YANKEE to the most distant site, X-RAY. Figures 8 and 9 show average daily albedo and net radiation totals, respectively, at the three sites. Albedo values (α) were derived from:

$$\frac{Q_0}{Q_i}$$

where Q_i is the value measured at Yankee and Q_0 the value at each site; R

TABLE 4

Mean Hourly Radiation Balance Values - 1982
($MJ\ m^{-2}\ h^{-1}$)
JD 170-207

Height	Zebra	Yankee	X-Ray
Q_i	0.946	0.946	0.946
$Q_i\alpha$	-0.497	-0.259	-0.192
Ii	0.949	0.949	0.949
Io	-1.212	-1.183	-1.172
R	0.186	0.453	0.531

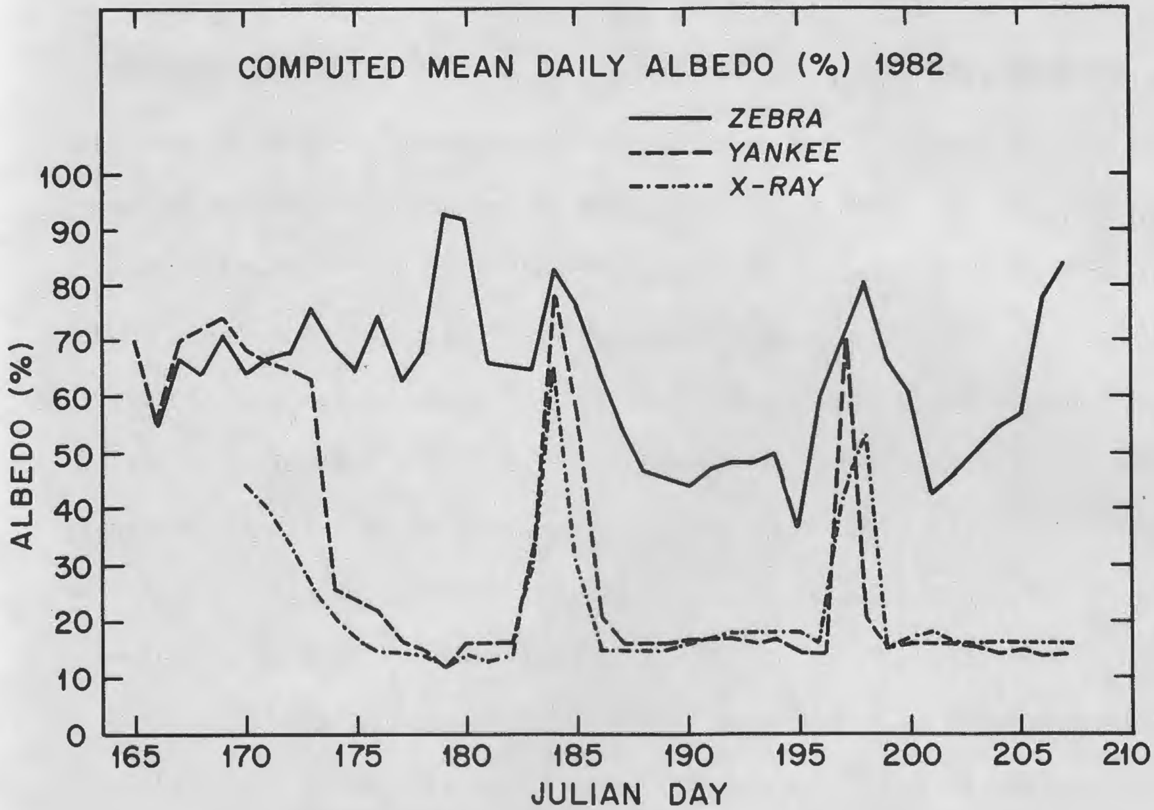

Figure 8 Mean daily albedo, 1982, for stations X-Ray, Yankee and Zebra.

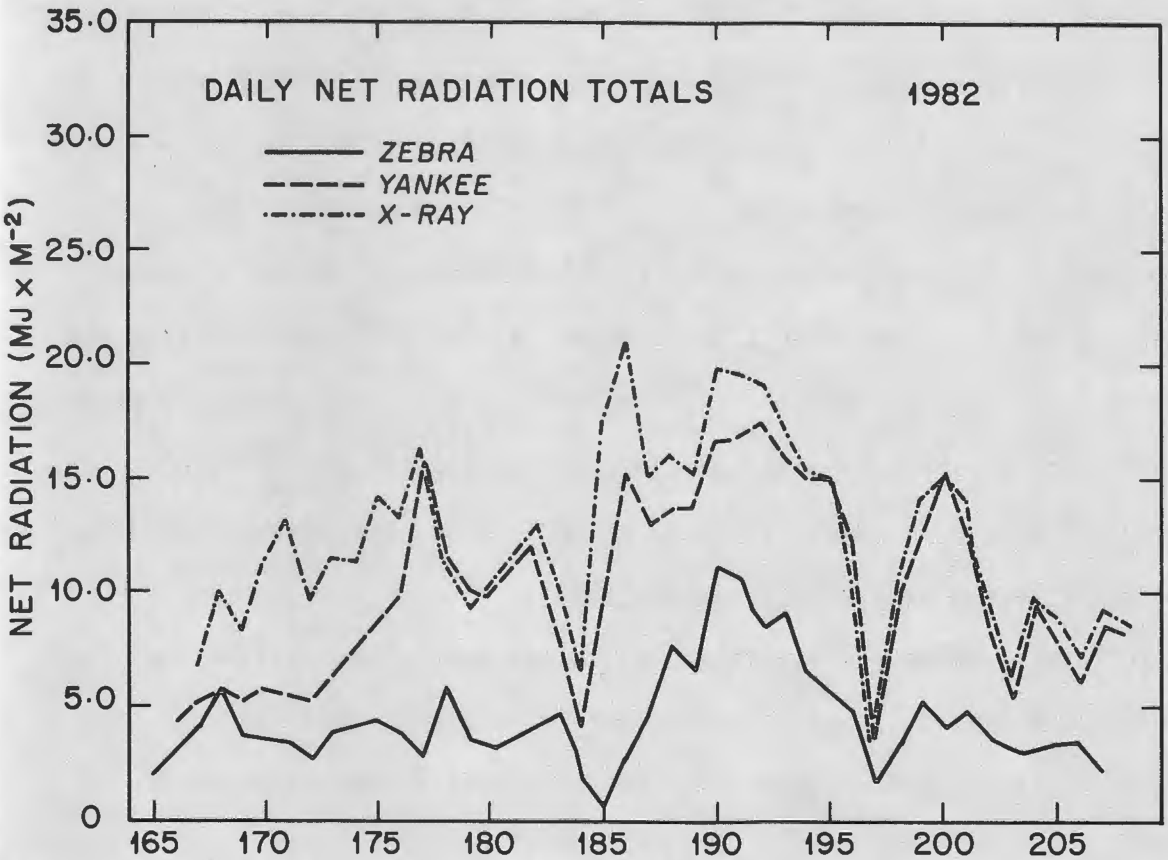

Figure 9 Mean daily net radiation, 1982, for stations X-Ray, Yankee and Zebra

was measured independently at each site. Clearly R is primarily dependent on albedo. The importance of mid-summer snowfall events (JD 183, 184, and 197, 198) is also apparent in reducing the amount of energy available at the surface. Albedo declined first at X-RAY and then at YANKEE. In fact, the initial value of 0.44 indicates that ablation had already begun by JD 170 at X-RAY and snow-free ground was visible first at this site. A base value of approximately 0.16 for both stations was reached by JD 178 (June 27) indicating complete removal of the snowpack. By contrast, at station ZEBRA, the original winter snowpack had not shown any appreciable reduction in albedo by that date. In fact it was not until early July (>JD 186) that any significant change in albedo took place on the ice cap (Figure 8). It is of particular interest that albedo began to decline first at the station farthest from the ice cap. This could be due to a lower mean winter snowpack at this site or to a lessening of any thermal effect of the ice cap with distance from the ice edge. Unfortunately, logistical problems prevented the establishment of this station until JD 170 which resulted in no radiation data at X-RAY for the critical period prior to JD 170. In 1983, a snow survey did reveal a reduction in snow depth from YANKEE to X-RAY which, if generally true, might explain the more rapid rise in albedo at the site farthest from the ice cap. It is possible that this gradient is related to drifting snow from the ice cap though it is not clear why snow would preferentially accumulate in the immediate vicinity of the ice cap itself which is just as exposed as the area around station X-RAY.

It is also of interest that net radiation values at X-RAY were consistently higher than at station YANKEE, nearer the ice cap edge, throughout the season (Figure 9). Several explanations for this are possible. Firstly, albedo at X-RAY was consistently lower than at YANKEE even after all snow had melted (though at that time the difference was very small). Secondly, it may be that our assumption of equal receipts of Q_i and I_i at all sites may be in error, but for this factor to account for the higher measured net radiation at X-RAY one would have to assume higher total radiation receipts at X-Ray than at YANKEE and this seems unlikely over the distances involved (approximately 5 km). Possibly a combination of these factors was important at times; nevertheless, even neglecting the contentious reasons for differences in R between X-RAY and YANKEE, it is abundantly clear that values of R over the ice cap and over the snow-free tundra nearby are drastically different. This is in strong disagreement with the conclusions of Ohmura (1982) who found similar values of R between tundra and the ablation area of polar glaciers despite differences in albedo. Ohmura's results seem inherently incorrect and our data clearly confirm this view. In 1982, the ice cap received only 35% of the net radiation on the surrounding tundra, which represents a profound reduction in radiative energy available for ablation.

In conclusion, there is evidence that net radiation was highest at the site farthest from the ice cap and that albedo fell at this site first. Whether this was the result of a higher snowpack around the ice cap edge (possibly as a result of snow drifting from the ice cap) or whether the ice cap exerted a thermal effect on snowmelt in the immediate vicinity of the ice cap in the early part of the ablation season is not clear. Seasonal net radiation totals beyond the ice cap were markedly higher than on the ice cap itself.

b) Temperature

Mean hourly temperatures and melting degree day totals, measured at three levels at stations X-RAY, YANKEE and ZEBRA, are shown in Table 5. At all levels, a clear gradient is apparent from X-RAY to ZEBRA with intermediate values at station YANKEE, near the edge of the ice cap. Melting degree day totals on the ice cap were only 40-65% of values at X-RAY. Differences between the ice cap site and the other two sites are statistically significant ($p = 0.001$); differences between the two tundra sites are not. The greatest difference between the three sites is at the 15 cm level as one might expect. This level is near the laminar boundary layer and thus more representative of surface temperatures than higher levels where turbulent overturning is more common.

Although the mean temperature at YANKEE, near the ice edge was intermediate between values on the tundra at X-RAY and on the ice at ZEBRA, it is not clear if this can be interpreted as an "ice-edge cooling effect." If this was the case, during periods of northerly airflow (i.e. involving advection of cooler air from the ice cap) temperatures at YANKEE should have been lower than at other times. Unfortunately, wind direction data were not accurately measured in 1982 but visual observations of direction indicated that the prevailing airflow was towards the ice cap, not away from it. Furthermore, stratification of temperature data from YANKEE revealed no statistically significant difference between times of northerly or southerly airflow. Further study of this question is needed before a definitive conclusion can be reached.

If station X-RAY is assumed to be beyond any thermal influence of the ice cap, the total cooling effect can be quantified by subtracting temperatures at ZEBRA from those at X-RAY. This gives mean values of

TABLE 5

Mean Hourly Temperatures and Melting Degree Day Totals,

JD 170-207, 1982 (^{o}C)

I. Mean Temperatures

Height	a. Zebra	b. Yankee	c. X-Ray	(c-a)*
300 cm	0.99	1.75	1.81	0.82
150 cm	1.05	1.77	2.03	0.98
15 cm	1.16**	2.98	3.02	1.86

*"Cooling effect" (see text)
** JD 178-207

II. Melting Degree Days*

Height	a. Zebra	b. Yankee	c. X-Ray
MDD_{300}	53 (65)	76 (94)	81
MDD_{150}	55 (60)	80 (87)	92
MDD_{15}	49 (40)	116 (95)	122

* Based on mean daily temperatures derived from (max. + min)/2.

Values in parenthesis express MDD as a percentage of values at X-Ray.

1.86 degrees C, 0.98 degrees C and 0.82 degrees C at 15 cm, 150 cm and 300 cm respectively. Thus the "cooling effect" is most apparent at lowest levels and decreases with height. Studies of the White Glacier, Axel Heiberg Island, have also attempted to quantify this cooling effect. Muller and Roskin-Sharlin (1967) calculated the difference between screen temperatures (approximately 150 cm) at their lower Ice and Base Camp stations. The former was in the center of a 1 km wide valley glacier (ablation zone) and the latter approximately 2 km away in the adjacent unglacierized valley. Both had similar elevations (approximately 200 m a.s.l.). These results indicated a mean cooling effect (for June, July and August 1961) of approximately 1.5 degrees C, somewhat higher than in this study. However, the topographic situation of the two areas is quite different with significantly more relief in the Axel Heiberg study; consequently, effects of cold air drainage, radiation from valley walls, shading, etc., may be important factors in that study. Nevertheless, the results indicate a similar thermal effect of 1-1.5 degrees C at 150 cm.

Muller and Roskin-Sharlin also arrived at two other interesting conclusions which can be tested with our data set. They noted that the "cooling effect" was greater on clear days with high global radiation receipts than on cloudy days and that the cooling effect becomes greater as the season progresses. Table 6 shows mean temperatures at the three stations and three levels for $\geqslant$ 7/10 and $\leqslant$ 3/10 cloud cover. As one might expect, temperatures are generally higher under relatively cloud-free conditions but the "cooling effect" is greater at such times than during cloudy periods (Table 6, column 5). This is probably because during relatively clear sky conditions, air temperatures over the tundra can rise rapidly (due to lower albedo and low specific heat of the surface) whereas

TABLE 6

Mean Hourly Temperatures and "Cooling Effect" (°C)
for Different Conditions of Cloudiness

Cloud Cover G.E. 7/10

	Zebra	Yankee	X-Ray	"Cooling Effect"
15 cm	0.83	2.21	2.64	1.81
150 cm	0.51	1.22	1.55	1.04
300 cm	0.39	1.10	1.36	0.97

Cloud Cover L.E. 3/10

	Zebra	Yankee	X-Ray	"Cooling Effect"
15 cm	2.45	3.28	4.32	1.87
150 cm	2.32	3.23	3.92	1.60
300 cm	2.41	3.50	3.59	1.18

snow and ice acts as an energy sink, so any increase in incoming radiation results in a smaller temperature increase over the ice cap. As a result the differential between the sites is enhanced under clear skies. Of course, this does not mean that clear skies favor ice cap survival, as higher temperatures over the ice cap and tundra increase the sensible heat flux to the ice and accelerate ablation.

Table 7 shows the "cooling effect" by sub-period. Muller and Roskin-Sharlin suggest that the increase in "cooling effect" as the summer progresses is due to the (almost) unlimited capacity of a glacier to absorb heat throughout the summer whereas (once snow cover has melted) the lower specific heat of the tundra surface and limited sub-surface heat flux results in a strong sensible heat flux to the atmosphere and much higher temperatures in the adjacent air layer. Consequently as the summer season progresses, the "cooling effect" increases. The St. Patrick Bay Ice Cap data also show a tendency for the cooling effect to increase as the season progresses. However, the maximum "cooling effect" occurred during the period JD 180-189, a period of generally clear skies and relatively high temperatures after snow-cover had melted from the tundra; these conditions are not inconsistent with Muller and Roskin-Sharlin's model.

Analysis of the low-level thermal structure of the atmosphere at the three sites provides further insight into the nature of an ice-cap "cooling effect." Seasonal mean lapse rates (JD 170-207)in the 15 cm to 150 cm level were -0.82, -0.79 and -0.29 degrees C m^{-1} at station X-RAY, YANKEE and ZEBRA respectively. The difference between the mean at the two tundra sites is not significant but between those and ZEBRA is highly significant ($p = 0.001$). These mean values reflect a higher frequency of

TABLE 7

"Cooling Effect" (°C) by 10-Day Intervals

	JD 170-179	JD 180-189	JD 190-199	JD 200-208
15 cm	1.78	2.52	1.31	1.83
150 cm	0.53	1.40	0.93	1.06
300 cm	0.53	1.09	0.81	0.89

inversions at the ice station, as a result of the continual presence of a cold snow or ice surface. This is further illustrated by Table 8 which shows the diurnal frequency of inversions at the three stations. Inversions reach a maximum frequency at all sites during low sun periods, as one would expect. Overall, inversions occur 32% of the time on the ice cap compared to only 11-13% at the other sites. During these periods sensible heat flux is directed towards the surface. Since the surface temperature can not increase above 0 degrees C, the inversion is not readily disturbed and the near surface air temperature remains low. Over the snow-free tundra, relatively high surface temperature results in an upward sensible heat flux, warming the near surface atmosphere. Thus, as air moves from snow-free to the snow and ice-covered surface the lower atmospheric temperature structure is modified as shown schematically in Figure 10.

It is of interest that the "cooling effect" has a pronounced diurnal pattern, with maximum values in late afternoon and minimum values during low-sun periods (Figure 11). This characteristic may reflect the higher frequency of stable conditions over the ice cap as compared to the tundra, particularly in the late afternoons. Although a pronounced diurnal variation in inversions was recorded at both sites (Table 8) the <u>difference</u> in inversion frequency between the sites follows a similar diurnal pattern to that of the "cooling effect."

In conclusion, a thermal gradient was observed along a transect perpendicular to the ice cap edge. This was maximized during relatively cloud-free periods. Maximum temperature differences between ice cap and tundra sites were observed at low levels (15 cm). The cooling effect of the ice cap was less at the start of the ablation season than

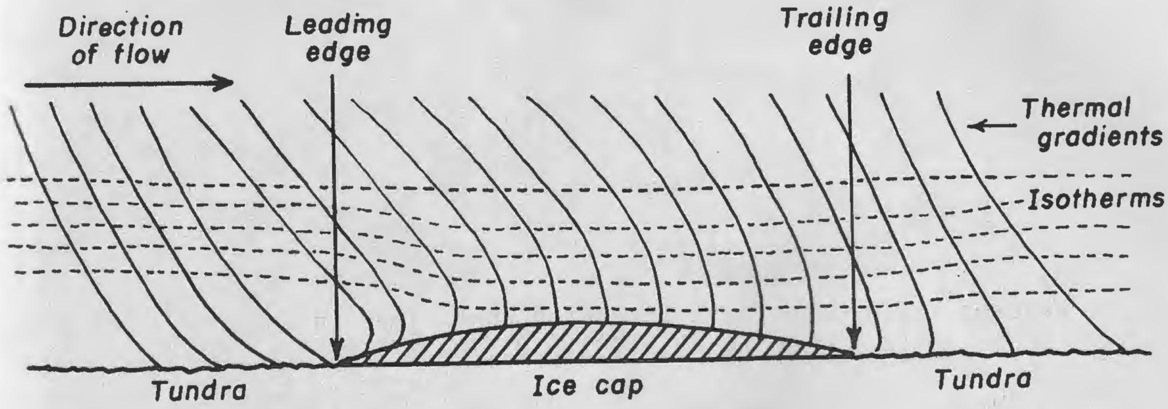

Figure 10 Schematic diagram of cooling effect of ice cap on lower atmosphere with wind direction from left to right (after Oke, 1978).

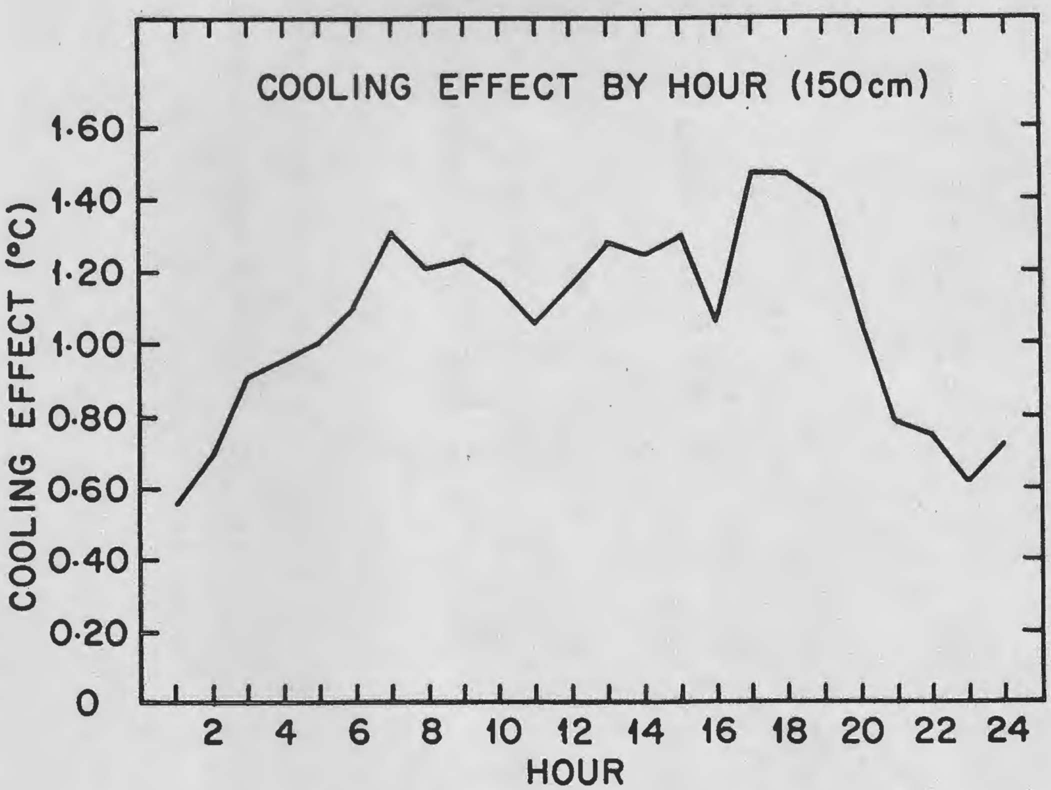

Figure 11 Mean hourly "cooling effect" (X-Ray - Zebra mean temperatures) at 150 cm level, based on J.D. 170 to J.D. 207 1982

TABLE 8

Percent Valid Cases with Inversion Conditions in 15 cm to 150 cm layer, 1982 (JD 170-207)

Hour	Zebra	Yankee	X-Ray
1	44	16	21
2	41	16	34
3	43	18	42
4	36	13	29
5	25	13	26
6	26	11	24
7	18	10	22
8	25	9	8
9	29	10	5
10	22	10	5
11	21	12	3
12	14	14	8
13	15	10	3
14	19	11	5
15	19	8	8
16	33	3	3
17	27	6	5
18	32	6	5
19	44	6	8
20	52	9	8
21	59	9	8
22	43	6	8
23	43	13	8
24	44	10	11
$\bar{x}$	32	11	13

subsequently. Inversions are more common over the ice cap than the tundra and a diurnal cooling effect, probably related to this difference, reaches a maximum in late afternoons.

TOPOCLIMATIC VARIATIONS: 1983

As noted earlier, climatic conditions in the summer of 1983 were markedly different than in 1982. This is clearly illustrated by comparing daily albedo and net radiation measurements (figures 12 and 13; cf. Figures 8 and 9). In 1983, surface albedo was considerably higher and net radiation values correspondingly lower. Furthermore, since the persistent snow cover in 1983 created similar surface conditions at all measurement sites, topoclimatic differences between the sites were greatly reduced. Except for brief melt episodes (e.g. JD 170-174 and 181-183 when frost-hummocks were exposed at X-RAY) albedo was similar at all sites for most of the season. Only after approximately JD 198 did the area around X-RAY become extensively snow-free, resulting in lower short-wave radiation losses for the season as a whole (Table 9). Net radiation at all sites was extremely low, and on some occasions (with clear skies) negative daily totals were recorded.

Mean temperatures and melting degree day (MDD) totals at the three stations are shown in Table 10. Temperatures were significantly lower in 1983; differences between the two seasons were greatest at the tundra site, X-RAY, and least on the ice cap (ZEBRA). The largest differences at all sites occurred at the 15 cm level (2.7 degrees C lower at X-RAY in 1983). Melting degree day totals were very similar at all sites in 1983, whereas in 1982 MDD totals at ZEBRA (15 cm level) were only 40% of those at X-RAY. Clearly, the extensive snow-cover in 1983 eliminated the topoclimatic effects which were manifested so clearly in 1982.

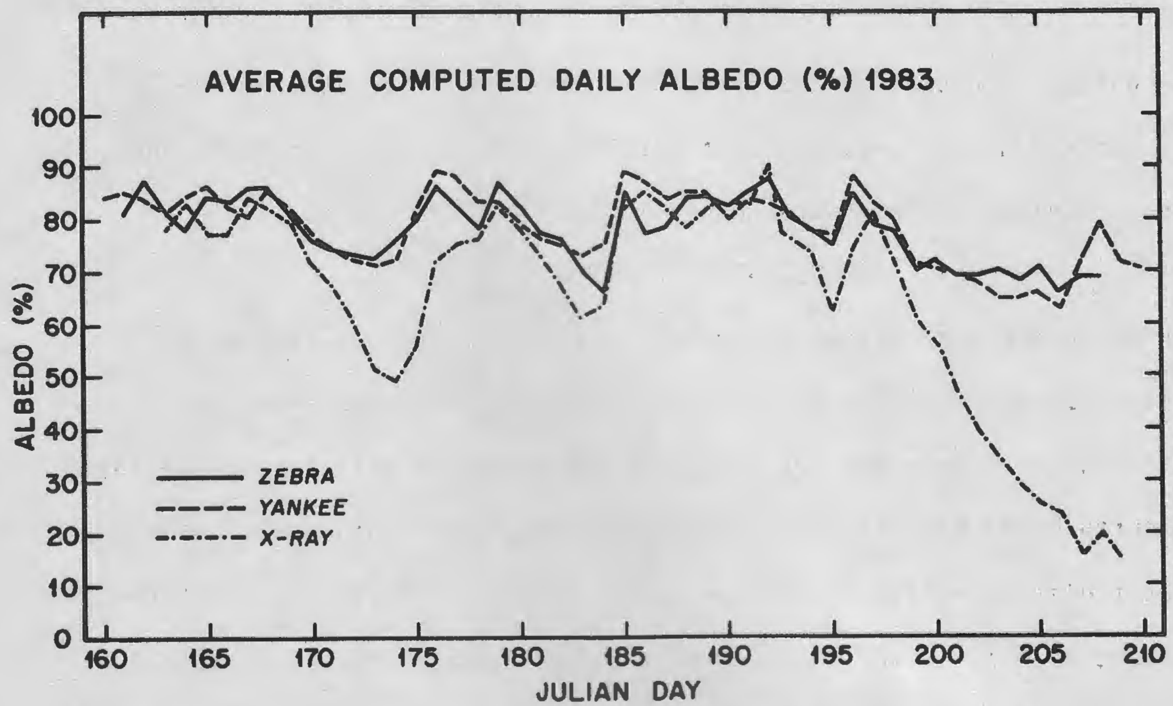

Figure 12 Mean daily albedo in 1983 at stations X-Ray, Yankee and Zebra.

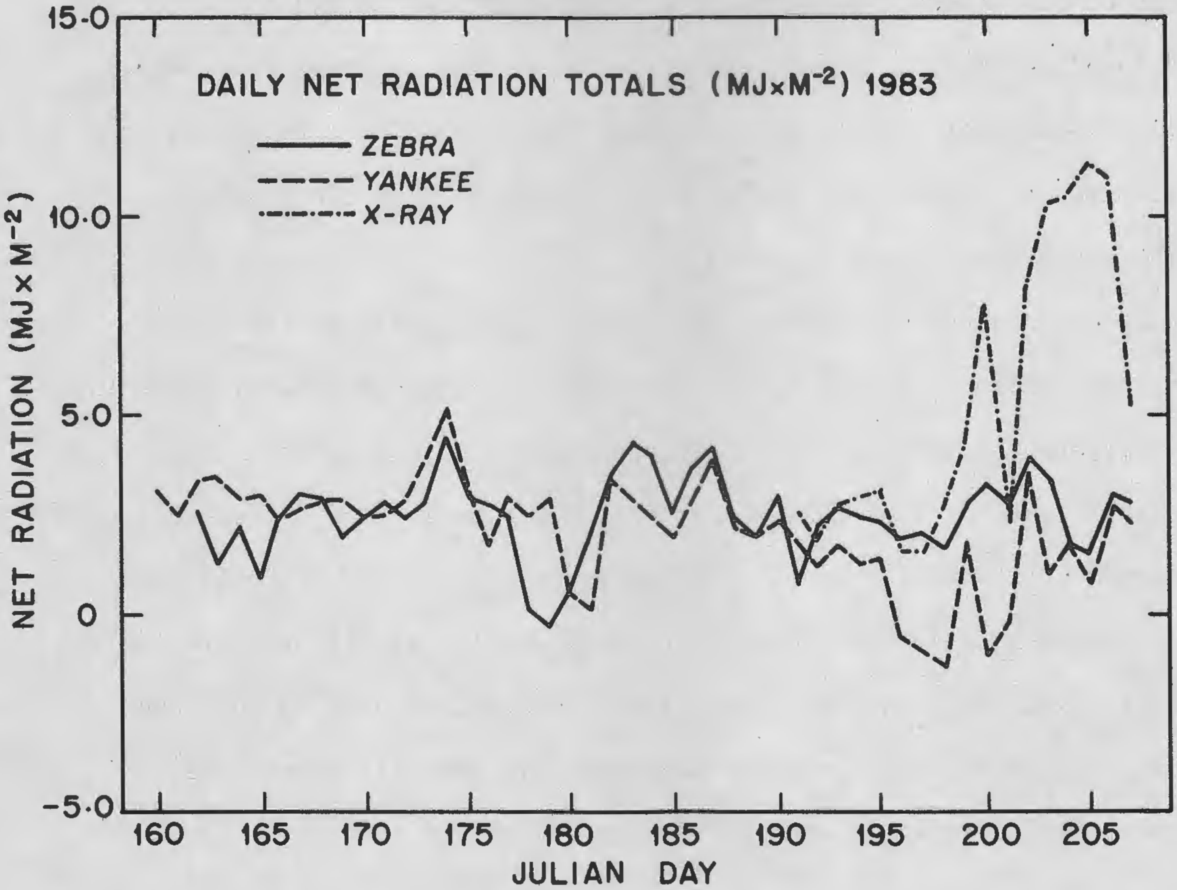

Figure 13 Mean daily net radiation in 1983 at stations X-Ray, Yankee and Zebra.

TABLE 9

Mean Hourly Radiation Values (MJ m^{-2} h^{-1})
JD 170-207

1983

	Zebra	Yankee	X-Ray
Qs	0.924	0.924	0.924
Qsα	-0.706	-0.713	-0.598
Ii	0.888	0.888	0.888
Io	-1.013	-1.020	[-0.994]*
R	0.093	0.079	[0.220]*

* Calculated only for JD 191-207 because of net radiation equipment failure prior to that period.

TABLE 10

Mean Hourly Temperatures and Melting Degree Day Totals
JD 170-207, 1983 (°C)

I. Mean Temperatures

	Zebra	Yankee	X-Ray
T_{300}	–	0.95	–
T_{150}	0.90	0.83	0.29
T_{15}	0.46	0.63	0.91

II. Melting Degree Days*

	Zebra	Yankee	X-Ray
MDD_{300}		69	
MDD_{150}	68	68	68
MDD_{15}	51	56	51

*Based on mean daily temperatures derived from (max + min)/2.

DISCUSSION

Topoclimatic differences observed in 1982 between the ice cap and tundra sites can be considered in terms of two conceptual models shown in Figure 14. Snow and ice cover, with a high albedo relative to tundra, limits net radiation and hence sensible and latent heat flux to the atmosphere. As ice has a high specific heat, it acts as a large sink for energy at the surface and this continues long after snow cover has melted from adjacent tundra regions. Surface temperature on the ice cap is limited to ≤ 0 degrees C so near-surface inversions are common, restricting turbulent heat exchange and energy flux to the surface. Low surface roughness over the ice cap enhances this effect. The net result is lower temperatures over the snow and ice surface which may favor diurnal riming and delay the seasonal decline in albedo. Lower temperatures over the snow and ice may lead to cold air advection to adjacent areas retarding melt and thereby delaying the exposure of tundra surfaces which would rapidly warm and reverse the advective effect. By contrast, a tundra/felsenmeer surface has a much rougher surface on which protruding rocks and vegetation may remain exposed above the regional snow surface. The substrate has a low albedo and low specific heat capacity. As a result, net radiation at the exposed surface is high, sub-surface heat flux is small, and surface temperature is essentially unlimited. Unstable temperature profiles which result, favor high sensible heat flux to the atmosphere, leading to high surface air temperature advection to adjacent areas and rapid removal of the snow cover. Tundra surfaces rapidly dry out reducing latent heat flux and directing net radiation into sensible heat flux to the the lower atmosphere. Warm air advection to the adjacent snow cover and ice cap will be minimal at first but increase

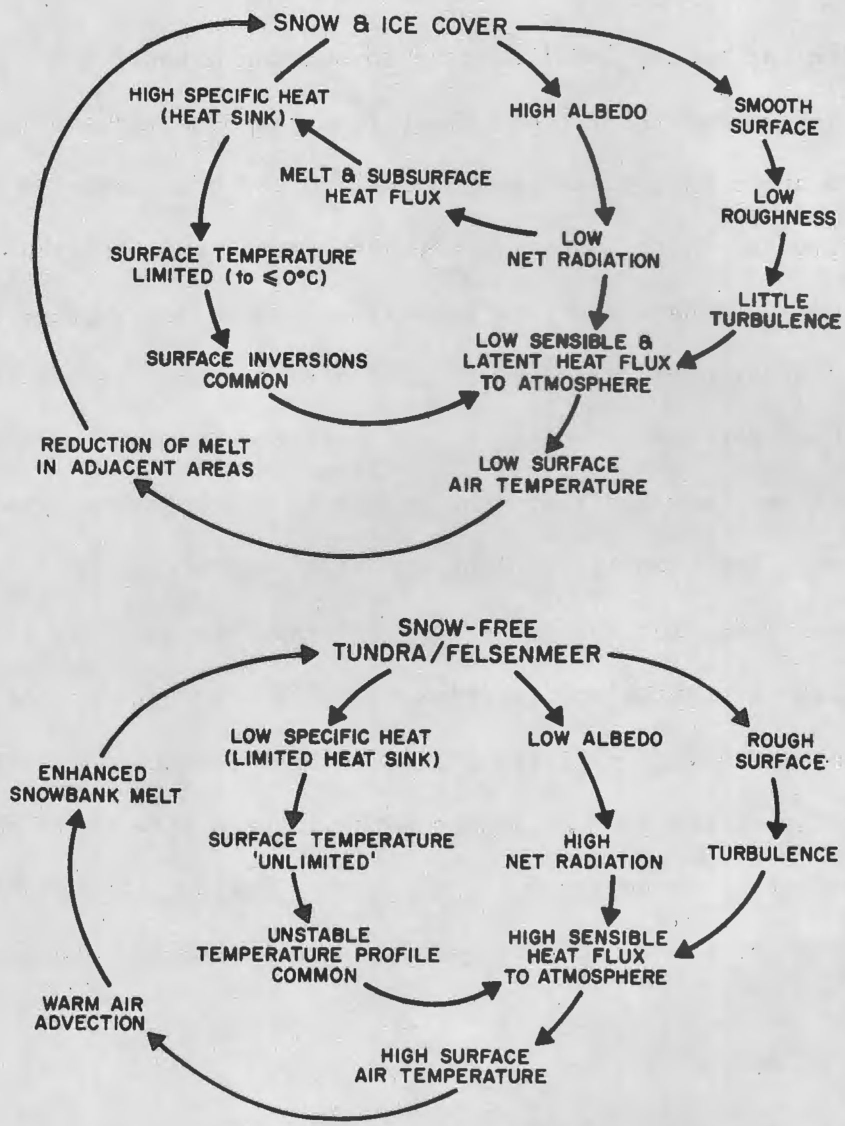

Figure 14 Conceptual model of feedbacks involved in a) maintenance of snow and ice cover, and b) maintenance of snow-free tundra/felsenmeer surfaces.

rapidly as the ablation season progresses and more land surfaces become exposed.

Does an ice cap modify local climate to such an extent that its preservation is favored? It seems clear from the observations made and the discussion above that conditions on the ice cap bring about a "cooling effect" relative to adjacent snow-free tundra areas, and that this cooling effect is absent when snow cover is extensive. However, whether the ice cap affects adjacent areas directly by cool air advection is not clear on the scale studied herein. Cooling of air over the ice cap is the result of heat flux to the snow and ice; the extent to which this occurs in a season will vary, but clearly prolonged cool air advection must be balanced by mass loss from the ice cap. If wind direction is persistently from a particular direction, the "leading edge effect" (Oke, 1978) shown schematically in Figure 10, would tend to increase ablation on the windward edge of the ice cap, whereas the leeward side would be relatively protected, or buffered. Over a long period, this might even favor "migration" of the ice cap downwind, given favorable topographic conditions.

SUMMARY

Meteorological measurements in the lowest 3 m of the atmosphere were conducted along a 5 km transect from the center of a small plateau ice cap (on northeastern Ellesmere Island) to the adjacent unglacierized tundra/felsenmeer. Differences in relief across the transect were <50 m and the entire area was completely unshaded. The major difference between the sites was thus the underlying surface and proximity to the ice cap. Measurements began when snow cover was extensive across the entire area, and continued through the ablation seasons (of 1982 and

1983). The objective was to assess the effect of the ice cap on modifying local climate. The following results were obtained:

1. Seasonal net radiation totals were highest at the site farthest from the ice cap and lowest on the ice cap. The ice cap site received only 35% of the net radiation on the surrounding tundra. Intermediate values were recorded near the ice cap edge.

2. A strong temperature gradient was observed between the tundra and the ice cap. This gradient was maximized at the 15 cm level. Melting degree days on the ice cap were only 40-65% of those on the adjacent tundra. Intermediate values were recorded near the ice cap edge. Maximum temperature differences between the sites occurred under clear skies after seasonal snow cover on the tundra had melted.

3. Low-level inversions are more common over the ice cap than over the tundra and a diurnal cooling effect, probably related to this difference, reaches a maximum in late afternoon.

4. In 1983, extensive and persistent snow cover eliminated any significant topoclimatic differences between the sites.

5. A conceptual model of feedback effects which tend to assist in the maintenance of a snow and ice cover is presented. Similarly, a model of surface-atmosphere interactions over snow-free tundra/felsenmeer is presented.

6. Observations indicate that the ice cap may bring about a 'cooling effect' relative to the adjacent snow-free tundra and that such an effect is absent when snow cover is extensive. Any cool air advection from the ice cap is the result of heat flux to the snow and ice. If this continued for a long time, mass losses from the ice cap would inevitably result.

7. Further studies are needed to isolate and quantify topoclimatic conditions on and around plateau ice caps of varying size.

ACKNOWLEDGEMENTS

This work was supported by the U.S. National Science Foundation, Grant ATM80-17745 to the University of Massachusetts. Logistical support was provided by the Polar Continental Shelf Project, Department of Energy, Mines and Resources, Ottawa. We are grateful to M. Palecki, C. Allen, M. Retelle, J. Fabel and R. Friend for assistance in the field.

REFERENCES

Ambach, W. 1974. On the influence of cloudiness on the net radiation balance of a snow surface with high albedo. Journal of Glaciology, 13(67), 73-84.

Bonacina, L.C.W., 1948. The self generating or automatic process in glaciation. Quarterly Journal of Royal Meteorological Society, vol 74, 85-88.

Bradley, R.S., and Serreze, M.C. 1983. Topoclimatic studies of a small plateau ice cap, northern Ellesmere Island, N.W.T., Canada, p. 57-59, in Abstracts of the 12th Arctic Workshop, Contribution No. 44, Dept. Geology and Geography, Univ. Massachusetts, Amherst, MA.

Bradley, R.S., and Serreze, M.C. 1985. Glacio-climatic studies of a High Arctic Plateau Ice Cap, Part 1: mass balance (submitted).

Braithwaite, R.J. 1978. Air Temperature and Glacier Ablation - A Parametric Approach. Unpublished Ph.D. Thesis, McGill Univ., University Microfilm. 146 pp.

Hattersley-Smith, G. and Serson, H., 1973. Reconnaissance of a small ice cap near St. Patrtick Bay, Robeson Channel, Northern Ellesmere Island, Canada. Journal of Glaciology 12(66), 417-421.

Hoinkes, H., 1970. Radiation budget at Little America V., 1957. pp. 163-284 in Isage Proceedings, Publication 86, IASH, Gentbrugge, Belgium.

Holmgren, B., 1971. Climate and energy exchange on a sub-polar ice cap in summer. Arctic Institute of North America, Devon Island Expedition, 1961-1963. Part F. On the Energy

Exchange of the Snow Surface at Ice Cap Station. Meddelanden fran Uppsala Universitets, Meteorologiska Institutionen, Nr. 112. 53 pp.

Ives, J.D., Andrews, J.T., and Barry, R.G., 1975. Growth and decay of the Lazurentide Ice Sheet and Comparaisons with Fenno-Scandinavia. Die Naturwissenschaften 62, 118-125.

Kellogg, W.W., 1975. Climatic feedback mechanisms involving polar regions. pp. 111-116 in Climate of the Arctic (G. Weller and S.A. Bowling, eds.). University of Alaska Press, Fairbanks.

Muller, F. and Roskin-Sharlin, N., 1967. A High Arctic climate study on Axel Heiburg Island, Canadian Archipelago, Summer 1961. Part 1, General Meteorology. Axel Heiburg Island Research Reports on Meteorology, 3, McGill University, Montreal, 82 pp.

Ohmura, A., 1982. Climate and energy balance on the Arctic tundra. Journal of Climatology 2, 65-84.

Oke, T.R., 1978. Boundary Layer Climates. London: Methuen and Co., Ltd., 372 pp.

Palecki, M., Serreze, M.C., and Bradley,R.S. 1985. Glacio-climatic studies of a high arctic plateau ice cap, part V: boundary layer observations (in preparation).

Serreze, M.C., and Bradley, R.S. 1985a. Glacio-climatic studies of a high arctic plateau ice cap, part III: Radiation Climate (submitted)

Serreze, M.C., and Bradley, R.S. 1985b. Glacio-climatic studies of a high arctic plateau ice cap, part IV: energy balance (in press).

GLACIO-CLIMATIC STUDIES OF A HIGH ARCTIC PLATEAU ICE CAP PART III: RADIATION CLIMATOLOGY

M.C. Serreze and R.S. Bradley

University of Massachusetts, Amherst.

ABSTRACT

Hourly measurements of incoming shortwave and longwave radiation, surface albedo and net radiation were made on an unshaded plateau ice cap on northeastern Ellesmere Island, in the summers of 1982 and 1983. Incoming shortwave radiation (Qi) is strongly dependent on solar angle whereas this is not so for incoming longwave radiation (Ii). All cloud types increase Ii, especially low dense clouds, snow and fog. Relative transmission of Qi is high in all cloud types compared to clouds at lower latitudes. With high surface albedo (>0.75) net radiation (R) is strongly and positively correlated with net infra-red radiation (In) but shows little relationship to net shortwave radiation (Qn). By contrast, with low surface albedo (<0.20) R is negatively correlated with In but positively related to Qn. Under high albedo conditions, an increase in cloud cover leads to higher values of R but under low albedo conditions R decreases as cloud cover increases. Maintenance of snow cover is favored by the normal seasonal progression of albedo and cloud cover changes (high albedo, clear skies to low albedo, cloudy conditions) which occur in the arctic.

INTRODUCTION

Meteorological observations were carried out in the summers of 1982 and 1983 on 'St Patrick Bay Ice Cap', northern Ellesmere Island, N.W.T., Canada (81°57' N, 64°10'W). The ice cap is situated on the Hazen Plateau at an elevation of ~850 m above sea level (Figure 1). Because the surrounding topography is so flat, the ice cap is completely unshaded so the effects of relief on topoclimate are minimized. Observations were initiated to determine the extent to which the ice cap assists in its own preservation by modification of the local climate (Bradley and Serreze, 1985). As part of the observation program, hourly measurements of

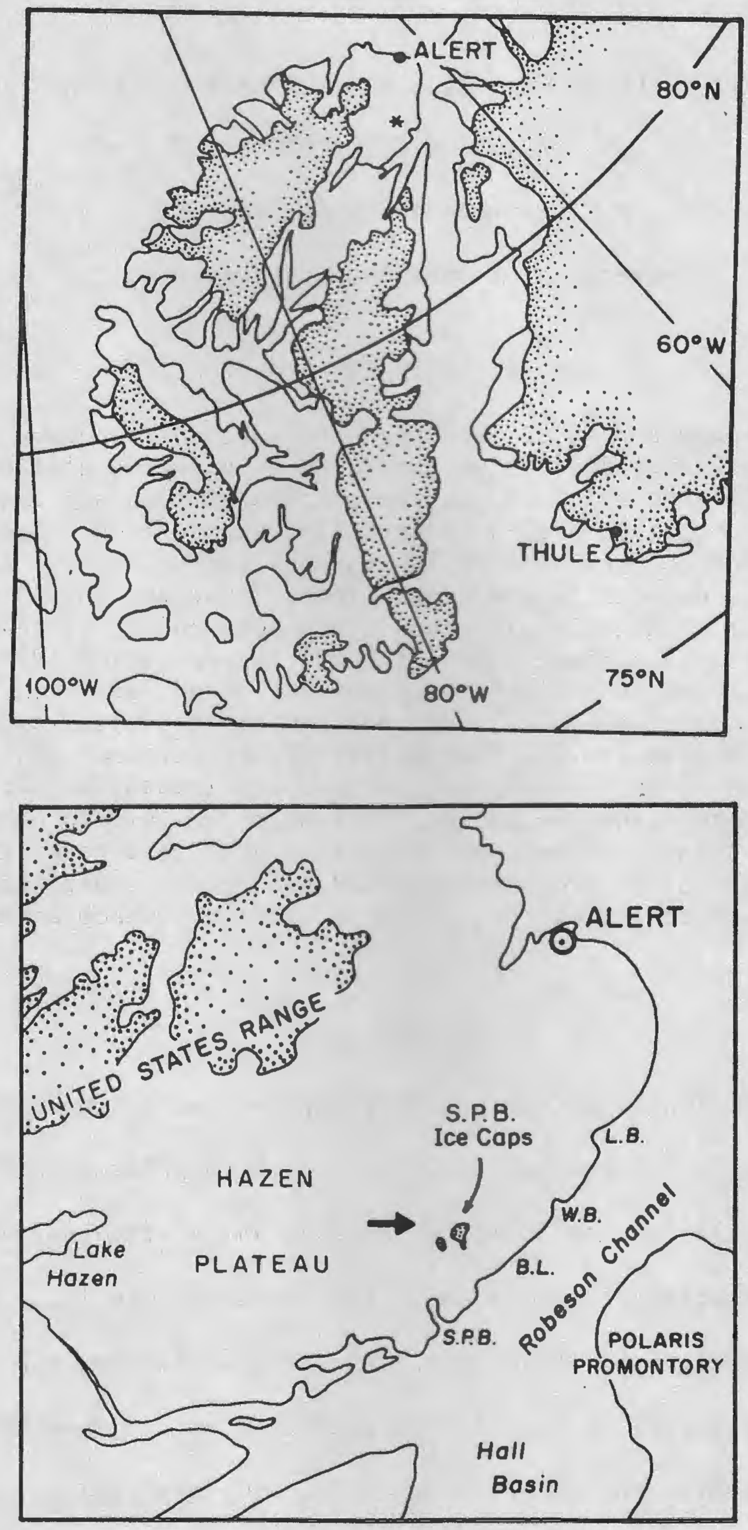

Figure 1 Regional location maps: S.P.B. = St. Patrick Bay, B.L. = "Beaufort Lakes;" W.B. = Wrangel Bay; L.B.= Lincoln Bay.

incoming short and long-wave radiation, cloud type and extent, surface albedo and net radiation were recorded. Instrumentation used is shown in Table 1. Here we describe results of the radiation measurements, stratified by cloud type, and discuss the relationships between surface albedo, cloud cover and net radiation, and their significance for ice cap mass balance.

OVERVIEW OF CONDITIONS IN 1982 AND 1983

Daily totals of incoming short radiation ($Q_{\downarrow}$) and long-wave radiation ($I_{\downarrow}$) recorded at station Yankee are shown in Figures 2 and 3. Large day-to-day variations in $Q_{\downarrow}$ are associated with synoptic scale events, with peaks associated with clear sky anticyclonic conditions. Near the solstice (Julian Day [JD] 172) approximately 77% (1982) and 74% (1983) of maximum short-wave radiation receipts at the top of the atmosphere, reached the surface. These values compare with a figure of 81% recorded by Holmgren (1971) on the Devon Island Ice Cap in late June; this higher value probably reflects the higher elevation (1320 m) of the Devon Island station as compared to St. Patrick Bay Ice Cap. Daily variations of $I_{\downarrow}$ are much less variable than $Q_{\downarrow}$ and, as might be expected, there is a close inverse relationship between the two variables which reflects the influence of cloud cover. Under clear skies, $Q_{\downarrow}$ is high but there is little counter-radiation ($I_{\downarrow}$). Conversely, under cloudy skies,

TABLE 1

Radiation Instruments Used in Study

Incoming and Reflected Short-wave Radiation (Qi and Qo

Eppley 'Black and White' Pyranometers, Model 8-48

Incoming Infra-red Radiation (Ii)

Eppley Precision Infra-red Radiometer (pyrgeometer)

Net Radiation (R)

'Fritschen type' Net Radiometers (Micromet Instruments)

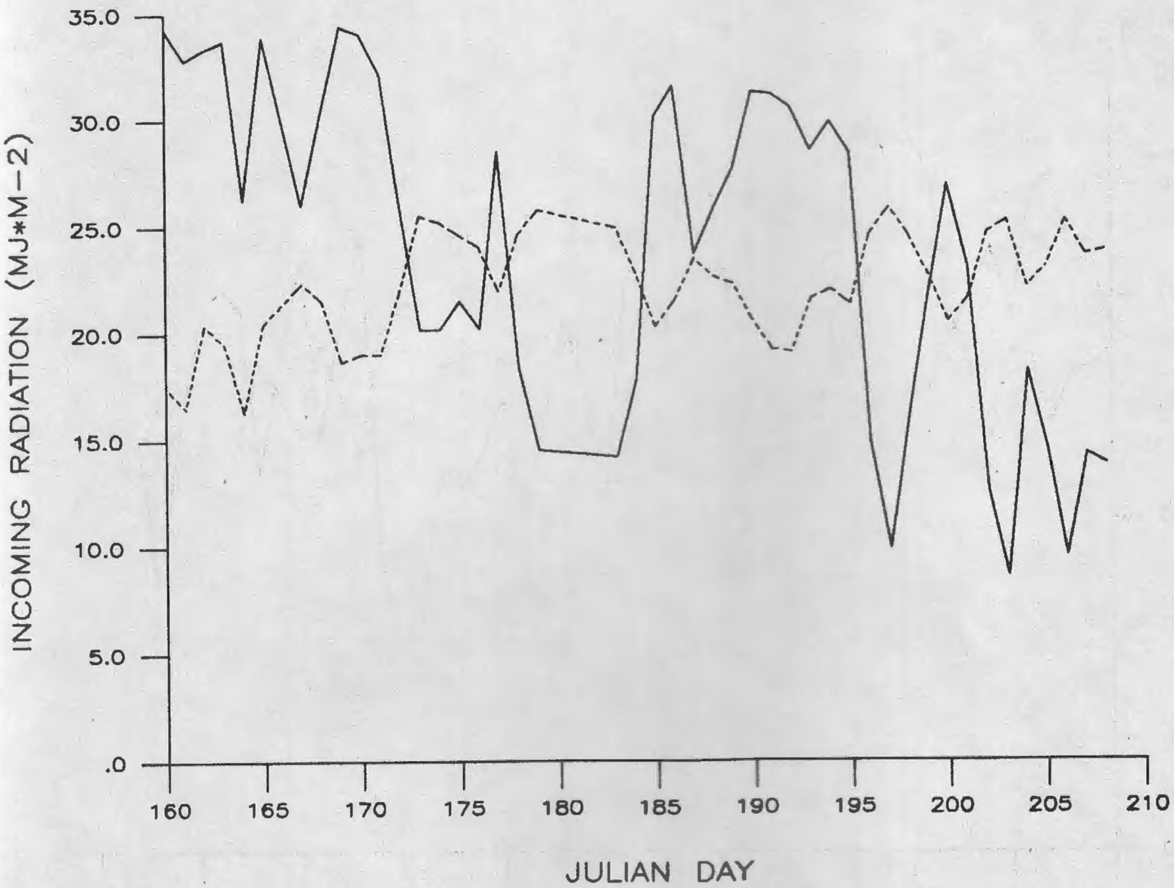

Figure 2: Daily receipt of incoming shortwave radiation (Qi) (dark line) and longwave radiation (Ii)(light line)in 1982 at Station Yankee.

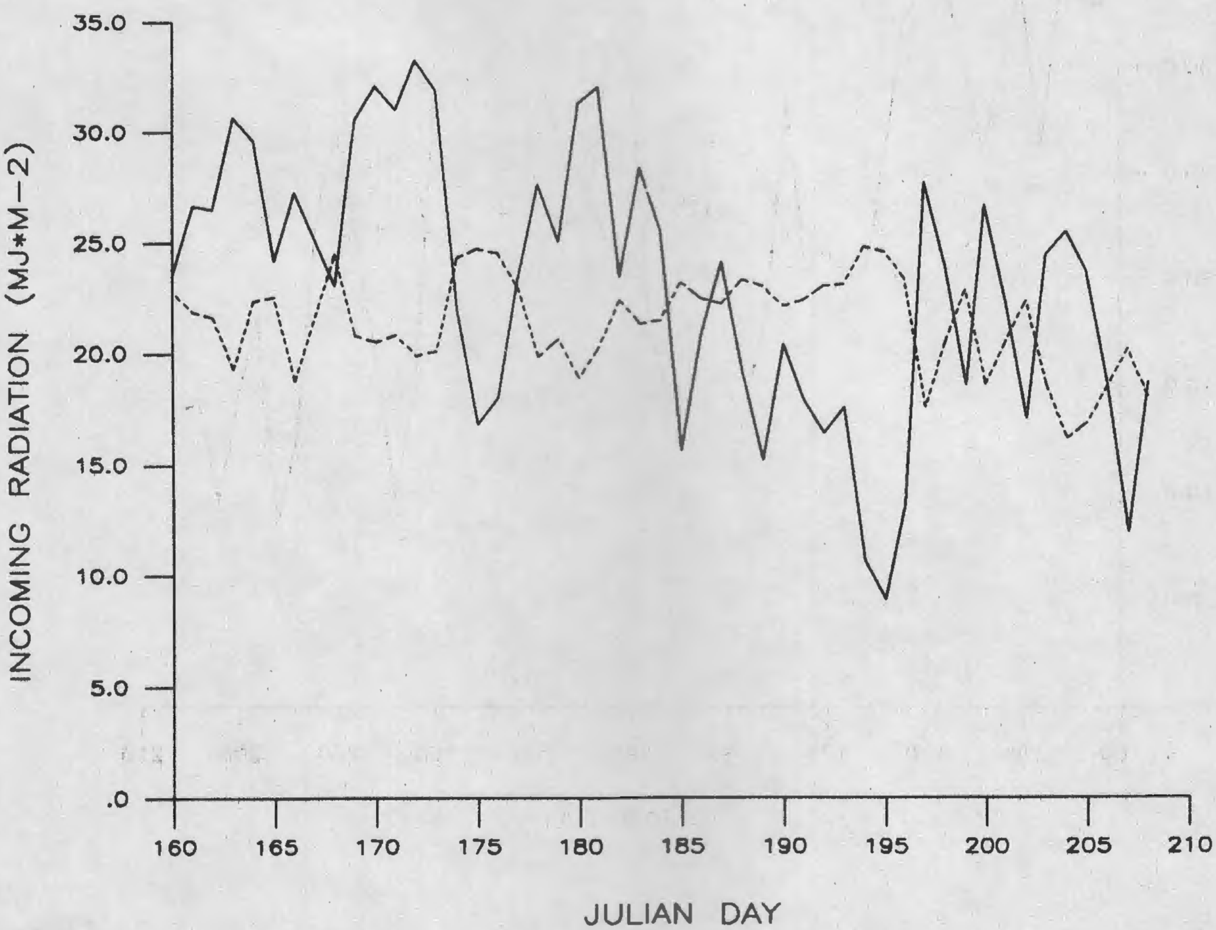

Figure 3: Daily receipts of incoming shortwave radiation (Qi)(dark line) and longwave radiation (i)(light line) in 1983 at station Yankee.

Q_i is lower but counter-radiation from clouds is increased. Indeed, under dense overcast conditions, I_i may exceed Q_i (e.g. J.D. 188-196 in 1983). The overall result of this inverse relationship between Q_i and I_i is that the daily variability of total radiation is much less then would be expected from measurements of Q_i alone.

Mean hourly totals of Q_i and I_i are shown in Figure 4; Q_i exhibits a clear diurnal pattern, with slightly lower values in 1983 when cloud cover was generally higher (averaging 7/10 in 1983, 6/10 in 1982). I_i shows little diurnal variation, reflecting the importance of atmospheric water vapor which undergoes little diurnal change. However,1983 values of Ii are lower than in 1982 due to the significantly colder conditions in the later year.

THE ROLE OF CLOUD COVER ON Q_i AND I_i

Two seasons of hourly cloud cover observations allow an analysis of the role of cloud cover on Qi and Ii. Hourly totals of Qi and Ii measured under clear skies and different cloud types are plotted against solar angle in Figures 5a and 5b and 6a and 6b. In the analysis, clear skies are defined as $\leq$3/10 cloud cover, and for each cloud type cloud cover was $\geq$7/10. A linear regression model has been adopted even though extrapolation to zero solar angle gives negative values of Qi. However, for the range of solar angle considered here, the simple regression seems

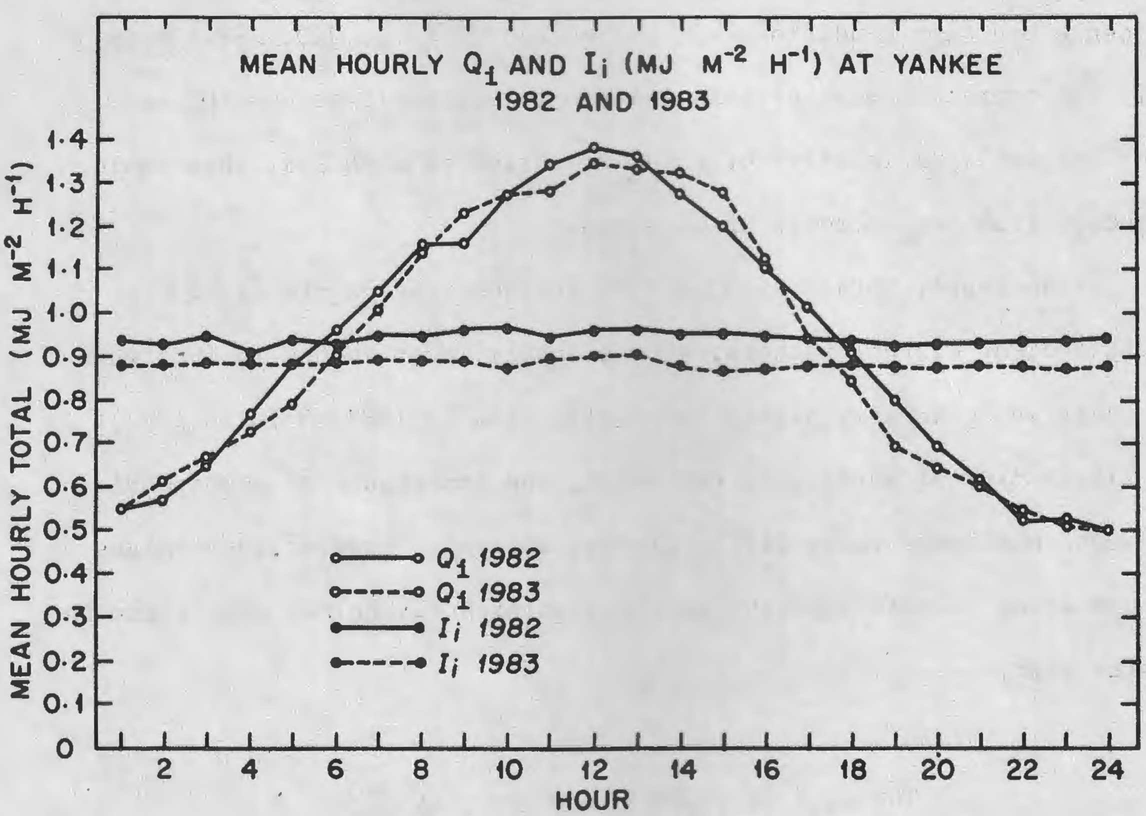

Figure 4: Mean hourly Qi and Ii at station Yankee in 1982 and 1983 (for Julian Days 170-207 in both years).

most appropriate. Although some scatter is inevitably introduced due to a comparison of hourly total radiation and (instantaneous) hourly cloud observations, and although observations took place over two seasons as surface albedo changed, the correlation coefficients between solar angle and Qi are uniformly high and extremely significant ($p = 0.001$). However, values of Ii are independent of cloud type and of solar angle.

To enable clear sky radiation receipts to be compared with those under different cloud conditions, the regression line for clear sky conditions (top left section of Figures 5a and 6a) is shown as a solid dark line in the other diagrams. Table 2 compares the relative transmission of Qi for various cloud types, for solar angles of 12° and 30°. Relative transmission is defined here as hourly Qi received under cloudy skies ($\geq$7/10 cloud-cover) as a percentage of hourly Qi received under clear skies ($\leq$3/10). The difference in relative transmission between these two solar angles is also shown (cf. Angstrom, 1934; Haurwitz, 1946, 1948; Holmgren, 1971; Liljequist, 1956; Vowinckel and Orvig, 1962). As one might expect, for the thinner, higher cloud types (cirrus/cirrostratus, altocumulus) relative transmission is high, while for the lower, thicker cloud types and for snowing conditions, relative transmission is much lower.

In comparison with clouds in temperate regions, arctic clouds are noted for their higher relative transmission. Angstrom (1934) arrived at an annual mean of 23% relative transmission under dense overcast

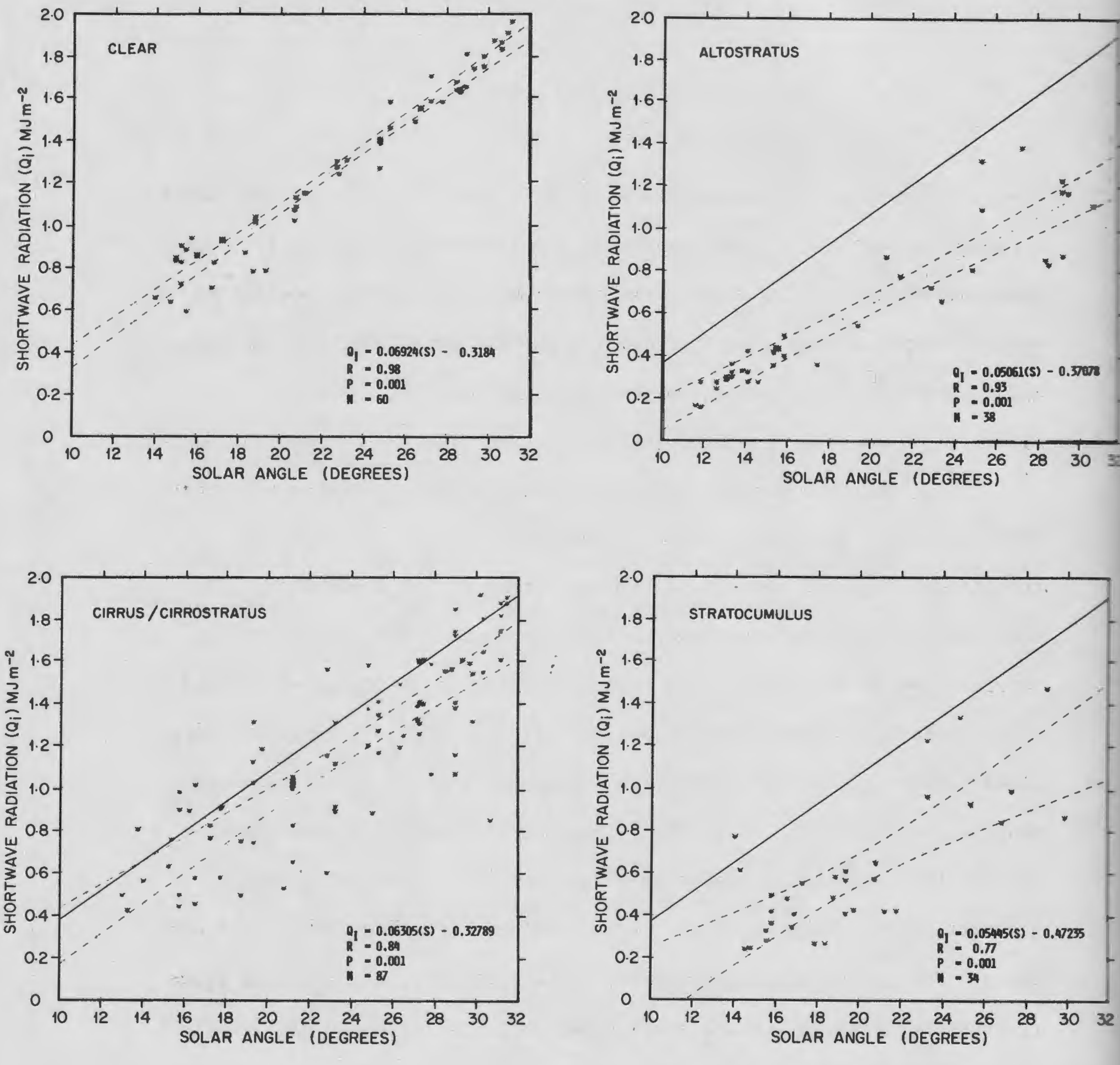

Figure 5a: Mean hourly Q_i (MJ m^{-2} h^{-1}) vs. solar angle for clear skies $\leqslant$ 3/10 cloud cover and different cloud types ($\geqslant$7/10 cloud cover. The regression line for each cloud type is shown enclosed by 95% confidence intervals. The regression equation, correlation coefficient (R) significance (P) and number of cases (N) for clear skies and the different cloud types are also shown. In the regression equation equations, solar angle is abbreviated as SA. The heavy line is the regression line for clear skies.

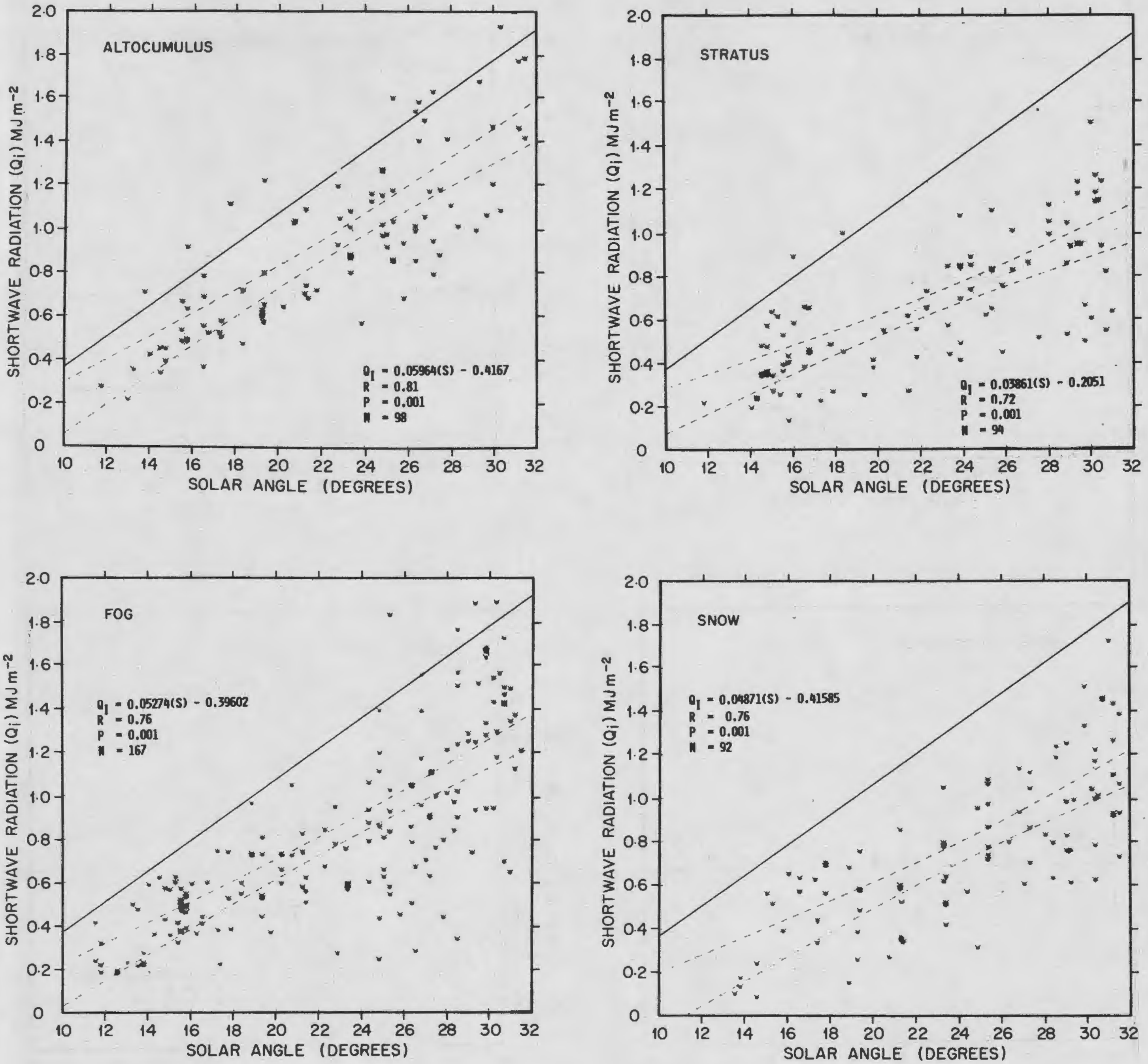
ALTOCUMULUS
Q_I = 0.05964(S) - 0.4167
R = 0.81
P = 0.001
N = 98
STRATUS
Q_I = 0.03861(S) - 0.2051
R = 0.72
P = 0.001
N = 94
FOG
Q_I = 0.05274(S) - 0.39602
R = 0.76
P = 0.001
N = 167
SNOW
Q_I = 0.04871(S) - 0.41585
R = 0.76
P = 0.001
N = 92
SHORTWAVE RADIATION (Q_i) MJ m^-2
SOLAR ANGLE (DEGREES)
0
0·2
0·4
0·6
0·8
1·0
1·2
1·4
1·6
1·8
2·0
10
12
14
16
18
20
22
24
26
28
30
32

Figure 5b

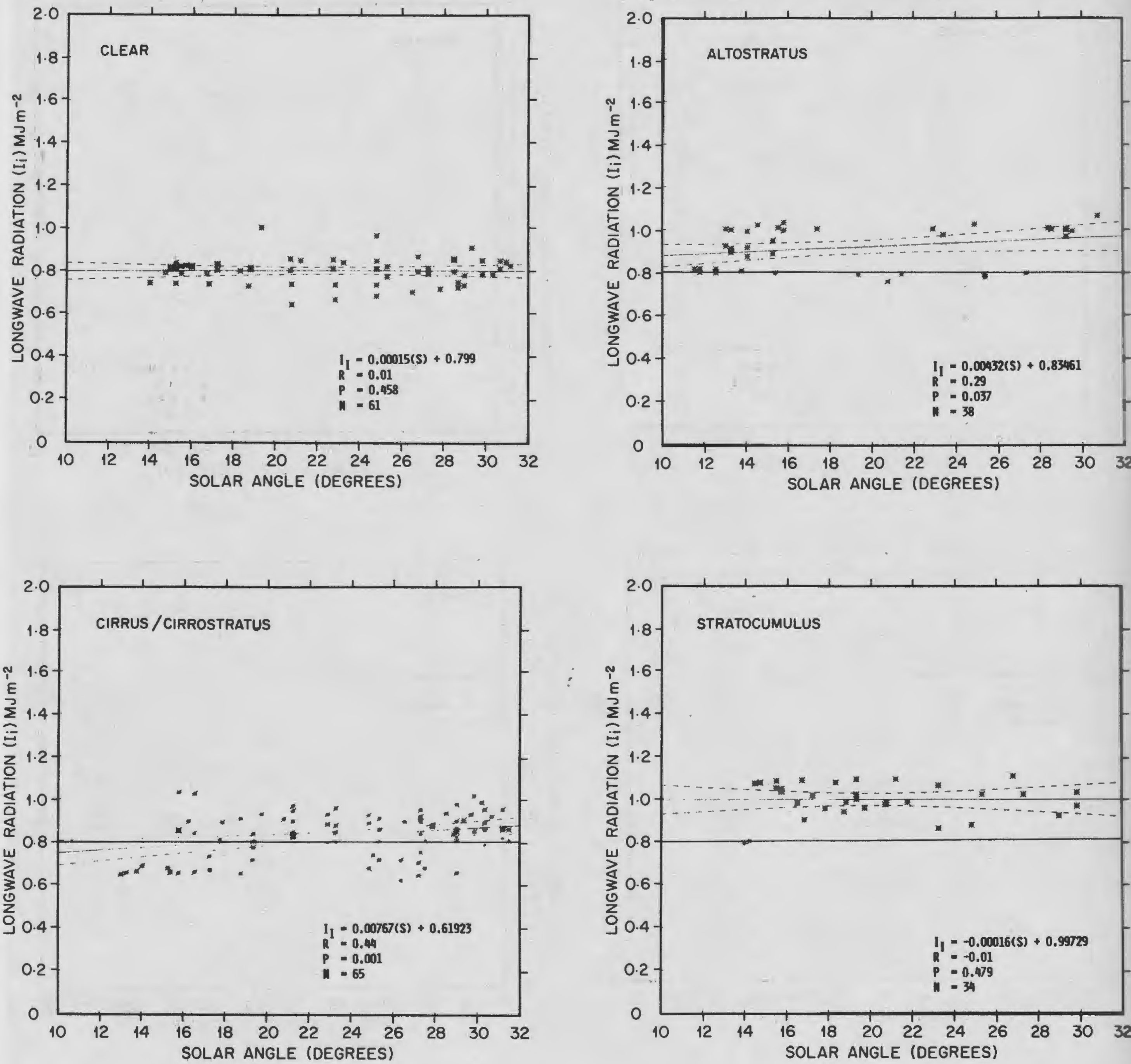

Figure 6a: Mean hourly I_i (MJ m^{-2} h^{-1}) vs. solar angle for clear skies $\leq$3/10 cloud cover and different cloud types ($\geq$7/10 cloud cover. The regression line for each cloud type is shown enclosed by 95% confidence intervals. The regression equation, correlation coefficient (R) significance (P) and number of cases (N) for clear skies and the different cloud types are also shown. In the regression equation equations, solar angle is abbreviated as SA. The heavy line is the regression line for clear skies.

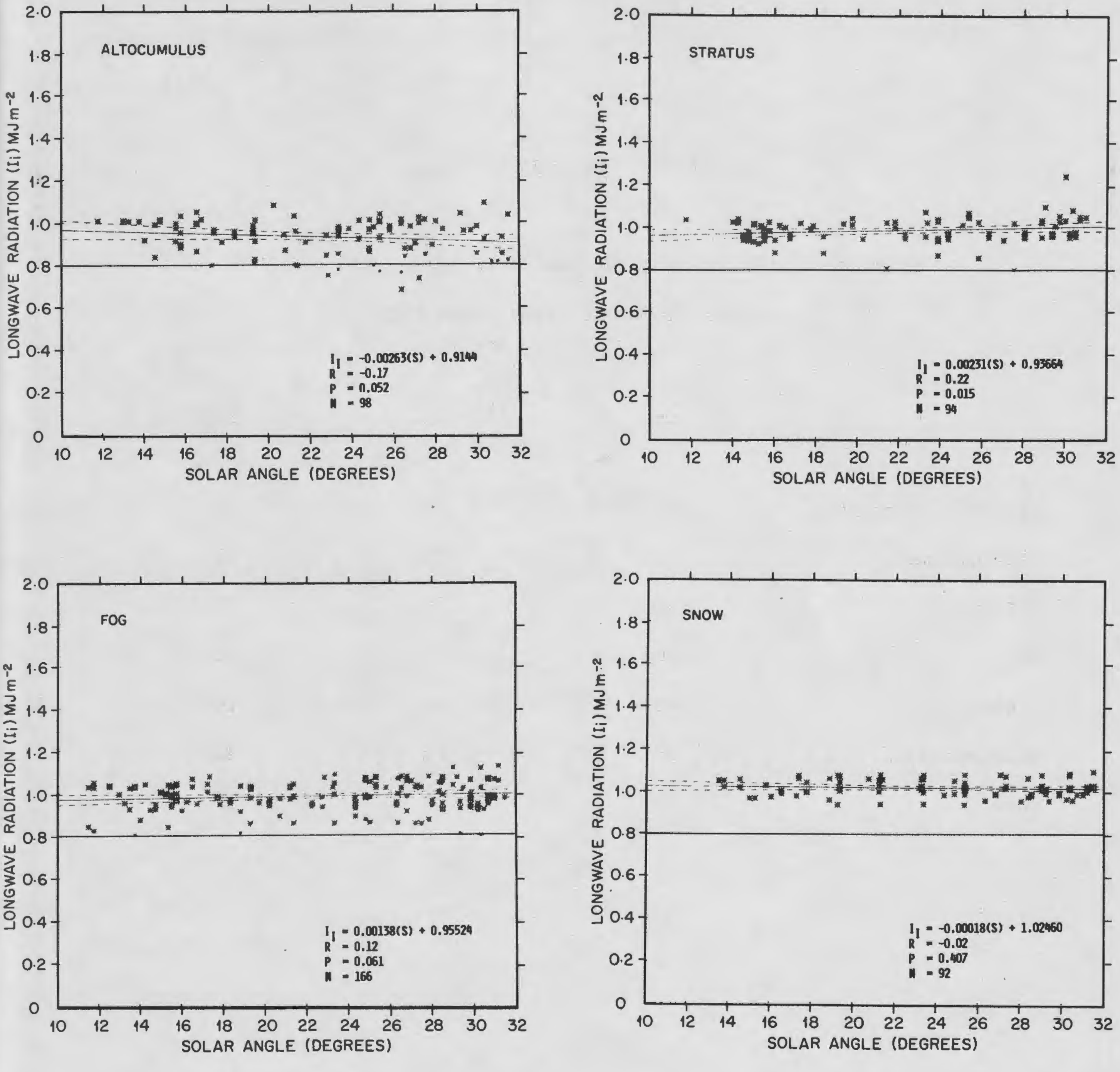
ALTOCUMULUS
I_I = -0.00263(S) + 0.9144
R = -0.17
P = 0.052
N = 98
STRATUS
I_I = 0.00231(S) + 0.93664
R = 0.22
P = 0.015
N = 94
FOG
I_I = 0.00138(S) + 0.95524
R = 0.12
P = 0.061
N = 166
SNOW
I_I = -0.00018(S) + 1.02460
R = -0.02
P = 0.407
N = 92
LONGWAVE RADIATION (I_i) MJ m^-2
SOLAR ANGLE (DEGREES)
0 0.2 0.4 0.6 0.8 1.0 1.2 1.4 1.6 1.8 2.0
10 12 14 16 18 20 22 24 26 28 30 32

Figure 6b

TABLE 2

Relative Transmission of Qi for Solar Angles 12° and 30°

Under Different Cloud Types (%)

	(a) 12°	(b) 30°	(c) b-a
Cirrus/cirrostratus	84	89	5
Altocumulus	58	78	20
Stratus	50	54	4
Fog	46	67	21
Altostratus	46	65	19
Stratocumulus	35	66	31
Snow	33	59	26

conditions in temperate regions. By contrast, in Antarctica, Liljequist (1956) arrived at a mean of 59.5%, while Holmgren (1971), on the Devon Ice Cap, noted even higher values of up to 70%. Both of the latter were summertime values. Table 3 also shows fairly high values of relative transmission, which lend support to the conclusions from these previous studies.

Vowinckel and Orvig (1962) suggested that the main factors that determine the relative transmission of clouds are surface albedo and cloud albedo. A high surface albedo is effective in enhancing relative transmission because it promotes multiple scattering between the cloud base and the ground. Empirical equations that describe this process have been devised by Angstrom (1934) and Liljequist (1956). Arctic clouds are also thinner than their temperate counterparts. Because cloud thickness and cloud albedo are thought to be positively correlated, the comparatively lower albedo of arctic clouds should also increase their relative transmission.

Griggs (1968) and Dave and Braslau (1975) showed that cloud albedo decreases with increasing solar angle. In temperate regions, the diurnal increase in solar angle, which by itself should lead to reduction of cloud albedo, is compensated for by an increase in cloud thickness in response to the pronounced diurnal increase in convection. As this should increase the cloud albedo, the diurnal range of relative transmission should be small, and, as Hewson (1943) argued, may be nearly

TABLE 3

Ranking of Ii for Different Cloud Types with Solar Angle of 20° (MJ $m^{-2} h^{-1}$)

		*
Cirrus/cirrostratus	0.773	96%
Clear skies	0.802	100%
Altocumulus	0.862	108%
Altostratus	0.921	115%
Stratus	0.939	117%
Fog	0.983	123%
Stratocumulus	0.994	124%
Snow	1.021	127%

* Relative to clear sky conditions at 20° solar angle.

zero. Conversely, in high latitude regions, where convection is limited, the diurnal range in cloud thickness is reduced, so the decrease in cloud albedo with increasing solar angle should be more pronounced. Thisprocess likely contributes to the noted high relative transmission of arctic clouds.

Figures 6a and 6b show that Ii is not dependent on solar angle. In comparison with clear sky conditions, all cloud types (except cirrus/cirrostratus at low solar angles) result in an increase in Ii. The effect is most pronounced for denser cloud types, snow and fog. This is summarized in Table 3 which ranks Ii according to the regression-derived value for a solar angle of 20°.It is clear that the cloud types associated with the highest receipts of Ii (stratocumulus, stratus, snow and fog) are also associated with low relative transmission of Qi (Table 2).

THE ROLE OF ALBEDO AND CLOUD COVER ON NET RADIATION

Interactions between cloud cover and the surface play a major role in the radiation balance of a region. Surface albedo is an important component in these interactions. Here we consider the role of albedo and cloud cover on net radiation (R) at the surface.

Tables 4 and 5 present correlation matrices between R,Qi,Ii, and the net long-wave (In = Ii +Io) and net short-wave (Qn =Qi+Qo) fluxes for conditions of high (>75%) and low (<20%) surface albedo. Data used were

TABLE 4

Correlation Matrix of R, Qi,Ii, In and Qn

for High Albedo Conditions (>75%)*

	Qi	Ii	In	Qn
Ii	-0.54 (741)			
In	-0.59 (741)	0.57 (741)		
Qn	0.90 (742)	-0.51 (741)	-0.66 (741)	
R	0.08 (742)	0.27 (741)	0.69 (741)	0.08 (742)

* The number of cases are shown in parentheses. All correlations are highly significant ($p = 0.001$) except for that of R and Qn.

TABLE 5

Correlation Matrix of R, Qi, Ii, In and Qn

for Low Albedo Conditions (<20%)*

	Qi	Ii	In	Qn
Ii	-0.55 (544)			
In	-0.86 (544)	0.72 (544)		
Qn	0.99 (544)	-0.54 (544)	-0.86 (544)	
R	0.96 (544)	-0.38 (544)	-0.69 (544)	0.96 (544)

* The number of cases are shown in parentheses. All correlations are highly significant($p = 0.001$).

from the ice cap station Zebra (which operated over a fairly stable snow cover in 1983) and from station Yankee which operated over a low albedo bare till surface in 1982 (Bradley and Serreze, 1985). Using these two data sets, the effects of cloud cover on R under conditions of high and low albedo can therefore be investigated.

HIGH ALBEDO (>75%)

Under conditions of high albedo, R is strongly correlated (positive) with In, and poorly correlated with Qi, Qn and Ii (Table 4). This is clearly seen in Figure 7 where R is plotted against In and Qn. Similar relationships were found by Ambach (1974), Hoinkes (1970), Holmgren (1971) and Kuhn, et al. (1975). They note that In is very dependent on cloud cover.

According to Ambach (1974), when the surface albedo is high, the radiation balance from clear (0/10 cloud cover) to overcast conditions (10/10 cloud cover) changes as follows:

$Qi(10/10) < Qi(0/10)$ $\quad$ $Ii(10/10) > Ii(0/10)$

$Qo(10/10) < Qo(0/10)$ $\quad$ $Io(10/10) \simeq Io(0/10)$

$Qn(10/10) < Qn(0/10)$ $\quad$ $In(10/10) > In(0/10)$

as a result, $R(10/10) > R(0/10)$.

Ambach (1974) argued that under 10/10 cloud cover, Qi and Qo are reduced by cloud albedo and absorption. Qn is therefore also reduced but must remain positive. Ii increases with cloud cover, due to enhanced

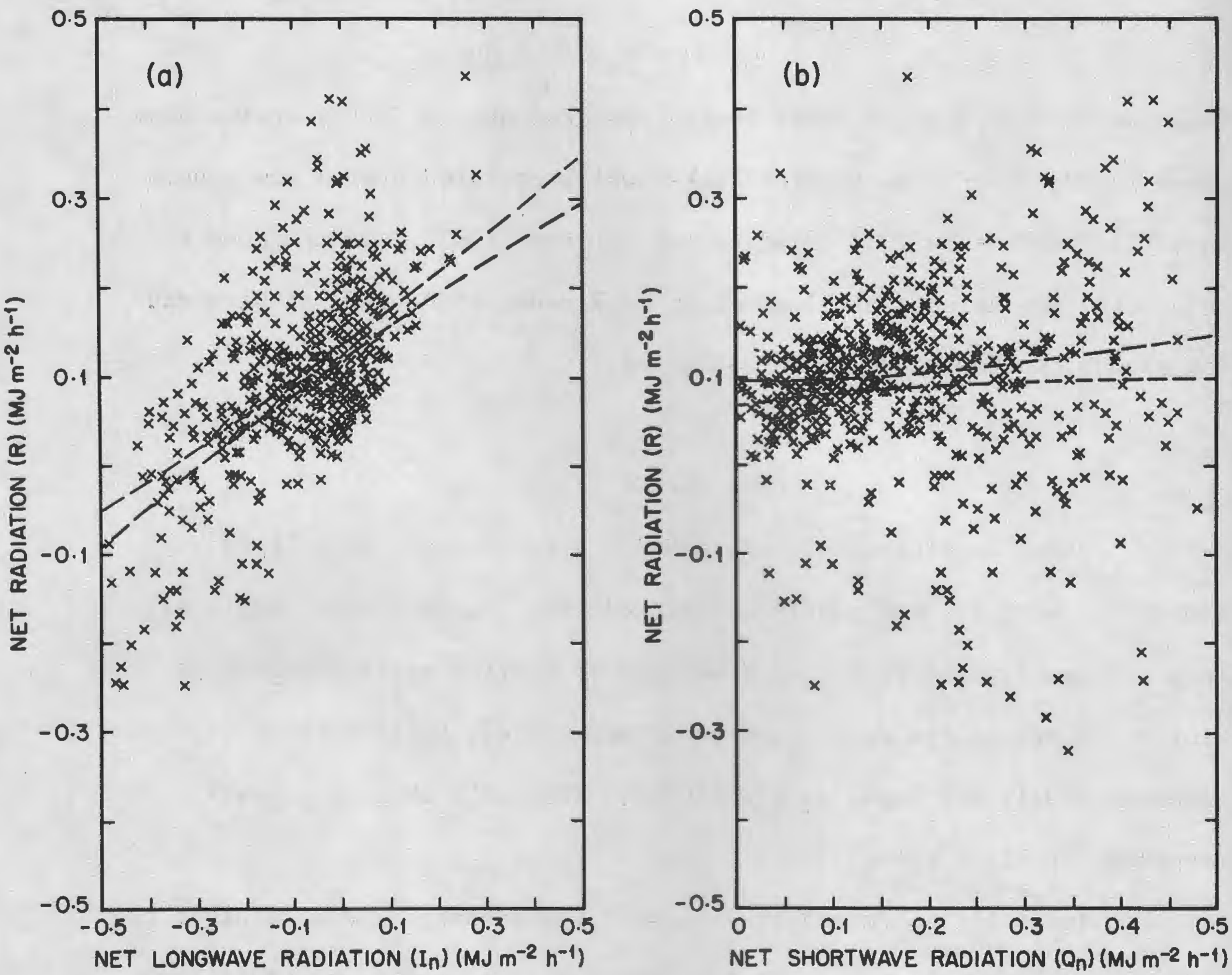

Figure 7: R vs. In (left) and Qn (right) for high albedo conditions (>75). The dotted lines on each plot are the 95% confidence intervals.

counter radiation. This is confirmed by the data shown in Figures 6a and 6b. Io depends on the surface temperature, and will be only marginally affected by an increase in cloud cover. Under clear skies (0/10), In is strongly negative, but under overcast conditions it can approach, or even exceed zero (Bolsenga, 1977). These relationships are supported in Table 4, where Ii and In (hence cloud cover) are both shown to be negatively correlated with Qi.

Evidently, with an extensive cloud cover, the increase in In more than makes up for the decrease in Qn, resulting in an increase in R. This effect is clearly illustrated in Table 6, in which hourly totals of Qn and In from the present study are stratified according to three conditions of cloud cover (in tenths, 0-2, 3-6, 7-10, and the difference between last and first groups). The change in R from condition (a) to condition (c) is significant at the 99.9% confidence level. There is also a reversal of sign.

LOW ALBEDO (<20%)

With conditions of low albedo (<20%), R is strongly correlated with Qi, Qn (positive), and In (negative), and is poorly correlated with Ii (Table 5). This is almost a complete reversal of the previously described situation (albedo >75%). These results agree well with those of Wilson (1973), who found an almost perfect linear relationship between Qi (and hence Qn) and R when the albedo was low. As before, R is plotted against Qn and In (Figure 8). In contrast to the previous situation, the

TABLE 6

Qn, In, and R Stratified According to Different Conditions of Cloud Cover with Surface Albedo >75%.

(MJ m-2 h-1)

	a) 0-2	b) 3-6	c) 7-10	(c-a)
Qn	0.247	0.241	0.103	-0.144
In	-0.208	-0.202	0.007	0.214
R	-0.040	0.039	0.112	0.152

TABLE 7

Qn, In, and R Stratified According to Different Conditions of Cloud Cover with Surface Albedo <20%.

(MJ m-2 h-1)

	a) 0-2	b) 3-6	c) 7-10	(c-a)
Qn	0.736	0.678	0.457	-0.279
In	-0.378	-0.364	-0.162	0.216
R	0.357	0.324	0.295	-0.062

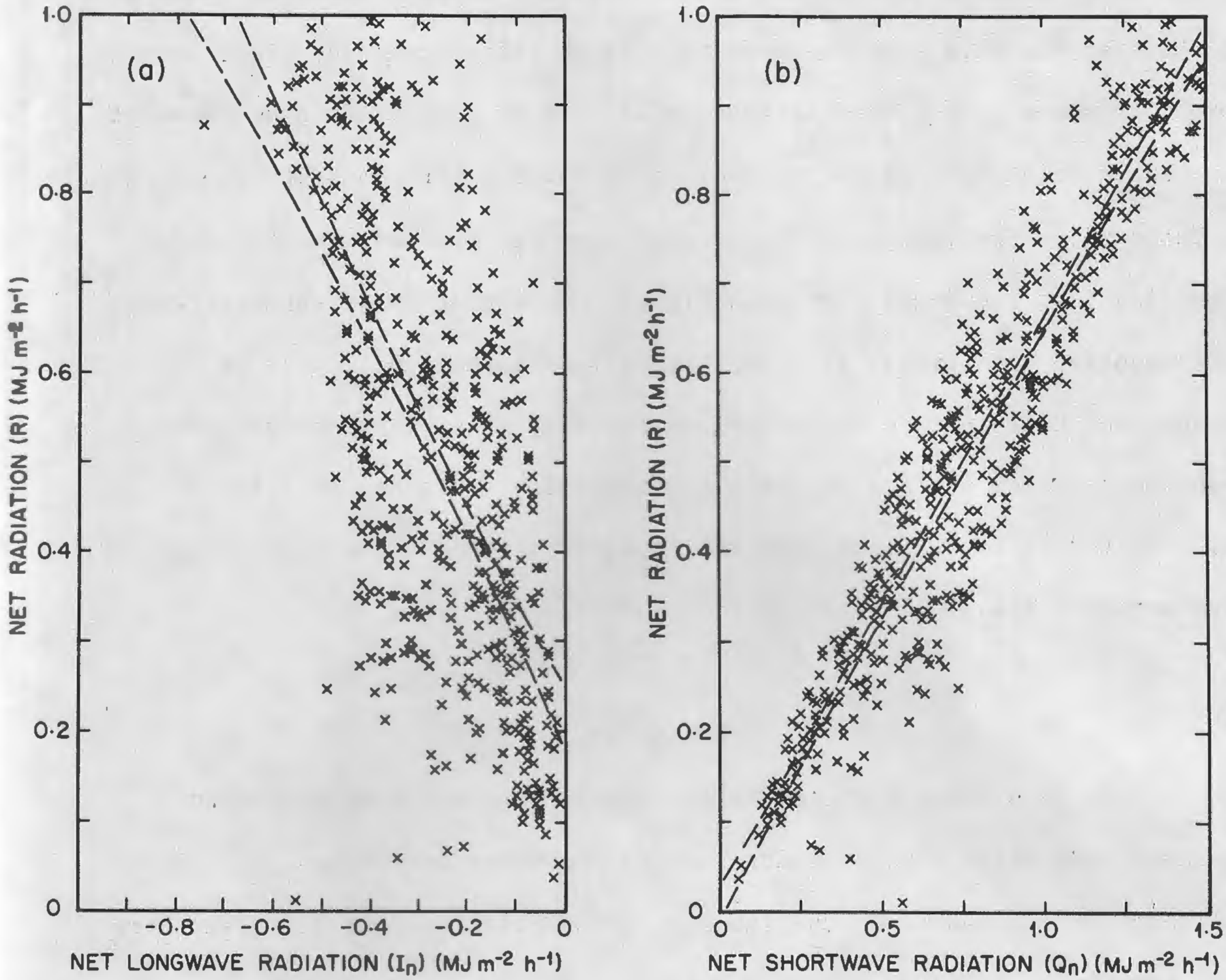

Figure 8: R vs.In (left) and Qn (right) for low albedo conditions (<20%). The dotted lines on each plot are the 95% confidence intervals.

variations in both Qn and In exert a strong influence on R. The influence of cloud cover on Qn and In is similar to that shown in Table 6; however, in this case the reduction in Qn with increasing cloudiness more than makes up for the increase in In. This results in a decrease of R. These relationships are made clear in Table 7 (in the same manner as in Table 6). The change in R from condition (a) to condition (c) is significant at the 99.9% confidence level. Note that In is substantially more negative than it was with the high albedo situation. This is because the till surface at Yankee was normally at a higher temperature than the snow/ice surface at Zebra and therefore had a higher value of Io. As the value of Ii at both stations was assumed to be identical, more negative values of In at Yankee resulted.

DISCUSSION

It is evident that the relationships between cloud cover and ground albedo exert a major control on R, and hence should have an influence on the health of the ice cap. The relationships discussed here find support in numerous other studies.

For example, Holmgren (1971) in a synoptic energy balance study on the Devon Island Ice Cap (N.W.T., Canada) noted that the lowest values of R were obtained when the surface was frozen and had a high albedo (Table 8). With the same surface characteristics but with an overcast sky, R rose dramatically. With a melting surface (lower albedo) and clear skies, again with light winds, R attained much higher values. Similar relationships were found by Alt (1978) on the Meighan Ice Cap (N.W.T., Canada).

Tables 6 and 7 show that the increase in R from relatively clear

TABLE 8

R at Devon Island Ice Cap Station Under
Different Weather Conditions (MJ m-2 h-1)
(after Holmgren, 1971,Part F,p.34)

Weather type	Sky	Wind	Surface	R
A	Clear	Light	Frozen	0.043
A	Overcast	Light	Frozen	0.083
B	Overcast	Strong	Melting	0.162
C	Clear	Light	Melting	0.158
C	Clear	Light	Frozen	0.014

(0-2 tenths) to cloudy (8-10 tenths) skies, when the surface albedo is high, is more than twice (R = 0.152 MJ m-2 h-1) the corresponding decrease in R when the surface albedo is low (R = -0.067 MJ m-2 h-1). This is intriguing, as it suggests that clear conditions in late spring (high albedo), by greatly reducing R from its already low values (and even reversing the sign) would tend to delay ablation. The reduction of R would seem to be doubly important at this time, as the sum of the net energy sources is, in general, already very small. Once ablation has commenced and the albedo drops off, the importance of Qn becomes established. Once this point is reached, cloudy conditions (by significantly reducing Qn) would be more favorable to the survival of a glacier.

In fact, cloud cover in the arctic does generally increase during the summer due to the increased availability of water vapor and the development of more unstable atmospheric conditions. This suggests that a snow cover may benefit from the normal pattern of both late spring (high albedo, clear skies) and summer (lower albedo, cloudy) conditions, which reduce ablation and thereby enhance its prospects for survival. This, of course, takes only radiative factors into account, and advection is sure to be more important in many cases. Nevertheless, the results do suggest that these interaction between albedo, the seasonal progression of cloud cover, and net radiation are important links in the persistence of seasonal snow cover.

REFERENCES

Alt, B.T. 1978. Synoptic climate controls of mass balance variations on Devon Island Ice Cap. Arctic and Alpine Research, 10, 61-80.

Ambach, W. 1974. On the influence of cloudiness on the net radiation balance of a snow surface with high albedo. J. Glaciology, 13(67), 73-84.

Angstrom, A. 1934. Total radiation from sun and sky at Abisko. Geografiska Annaler, 58A, 71-81.

Bolsenga, S.J. 1977. Radiation balance over a continuous snow surface: A review. U.S. Dept. Commerce, NOAA, Great Lakes Environmental Research Laboratories, Contribution 108, 88 pp.

Bradley, R.S. and Serreze, M., 1985. Glacio-climatic studies of a high arctic plateau ice cap part II: topoclimate (submitted).

Dave, J.V. and Braslau, N. 1975. The effect of cloudiness on the transmission of solar radiation through realistic model atmosphere. J. Applied Meteorology, 14, 388-395.

Griggs, M. 1968. Aircraft measurements of albedo and absorption of stratus clouds and albedo. J. Applied Meteorology, 1, 1012-1017.

Haurwitz, B. 1946. Insolation in relation to cloud type. J. Meteorology, 3, 123-124.

Haurwitz, B. 1948. Insolation in relation to cloud type. J. Meteorology, 5, 110-113.

Hewson, E.W.1943. The reflection, absorbtion, and transmission of solar radiation by fog and cloud. Quarterly J. Royal Meteorological Society, 69, 47-62.

Hoinkes, H. 1970. Radiation budget at Little America V., 1957. pp. 163-284 in Isage Proceedings, Publication 68, IASH, Gentbrugge, Belgium.

Holmgren, B.1971. Climate and energy exchange on a sub-polar ice cap in summer. Arctic Institute of North America, Devon Island Expedition, 1961-1963. Part E. Radiation Climate. Meddelanden fran Uppsala Universitets, Meteorologiska Institutionen, Nr. 111. 111 pp.

Kuhn, M., Kundla, L.S., and Stroschein, A. 1975. The radiation balance of Plateau Station, Antarctica, 1966,-1967 pp. 41-73 in Meteorological Studies of Plateau Station, Antarctica. Institut fur Meteorologie und Geophysik der Universitet, Innsbruck, Austria.

Liljequist, G.H. 1956. Energy exchange of an arctic snowfield, Norwegian-British-Swedish Antarctica Expedition, 1949-1952. Scientific Results, Part 1E, Vol 2. Norsk Polarinstitut, Oslo, 184 pp.

Vowinckel, E. and Orvig, S. 1962. Relation between solar radiation and cloud type in the arctic. J. Applied Meteorology, 1, 552-559.

GLACIO-CLIMATIC STUDIES OF A HIGH ARCTIC PLATEAU ICE CAP:

PART IV: ENERGY BUDGET

M.C. Serreze and R.S. Bradley

University of Massachusetts, Amherst

ABSTRACT

Measurements of energy budget terms were made at 850 m on a small ice cap and on a nearby tundra/felsenmeer surface in June and July 1983. Both sites remained snow-covered for most of the season. Sensible and latent heat fluxes were larger over the ice cap, probably due to high wind speeds resulting from smoother surface conditions. Sensible heat flux at both sites showed diurnal variations related to changes in stability in the lower atmosphere (15-150 cm). Over the ice cap, sensible heat flux was generally directed downward due to the strong inversions commonly present there. Sensible and latent heat terms were markedly different with changes in airflow over the region. Totals of energy budget terms at the ice cap stations for the period of record are presented.

INTRODUCTION

Meteorological observations on and around the "St Patrick Bay Ice Cap" on northeastern Ellesmere Island, were carried out in the summers of 1982 and 1983 in order to assess the effect of the ice cap on local climate. Details of instruments used and results obtained have been described elsewhere (Bradley and Serreze 1985a and b; Serreze and Bradley, 1985; Palecki, et al., 1985). Here we discuss the results of energy budget measurements made in 1983 (from June 14 to July 29; Julian Day [JD] 165-210).

ENERGY BUDGET TERMS

The energy budget is defined as the apportionment of net radiation (the balance between incoming and outgoing short and longwave radiation) between the non-radiative surface energy fluxes and storage terms. For a glacier, it can be expressed as follows (Paterson, 1981):

$$R + Qh + Qe + P - \Delta G - M = 0 \qquad \text{(Equation 1)}$$

where:

R = Net radiation (defined above)

M = Energy used to melt snow and ice

ΔG = Change in heat content to a depth where heat transfer is negligible

Qh = Transfer of energy between the atmosphere and surface by conduction (negligible) and convection (sensible heat)

Qe = Transfer of energy between the atmosphere and the surface by evaporation and condensation (latent heat).

P = Heat supplied by precipitation.

R, Qh and Qe are positive when directed toward the surface. P and ΔG are positive when the snowpack gains heat while M is positive when there is melt.

In 1983, Qh, Qe and R were measured at stations Zebra (ice cap) and Yankee (tundra) and despite an essentially complete snow cover at both sites, some interesting differences were noted. ΔG was measured in the snowpack at Yankee. Although ΔG and M were not measured at Zebra they were combined and determined (as a residual) which allows some check on the energy budget at this site.

The turbulent fluxes of Qh and Qe at Zebra and Yankee were calculated as follows (Sellers, 1965):

$$Qh = pCpk^2(\Delta\bar{u}\Delta\bar{T})/\ln(z_2/z_1)^2 \ \ Wm^{-2} \qquad \text{(Equation 2)}$$

$Qe = pLk^2(\Delta\bar{u}\Delta\bar{q})/(\ln z_2/z_1)^2$ W m^{-2} (Equation 3)

Where p and Cp are the density and specific heat of air, k is Von Karmen's constant (0.4), L is the latent heat of evaporation, and $\bar{u}$, $\bar{T}$, and $\bar{q}$ are the time-averaged wind speed, temperature, and specific humidity at heights z_1 and z_2.

Wind speed, temperature, and relative humidity were recorded hourly at 15 (z_1) and 150 (z_2) cm. The instruments used are described in Bradley and Serreze (1985b). The values of p, Cp, and L were obtained from the Smithsonian Meteorological Tables.

The saturation vapor pressure over ice and water (es and ew respectively, in Nm-2) at z_1 and z_2 were obtained from equations described by Williams (personal communication):

a) over ice, 203.15°K $\leq$ T $\leq$ 273.15°K

es = 610.64*EXP (22.457 ((T - 273.15)/(T - 0.56)) (Equation 4)

b) over water, 273.15°K $\leq$ T $\leq$ 298.15°K

ew = 610.64*EXP(17.491 ((T - 273.15)/(T - 0.56)) (Equation 5)

The values obtained were multipled by the relative humidity to yield vapor pressure (e). Using an assumed atmospheric pressure of 91000 Pa, q was calculated as follows:

q = (0.622 e)/91000 g kg-1 (Equation 6)

MEASUREMENT DIFFICULTIES

There were a number of occasions, during particular weather conditions, when the quality of the collected data suffered. The most common problem was the collection of rime on the anemometer cups. Rime preferentially collected on the upper anemometer (150 cm), resulting in an under-representation of Δu. At Yankee, which was close to base camp, rime could be removed frequently. However, due to the extremely poor visibility during riming conditions, station Zebra was sometimes left unattended for several days. On such occasions, rime sometimes collected in sufficient amounts that the data recorded could not be used. A similar problem sometimes occurred with the temperature and relative humidity sensors.

At both stations, during clear, calm conditions, it was occasionally noted that the lower anemometer cup was slowly spinning while the upper instrument remained still. This could have resulted from a very low-level katabatic flow that only occurred when the existing circulation was very weak. Although interesting, such observations were eliminated from consideration, as the wind gradients in no way followed a logarithmic profile. On the same kind of days, especially during low sun hours, the upper (150 cm) temperature sensors were sometimes prone to direct solar heating. By making the temperature gradients more positive, this tended to emphasize positive values of Qh. As these same sensors also measured relative humidity, any direct solar heating (by increasing temperature and decreasing relative humidity) could also have caused errors in the calculation of Qe. The combined effect of all of these events resulted in ~20% of the data being discarded.

DIURNAL CHANGES IN ENERGY BUDGET COMPONENTS

In order to understand some aspects of the energy budget at each station it is first necessary to examine the record of atmospheric stability immediately above the surface at each observation site. Average lapse rates in the 15-150 cm layer are shown in Figure 1. It is clear the stability at station Yankee was greatest during the early and late hours of the day. At Zebra, there were also two peaks in diurnal stability, but they occurred later in the morning and earlier in the evening than those at Yankee. At both stations, stability decreased in the late afternoon hours although instability was more common at Yankee. Overall, inversions were present 53% of the time at Zebra and 40% of the time at Yankee (Bradley and Serreze, 1985b).

Figures 2 and 3 show mean hourly totals of Qh, Qe and R at stations Zebra and Yankee (positive values denoting an energy flux towards the surface). Marked diurnal variations in all components are apparent. It is also clear that daily changes of stability at each site and recorded values of Qh are strongly related (cf. Figure 2 and 3 with Figure 1). At station Yankee (except for early and late in the day) Qh was generally directed away from the surface, with minimum values corresponding to the period of maximum instability at that site. At station Zebra, where stable conditions were more common, Qh was positive for almost the entire day, on average. It became negative for only a short period, centered on 1500h, when the daily energy surplus was near its maximum. A time lag of ~3 hours occurred between the time of maximum R and the time of most negative Qh.

At both stations, Qe was generally negative (i.e. evaporation from the surface) and was greatest in mid-afternoon. During nightime conditions

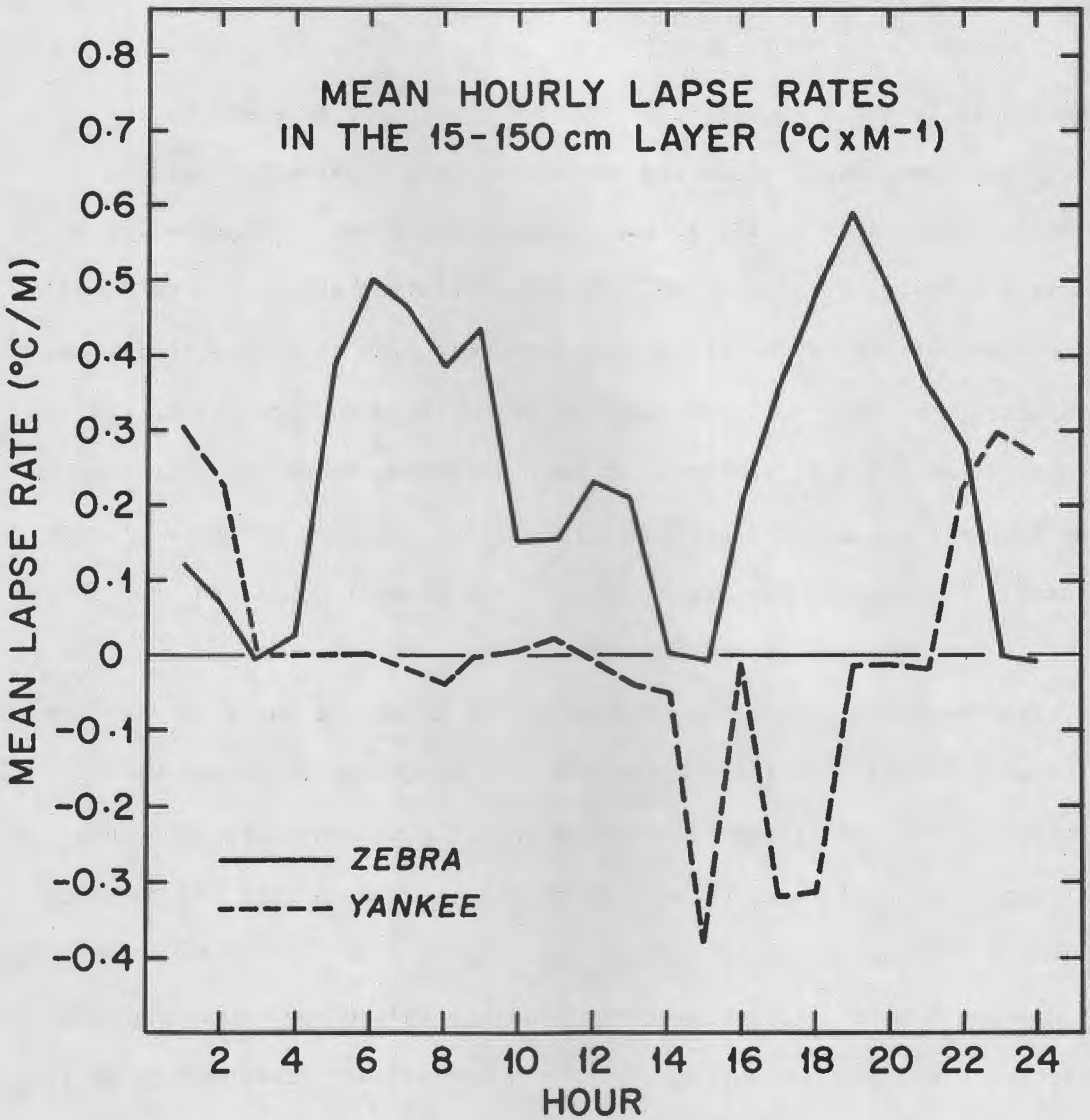

Figure 1 Mean hourly lapse rates at Zebra and Yankee, JD 165-210, 1983 (150 cm -15 cm temperature).

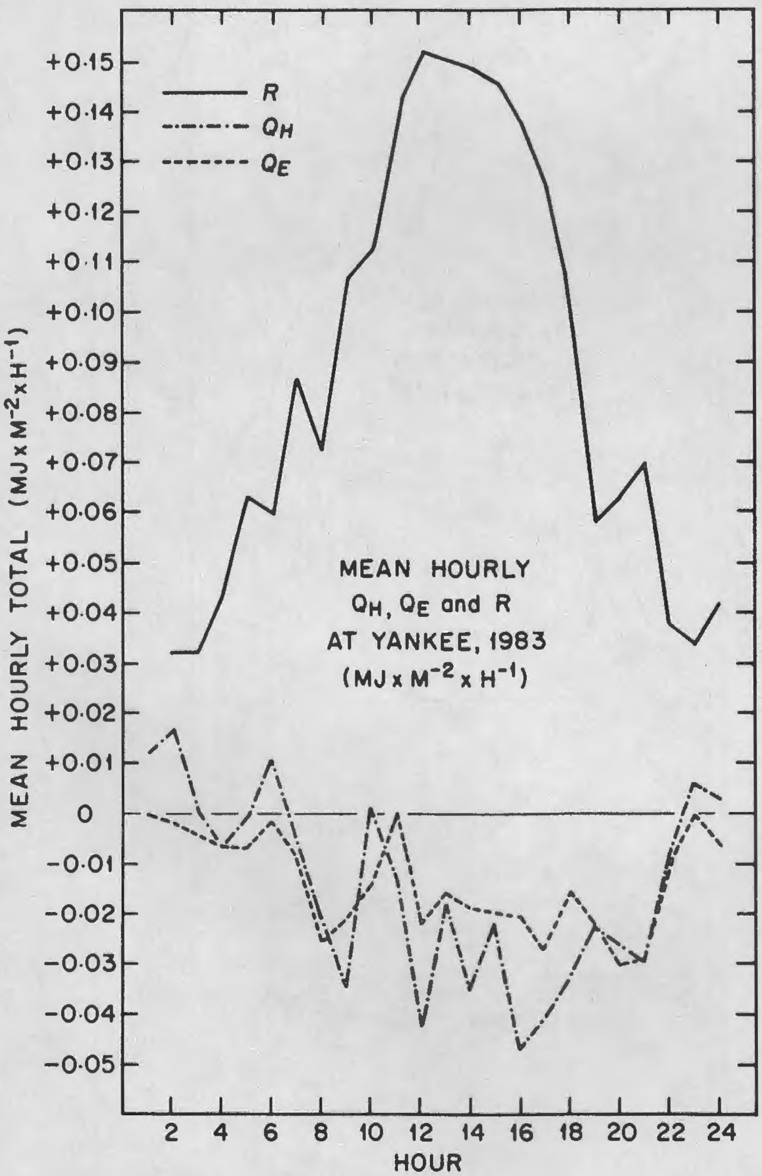

Figure 2 Mean hourly Qh, Qe and R at Yankee, JD 165-210, 1983.

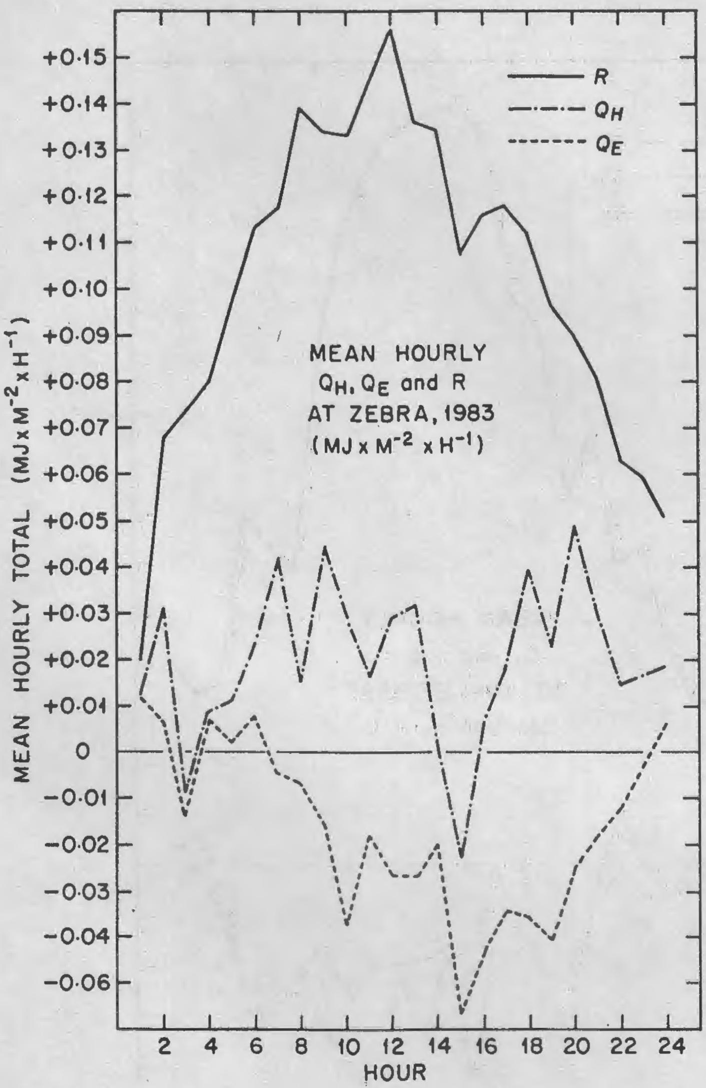

Figure 3 Mean hourly Qh,Qe and R at Zebra, JD 165-210,1983.

(low sun) Qe became less negative, even attaining positive values at Zebra (i.e. condensation at the surface). At station Zebra, Qh and Qe were commonly directed in different directions. With a stable temperature profile, Qh must be directed toward the surface, however, stable conditions will only affect the magnitude of Qe. As long as there is a negative specific humidity gradient (a common daytime situation) Qe will be directed away from the surface. Conversely at station Yankee, both Qh and Qe were usually directed away from the surface, indicating that both vapor and temperature gradients were usually negative.

Despite the pervasive snow cover at both stations, the vertical surface relief at Yankee was much greater (~20 cm) than at Zebra (~5 cm). This is because the surface underlying the snow cover at Yankee was hummocky till, while the surface underlying the snow cover at Zebra was fairly smooth glacial ice. By its influence on wind, temperature, and specific humidity gradients, this difference in surface relief between the two stations probably accounted for many of the measured differences in Qh and Qe.

Mean seasonal wind speeds at 150 cm (u150 cm) and Δu were computed for both stations. The results are as follows (ms-1);

	Zebra	Yankee
u150 cm	3.1	2.7
Δu	0.9	0.4

The difference between the stations in u150 cm and Δu is significant ($p = 0.1$).

The effect of surface relief on the windfields is examined in further detail in Figure 4 which plots hourly u150 cm for both stations and Figure 5 which compares hourly Δu. At Zebra, u150 cm was higher, resulting in larger values of Δu. This probably accounts for the larger absolute magnitude of the turbulent fluxes there, as compared to Yankee. Diurnal trends in u and Δu were probably the result of the diurnal trend of stability on a regional scale. However, the differences between stations point to significant differences in microclimate, despite the fact that both sites were snow-covered.

In summary, it is clear that an important difference between the two sites -- one snow-covered tundra/felsenmeer and the other snow-covered glacier ice -- is the magnitude and direction of sensible heat transfer. This is related to the temperature gradients and wind profiles near the surface which were significantly different in spite of the apparent homogeneity of the snow-covered surface for much of the measurement period. However, the fact that station Zebra was underlain by ice, which absorbed heat to a greater depth than the tundra underlying station Yankee, meant that surface snow temperature at Zebra was generally lower than at Yankee (until regional melt conditions prevailed). This meant that surface inversions tended to be stronger and more persistent at Zebra than at Yankee. Thus, the material underlying the surficial snow layer played a role in determining low-level stability conditions.

It must be noted that the foregoing discussion assumes that the measured flux of sensible heat at the surface <u>over the 15-150 cm layer</u> is truly representative of the surface flux. However, this may not be a reasonable assumption at all times since strong surface inversions may be

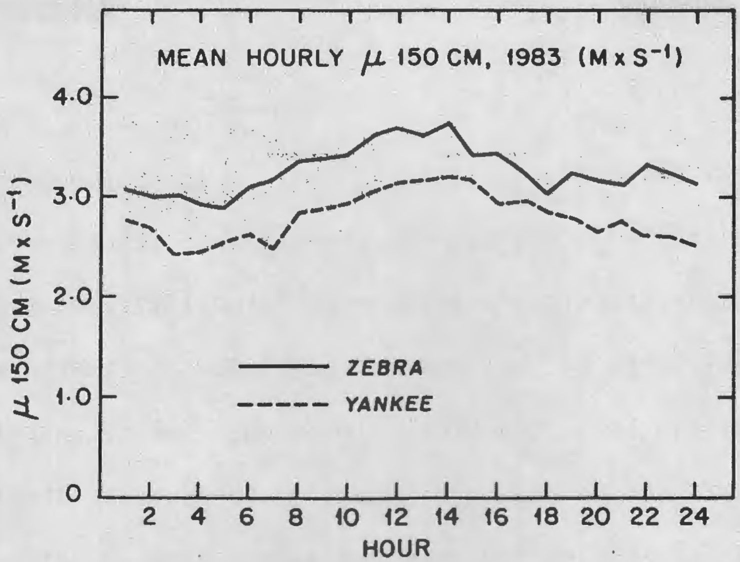

Figure 4 Mean hourly u150 cm at Zebra and Yankee, JD 165-210, 1983.

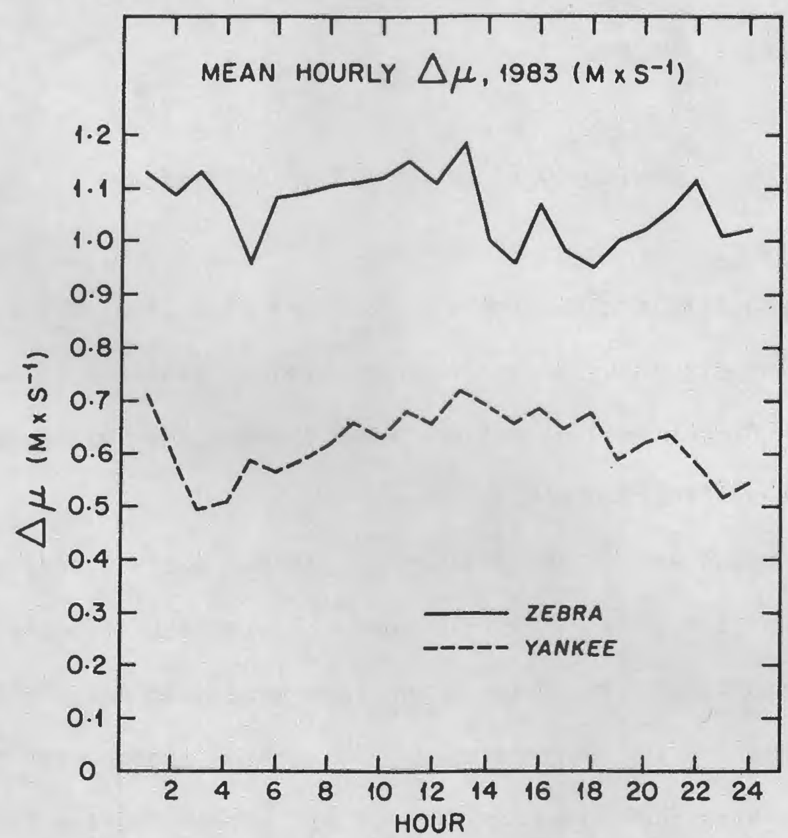

Figure 5 Mean hourly Δu at Zebra and Yankee, JD 165-210, 1983.

below the lowest measurement level (15 cm)., It was common at Yankee for the 15 cm level to be $\geq 0°C$ while the snow-surface itself remained below 0°C and a negative temperature gradient (instability) was present from 15-150 cm. Estimates of Qh based on the 15-150 cm temperature gradient at such times would be in the wrong direction. Unfortunately, surface temperatures were not continuously measured (because of difficulties associated with heating of the sensors) so it is not possible to quantify how important this effect might have been. However, is is clear that, depending on the strength and frequency of the near surface (0-15 cm) inversion, overall estimates of Qh based on the 15-150 cm temperature gradients may be in error.

WIND ROSES OF Qh AND Qe AT YANKEE

Some insight into reasons for the observed climate at a location can be determined by examining wind roses of climatic elements (Alt, 1975). Wind roses of Qh, Qe, wind direction, wind speed, temperature and relative humidity are shown in Figure 6.

The roses of Qh and Qe are similar in overall shape. Fairly negative values for both fluxes were the rule when the wind was from the NNE and the south. This is because these directions were associated with both high wind speeds and low temperatures. High wind speeds result in large values of Δ u while the advection of cold air across the ice cap would tend to favor negative temperature gradients. The combination of these factors probably accounts for the strong sensible heat loss (negative Qh). The cold air probably also had a low vapor pressure, thereby

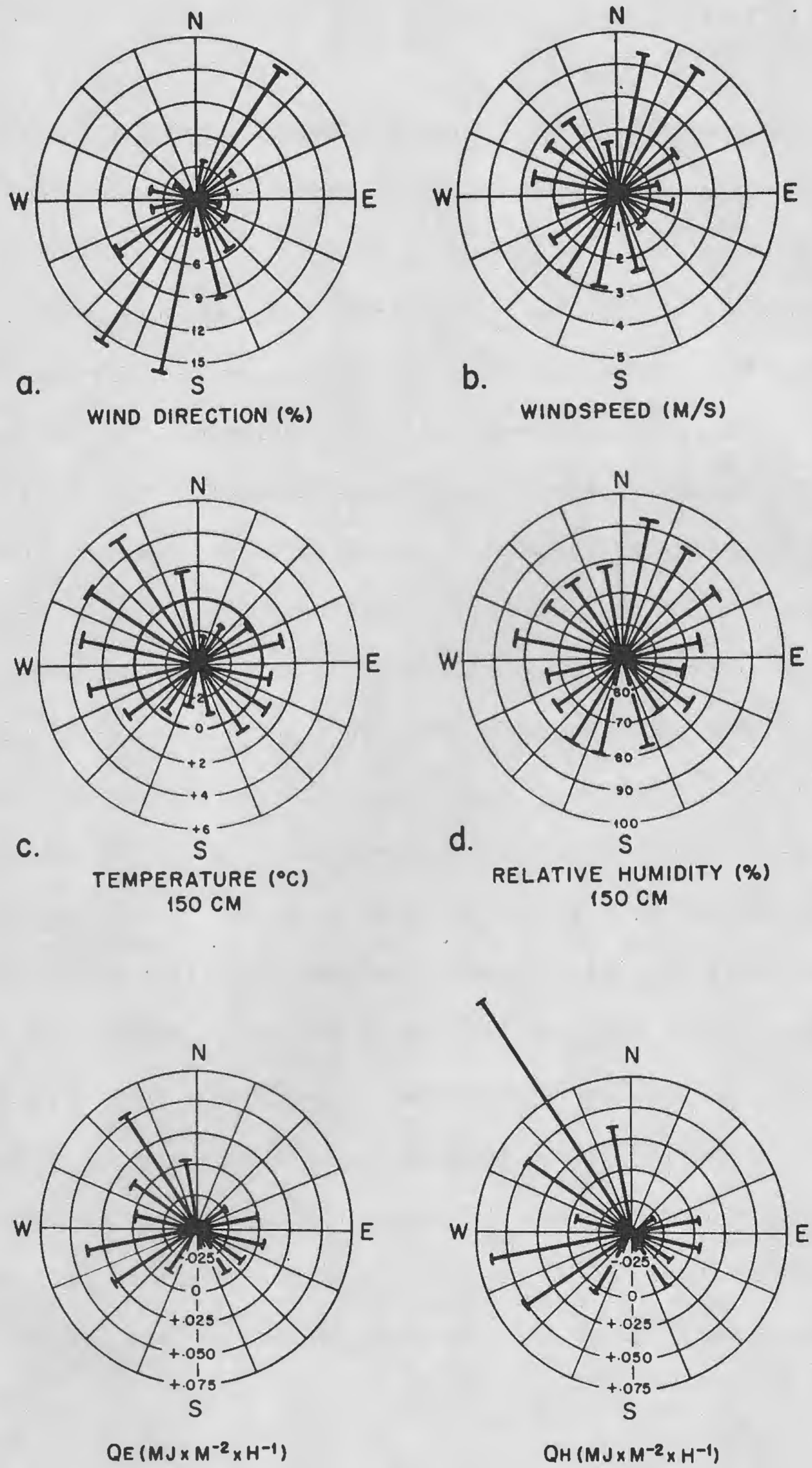

Figure 6 Hourly wind direction frequency at Yankee, JD 165-210, 1983, and mean hourly values of Qh, Qe, wind speed, temperature and relative humidity stratified by wind direction.

strengthening the near-surface vapor gradient. Combined with the high wind speeds, this probably accounts for the strong evaporation (strongly negative Qe).

With an easterly wind component, both Qh and Qe were small in magnitude. This is because the wind speeds from this direction were also low, reducing Δ u and the momentum flux. Conversely, Qh and Qe both tended to become positive when there was a westerly component to the wind. This is because these wind directions were associated with higher temperatures (Figure 6). This inflow of warm air tended to favor advection inversions, resulting in positive values of Qh. These positive values of Qh were also generally large in magnitude, a result of high wind speeds from this direction. The large positive spike of Qh with a NW wind was based on only a few observations so it is unclear how much significance should be attached to these values.

The generally positive values of Qe with a westerly wind component arises from the fact that the associated temperatures were fairly high which would favor high vapor pressures. Evidently, advected air from this direction carried enough moisture to reverse the vapor gradient. The combination of high temperatures and positive Qh and Qe suggests that the relative frequency of westerly airflows may have a significant impact on the mass balance of the ice cap (also see Bradley and Serreze, 1985a).

CHANGE IN HEAT STORAGE (ΔG) OF SNOWPACK AT YANKEE

The change in heat storage of a vertical column of snow is dependent on a number of processes, most importantly, conduction, radiation absorbed at depth, and the refreezing of meltwater or rain within the snowpack. Air circulation and the movement of water vapor can also transfer heat within the snowpack (Paterson, 1981), but these factors are generally of lesser importance. The change in heat storage of ice is mainly by conduction and radiation absorbed at depth. The change in heat storage of a vertical column of snow or ice to a depth where heat transfer is negligible* can be calculated as follows:

$$\Delta G = (T_2 - T_1) p \; Cs \; d \quad J \; m{-}2 \qquad \text{(Equation 7)}$$

where T and T are the temperature at times 1 and 2 (°K), d is the thickness of the layer where $T_2 - T_1$ is measured, p is the density of the snow (k gm-3), and Cs is the density-independent specific heat of snow or ice (2090 J kg-1 K-1). Δ G is positive when there is a net heat gain within the snowpack.

At Yankee, thermistors were placed at two depths within the snowpack (-0.02cm, -0.20cm) and at the original snow/tundra interface (-0.37 cm). By taking half-distances between these depths, three values of d were defined (d = 0.11 cm, d = 0.18 cm, d = 0.37 cm). $T_2 - T_1$ was calculated within each of these layers and was assumed to remain constant with depth within each layer. The density of the snowpack increased throughout the season, so the thickness of each layer also decreased.

---

*Note that this is a calculation of ΔG within the snowpack only. The actual depth to which heat transfer is negligible is unkown, and likely extends to a shallow depth below the tundra surface.

These changes were duly noted and the data accordingly adjusted.

Measurement of ΔG within a snowpack, although straightforward in theory, is in practice subject to error. Density changes and depth of the snowpack are difficult to measure accurately. Density is especially difficult to measure when meltwater or rain refreezes at depth because the development of ice layers and lenses make the snow cover inhomogeneous, so density can change irregularly with depth. The cables for the thermistors may offer pathways for the percolation of meltwater, so that measured temperatures may not be representative of the snowpack as a whole. Snow is also a semi-transparent medium, and allows the penetration of short-wave radiation at depth. This can cause undue heating of the upper thermistors. Because of these sources of error, it is difficult to measure ΔG with anywhere near the resolution that, for instance, radiative fluxes can be measured. The results presented here should be viewed with these caveats in mind.

Figure 7 plots mean hourly ΔG and shows a marked diurnal trend. The snowpack underwent a slight loss of heat in the early and late hours of the day. At these times, the sum of the other energy sources (R and Qh) were at their minimum. During the high-sun hours, ΔG became positive. The bulk of the heat gain during these hours was due to radiation absorbed at depth. The maximum change in storage occurred at 1400 h, several hours after the time of maximum R.

Daily values of ΔG are presented in Figure 8. The day-to-day changes were largely due to the combined effects of R, Qh, Qe, and on one occasion, precipitation (P). Two major events within the record are

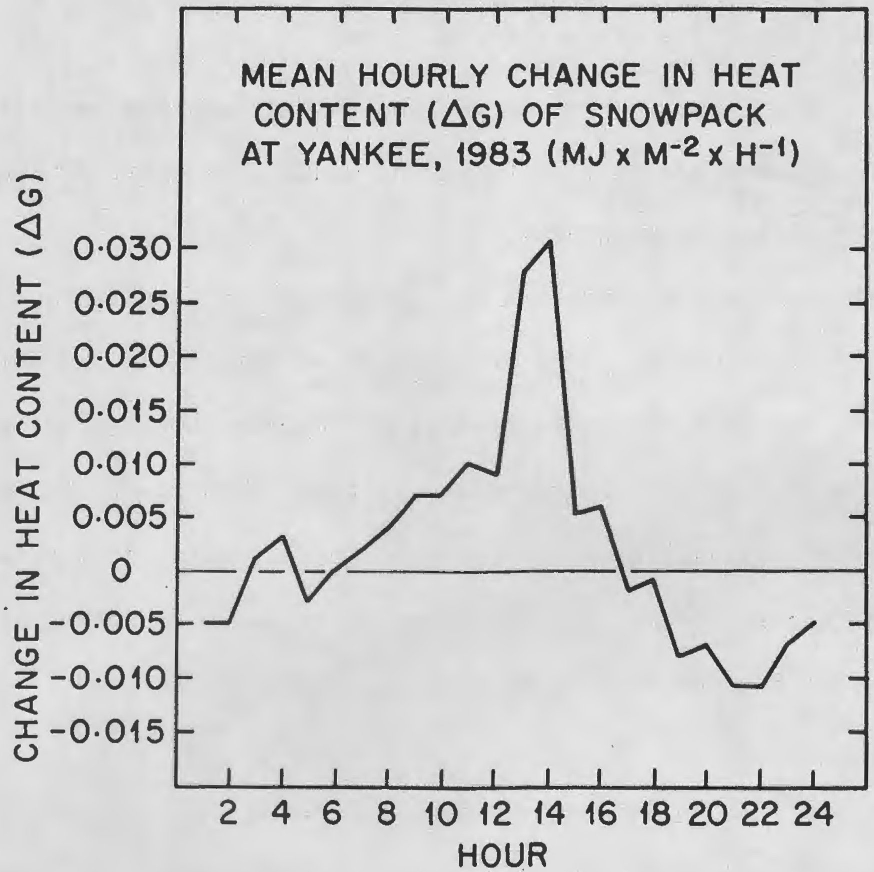

Figure 7 Mean hourly ΔG at Yankee, JD 165-210, 1983.

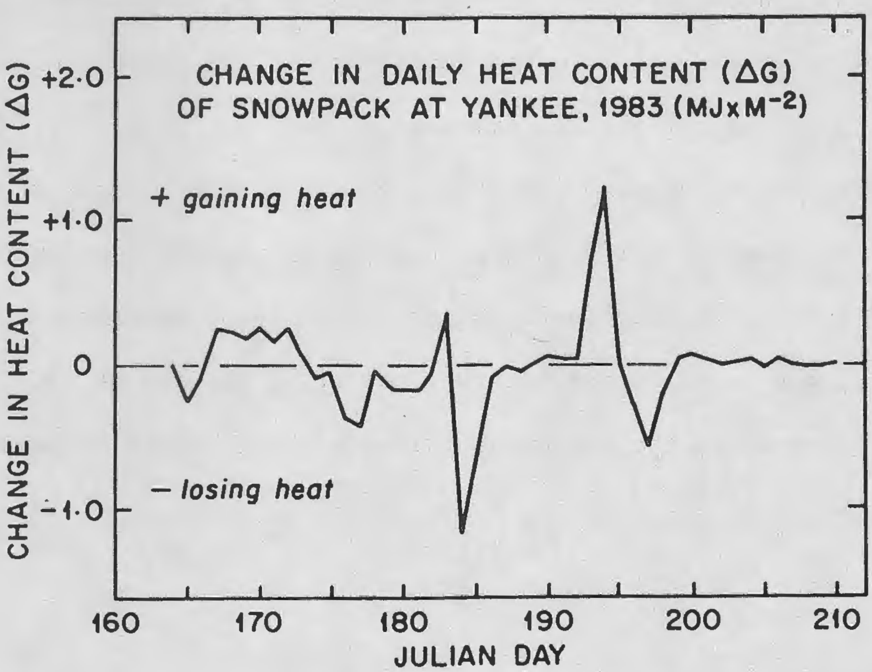

Figure 8 Daily ΔG at Yankee, JD 165-210, 1983.

of interest. The first was the large loss in heat storage on Julian Day 184. This day was characterized by strong winds (strongest of the season), fog, and low temperatures.

The other significant event was the large gain in heat storage from J.D. 192-195. This corresponded to a period of rain (0.70 cm) which rapidly warmed the snowpack by refreezing at depth. During this event, the snowpack became almost isothermal. In fact, after J.D. 200, ΔG remained nearly constant, at close to zero, corresponding to isothermal conditions in the snowpack. In this regard, it is worth noting that on J.D. 199, runoff was observed on a smaller, ice cap to the west.

THE ENERGY BUDGET AT ZEBRA

The energy budget at the surface is defined in Equation 1. Here, we provide a check on the energy budget at Zebra. By summing R, Qh and Qe for the season along with an estimated value of P, the combined contributions of ΔG and M to the energy budget can be determined as a residual in the energy balance equation.

As noted above, because 20% of the hourly totals of Qh and Qe had to be discarded (due to poor data quality) the values for the fluxes do not represent complete totals (as compared to the total measurement season). Altogether, 878 valid hourly observations of R, Qh, and Qe were used. Based on these data, the following values of heat budget components were obtained:

$$
\begin{aligned}
P &= +2 \\
R &= +92 \\
Qh &= +16 \\
\underline{Qe} &= \underline{-32} \\
G{+}M &= +78
\end{aligned}
$$

The value of P represents the re-freezing of 0.70 cm of rain within the snowpack (on J.D. 193-195).

A minimum estimate of M was determined from a calculation of the total mass loss from a snowpit adjacent to Zebra. The measured loss of 4.6 cm w.e. corresponds to a consumption of 15 MJ m^{-2}. This is a minimum estimate, as free water stored within the snowpack is unacccounted for.

From stake measurements, it was determined that ~5 cm of superimposed ice had formed on the ice cap. Part of this superimposed ice represents the refreezing of liquid precipitation, while the remainder is refrozen meltwater. Although the superimposed ice therefore required some snowmelt, consuming energy, an equivalent amount of energy was released when the meltwater refroze, so there was no net energy gain or loss to the system.

Subtracting this (minimum) estimate of M from the original residual yields a value of 63 MJ m^{-2}, which corresponds to any additional M and ΔG (as well as measurement error). No estimate of ΔG alone is available for the ice cap site.

The energy unaccounted for is less than total R, which indicates that the heat budget closes with a tolerable degree of accuracy (at least within the right order of magnitude). The agreement is not bad at all when it is considered how small all of the heat budget terms are. For example, the largest term, R, represents the amount of short-wave energy (Qh) that would be received on only three clear days near the solstice and total Qh for the 37-day record corresponds to considerably less than the short-wave energy that would be received on a single day.

SUMMARY

Energy budget measurements on the St. Patrick Bay Ice Cap during June and July 1983 were carried out at two sites, one in the center of the ice cap (station Zebra) and the other on tundra/felsenmeer near the edge of the ice cap (station Yankee). Both sites remained snow-covered for most of the period of record.

Diurnal changes in Qh were related to changes in stability conditions in the 15-150 cm layer above the ice cap surface. The overall magnitude (absolute values) of the turbulent fluxes (Qh and Qe) was larger at the ice cap site than the snow-covered felsenmeer site. This is probably due to the smoother surface conditions at Zebra which consequently led to higher windspeeds (u 150 cm) and larger values of Δ u. Whether the difference in Qh and Qe between a smooth and an uneven snow-covered surface has any implication for the survival of a snow-cover (i.e. a "self-preserving effect") depends on the net effect of these fluxes, their magnitude and direction, and their influence on other terms of the energy budget. Further study of this question is warranted.

Stratification of Qh, Qe, windspeed, temperature and relative humidity by wind direction at station Yankee indicates that the relative frequency of different synoptic conditions has a significant impact on the mass balance of the ice cap. For example, NNE and SSE airflows were rather common in 1983, and were associated with high windspeeds, low temperatures, and a tendency for both Qh and Qe to become negative, factors that would contribute to the health of the ice cap. Conversely, a westerly airflow, although uncommon in 1983, was associated with high temperatures and positive Qh and Qe, conditions detrimental to the health of the ice cap.

If the conditions associated with certain wind directions are the same from year to year (which only further investigation could ascertain) an analysis of past synoptic patterns may provide some clue as to the mass balance history of the ice cap. Bradley and Serreze, (1984a) made gross estimates of mass balance history of the ice cap for the last several decades by examining melting degree day data from Alert, approximately 40 km north of the ice cap. However, these data may only be applicable to a small coastal strip of northeastern Ellesmere Island, and may not always be representative of conditions over the ice cap. Hence, an analysis of energy budget terms in relation to synoptic circulation patterns (as for example carried out by Alt, 1975; 1978) would be a more useful way of looking at long-term changes in mass balance of the St. Patrick Bay Ice Cap.

REFERENCES

Alt, B., 1975. The Energy Balance of Meighen Ice Cap, N.W.T., Vols. 1 and 2, Polar Continental Shelf Project, Department of Energy, Mines and Resources, Ottawa.

Alt, B., 1978. Synoptic climate controls of mass balance variations on Devon Island ice cap. Arctic and Alpine Research, 10, 61-80.

Bradley, R.S. and Serreze, M.C., 1985a. Glacio-climatic studies of a high Arctic plateau ice cap, part I, mass balance (submitted.

Bradley, R.S. and Serreze, M.C., 1985b. Glacio-climatic studies of a high Arctic plateau ice cap, part II, topoclimate (submitted).

Palecki, M., Serreze, M.C. and Bradley, R.S., 1985. Glacio-climatic studies of a high Arctic plateau ice cap, part V, boundary layer observations (in preparation).

Paterson, W.S.B., 1981. The Physics of Glaciers, Pergamon Press, Oxford, 380 pp.

Sellers, W.D., 1965. Physical Climatology, University of Chicago Press, Chicago, 272 pp.

Serreze, M.C. and Bradley, R.S., 1985. Glacio-climatic studies of a high Arctic plateau ice cap, part III, radiation climatology (submitted).

GLACIO-CLIMATIC STUDIES OF A HIGH ARCTIC PLATEAU ICE CAP: PART V: BOUNDARY LAYER CONDITIONS

M.A.Palecki, M.C.Serreze and R.S.Bradley

University of Massachusetts, Amherst.

ABSTRACT

Thirty-nine low altitude (<400 m) soundings were made over St. Patrick Bay Ice Cap (81°57'N, 64°13'W) during June and July 1983. Measurements of dry-bulb and wet-bulb temperature, wind direction and speed and air pressure were made by a radio-equipped instrument package suspended from a tethered, helium-filled balloon. Flights took place in predominantly anticyclonic conditions. The data present a unique, high-resolution, view of conditions in the boundary layer above a near isothermal snowpack on a high altitude plateau in the Arctic. Case studies of the flights reveal a variety of macro-, meso-, and microscale processes affecting the local atmospheric conditions, and, thus, the energy and mass balance of the ice cap.

INTRODUCTION

Meteorological measurements on and around a small plateau ice cap on northern Ellesmere Island, N.W.T., Canada were carried out in the summers of 1982 and 1983 (Figure 1). The objective was to study the role of the ice cap in modifying local climate with a view to understanding the role of feedback mechanisms which might be effective in plateau glacierization. Observations at the surface, along a transect from the ice cap center to the adjacent unglacierized (felsenmeer) plateau surface, provided a measure of any "cooling effect" which the ice cap might exert (Bradley and Serreze, 1985a). However, it was hypothesized that the ice cap would also have an effect on the lower atmosphere by modifying boundary layer conditions above, and perhaps (to some unknown extent) around the ice cap. Analysis of standard radiosonde data (e.g. Bilello, 1966) is not very helpful in addressing this question. Such data are almost exclusively made at widely separated drifting ice stations or at coastal sites which

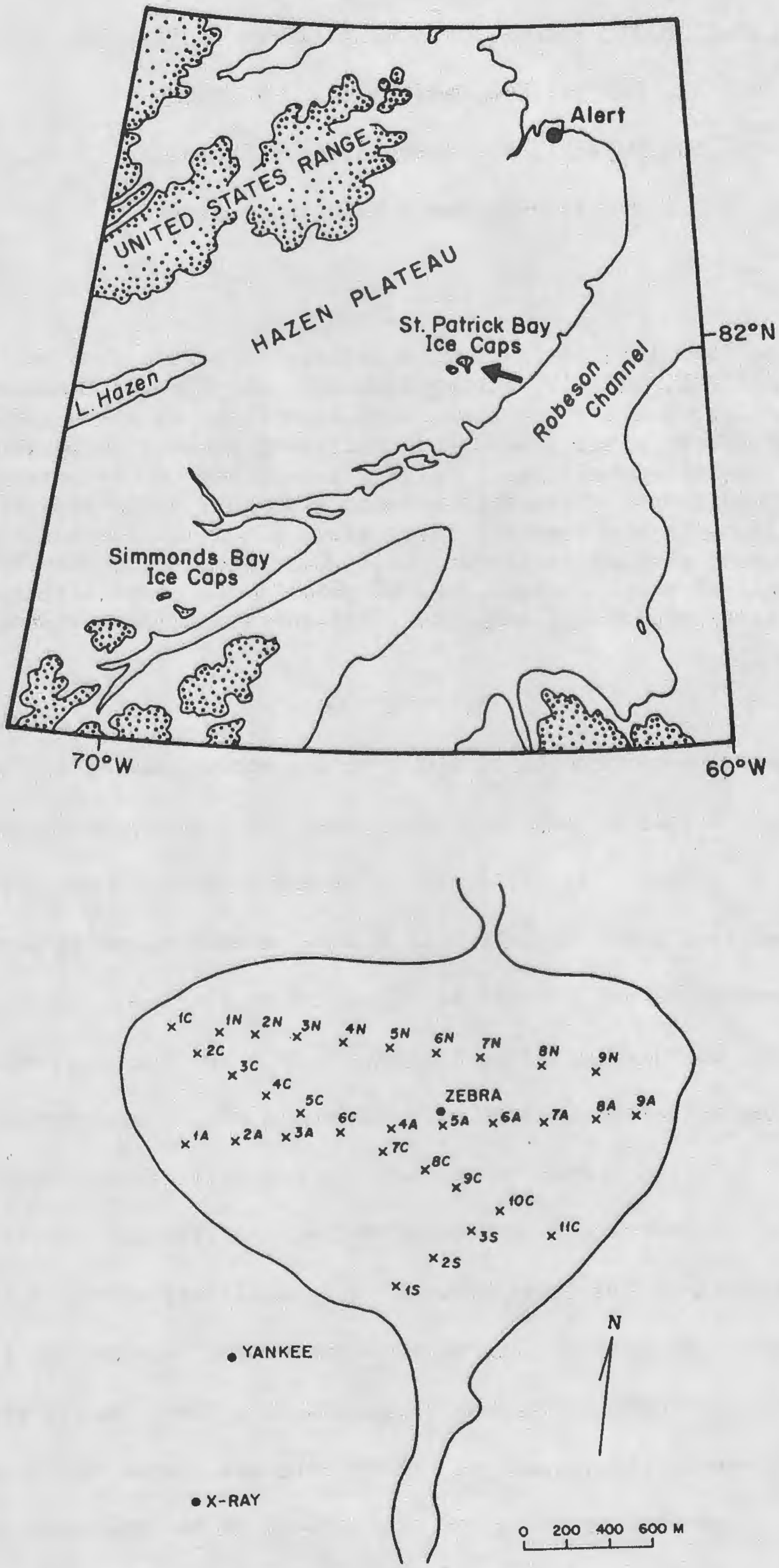

Figure 1 Location of ice cap and of launch sites X-Ray, Yankee and Zebra on and around the ice cap.

are not representative of surface conditions inland, particularly in summer.

Furthermore, conventional radiosonde data are relatively coarse, with observations generally recorded at vertical intervals of >100 m. In short, to study the effect of an ice cap on the lower boundary layer, detailed soundings directly over the ice cap are needed at regular intervals. Such observations are rarely carried out because of the logistical difficulties involved. In particular, the transportation of helium to the field site poses significant problems. Nevertheless, in the summer of 1983 a tethered instrumented balloon was used to record the fine structure of the lower atmosphere (up to 400m) over the St. Patrick Bay Ice Cap (81°57'N, 64°13'W)(Figure 1). The original objective was to record soundings over the snow-free tundra and over the adjacent ice-cap. However, due to low summer temperatures in 1983, snow-cover persisted across the plateau throughout the summer (Bradley and Serreze, 1985b) making it impossible to compare conditions over contrasting surfaces as planned. In spite of this, the observation program produced a unique set of soundings over a near-isothermal snowpack during conditions of continuous daylight.

INSTRUMENTATION AND OBSERVATION PROGRAM

Measurements of wet and dry bulb temperature, pressure, wind speed and direction were made with a Tethersonde (TM) system. Details of the instruments are given in Table 1. The Tethersonde comprises a direction were made with a Tethersonde (TM) system. Details of the

TABLE 1

Tethersonde* Instrumentation

Dry bulb temperature and wet bulb depression:	2 precision, interchangeable linearized thermistors (accuracy ±0.2°C)
Pressure:	piezoresistive aneroid, automatically adjusted for temperature change (accuracy ±1.0 mb)
Wind Speed	3 cup anemometer with continuous voltage generation (accuracy ±0.25 m/s).
Wind direction	Magnetic needle locked to a circular potentiometer (accuracy ±2°)

*Tethersonde is a trade mark of Atmospheric Instrumentation Research, (AIR) Boulder, Colorado.

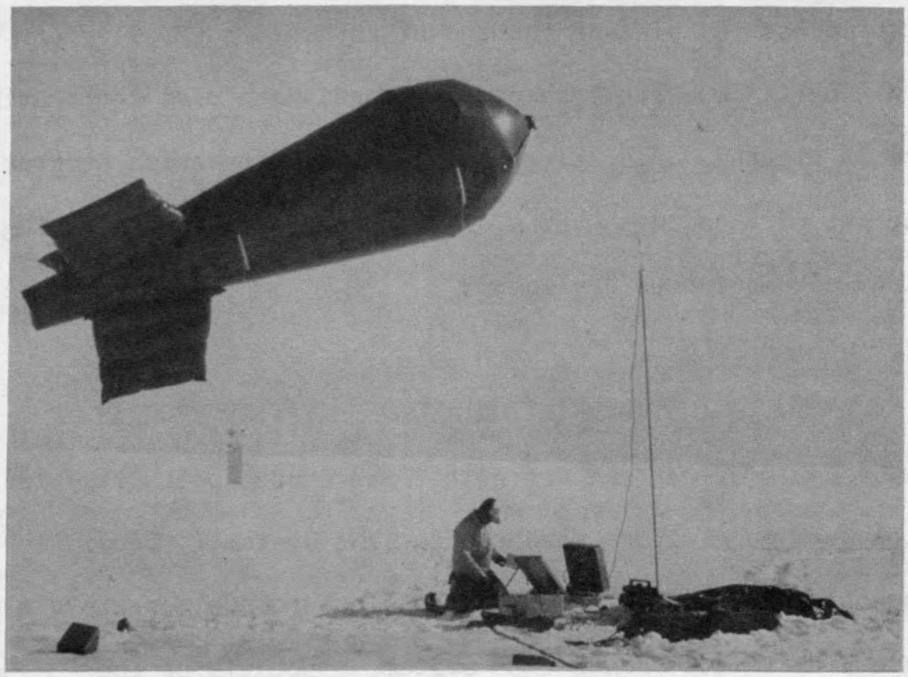

Figure 2. The Tethersonde (TM) system ready for launch at station Yankee. The instrument package is suspended from the balloon. Ground receiving station and power winch are on the right.

instruments are given in Table 1. The Tethersonde comprises a radio-equipped instrument package (1.2 kg) suspended from a 15 m^3 helium-filled balloon tethered to a power winch (Figure 2). As the balloon ascended, the on-board sensors were scanned at a pre-set interval and data were transmitted to a ground receiving station. Data were recorded on a cassette tape for later analysis.

Thirty-nine soundings were made on six days, generally at two-hour intervals (Table 2). Soundings took place at three different sites (Figure 1): at ice cap Station Zebra on Julian Days (JD) 173, 180 and 203; at Station X-Ray on JD 197 and 200; and at Station Yankee on JD 204-205. Station elevations differ by less than 50 m. The snowpack at Zebra was considered to be near isothermal on JD 172 and was probably near isothermal during flights after this. The flights at X-Ray took place over a thin, patchy snow cover interspersed with frost-heaved till and felsenmeer. The flights at Yankee took place over a thin but almost continuous isothermal snow cover.

Flights were restricted to only six days because of limitations of the system, logistical problems and meteorological conditions. The large balloon became unstable and could not be flown when wind speeds exceeded 8-10 m/sec. The balloon used a large volume of helium ($15m^3$) which had to be transported in heavy ($\sim$60 kg) cylinders to the field site. In addition two car batteries and a portable generator were needed for the winch and ground receiving station. Only four cylinders could be taken to the ice cap because of weight limitations. Overall the complete system and four helium tanks weighed $\sim$350 kg. Furthermore, no field building or

TABLE 2

Summary of Tethered Balloon Flights St. Patrick Bay Ice Cap

SITE	DATE (Julian Days)	TIME (hour)	METEOROLOGICAL CONDITIONS	REMARKS
X-Ray	7/16/83 (188)	1400,1600,1800 2000,2200,0000	Clear, light breeze from North. Temperature <0°C.	
	7/19/83 (200)	1400,1600,1800 2000,2200,0000	Clear, calm, Temperature >0°C	Several flights to elevations >400 m.
Yankee	7/23/83-7/24/83 (204-205)	1400,1600,1800 2000,2200,0000 0200,0400,0600 0800,1000,1200	Generally clear, periods of high thin cirrus, gradual advance of altocumulus late morning of 7/24. Winds calm.	A complete diurnal study Excellent flights.
Zebra	6/22/83 (173)	0000,0200,0400 0600,0800,1000	High, thin cirrus, light breeze from SE. Temperature >0°C	Unable to achieve high altitudes due to wind. Ascent date for 1000 flight lost due to equipment failure.
	6/29/83-6/30/83 (180-181)	1600,1800,2000 2200,0000,0200	Clear and calm. Temperature >0°C	Optimum conditions. Excellent flights.
	7/22/83 (203)	1000,1200,1400	Clear, light breeze from NE. Temperature >0°C	

tent large enough to protect the inflated balloon was available, therefore, the balloon was inflated only when weather conditions were good. This provided observations under generally anticyclonic conditions with relatively low wind speeds (Table 2). Hence, although the observations are not representative of a wide range of meteorological conditions, they do reflect those occasions when any 'ice cap effect' on the boundary layer was likely to be maximized.

Data were recorded during both balloon ascents and descents. However, data from the upward flights were most consistent. Because of the system design and its response to wind speed and wind shear changes, downward flight data were less useful. Similar problems were noted by Whiteman (1980). In the following section, only ascent data were used. In general, these data were considered to be excellent.

DATA ANALYSIS

From the parameters measured (temperature, wet bulb depression, wind speed and direction and pressure differential, from the surface) the following variables were computed using the formulae in Table 3: height, potential temperature, specific humidity and Richardson numbers (Ri). However, there were problems in computing Richardson numbers based on the wind speed data recorded 'instantaneously' at each level. Any errors in the wind speed gradient greatly affect the value of Ri (Table 3) and may lead to erroneous estimates. This should be kept in mind when considering the values of Ri reported below.

The layer of air near the surface is affected by four basic processes:

TABLE 3

Formulae Used in Derivation of Variables

Saturated Vapor Pressure: $$e_s = 6.1078 \times 10^{\left(\frac{7.5T}{237.3 + T}\right)}$$

Vapor Pressure: $$e = e_{sw} - 0.00066\ (1 + 0.00115\ T')\ P\ (T - T')$$

Thickness of Air Layer: $$\Delta H = 14.636(T_1 + T_2)\ \ln \frac{P_1}{P_2}$$

Height: $$H_n = \sum_{i=1}^{n} (\Delta H)_i$$

Potential Temperature: $$\Theta = (T + 273.15)\left(\frac{1000}{P}\right)^{0.286}$$

Richardson Number: $$Ri = \frac{9.807\ (\Delta\Theta/\Delta H)}{\Theta(\Delta u/\Delta H)^2}$$

Specific Humidity: $$q = \frac{0.622e}{P - 0{,}378e}$$

All formulae are from Atmospheric Instrumentation Research (1977) except for the specific humidity formula from Oke (1974).

turbulent flux, clear-air radiation, surface radiation, and advection/subsidence. Significant turbulent flux is limited to the planetary boundary layer (PBL) reaching zero near its top. Clean-air radiation affects all atmospheric layers simultaneously, while surface radiation affects only the lowest layer of air directly. The balance of radiative fluxes in a layer is controlled by air temperature, moisture content, and the radiative features of nearby air layers. Advection/subsidence processes introduce air masses with different properties into the local environment. The interactions of these four processes create the temperature, humidity and wind profiles observed.

FLIGHTS ON JULIAN DAYS 204 AND 205 (JULY 23 AND 24)

The most detailed series of soundings were obtained at Station Yankee on JD 204-205. Twelve high quality soundings were obtained over a 24 hour interval during generally clear anticyclonic conditions. Their major features are summarized in Table 4. Using the data collected during this diurnal cycle, the planetary boundary layer (PBL, defined as the height at which Ri was greater than 0.5) was generally in the range of 8-12 m. This was only exceeded during a period of turbulence between 0300 and 0700 on JD 205 (Table 4). On this basis, the surface layer (generally cosidered to be 5-10% of the depth of the planetary boundary layer) was estimated as 0.4-1.2 m. Observations of this layer are discussed in Bradley and Serreze (1985a). Here, we discuss the sequence of changes which took place in the lowest 300-350 m of the atmosphere over the snow-covered plateau surface.

TABLE 4

Yankee Flights JD 204-5

Hour	Net	LWout	T_o	h_1	$dT_1/100m$	h_{2b}	h_{2t}	$dT_2/100m$	h_u	h_R
1400	0.146	1.079	2.50	15	6.36	148	186	2.47	70	10
1600	0.357	0.813	2.80	20	3.89	86	130	2.95	-	11
1800	0.246	0.817	3.18	51	1.76	82	141	2.39	42	10
2000	0.037	0.937	2.53	18	4.35	41	94	3.19	47	8
2200	-0.032	0.954	2.85	57	3.86	-	-	-	20	8
2400	-0.121	0.963	2.79	81	2.63	-	-	-	15	8
0200	-0.143	1.031	2.55	72	0.64	77	162	2.35	44	2
0400	-0.069	1.008	3.07	-	-	56	136	2.81	53	35
0600	-0.120	1.147	3.70	3	3.33	77	178	1.58	-	-
0800	-0.056	1.107	1.96	21	2.50	49	89	5.15	16	8
1000	0.034	1.095	2.60	47	0.96	57	92	4.91	19	12
1200	0.198	1.031	3.60	17	0.73	61	110	3.63	41	9

Key

Net: Net Radiation (MJ $m^{-2}hr^{-1}$) LWout: Outgoing longwave radiation (MJ $m^{-2}hr^{-1}$)
T_o: Surface temperature (°C) h_1: Height of surface inversion (m)
$dT_1/100m$: Temperature gradient in the surface inversion (°C/100m).
h_{2b}: Base height of above surface inversion (m) h_{2t}: Top height of above surface inversion (m)
$dT_2/100m$: Temperature gradient in the above surface inversion (°C100m)
h_u: Height of maximum wind speed h_R: Height of lowest layer where Ri = 0.5.

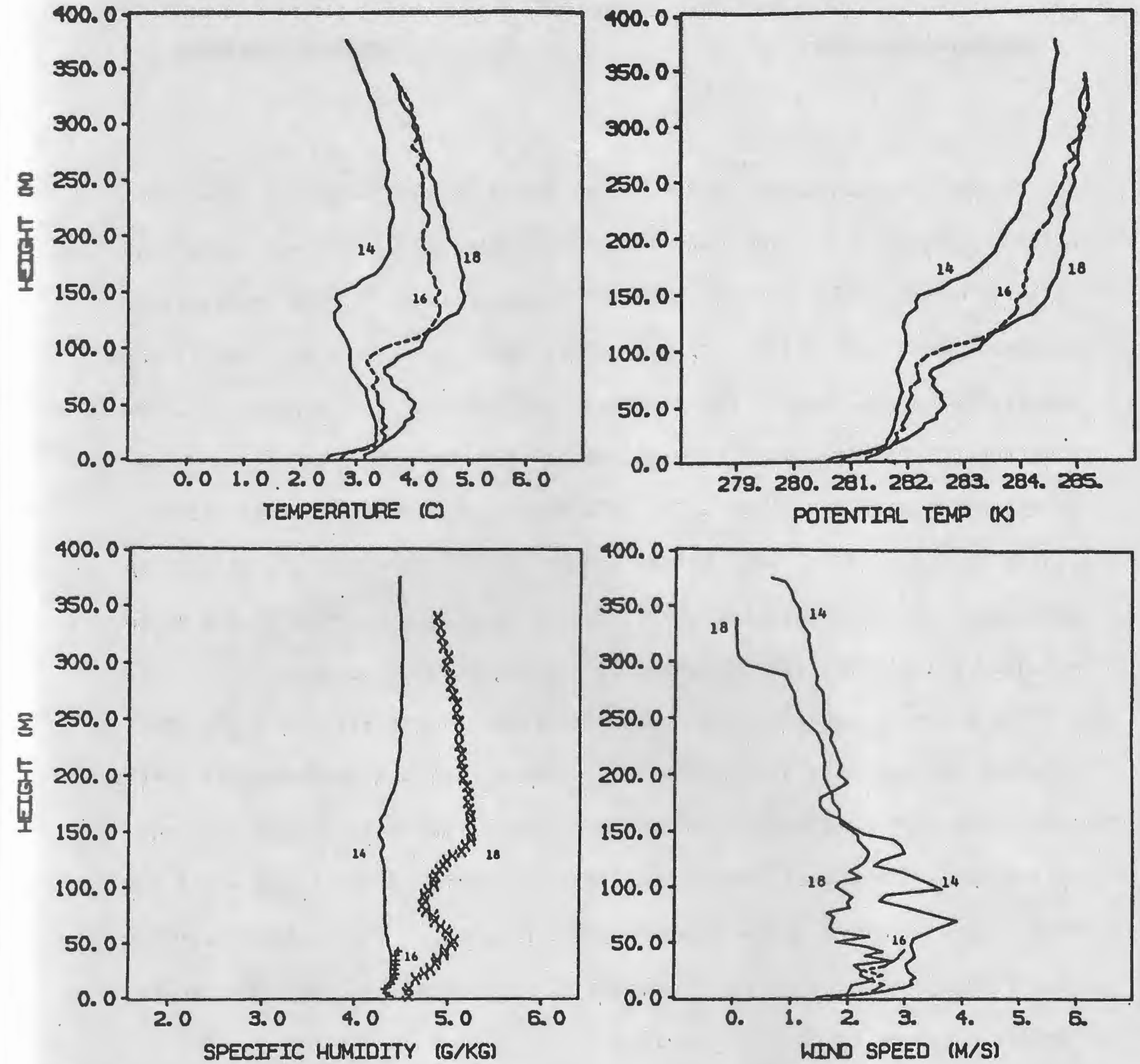

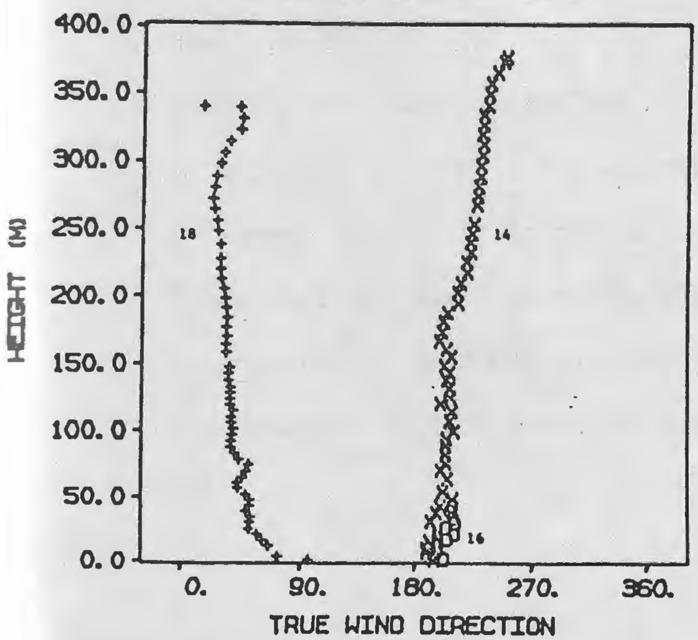

Figure 3:

Station Yankee flight profiles
for Julian Day 204 (1400-1800 hours).

By early afternoon on JD 204, there was a double inversion structure evident (Figure 3). The lower inversion appears to have been associated with turbulent cooling of air brought to the surface. A large slightly stable layer extended to 150 m. There was no moisture gradient in this layer, indicating that it was probably detached from the surface. This also account for its jet-like wind speeds that are 2 m/s faster than the layers below or above (Figure 3). Finally, large calculated Ri values (Table 5) indicate the well stratified nature of this layer. The air in this layer had been advected over a snow free valley, across a side slope, and only briefly over the snowpack to the SSW of Station Yankee.

The second inversion layer coincided with a lower wind velocity, an increase in moisture, a decrease in Ri number, and the beginning of a wind vector rotation (Figure 3). This inversion is probably due to regional subsidence, with the air above more representative of the large scale air mass. The rotation of the wind vector clockwise, pointing more toward high pressure, indicates the weakening of wind shear with height that is readily apparent in the wind profile.

Alternatively, the second inversion level in flight 1400 may in fact be the remnant of a surface inversion from the previous low-sun period. This would indicate that 150 m is the extent of the PBL over the area on a mesoscale level. The 150 m layer may be a remnant of active convective mixing from the morning. To differentiate between large, medium, and micro scale mechanisms, time marches of the profiles must be examined. When comparing the 1400 and 1600 profiles (Figure 3), it is immediately

TABLE 5

Richardson Numbers: Selected levels, Yankee Flight

JD 204 (July 23, 1983)

Hour	Bottom (m)	Top (m)	Midpoint (m)	Richardson No.
1400	1	13	7	0.21
	13	64	39	3.38
	64	107	86	1.23
	107	144	125	0.94
	144	174	159	0.70
	194	253	223	6.29
	281	311	294	11.55
	342	358	350	1.85
1600	2	13	7	0.03
	13	41	27	2.44
1800	1	17	9	0.287
	17	34	28	5.18
	34	78	56	-0.17
	78	132	104	6.53
	132	164	148	1.30
	163	227	195	4.32
2000	1	16	9	0.55
	16	48	32	0.61
	1	95	48	13.65
	48	110	79	3.16
2200	3	17	10	0.74
	1	47	24	2.41
	25	52	39	0.94
	52	104	78	2.83
2400	1	16	8	0.45
	1	28	14	5.66
	16	55	36	0.23
	55	106	81	28.80
	106	152	129	5.98

apparent that the second inversion moved down about 60 m, leaving its structure intact. The layer of air above the inversion uniformly warmed by 0.5°C. It is likely that the warming was due to the movement of this air downward. Thus, by examining the relationships of different variables within each flight and comparing them with subsequent profiles, a physical process can be identified more clearly.

The wind maxima observed in the lower atmosphere are perhaps unexpected. However, they are relatively common during stable evenings in mid-latitudes, and certainly seem common in the balloon data profiles. There are many situations when such jets may develop: directly above the PBL under anticyclonic conditions (Thorpe and Guymer, 1977; Garratt and Brost, 1981); as a result of the oscillation of mesoscale pressure gradients (Hahn, 1981); due to a step change in surface roughness (Korrell, et al., 1982); as a result of flow between two stable layers (Hsu, 1979) and flow within a stable layer (Li, et al., 1983). There is a unifying tendency in all such jet formations: they exist in areas of low shear stress (Mahrt, 1981; Mahrt, et al., 1979). Stable stratification may develop above a turbulent boundary layer due to advection/subsidence and clear-air radiative cooling. The winds become decoupled from those below and rotate away from the geostrophic direction. Eventually winds at all layers rotate, and significant shear is developed. This shear can eventually build-up to the point that there is a penetrative turbulence event that decreases the wind shear and flattens the wind profile. With large wind shear and stable temperature gradients, wind jets will usually be located at levels with a high

Richardson number. It is therefore is of interest that there is generally an associated wind jet just above layers with a high Richardson number on flights between 1400-2400 (Figure 3 and 4; Table 5).

The general evolution of temperature and wind profiles are closely linked, relating to the stability of the air layer. There are turbulent interludes (Panofsky and Dutton, 1984) that cause interaction between the turbulent boundary layer and the layer above it (which may be a jet). Normally, in the lowest part of the turbulent boundary layer total cooling is maintained by radiational cooling and by turbulent warming. In the middle part, total cooling is maintained by heat flux divergence (cold air is brought from the surface by returning turbulence). Then in the uppermost layer, cooling is again dominated by radiative loss (Garratt and Brost, 1981). When air above is cooled radiatively, the stratification can cause the penetrative turbulence mentioned earlier. This has a temperature effect exclusive of the wind velocity decrease. The air mixed in the lower jet layer is cooled down, while the air in the turbulent boundary layer is warmed up. This process of warming the surface has been recognized as a major control on surface temperatures over a snowpack (Halbertstam and Melendez, 1979). In fact, just such an event occurred betweeen 0300-0700 causing the surface temperature to rise 1.15°C from the 0200 to the 0600 flights, and the planetary boundary layer to double in thickness (Figure 5).

Specific humidity gradients can be small or large, elevated or surface-based. All types have been observed in the balloon data. A

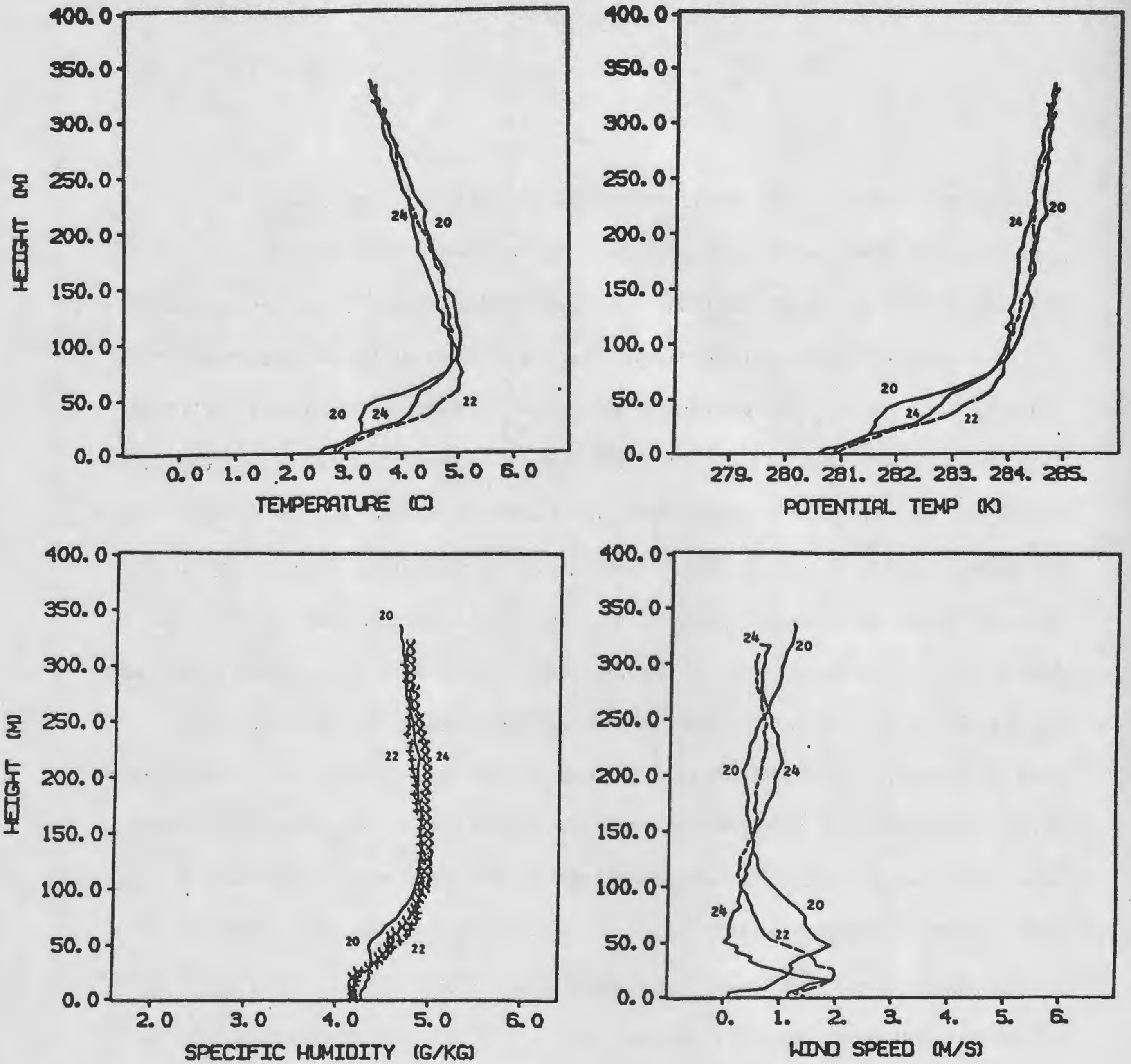

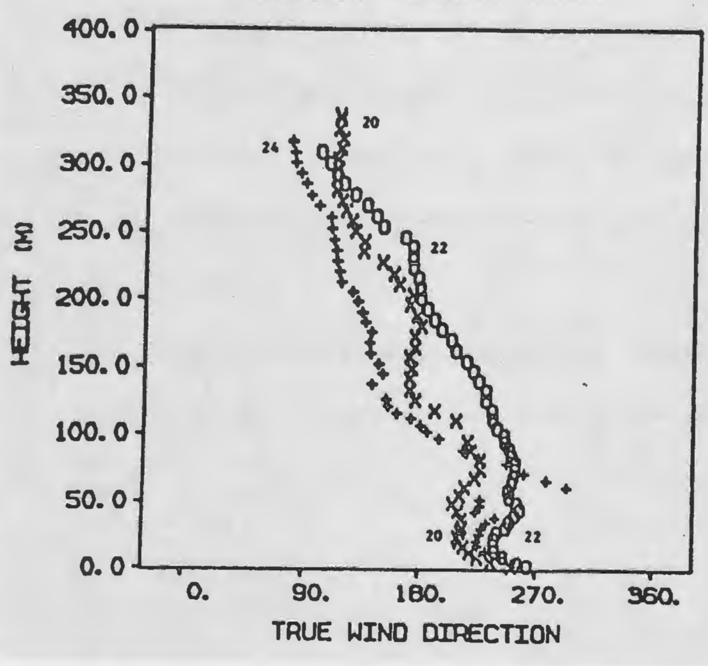

Figure 4:

Station Yankee flight profiles
for Julian Day 204 (2000-2400 hours).

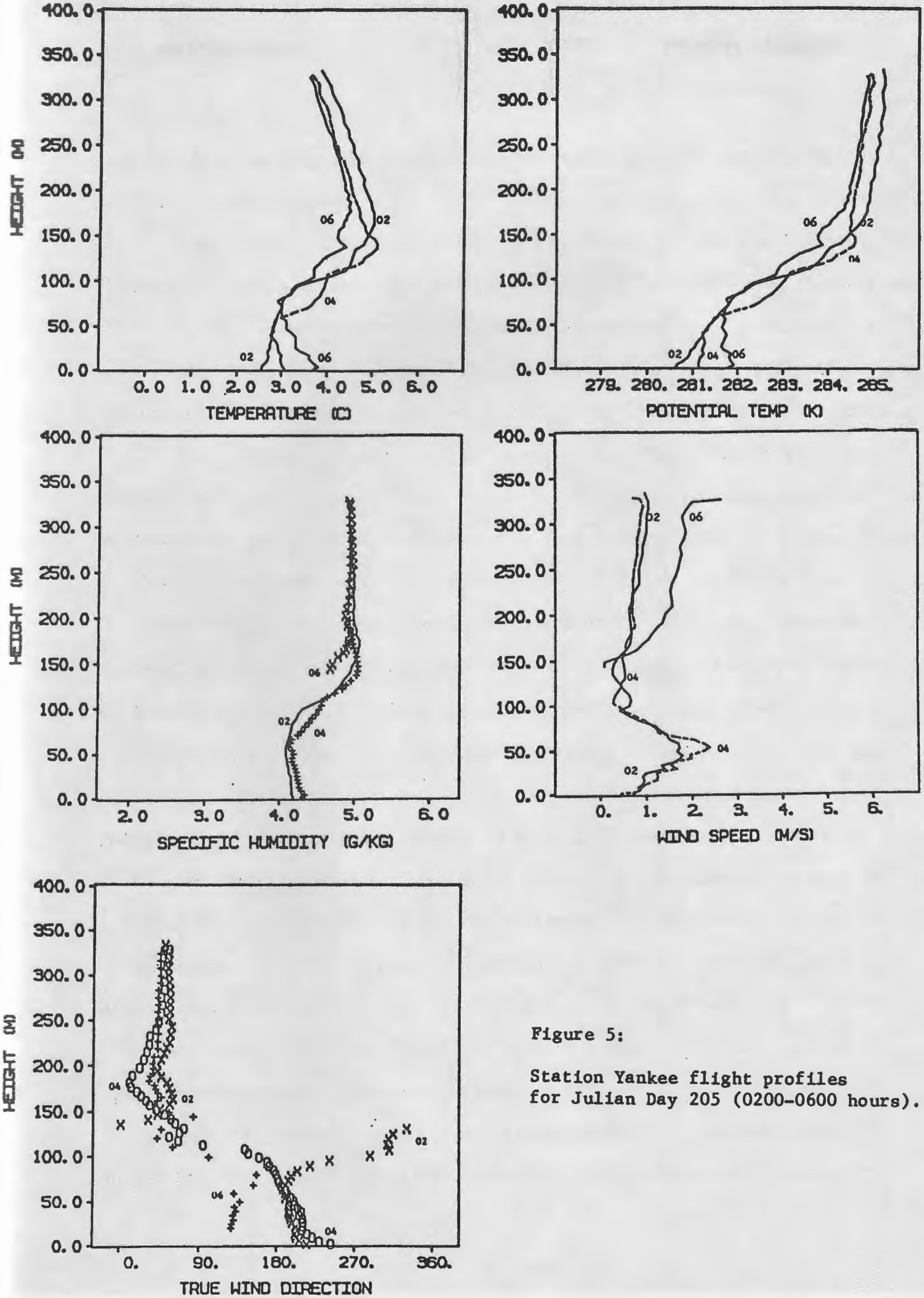

Figure 5:

Station Yankee flight profiles
for Julian Day 205 (0200-0600 hours).

noticeable positive gradient at the surface may be a good example of the drying power of snow (Treidl, 1970), as turbulent interactions in the nocturnal boundary layer remove heat and water vapor. A noticeable gradient at an elevated position is probably indicative of two different air masses of local and regional temperature and stability.

The flights at Yankee presented an interesting sequence of events (Figures 3-6). During the late afternoon and early evening, subsidence continued until the surface inversion and subsidence inversion were indistinguishable (Figure 4). By 1800, wind had slowed down and the wind jet altitude had lowered. This was probably in response to the reduction of local pressure gradients with height as the solar energy diminished over snow-free areas. Wind direction switched to NE at higher levels, rotating gradually with height. Since winds remained NE at high levels and increased in strength the next day, it is likely that the weakening in the evening winds were due to the location of a macroscale high pressure center very close by.

The transitional period from 2200 to 0200 showed clearly the evolution of temperature structures (Figures 4 and 5). The maximum rate of clear-air radiational cooling was at the top of the inversion, declining with temperature both above and below the maximum inversion temperature level. The lowest sun occurred before the 2400 flight, which was already showing cooling at the upper part of its inversion. The lowest part of the boundary layer was growing increasingly neutral, as radiative warming (flux from the surface and warmer air layers) counteracted the cooling effects of a very weak PBL. Table 4 shows that the cooling at the top of

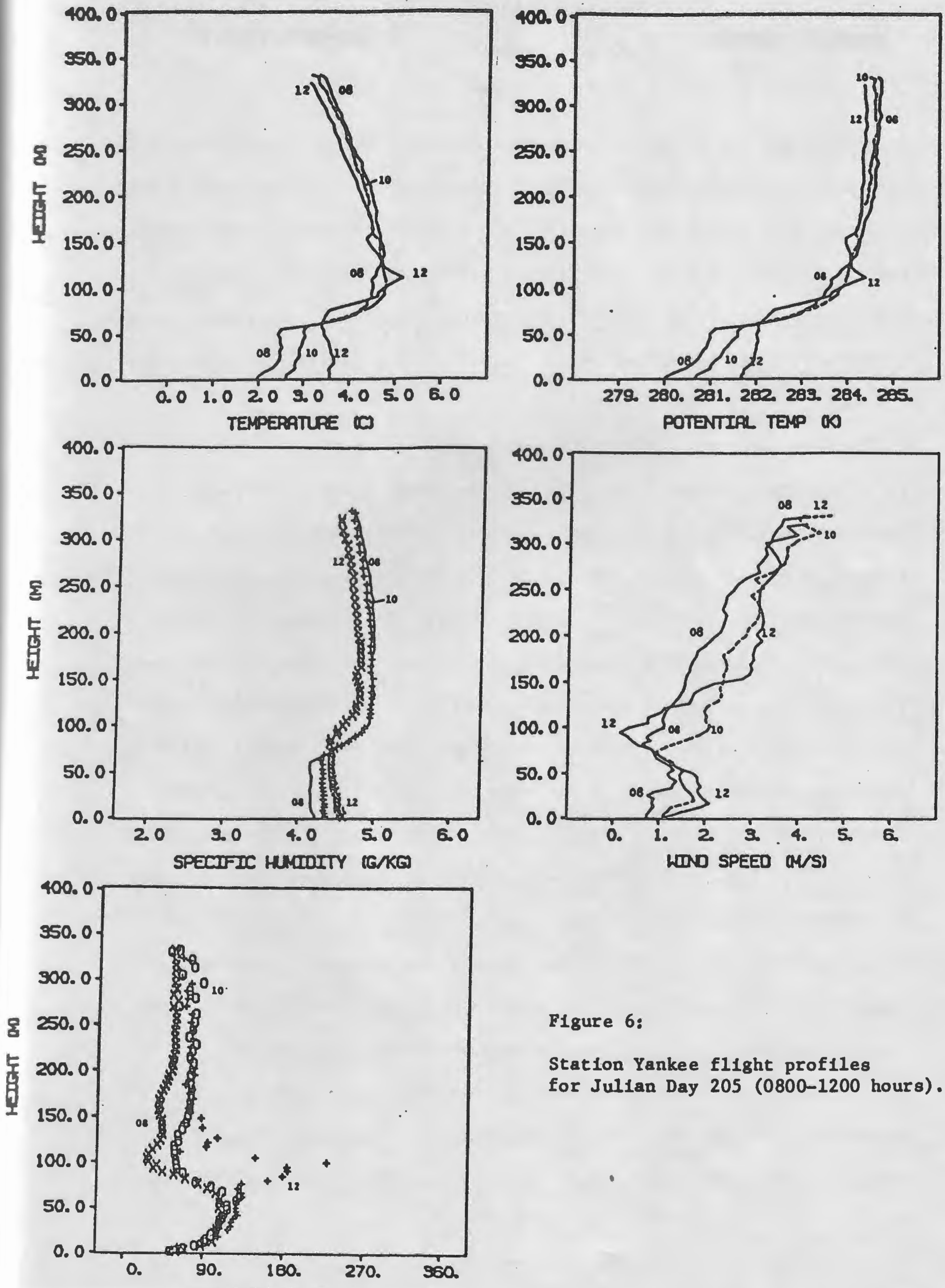

Figure 6:

Station Yankee flight profiles
for Julian Day 205 (0800-1200 hours).

the inversion took place at the rate of 1.16°C/hr between 2400 and 0200, with the surface cooling at a rate of only 0.12°C/hr. While some of the radiative flux warmed the lower PBL, almost all of it went toward warming the significantly cooler layer above the original inversion height. Thus, through purely radiative effects in the clear air, the lowest layer of the atmosphere has become quite neutral, with a stable inversion layer now significantly removed from the ground.

Between 0200 and 0800 it is clear that something happened that calls for a different explanation. The wind jet above the PBL increased in speed to the point that wind shear overcame the weakened temperature stratification and created turbulence in the shear zone (Panofsky and Dutton, 1984; Halberstam and Melendez, 1979). This mixing cooled the area above the shear zone (intensifying the inversion above surface level) and warmed the surface layer and expanded PBL. It should also be noted that not only wind velocity shear took place, but severe wind directional shear also occurred, adding to the turbulence. The specific humidity during this time period was in two modes, drier at the surface and moister above. This indicates that the wind direction shear was caused by local and regional winds with different sources.

After 0600, the stratified lower atmosphere returned. Weakly stable temperature gradients were capped by a thin inversion layer that lowered slightly to an equilibrium position between turbulent and clear air radiative fluxes. During the morning (Figure 6) the second inversion maintained the same level even as the lower layer underwent a 1.5°C warming. The inversion was restricted by an increase in wind speed above

75-100 m, constantly advecting air with the same temperature profile from a regional air mass. The PBL was very shallow, with a weak radiative inversion close to the surface. There was still a jet above the PBL, with the maximum jet level more or less coinciding with the level at which the wind direction vector rotated. Differences in moisture were still apparent between the upper and lower layers.

FLIGHTS ON JULIAN DAY 180-181 (JUNE 29 AND 30)

The flights on JD 180-1 over the central part of the ice cap (Station Zebra) are noteworthy in that they demonstrate the development of shallow, very strong surface inversions as the sun lowered in elevation (Figures 7 and 8). Wind decreased in the late afternoon which enabled wind jets to develop at low elevations, with their own directional dependencies. By mid-evening, though, winds had picked up from the SSE, with increasing temperatures and a steady wind direction throughout. Moisture content of the air increased steadily throughout the flights. There may have been a general subsidence taking place also, as a weak elevated inversion layer "passed through" the surface profile (Figure 7). Again the PBL was limited by stable stratification at the surface.

FLIGHTS ON JULIAN DAY 203 (JULY 22)

The flights on JD 203 at Station Zebra took place around the local solar maximum (Figure 9). The most interesting feature present was the wind shift from east to west and back to east in the four hour period.

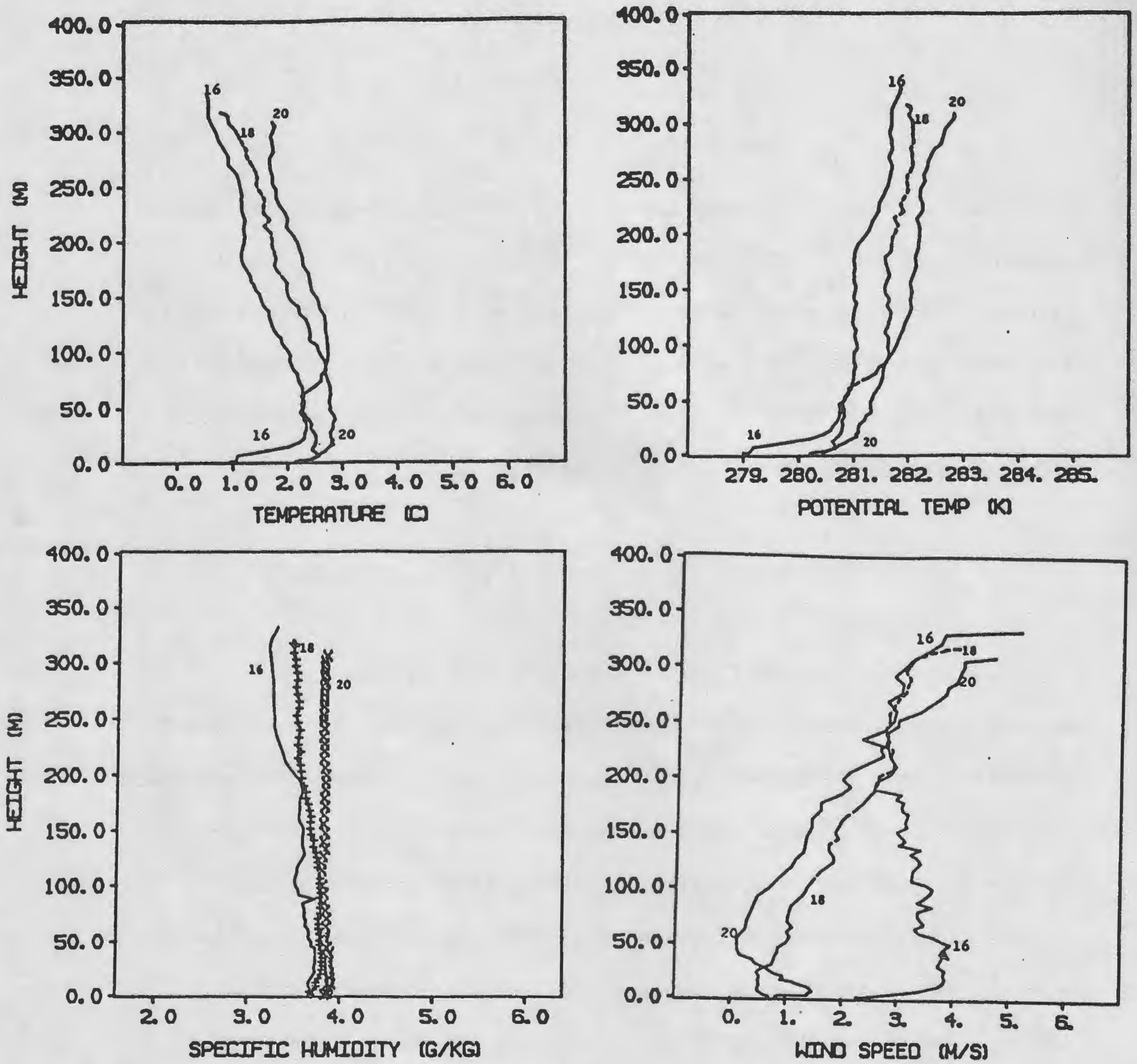

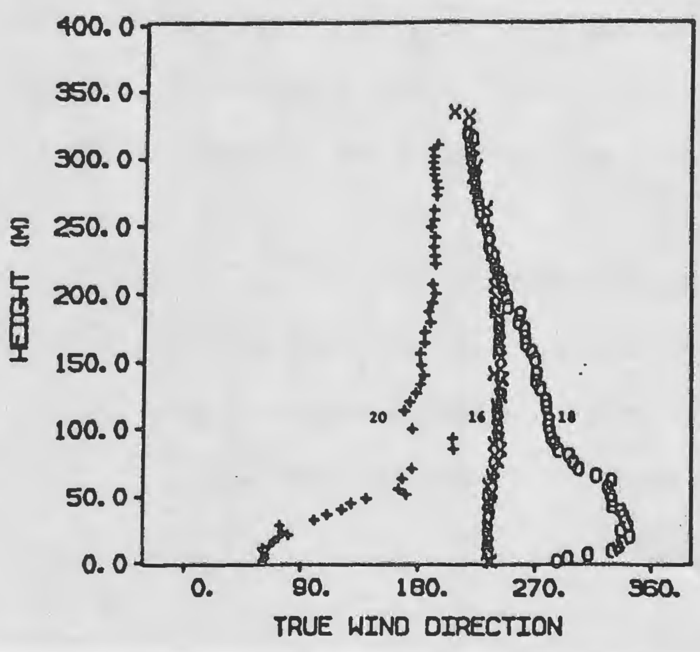

Figure 7:

Station Zebra flight profiles for Julian Day 180 (1600-2000 hours).

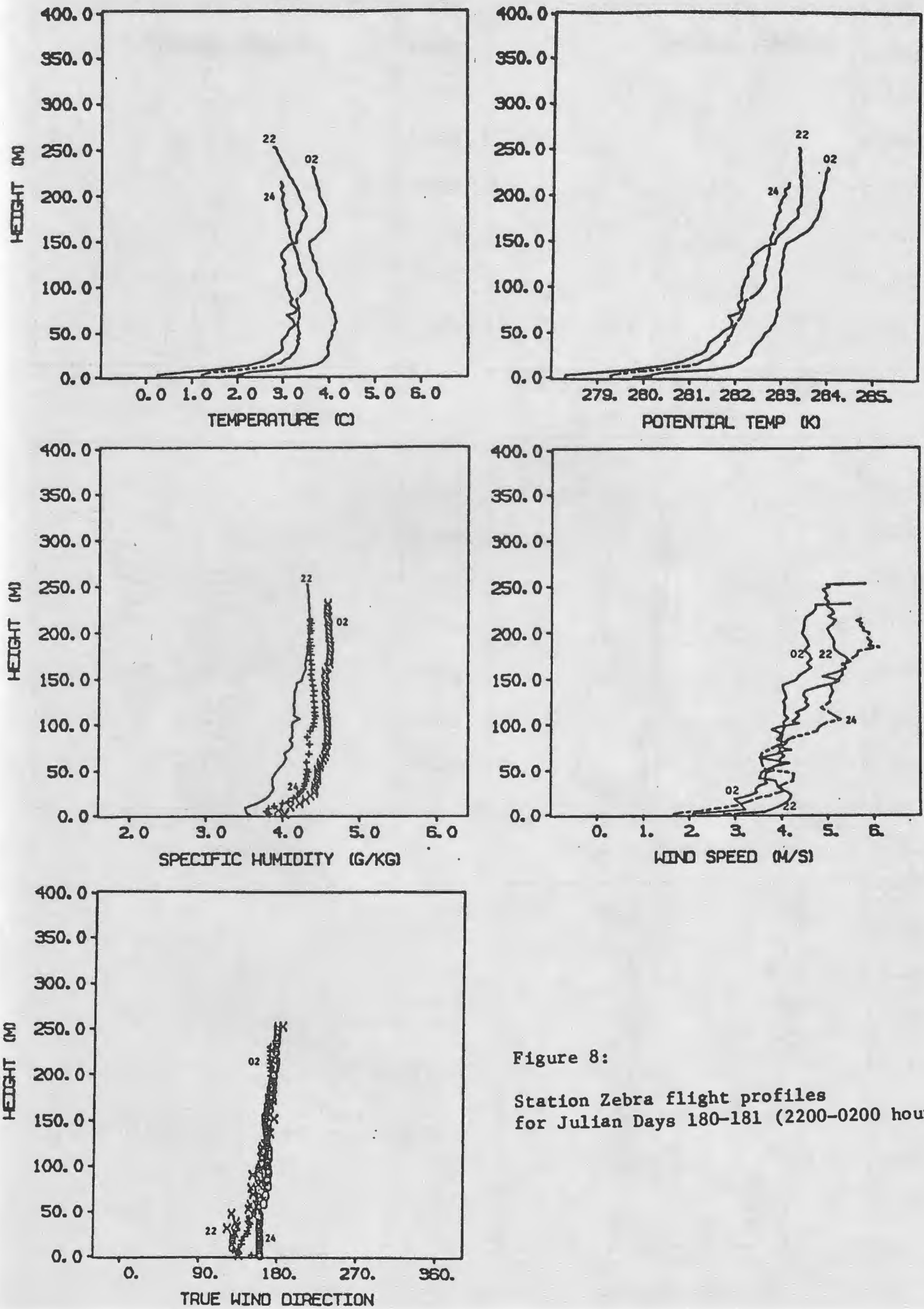

Figure 8:

Station Zebra flight profiles
for Julian Days 180-181 (2200-0200 hours).

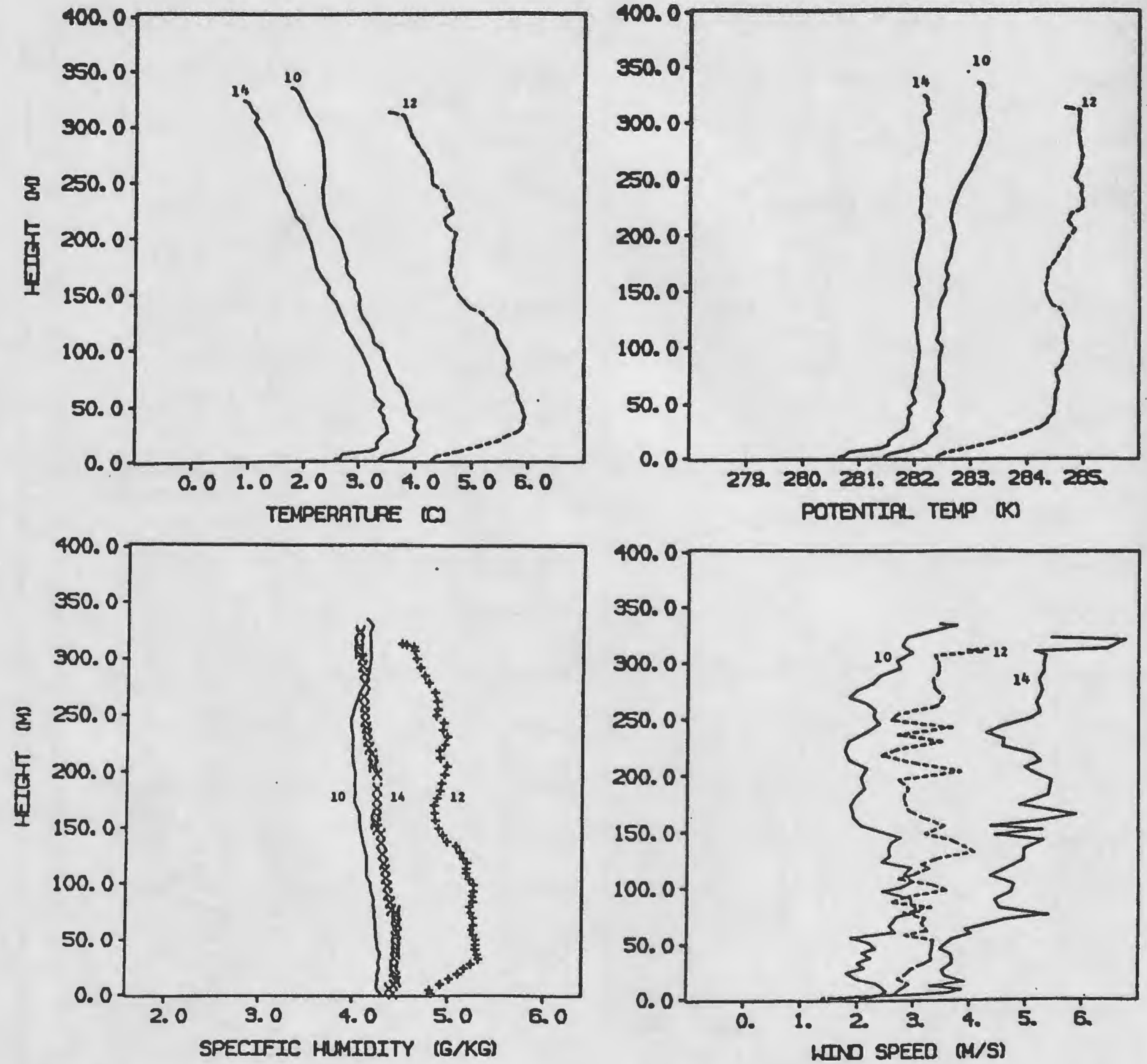

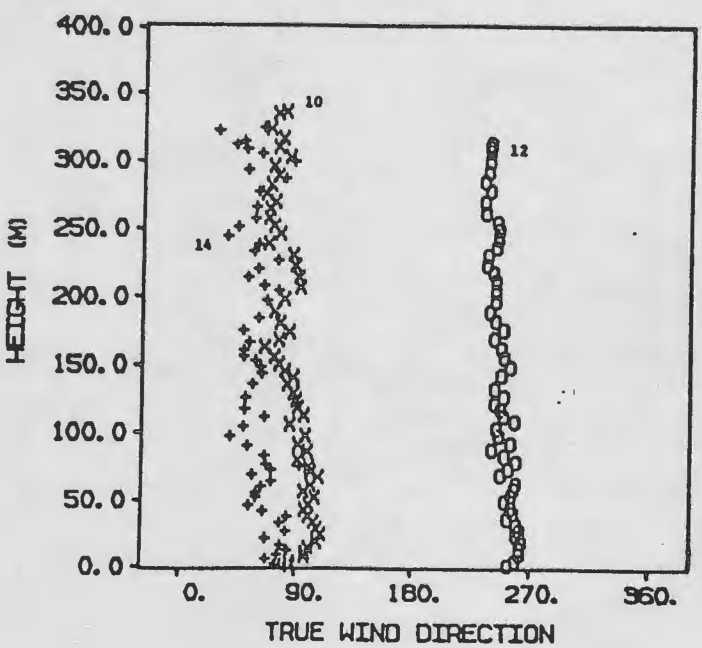

Figure 9:

Station Zebra flight profiles
for Julian Day 203 (1000-1400 hours).

The hour with the wind from the west indicated the generally warmer nature of air flow from this direction after the snow had melted in the lowlands to the west. The east winds were both cooler and drier, as they came from the pack ice covered channel. The cause of the wind shift may be a local wind system funneling through low spots in the topography, alternating between cold air off the coast and warm air inland, similar to a mesoscale land-sea breeze.

FLIGHTS ON JULIAN DAY 200 (JULY 19)

The flights on JD 200 at Station X-Ray provide another good example of a subsidence inversion propagating downward (Figures 10 and 11). From 1400-2400, a mass of air descended, warming the lower 350 meters of the atmosphere as the day progressed. Intermediate elevation increased in temperature by 5°C, and near-surface layers increased by 3°C, even as the sun declined. Such events may have a significant impact on ablation on the plateau. The layer of subsiding air was very stratified and had high wind speeds. Subsidence was weaker in the last four hours, allowing local wind systems to create fine surface jets.

CLIMATIC IMPLICATIONS OF ATMOSPHERE-SURFACE INTERACTIONS

As mentioned earlier, the main processes affecting atmosphere-surface interactions are turbulent boundary layer fluxes, surface and clear-air radiative fluxes, advection, and subsidence. The balloon data have shown that all these processes are important during the short melt season of this high Arctic plateau. Clear-air radiative loss stratifies lower

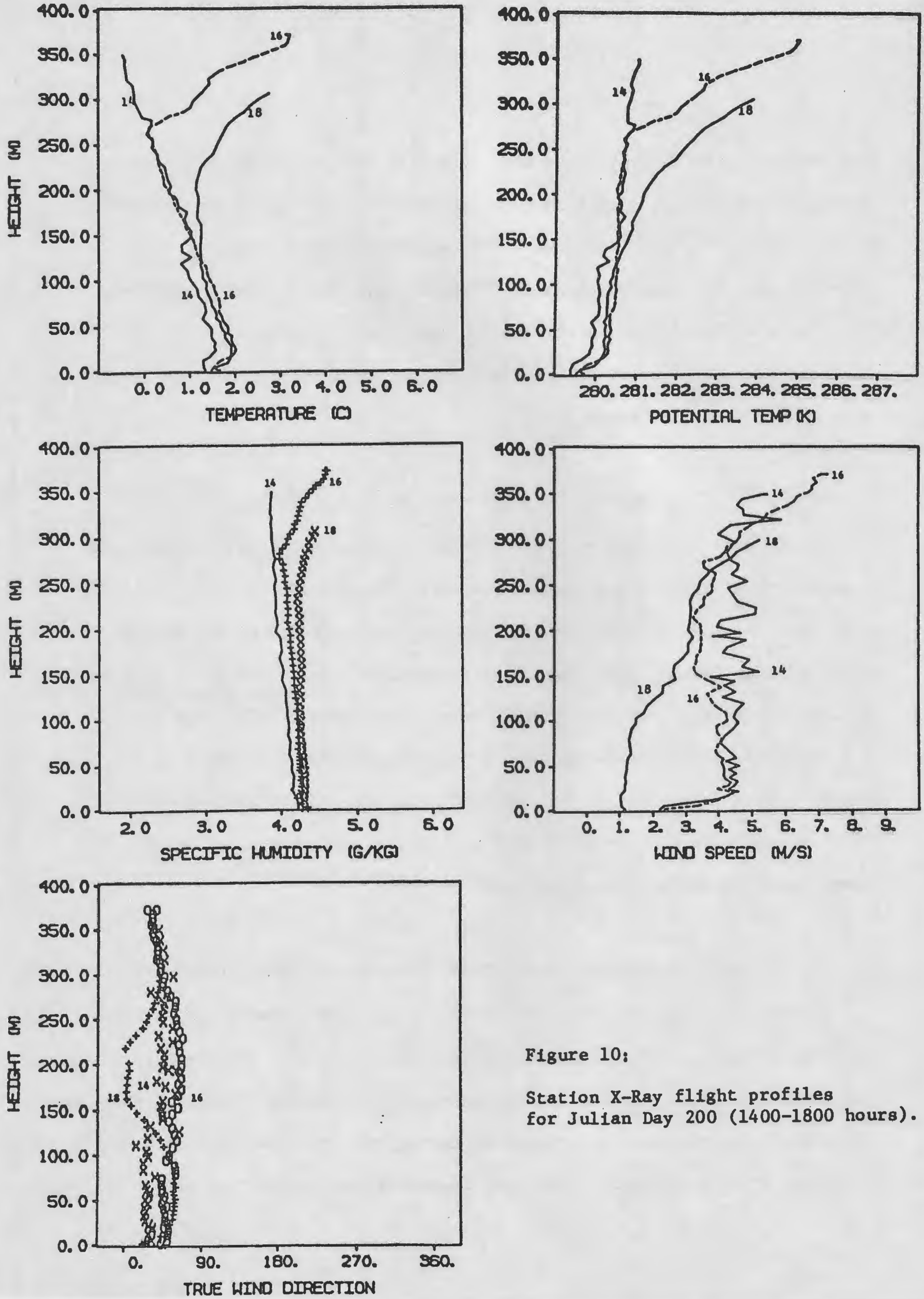

Figure 10:

Station X-Ray flight profiles
for Julian Day 200 (1400-1800 hours).

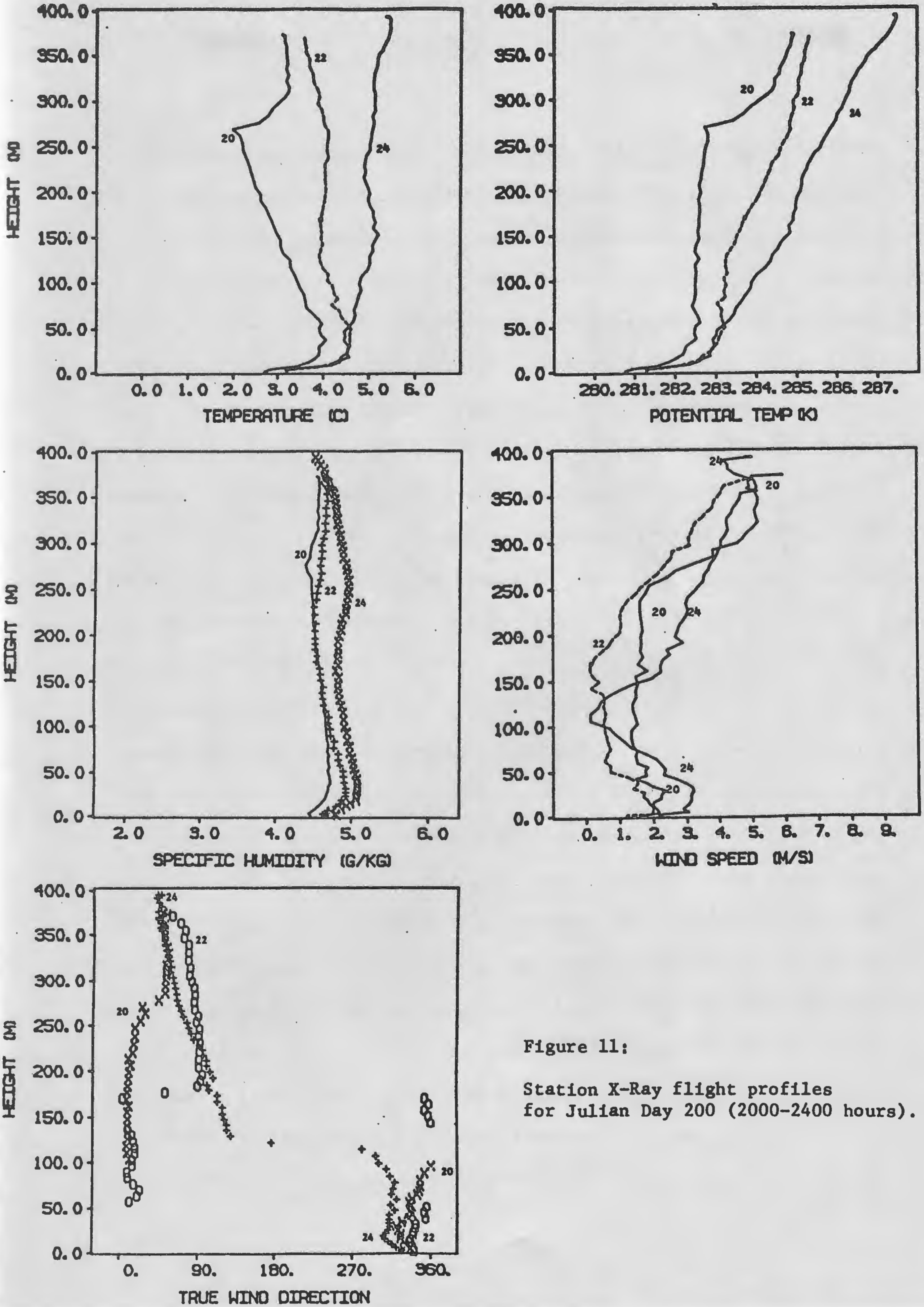

Figure 11:

Station X-Ray flight profiles for Julian Day 200 (2000-2400 hours).

layers and limits the range of turbulent fluxes that would normally be expected to freely carry away heat and water vapor from the surface. The air near the surface was almost always cooler and drier than the air above. However, this was not a static condition; in the normal evolution of the surface inversion, a low-level wind jet formed in the layer of air above the inversion. By increasing wind shear in this region, the stratified jet was eventually invaded by penetrative turbulence from the inversion layer. The air above the inversion was cooled. More importantly, though, the surface temperature was increased by over 1°C for several hours, until this extra heat was transferred to the surface. Such a sequence of events has not been widely observed and could be very important in ice and snow mass balance (Halberstam and Melendez, 1979).

An important regional consideration is the extent of bare ground. Areas that are not snow-covered create convective turbulence by heating the atmosphere. Not only is the warm air available for advection, but the upward convection causes air over non-convective surfaces (e.g. ice caps) to subside. The balloon flights have demonstrated that subsidence is a very effective warming process on the high Arctic plateau.

On the local level, there is the possibility that an oscillating wind system exists, due to differing pressure gradients created by non-uniform surface heating and topography. This may affect the ice and snow adversely, depending on the extent of bare ground immediately around. At the St. Patrtick Bay Ice Cap, there is also the possibility of relatively cool breezes from the ice-covered Robeson Channel (and Greenland beyond). The distinct separation of local winds and regional flow under conditions of light geostrophic winds causes the lower layer of air to have different characteristics than the free atmosphere.

In light of this research, several approaches to examining atmosphere-glaciation level relationships can be looked at. Problems are abundant in trying to extrapolate temperature upward from a near sea level weather station to plateau surfaces (Bradley, 1972). In fact, our conclusion is that there is in general no way to predict the various topographic and surface effects on temperature profiles knowing only sea-level surface temperature. Actual upper air soundings are the minimum needed to discuss relationships between atmospheric and surface processes (Kuhn, 1979; Braithwaite, 1979). However, the determination of a statistical relationship between a certain isotherm and glaciation level a short distance away may be possible (e.g.Bradley,1975) with the slope and intercept representing averages of local physical processes taking place.

It is important to remember that surface-scale processes can be quite overwhelmed by synoptic scale atmospheric conditions. Recent changes in freezing level indicate gross atmospheric conditions may have favored the glacierization of upland surfaces (Bradley, 1973). However, Alt (1979) has found that occasional periods of persistent high pressure over the area have, in the past, resulted in extremely negative mass balance conditions, eliminating the accumulation of snow and ice from many previous years. At such times, warm air advection was important in enhancing ablation, but the results of this study suggest that at higher altitudes subsidence was probably equally important.

In conclusion, it is clear that more research is needed on this important problem of localized surface effects. The feedbacks of the surface-atmosphere system are not known well at all on this scale. The balloon system approach, though cumbersome, has provided excellent data with which to identify important processes. An improved approach to utilizing the balloon system could include making several rapid ascents with little time in between (Mahrt, et al., 1979) and averaging the results, or stopping the ballooon every fifty meters to gain information from each level for ten minutes (Trombetti and Tampieri, 1983). These averaged results would be more useful in using profile relationships and Richardson numbers that should be based on time averages. Finally, upper air and synoptic data should be included in future studies to specifically identify and quantify surface-atmosphere-climate relationships.

REFERENCES

Alt, B., 1979. Investigation of summer synoptic climate controls on the mass balance of Meighen Ice Cap. Atmosphere-Ocean 17, 181-199.

Atmospheric Instrumentation Research, 1977. Tethersonde Operations Manual. A.I.R., Boulder, Colorado.

Bilello, M. 1966. Survey of Arctic and Subarctic Temperature Inversions: Technical Report 161, U.S. Army Material Comman, CRREL, Hanover, New Hampshire, 38 pp.

Bradley, R.S., 1972. The problem of inversions in estimating the height of glaciation limits in arctic regions. Arctic and Alpine Research, 4, 359-360.

Bradley, R.S., 1973. Recent freezing level changes and climatic deterioration in the Canadian Arctic archipelago. Nature 243, 398-400.

Bradley, R., 1975. Equilibrium-line altitudes, mass balance, and July freezing-level heights in the Canadian High Arctic. Journal of Glaciology 14, 267-274.

Bradley, R.S. and Serreze, M.C., 1985a. Glacio-climatic studies of a High Arctic plateau ice cap: Part II: topoclimate (submitted).

Bradley, R.S. and Serreze, M.C., 1985b. Glacio-climatic studies of a High Arctic plateau ice cap: Part I: mass balance. (submitted).

Braithwaite, R. 1979. Glacier energy balance and air temperature: comments on a paper by Dr. M. Kuhn. Journal of Glaciology 22, 501-503.

Garratt, J. and Brost, R., 1981. Radiative cooling effects within and above the nocturnal boundary layer. J. Atmospheric Sciences 38, 2739-2746.

Hahn, C., 1981. A study of the durnal behavior of boundary-layer winds at the Boulder Atmospheric Observatory. Boundary-Layer Meteorology 21, 231-245.

Halbertstam, I. and Melendez, R., 1979. A model of the planetary boundary layer over a snow surface. Boundary-Layer Meteorology 16, 431-452.

Hsu, S., 1979. Mesoscale nocturnal jetlike winds within the planetary boundary layer over a flat, open coast. Boundary-Layer Meteorology 17, 485-494.

Korrell, A., Panofsky, H. and Rossi, R., 1982. Wind profiles at the Boulder Tower. Boundary-Layer Meteorology 22, 295-312.

Kuhn, M., 1979. On the computation of heat transfer coefficients from energy-balance gradients on a glacier. J. Glaciology 22, 263-272.

Li, Xing-sheng, Gaynor, J. and Kaimal, J., 1983. A study of multiple stable layers in the nocturnal lower atmosphere. Boundary-Layer Meteorology 26, 157-168.

Mahrt, L., Heald, R., Lenschow, D., Stankov, B. and Troen, I., 1979. An observational study of the structure of the nocturnal boundary layer. Boundary-Layer Meteorology 17, 247-264.

Mahrt, L., 1981. The early evening boundary layer transition. Quarterly Journal of the Royal Meteorology Society 107, 329-343.

Oke, T., 1974. Boundary layer climates. Methuen and Company, Ltd., London. 372 pp.

Panofsky, H. and Dutton, J., 1984. Atmospheric Turbulence. John Wiley and Sons, New York. 397 pp.

Thorpe, A. and Guymer, T., 1977. The nocturnal jet. Quarterly Journal of the Royal Meteorological Society 103, 633-653.

Treidl, R., 1970. A case study of warm air advection over a melting snow surface. Boundary-Layer Meteorology 1, 155-168.

Trombetti, F. and Tampieri, F., 1983. An interpolation method of randomly distributed atmospheric data in the height-time domain. Boundary-Layer Meteorology 25, 159-170.

Whiteman, C., 1980. Breakup of Temperature Inversions in Colorado Mountain Valleys. Atmospheric Science Paper No. 328, Climatology Report No. 80-82, Department of Atmospheric Sciences, Colorado State University, Fort Collins, Colorado. 250 pp.

ASPECTS OF THE PRECIPITATION CLIMATOLOGY OF THE CANADIAN HIGH ARCTIC

R.S. Bradley and J.K. Eischeid

University of Massachusetts, Amherst

ABSTRACT

Most precipitation in the High Arctic results from a relatively small number of discrete precipitation events. The synoptic circulation patterns giving rise to these events is investigated for significant precipitation (SP) events at Alert. Four major synoptic type sequences are shown to be important. Precipitation events are then examined in relation to temperature. Precipitation is positively correlated with temperature and, in winter, days with precipitation are significantly warmer than other days. The implications of these facts for the interpretation of ice core oxygen isotope records is investigated. There is no *a priori* reason why ice core oxygen isotope records should be related to mean annual temperature. Oxygen isotopes should reflect accumulation changes. The available data shows that this is only true for two periods in the Dye-3 record. Further research on the proper interpretation of ice core oxygen isotope records is needed.

INTRODUCTION

Although long-term meteorological observations are quite sparse, it is well known that precipitation amounts in the High Arctiuc are extremely low and the area can justifiably be described as a polar desert (Bovis and Barry, 1974; Maxwell, 1980). In the Queen Elizabeth Islands of northern Canada, precipitation records (mostly from coastal sites near to sea-level) indicate a range of 75-170 mm per year; the only inland record (from Lake Hazen) indicates that even lower amounts (25-50 mm) may occur in interior lowlands (Table 1). Analysis of the daily precipitation records from High Arctic stations points to another

TABLE 1

Annual Precipitation Amounts

(after Fristrup, 1961; Putnins, 1970; Bradley and England, 1978)

Station	Location	Elevation	Period of Record	Total Precipitation	Adjusted Total(mm*)
Alert	82°30'N,62°20'W	63	1951-1975	158	170
Eureka	80°00'N,85°56'W	10	1947-1975	60	76
Isachsen	78°47'N,103°32'W	25	1948-1975	105	125
Resolute A	74°43'N,94°59'W	64	1947-1972	134	154
Thule	75°32'N,68°45'W	60	1951-1970	139	153
Jorgen Bronlunds	82°10'N,30°30'W	5	1948-1950	55	
Nord	81°36'N,16°40'W	35	1952-1956	204	
L.Hazen	81°49'N,71°18'W		1957-1958	25	50**

* Assuming daily trace recordings = 0.127 mm

** Estimate based on observations of snow depth and density on Lake Hazen (Jackson, 1960).

important characteristic of precipitation in these regions: most precipitation occurs on a relatively small number of days per year. At Alert, for example, 80% of all precipitation results from precipitation events $\geq$ 1 mm which occur on only 22% of days. Similarly, at Thule, Greenland, 73% of all precipitation occurs on less than 10% of days. Here, we examine precipitation events in more detail to determine (a) what circulation patterns give rise to the bulk of High Arctic precipitation and (b) what is the proper interpretation of the oxygen isotope content of precipitation from the High Arctic..

PRECIPITATION EVENTS

Since the bulk of precipitation in the High Arctic results from a relatively small number of events it is of interest to examine these events in some detail. A "substantial precipitation" (SP) event is defined here as any one day, or sequence of consecutive days, on which precipitation occurred resulting in a cumulative total exceeding 5% of the annual mean. Using long-term data from Alert (1951-1981) the 5% threshold for this analysis is 7.7 mm. On this basis, 151 SP events occurred in the 31 year period of study (~ 5 SP events per year). SP events ranged in duration from 1 to 15 days, averaging ~ 4 days per event (Table 2). Overall, SP events accounted for 48% of mean annual precipitation yet they occurred on only ~ 6% of days per year. Of course, the contribution of SP events to total annual precipitation varies from year to year (Figure 1); in 1975 they were responsible for only 24% of the yearly total

TABLE 2

Substantial Precipitation (SP) Events at Alert, N.W.T. (1951-1981)

Mean Annual Precipitation:	155.3 mm (6.11 inches)
Minimum amount for SP event	7.7 mm
Mean No. SP events per year	4.9
Mean No. days per SP event	4.3
Max. No. days per SP event	15
Min. No. days per SP event	1
Mean precipitation per event	15.3 mm
Max. Precipitation per event	41.6 mm
Max. frequency of SP events	August (26% of all events)

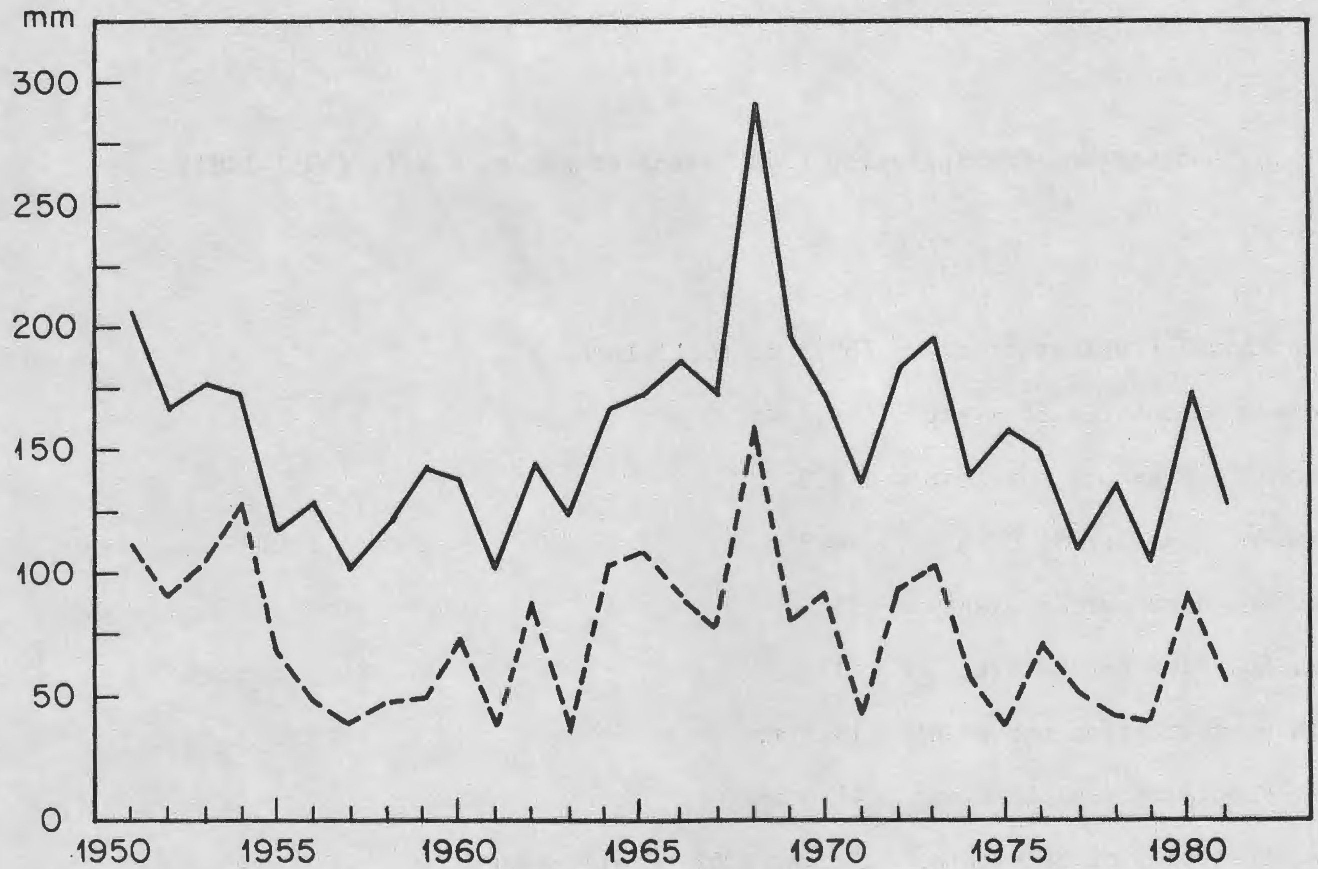

Figure 1. Annual precipitation at Alert (solid line) and total amount from SP events (dashed line). There are approximately 5 SP events per year on average (Table 2).

whereas in 1954 they resulted in 73% of the annual amount.

Monthly frequencies of SP events are shown in Figure 2. Their occurrence is clearly at a maximum in late summer/early Fall. The three months of July-September account for 64% of all SP events.

SYNOPTIC CIRCULATION PATTERNS AND SP EVENTS

In order to understand the circulation patterns which bring about SP events, 104 case studies in the period 1951-70 were examined. These occurred on 6% of days and resulted in 50% of precipitation in the period. Using sea-level pressure maps for the polar regions (European Meteorological Bulletin) synoptic circulation patterns on days with substantial precipitation and on the preceding 2-3 days were examined. Although there are, no doubt, many inaccuracies in the charts for this area because of the limited synoptic reporting network, it was nevertheless clear that four basic patterns (sequences of synoptic types) accounted for most SP events (91% of the total) over the 1951-70 period. The four sequences are as follows (see Figure 3 and Table 3):

A. Low pressure center tracking across the central Arctic Islands.

A low pressure center enters the archipelago generally between the mainland coast and Ellef Ringnes Island crossing to northern Baffin Island, Devon Island or southern Ellesmere Island. Precipitation at Alert is associated with southerly airflow as the low moves eastwards. This type is relatively uncommon (6% of SP events).

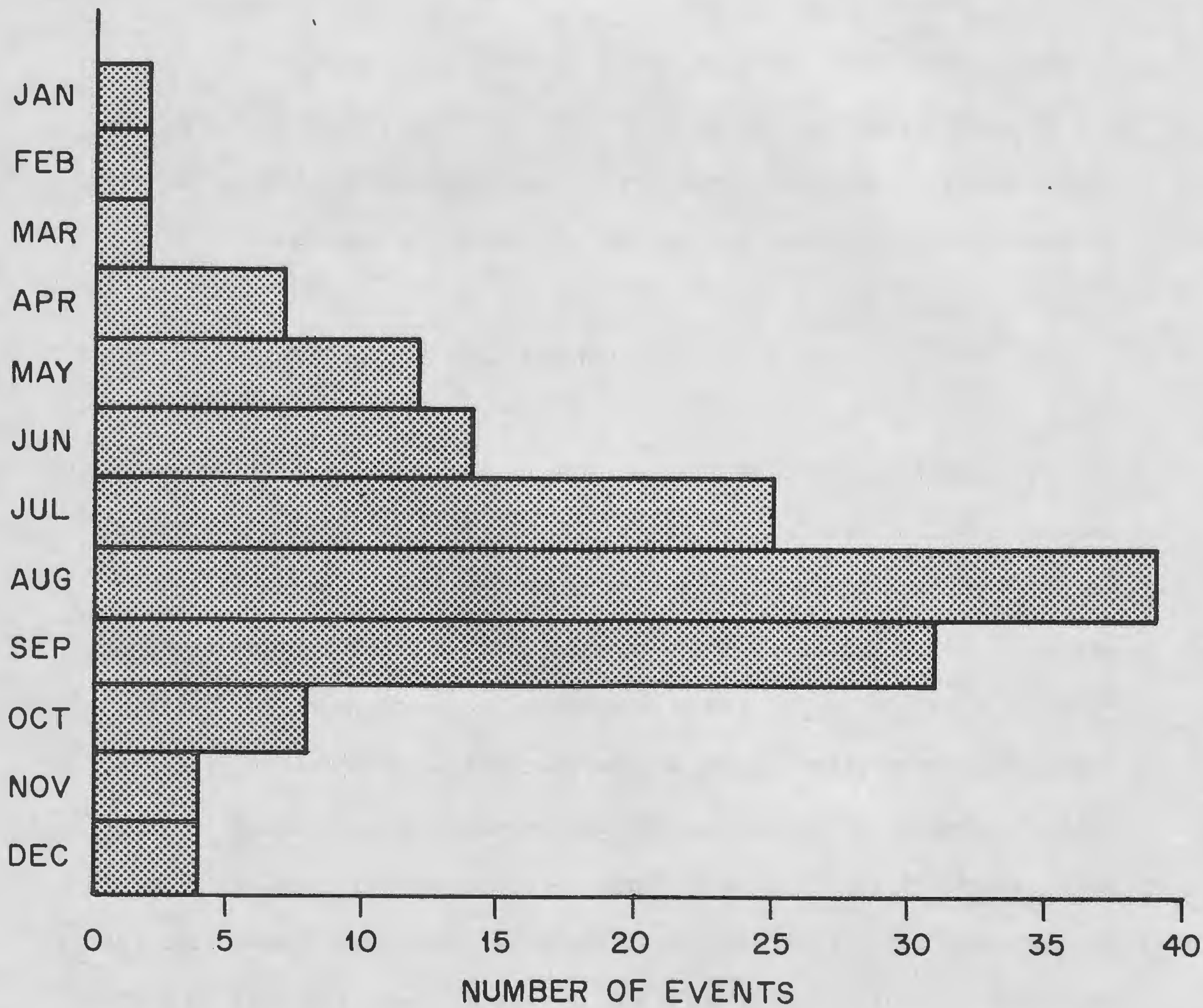

Figure 2. Frequency histogram of SP events by month at Alert, 1951-81.

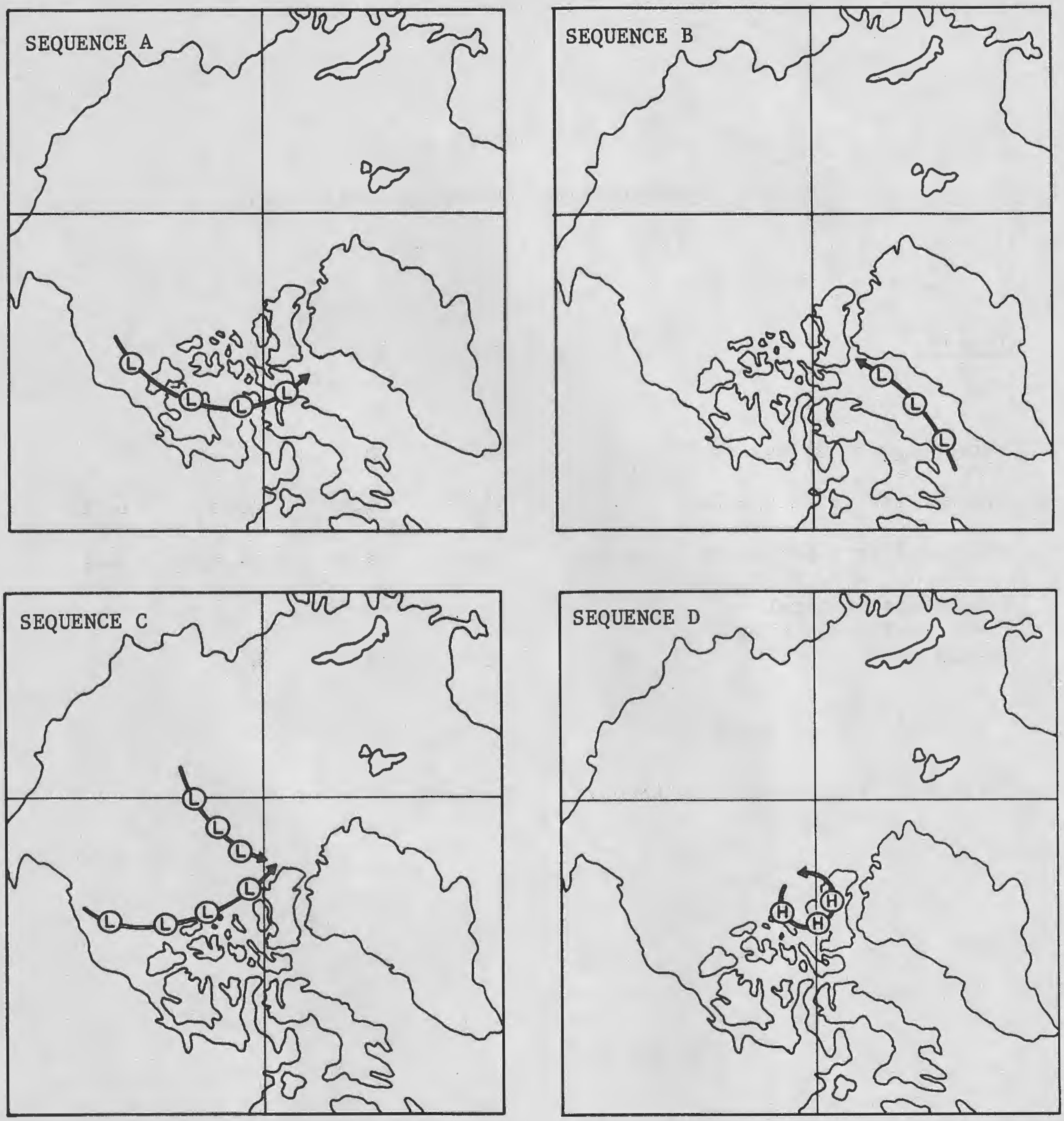

Figure 3. Principal features of synoptic circulation type sequences A,B,C and D.

TABLE 3

Synoptic Type Statistics (1951-1970)

Types*	A	B	C	D	E
Percentage of SP events	6	16	30	40	9
Average precipitation (mm)	18.5	13.9	14.6	15.3	14.1
Average # days per event	5.2	3.7	3.7	4.6	4.7
Percentage of total Precipitation (during SP events only)	4	16	30	42	8

*Type E = indeterminate patterns.

B. Low pressure center tracking northward up Baffin Bay.

Low pressure centers may reach the vicinity of northern Ellesmere Island, or northern Baffin Bay having tracked across Baffin Island (from the southwest) or directly up Davis Strait from Labrador. Some of these types may originate with depressions crossing the southern arctic islands on a track parallel to, but south of, the typical "sequence A" track. The low may decay in northern Baffin Bay, move around the northern coast of Greenland or over central Ellesmere Island. Depending on the precise track, moist southerly air may reach northern Ellesmere or airflow may be off the Arctic Ocean. This type is not very common (16% of SP events studied).

C. Low pressure center tracking from the Beaufort Sea.

Low pressure centers commonly move from the Beaufort Sea (north of Alaska) skirting the western edge of the arctic islands. A trailing cold front may cross the area. A related type involved a more direct path from the Arctic Oceaqn proper, often crossing near the North Pole towards northern Ellesmere Island. These types account for 30% of SP events.

D. High pressure center south or southwest of Ellesmere Island.

High pressure centers often move slowly south and southwest of Ellesmere Island resulting in northerly airflow from the Arctic Ocean. This type accounts for most SP events (40%).

These circulation sequences are similar in many ways to the major synoptic types identified by Alt (1975) in a study of energy budget and mass balance data from Meighen Island. Alt's type I is similar to our synoptic type sequence B and Alt's type II to our type sequence C. Interestingly, Alt found that her type II circulation patterns resulted in large amounts of precipitation on the ice cap, just as they do at Alert.

It is surprising that the "Baffin Bay track" (type B) is not more important for precipitation at Alert. Most climatologies point to this as the principal track for depressions into the High Arctic (e.g. Klein, 1957; Reed and Kunkel, 1960; Wilson, 1967). However, in terms of significant precipitation events, the Beaufort Sea track is more important. It is also of interest that most of the significant precipitation events are associated with northerly airflow from the Arctic Ocean. Presumably, with more open water conditions off the coast, precipitation amounts associated with this type would be even greater.

The results of this study confirm the views of Jackson (1961), Alt (1975) and Bradley and England (1979) that the movement of low pressure centers along the western edge of the Arctic Islands may contribute significantly to total annual precipitation. Over the period 1951-70 such events, occurring on only 5-6 days per year, contributed 15% of annual precipitation, on average. Any increase in the frequency of these types would have a major impact on annual precipitation totals. Similarly, northerly airflow associated with (on average) 9 to 10 days of slowly-moving high pressure south and southwest of Ellesmere Island (type sequence 4) results in 20% of annual precipitation at Alert. With more open leads, this figure could increase greatly. This inference has some support from the data in Figure 4 which shows mean precipitation from sequence D circulation patterns, by month. Precipitation amounts reach a peak in September when open water is most abundant.

THE INTERPRETATION OF ICE CORE ISOTOPIC RECORDS

Although ice cores can provide a vast amount of paleoclimatic information, ranging from atmospheric composition and turbidity to solar output variations (Bradley, 1985), attention continues to focus on the oxygen isotope record within the ice (e.g. Dansgaard, et al., 1982, 1984; Fisher, et al., 1983). Following the work of Dansgaard (1964) and Dansgaard, et al. (1973) who regressed mean annual temperature at various locations with $\delta^{18}O$ in precipitation, it has generally been assumed that the $\delta^{18}O$ record is a direct proxy of mean annual temperature. However, this is not a physically meaningful relationship. The ice core record itself is obviously a record of precipitation and the bulk of high arctic precipitation only occurs on a small fraction of days per year, as noted earlier. Why should the mean temperature of 365 days, many of which are dominated by strong winter surface inversions under anticyclonic conditions, be related to $\delta^{18}O$ in precipitation on the relatively few days per years when snow falls? One possible solution is that the mean temperature of "precipitation days" co-varies with that of mean annual temperature (i.e. of all days per year). However, there is very little

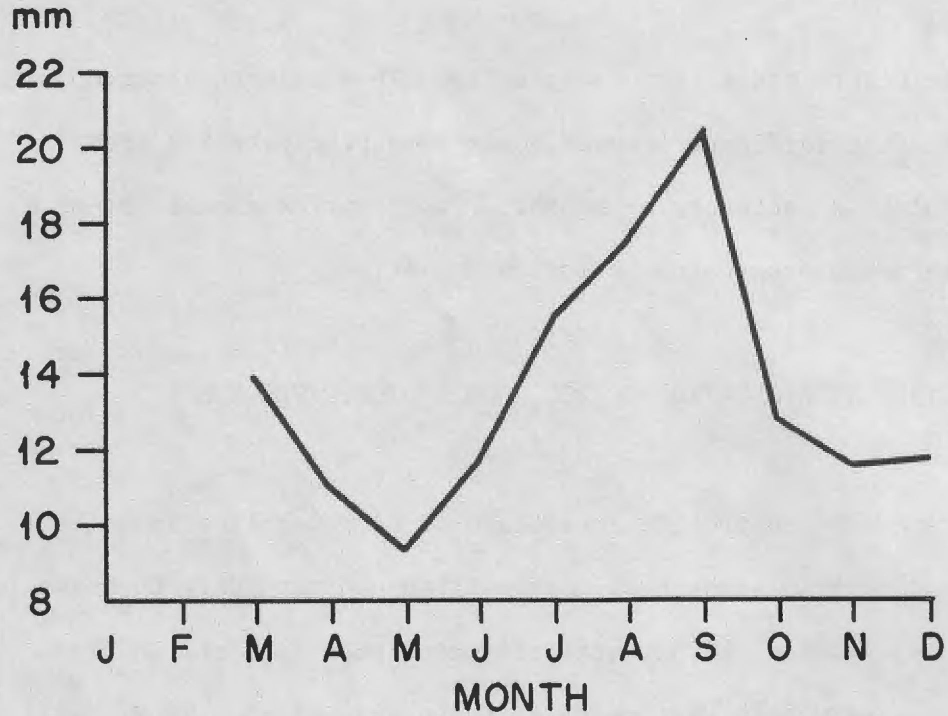

Figure 4. Average precipitation at Alert per SP event, resulting from synoptic circulation type sequence D (1951-70).

correspondence between such records, as Figure 5 illustrates. This is also true at Resolute, Eureka, Isachsen and Thule (not shown).

It is noteworthy that the "mean precipitation day" temperature is significantly warmer than mean annual temperature (Figure 5). If the same data are examined on a monthly basis, it is clear that this is not true for summer months (Figures 6 and 7). Days with precipitation are warmer than the mean of "all days" (which includes precipitation days) from September to May. At Thule, the difference reaches 8°C in March. This is because precipitation-bearing systems involve the advection of warm air into the Arctic. In summer months, precipitation days are <u>cooler</u> than the mean of all days because summer precipitation events generally interrupt periods with relatively clear skies and strong radiation receipts. Nevertheless, in almost <u>all</u> months at the 5 high arctic weather stations studied (Resolute, Eureka, Isachsen, Thule and Alert) precipitation amounts are positively correlated with mean temperature on the same days. That is, the heavier the precipitation the higher the temperature, even in summer, again because of the importance of warm air advection in bringing moisture to high latitudes.

In summary, there is no <u>a priori</u> reason to expect $\delta^{18}O$ in precipitation to correlate with mean annual temperature; indeed, "precipitation day" mean temperature shows very little correlation with yearly averages. Precipitation days are generally warmer than other days, except in summmer. In all months, precipitation amounts are

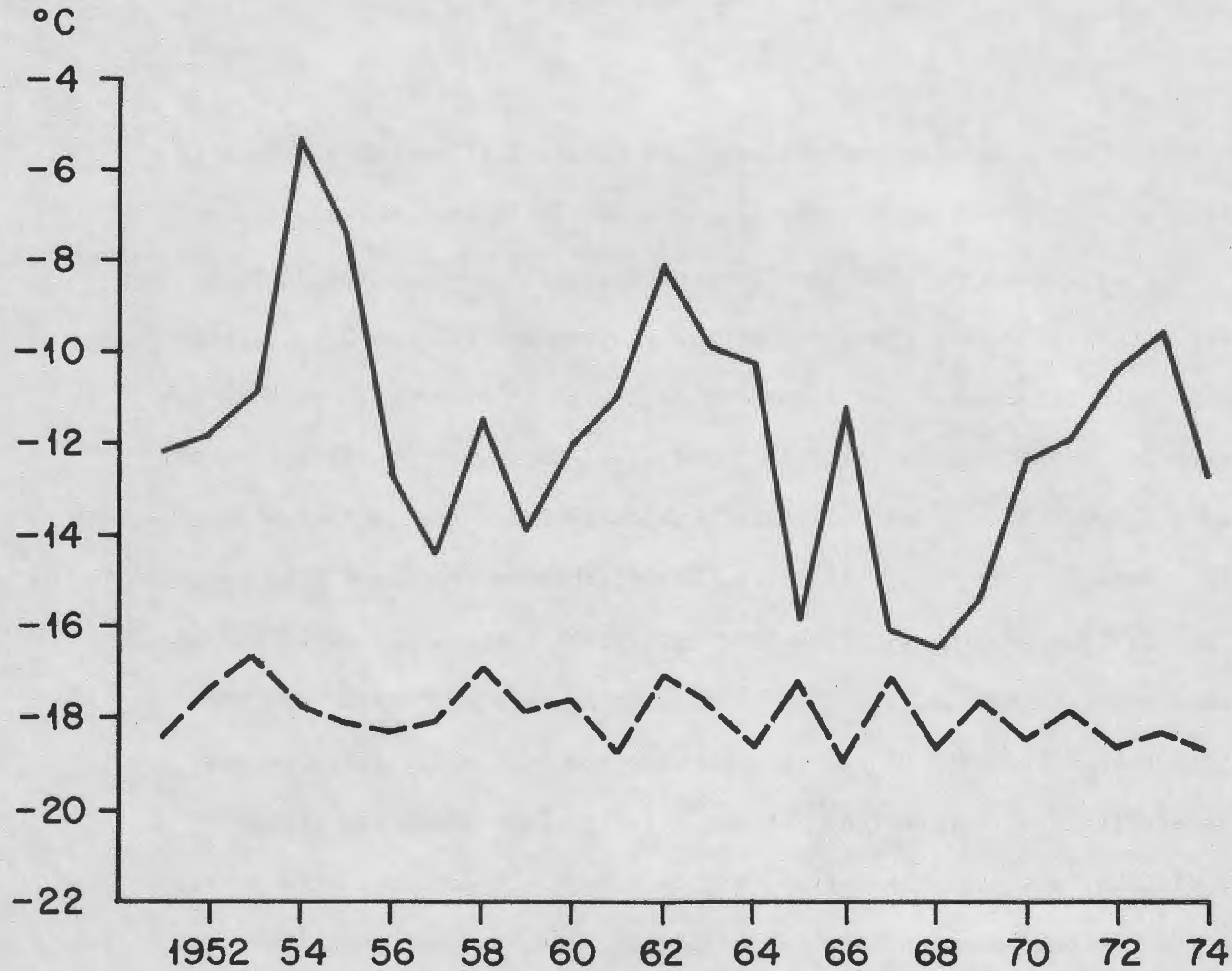

Figure 5. Mean annual temperature at Alert (dashed line) and mean temperature on days with precipitation ≥ 1 mm.

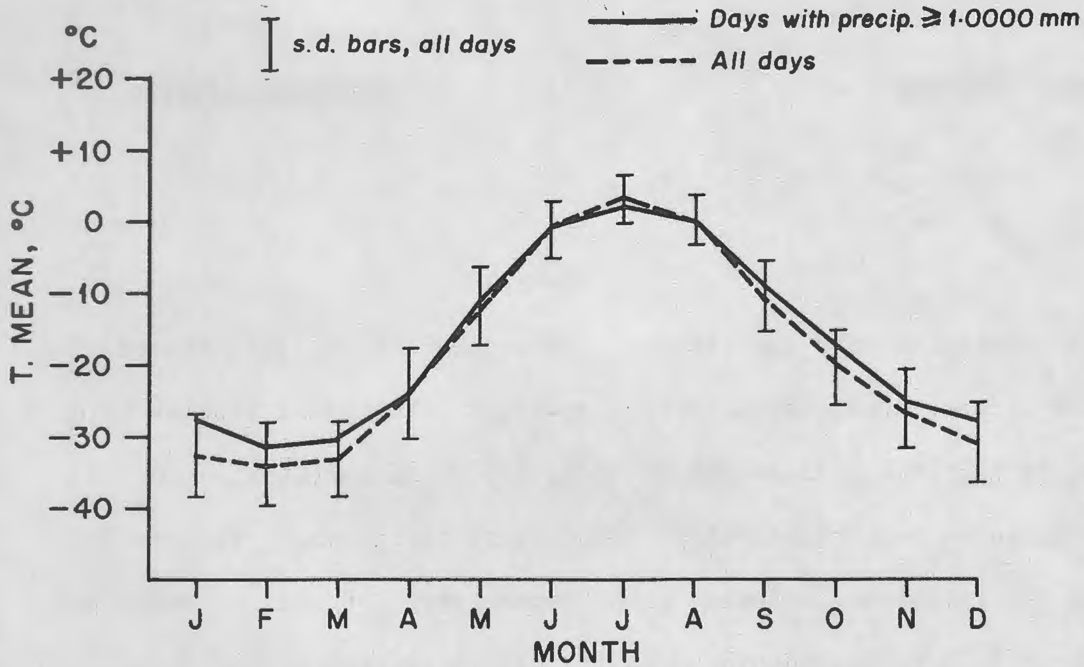

Figure 6. Mean monthly temperature at Alert on all days (dashed line) and on days with $\geq$ 1 mm of precipitation (solid line). Vertical bars indicate ±1 standard deviation for mean monthly temperature.

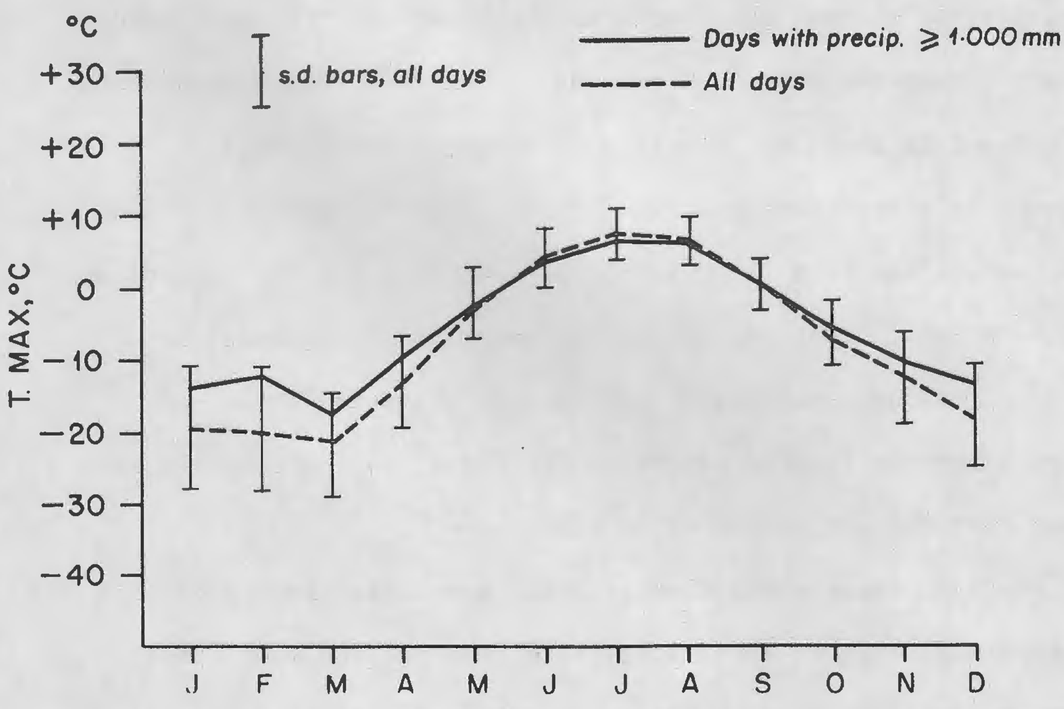

Figure 7. Mean monthly temperature at Thule on all days (dashed line) and on days with $\geq$ 1 mm of precipitation (solid line). Vertical bars indicate ± 1 standard deviation for mean monthly temperature.

positively correlated with temperature. What are the implications of these facts for ice core oxygen isotope studies? Empirical studies (e.g. Picciotto, et al, 1960; Aldaz and Deutsch, 1967) indicate that $\delta^{18}O$ should increase as mean condensation temperature increases. We have shown that precipitation increases with temperature. Hence, it might be expected that $\delta^{18}O$ values should be positively correlated with precipitation amounts and that very low $\delta^{18}O$ values should correspond to dry (low accumulation) conditions. Unfortunately, there are very few long-term records of precipitation or accumulation at ice core sites. However, Reeh, et al, (1978) have reconstructed accumulation rates at three sites (Dye-3, Milcent and Crete) on the Greenland ice sheet which can be directly compared with $\delta^{18}O$ records. The $\delta^{18}O$ and accumulation record from Dye-3 is shown in Figure 8. Although the overall correspondence is poor, there are two periods, from 1320 A.D. to the early 16th century and from 1850 to the present when the two records are reasonably in phase. That is, heavier accumulation corresponds to higher $\delta^{18}O$. For the remainder of the period, there is little correspondence between the two records. At Crete, the correlation is equally poor over the period 1100-1970 A.D.

Oxygen isotopic records are clearly not a meaningful indicator of annual temperature. It is more likely that they reflect some other factor, such as distance to moisture source (e.g. Koerner and Russell, 1979; Bromwich and Weaver, 1983). There is reason to believe that they

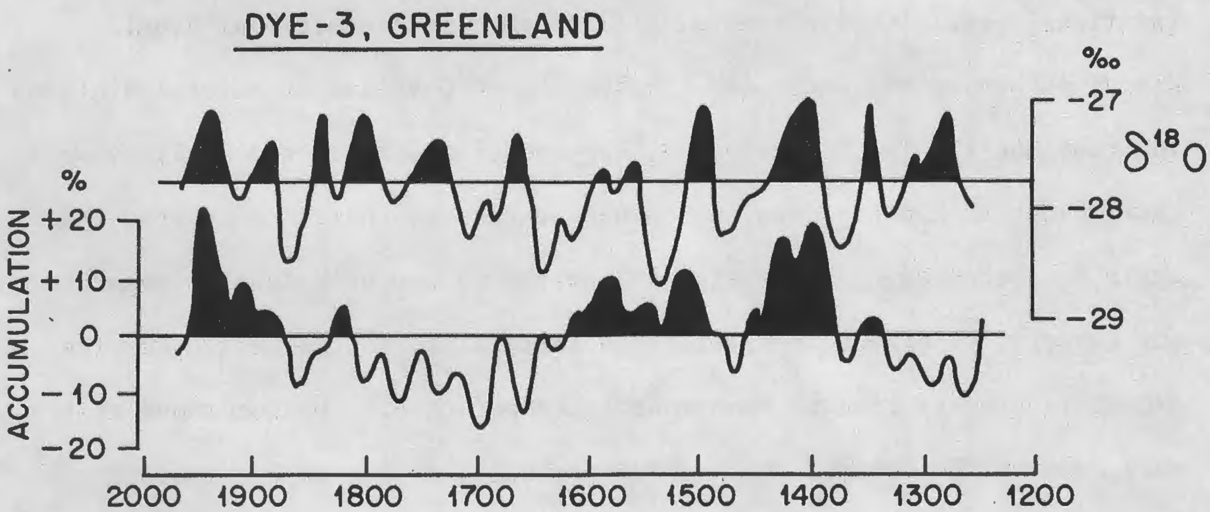

Figure 8. The record of $\delta^{18}O$ in an ice core from Dye-3, Greenland (above) and of accumulation expressed as departures (%) from the long-term mean (after Reeh, et al., 1978).

should provide information on changes in precipitation amount. However, the available evidence is equivocal. A major problem in understanding the oxygen isotope record is a lack of data on the isotopic composition of individual precipitation events. Although the International Atomic Energy Authority has monitored tritium and $\delta^{18}O$ values at several stations in Greenland (Thule, Scoresbysund, Groennedal and Nord) the analyses were carried out on monthly data, so cannot be tied to individual storms and their trajectories. It is also impossible to use such data to separate any temperature effect from "distance to moisture source" since sea ice extent is closely tied to mean monthly temperature. We recommend that more research be focused on the interpretation of the oxygen isotope records in high latitude snow and ice. In particular, it would be extremely useful if a monitoring network were established to collect precipitation samples and determine $\delta^{18}O$ on a storm-by-storm basis. These data could then be examined in relation to precipitation amount, synoptic circulation pattern and sea-ice position. With such a data base, the valuable $\delta^{18}O$ record in ice cores could be interpreted in a much more meaningful way.

REFERENCES

Aldaz, L. and Deutsch, S., 1967. On a relationship between air temperature and oxygen isotope ratio of snow and firn in the South Pole region. Earth and Planetary Science Letters, 3, 267-274.

Alt, B.T., 1975. The energy balance climate of Meighen Island Ice Cap, N.W.T., vols 1 and 2, Polar Continental Shelf Project, Dept. Energy, Mines and Resources, Ottawa.

Bovis, M. and Barry, R.G., 1974. A climatological analysis of north polar desert areas, pp. 23-31 in Polar Deserts and Modern Man, Smiley, T.L. and Zumberge, J.H., eds., University of Arizona Press, Tucson, Arizona.

Bradley, R.S., 1985. Quaternary Paleoclimatology, G. Allen and Unwin, Boston and London, 472 pp.

Bradley, R.S. and England, J., 1979. Synoptic climatology of the Canadian High Arctic. Geografiska Annaler, 61A, 187-201.

Bromwich, D.H. and Weaver, C.J., 1983. Latitudinal displacement from main moisture source controls $\delta^{18}O$ of snow in coastal Antarctica. Nature, 301, 145-147.

Dansgaard, W., 1964. Stable isotopes in precipitation. Tellus, 16, 436-468

Dansgaard, W., Johnsen, S.J., Clausen, H.B. and Gundestrup, N., 1973. Stable isotope glaciology. Meddelelser om Gronland, 197, 1-53.

Dansgaard, W., Clausen, H.B., Gundestrup, N., Hammer, C.U., Johnsen, S.J., Kristinsdottir, P.M. and Reeh, N., 1982. A new Greenland deep ice core. Science, 218, 1273-1277.

Dansgaard, W., Johnsen, S.J., Clausen,H.B., Dahl-Jensen, D., Gundestrup, N., Hammer, C.U. and Oeschger, H. 1984. North Atlantic climatic oscillations revealed by deep Greenland ice cores, pp. 288-298 in Climate Processes and Climate Sensitivity, Hansen, J.E. and Takahaski, T., eds., American Geophysical Union, Washington, D.C.

Fisher, D.A., Koerner, R.M., Paterson, W.S.B., Dansgaard, W., Gundestrup, N. and Reeh, N., 1983. Effect of wind scouring on climatic records from ice-core oxygen isotope profiles. Nature, 301, 205-209.

Jackson, C.I., 1961. Summer precipitation in the Queen Elizabeth Islands. Folia Geographica Danica, 9, 140-1,53.

Klein, W.H., 1957. Principal tracks and mean frequencies of cyclones in the northern hemisphere. Research Paper No. 40, U.S. Weather Bureau, Washington, D.C. 22 pp.

Koerner, R.M. and Russell, R.P., 1979. $\delta^{18}O$ variations in snow on the Devon Island Ice Cap, Northwest Territories, Canada. Canadian J. Earth Science, 16, 1419-1427.

Maxwell, J.B., 1980. The Climate of the Canadian Arctic Islands and Adjacent Waters, Vol. 1, Environment Canada, Hull, Quebec.

Picciotto, E., DeMaere, X. and Friedman, I., 1960. Isotopic composition and temperature of formation of Antarctic snows. Nature, 187, 857-859.

Reed, R.J. and Kunkel, B.A., 1960. The Arctic circulation in summer. J. Meteorology, 17, 489-506.

Reeh, N., Clausen, H.B.,Dansgaard, W.,Gundestrup, N.,Hammer, C.U. and Johnsen, S.J., 1978. Secular trends of accumulation rates at three Greenland stations. J. Glaciology, 20, 27-30.

Wilson, C., 1967. Cold Regions Climatology Introduction. Northern Hemisphere I. Cold Regions Research and Engineering Laboratory, Hanover, New Hampshire, 141 pp.

Cumulus over Base Camp,
"St. Patrick Bay" Ice Cap,
N.E. Ellesmere Island, N.W.T., Canada